Methods in Molecular Biology 2579

Springer Protocols

Zhixiang Wang *Editor*

Cell-Cycle Synchronization

Methods and Protocols

Humana Press

METHODS IN MOLECULAR BIOLOGY

Series Editor
John M. Walker
School of Life and Medical Sciences
University of Hertfordshire
Hatfield, Hertfordshire, UK

For further volumes:
http://www.springer.com/series/7651

For over 35 years, biological scientists have come to rely on the research protocols and methodologies in the critically acclaimed *Methods in Molecular Biology* series. The series was the first to introduce the step-by-step protocols approach that has become the standard in all biomedical protocol publishing. Each protocol is provided in readily-reproducible step-by-step fashion, opening with an introductory overview, a list of the materials and reagents needed to complete the experiment, and followed by a detailed procedure that is supported with a helpful notes section offering tips and tricks of the trade as well as troubleshooting advice. These hallmark features were introduced by series editor Dr. John Walker and constitute the key ingredient in each and every volume of the *Methods in Molecular Biology* series. Tested and trusted, comprehensive and reliable, all protocols from the series are indexed in PubMed.

Cell-Cycle Synchronization

Methods and Protocols

Edited by

Zhixiang Wang

Department of Medical Genetics, University of Alberta, Edmonton, AB, Canada

Humana Press

Editor
Zhixiang Wang
Department of Medical Genetics
University of Alberta
Edmonton, AB, Canada

ISSN 1064-3745 ISSN 1940-6029 (electronic)
Methods in Molecular Biology
ISBN 978-1-0716-2735-8 ISBN 978-1-0716-2736-5 (eBook)
https://doi.org/10.1007/978-1-0716-2736-5

This Humana imprint is published by the registered company Springer Science+Business Media, LLC, part of Springer Nature.
The registered company address is: 1 New York Plaza, New York, NY 10004, U.S.A.

Preface

The cell cycle is a series of events that drives cells to divide and produce two new daughter cells. The typical cell cycle in eukaryotes is composed of the following phases: G1, S, G2, and M phases. G1, S, and G2 phases are collectively known as interphase. M phase consists of two coupled processes: mitosis and cytokinesis. In mitosis, a cell's nucleus divides, and in cytokinesis, a cell's cytoplasm divides to form two daughter cells. Mitosis is further divided into five subphases including prophase, prometaphase, metaphase, anaphase, and telophase. Progression through each cell cycle phase is dependent on the proper completion of the previous one. Cells can also exit from cell cycle to enter quiescence or G0 phase by temporarily or reversibly stopping division. In prokaryotes, the cell cycle is divided into the B, C, and D periods. The B period extends from the end of cell division to the beginning of DNA replication. DNA replication occurs during the C period. The D period refers to the stage between the end of DNA replication and the splitting of the bacterial cell into two daughter cells.

Cell cycle progression is mediated by cyclin-dependent kinases (CDKs) and their regulatory cyclin subunits. CDKs, such as CDK4/6, CDK2, and CDK1 (also known as CDC2), are serine/threonine kinases with a wide variety of substrates. CDKs are activated mainly by binding to their cyclin partners, whose expressions rise and fall throughout the cell cycle to mediate the temporal activation of each CDKs. Various cell cycle checkpoints exist to ensure that critical processes are engaged prior to progression to the next phase. These cell cycle checkpoints are the G1 (restriction) checkpoint, the G2/M DNA damage checkpoint, and the spindle assembly checkpoint (SAC).

Cell synchronization is a process to bring the cultured cells at various stages of the cell cycle to the same phase. Cell synchronization is a vital method in the study of cell cycle progression and regulation because it allows population-wide data to be collected rather than relying solely on single-cell experiments. Cell synchronization could be achieved in many different ways. Traditionally, the types of synchronization are broadly categorized into two groups: synchronization by non-chemical inhibitors and synchronization by chemical blockade. Synchronization by non-chemical inhibitors includes physical fractionation, changes to cell environments, and genetic manipulation. Synchronization by physical fractionation is based on cell density and size, cell surface epitopes and DNA contents, as well as light scatter and fluorescent emission. Flow cytometry and centrifugal elutriation are the two commonly used methods. Serum starvation, contact inhibition, mitotic shake-off, and genetic manipulation are also used as non-chemical methods. Cell synchronization by using chemical inhibitors is a major approach used by many researchers. As each specific cell cycle phase has its own protein expression profile and is regulated differently from other cell phase, specific chemical inhibitors have been identified and used to inhibit the cell cycle at specific cell cycle phase. While chemical blockade is typically more effective and precise than physical separation, chemical manipulations may disrupt cellular function and/or kill a portion of cells.

This volume is divided to four parts. Part I contains four review articles that provide a general overview regarding the cell cycle control and synchronization. Part II provides five protocols used to synchronize mammalian cells to various cell cycle phase including mitotic subphases. Part III contains four protocols for the synchronization of unicellular organisms. Part IV provides five protocols for the analysis of cell cycle progression.

These protocols cover a broad range of cell types, including cultured cell lines and the primary cells, and various unicellular organisms, including fission yeast, budding yeast, parasite *Leishmania amazonensis*, and parasite *Trypanosoma brucei*. These protocols cover all the common methods used for cell cycle synchronization including centrifugal elutriation (Chapters 11 and 12), serum starvation (Chapters 7 and 9), nitrogen depletion (Chapter 13), genetic manipulation (Chapters 12 and 13), pheromone treatment (Chapter 12), double thymidine block (Chapters 5, 6, 7, 8, and 9), hydroxyurea inhibition (Chapters 10, 12, and 13), Nocodazole treatment (Chapters 6, 8, 9, and 12), GM132 treatment (Chapters 6 and 8), Roscovitine treatment (Chapter 7), RO-3306 treatment (Chapter 9), blebbistatin treatment (Chapter 8), and STLC (S-Trityl-L-cysteine) treatment (Chapter 6).

The format of the protocols is standardized to be followed accurately and easily. Each protocol is composed of four sections: Introduction, Materials, Methods, and Notes. The protocols are useful for both the newcomers to the field and more experienced scientists.

Edmonton, AB, Canada ***Zhixiang Wang***

Contents

Contributors

Asra Almubarak • *Department of Medical Genetics, University of Alberta, Edmonton, AB, Canada*

Luiz H. C. Assis • *Telomeres Laboratory, Department of Chemical and Biological Sciences, Biosciences Institute, São Paulo State University (UNESP), Botucatu, SP, Brazil*

Corinna Benz • *Division of Biomedical and Life Sciences, Faculty of Health and Medicine, Lancaster University, Lancaster, UK*

Fred B. Berry • *Department of Medical Genetics, University of Alberta, Edmonton, AB, Canada; Department of Surgery, University of Alberta, Edmonton, AB, Canada*

David N. Brindley • *Department of Biochemistry, Cancer Research Institute of Northern Alberta, University of Alberta, Edmonton, AB, Canada*

Maria Isabel N. Cano • *Telomeres Laboratory, Department of Chemical and Biological Sciences, Biosciences Institute, São Paulo State University (UNESP), Botucatu, SP, Brazil*

Gordon K. Chan • *Department of Oncology, University of Alberta, Edmonton, AB, Canada; Experimental Oncology, Cross Cancer Institute, Edmonton, AB, Canada; Cancer Research Institute of Northern Alberta, University of Alberta, Edmonton, AB, Canada*

Kyle Cheung • *Molecular Science Program, Yeates School of Graduate Studies, Toronto Metropolitan University (formerly Ryerson University), Toronto, ON, Canada*

Loraine L. Y. Chiu • *Department of Chemical Engineering, Ryerson University, Toronto, ON, Canada; Li Ka Shing Knowledge Institute, St. Michael's Hospital, Toronto, ON, Canada*

Marcelo S. da Silva • *DNA Replication and Repair Laboratory (DRRL), Department of Chemical and Biological Sciences, Biosciences Institute, São Paulo State University (UNESP), Botucatu, SP, Brazil*

Vitor L. da Silva • *Telomeres Laboratory, Department of Chemical and Biological Sciences, Biosciences Institute, São Paulo State University (UNESP), Botucatu, SP, Brazil; DNA Replication and Repair Laboratory (DRRL), Department of Chemical and Biological Sciences, Biosciences Institute, São Paulo State University (UNESP), Botucatu, SP, Brazil*

Arthur de Oliveira Passos • *DNA Replication and Repair Laboratory (DRRL), Department of Chemical and Biological Sciences, Biosciences Institute, São Paulo State University (UNESP), Botucatu, SP, Brazil*

Beatriz C. D. de Oliveira • *Telomeres Laboratory, Department of Chemical and Biological Sciences, Biosciences Institute, São Paulo State University (UNESP), Botucatu, SP, Brazil*

Leilane S. de Oliveira • *Telomeres Laboratory, Department of Chemical and Biological Sciences, Biosciences Institute, São Paulo State University (UNESP), Botucatu, SP, Brazil*

Yete G. Ferri • *Telomeres Laboratory, Department of Chemical and Biological Sciences, Biosciences Institute, São Paulo State University (UNESP), Botucatu, SP, Brazil*

Veronica S. Fontes • *Telomeres Laboratory, Department of Chemical and Biological Sciences, Biosciences Institute, São Paulo State University (UNESP), Botucatu, SP, Brazil*

Brianna L. Greenwood • *Department of Biochemistry, University of Alberta, Edmonton, AB, Canada*

Joanne D. Hadfield • *Department of Oncology, University of Alberta, Edmonton, AB, Canada; Experimental Oncology, Cross Cancer Institute, Edmonton, AB, Canada; Cancer Research Institute of Northern Alberta, University of Alberta, Edmonton, AB, Canada*

Md Gulam Musawwir Khan • *Radiobiology and Health, Canadian Nuclear Laboratories, ON, Canada*

Zohreh Kianfard • *Molecular Science Program, Yeates School of Graduate Studies, Toronto Metropolitan University (formerly Ryerson University), Toronto, ON, Canada*

Hamid Maadi • *Department of Oncology, Cross Cancer Institute, University of Alberta, Edmonton, AB, Canada*

Sirasie P. Magalage • *Molecular Science Program, Yeates School of Graduate Studies, Toronto Metropolitan University (formerly Ryerson University), Toronto, ON, Canada*

Stephany C. Paiva • *Telomeres Laboratory, Department of Chemical and Biological Sciences, Biosciences Institute, São Paulo State University (UNESP), Botucatu, SP, Brazil*

Daniel Rappaport • *Molecular Science Program, Yeates School of Graduate Studies, Toronto Metropolitan University (formerly Ryerson University), Toronto, ON, Canada*

Aja M. Rieger • *Department of Medical Microbiology and Immunology, University of Alberta, Edmonton, AB, Canada*

Sarah A. Sabatinos • *Molecular Science Program, Yeates School of Graduate Studies, Toronto Metropolitan University (formerly Ryerson University), Toronto, ON, Canada; Department of Chemistry and Biology, Toronto Metropolitan University (formerly Ryerson University), Toronto, ON, Canada*

Mark E. Shiburah • *Telomeres Laboratory, Department of Chemical and Biological Sciences, Biosciences Institute, São Paulo State University (UNESP), Botucatu, SP, Brazil*

Mohammad Hasan Soheilifar • *Department of Medical Laser, Medical Laser Research Center, Yara Institute, ACECR, Tehran, Iran*

Sargun Sokhi • *Department of Oncology, University of Alberta, Edmonton, AB, Canada; Cancer Research Institute of Northern Alberta, University of Alberta, Edmonton, AB, Canada*

David T. Stuart • *Department of Biochemistry, University of Alberta, Edmonton, AB, Canada*

Omar D. Subedar • *Department of Chemical Engineering, Ryerson University, Toronto, ON, Canada; Li Ka Shing Knowledge Institute, St. Michael's Hospital, Toronto, ON, Canada*

Xiaoyun Tang • *Department of Biochemistry, Cancer Research Institute of Northern Alberta, University of Alberta, Edmonton, AB, Canada*

Michael D. Urbaniak • *Division of Biomedical and Life Sciences, Faculty of Health and Medicine, Lancaster University, Lancaster, UK*

Stephen D. Waldman • *Department of Chemical Engineering, Ryerson University, Toronto, ON, Canada; Li Ka Shing Knowledge Institute, St. Michael's Hospital, Toronto, ON, Canada*

Richard C. Wang • *Johns Hopkins School of Medicine, Baltimore, MD, USA*

Yi Wang • *Radiobiology and Health, Canadian Nuclear Laboratories, ON, Canada; Department of Biochemistry, Microbiology and Immunology, University of Ottawa, Ottawa, ON, Canada*

Zhixiang Wang • *Department of Medical Genetics, University of Alberta, Edmonton, AB, Canada*

PING WEE • *Department of Medical Genetics, University of Alberta, Edmonton, AB, Canada*
JIHANG YU • *Radiobiology and Health, Canadian Nuclear Laboratories, Chalk River, ON, Canada*

Part I

Introduction and Review

Chapter 1

Cell Cycle Progression and Synchronization: An Overview

Zhixiang Wang

Abstract

The cell cycle is the series of events that take place in a cell that drives it to divide and produce two new daughter cells. Through more than 100 years of efforts by scientists, we now have a much clearer picture of cell cycle progression and its regulation. The typical cell cycle in eukaryotes is composed of the G1, S, G2, and M phases. The M phase is further divided into prophase, prometaphase, metaphase, anaphase, telophase, and cytokinesis. Cell cycle progression is mediated by cyclin-dependent kinases (Cdks) and their regulatory cyclin subunits. However, the driving force of cell cycle progression is growth factor-initiated signaling pathways that controls the activity of various Cdk-cyclin complexes. Most cellular events, including DNA duplication, gene transcription, protein translation, and post-translational modification of proteins, occur in a cell-cycle-dependent manner. To understand these cellular events and their underlying molecular mechanisms, it is desirable to have a population of cells that are traversing the cell cycle synchronously. This can be achieved through a process called cell synchronization. Many methods have been developed to synchronize cells to the various phases of the cell cycle. These methods could be classified into two groups: synchronization methods using chemical inhibitors and synchronization methods without using chemical inhibitors. All these methods have their own merits and shortcomings.

Key words Cell cycle, G1 phase, S phase, G2 phase, M phase, Synchronization, Cdks

1 Introduction

Cell theory was developed in the middle of the nineteenth century, marking the start of the cell cycle research [1–3]. By the turn of the twentieth century, the cell cycle had become a subject of intense study. Microscopists and embryologists became able to describe the cytology of cell division in great detail; however, the underlying mechanisms driving cell division were still mostly unknown. In the late 1970s and 1980s, the advancement of modern molecular biology provided the means and knowledge to study the molecular mechanisms regulating the cell cycle. Cell biologists, biochemists, and geneticists joined forces and demonstrated that the basic processes and control mechanisms of the cell cycle were universal among eukaryotes.

Zhixiang Wang (ed.), *Cell-Cycle Synchronization: Methods and Protocols*, Methods in Molecular Biology, vol. 2579,
https://doi.org/10.1007/978-1-0716-2736-5_1,

Through more than 100 years of efforts by scientists, we now have a much clearer picture of cell cycle progression and its regulation. The cell cycle, or the cell division cycle, is the series of events in a cell that drives it to divide and produce two new daughter cells. The typical cell cycle in eukaryotes is composed of four phases: G1, S, G2, and M. G1, S, and G2 are collectively called interphase. The M phase is comprised of mitosis, during which the cell's nucleus divides, and cytokinesis, during which the cell's cytoplasm divides to form two daughter cells. Mitosis and cytokinesis are tightly coupled together. Mitosis is further divided into 5 sub-phases: prophase, prometaphase, metaphase, anaphase, and telophase (Fig. 1). Each phase of cell cycle progression relies on the proper completion of the previous cell cycle phase. A cell can also exit from the cell cycle to enter the G0 phase, a state of quiescence [4, 5].

Cell cycle progression is mediated by cyclin-dependent kinases (Cdks) and their regulatory cyclin subunits. Cdks, such as Cdk4/6, Cdk2, and Cdk1, are serine/threonine kinases with a wide variety of substrates. Cdks are activated mainly by binding to their cyclin partners, which expressions rise and fall throughout the cell cycle to mediate the temporal activation of each Cdk. Various cell cycle checkpoints exist to ensure that critical processes are engaged prior to progression to the next phase. There are three major cell cycle checkpoints: the G1/S checkpoint (also referred as the restriction point), the G2/M DNA damage checkpoint, and the spindle assembly checkpoint (SAC) [6–8]. Growth factors (GFs) also play an important role in the regulation of the cell cycle. GFs are a group of proteins that stimulate the growth of specific tissues. Each GF binds to a specific cell-surface receptor, initiating an intracellular signaling pathway that drives cell division and proliferation. One specific group of GF receptors that possess tyrosine kinase activity, termed receptor tyrosine kinases (RTKs), are particularly important in cell cycle regulation. GFs drive the cell cycle by activating RTKs and downstream signaling pathways, which in turn regulate Cyclin-Cdk complexes [9, 10].

When studying the cell cycle, it is desirable to have a population of cells that are traversing the cell cycle synchronously, as it allows population-wide data to be collected rather than relying solely on single-cell experiments [4]. This is achieved through a process called cell synchronization, where a population of cultured cells at different phases of the cell cycle are brought to the same phase. Through the years, many protocols have been developed to synchronize cells to each cell cycle phase with specificity and efficiency [11–14].

In this review, we will provide a brief overview of historically important findings in cell cycle research, describe the process of cell cycle progression through various cell cycle phases, and discuss commonly used methods in cell cycle synchronization.

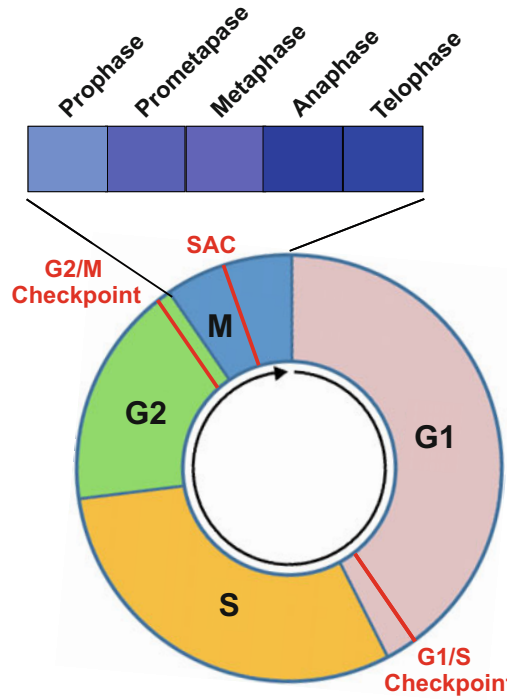

Fig. 1 Diagram to illustrate a complete cell cycle progression through four cell cycle phases (G1, S, G2, and M) and three major checkpoints (G1/S, G2/M, and SAC). M phase is further divided into Prophase, Prometaphase, Metaphase, Anaphase, and Telophase

2 Early History of Cell Cycle Discovery

Cell theory was developed in the middle of the nineteenth century. This theory had three main principles: (1) Every living organism is composed of one or more cells; (2) cells are the basic unit of life for all living organisms; and (3) cells only arise from pre-existing cells. The first two principles were contributed by German physician and physiologist Theodor Schwann and German botanist Matthias Jakob Schleiden, while the third principle was contributed by German scientist and physician Rudolf Virchow. Importantly, Virchow's discovery that all cells arise from pre-existing cells marks the beginning of cell cycle research [1–3] (Fig. 2).

In the late nineteenth century, early light microscopic studies showed that cell division followed mitosis. Through his observations of cell division, German biologist and founder of cytogenetics Walther Flemming was able to observe and describe the sequence of chromosome movements in mitosis. Flemming's discovery was proved correct decades later by the study of live dividing cells [15], which further showed that mitosis could be broken down into distinct morphological stages. However, the only observable

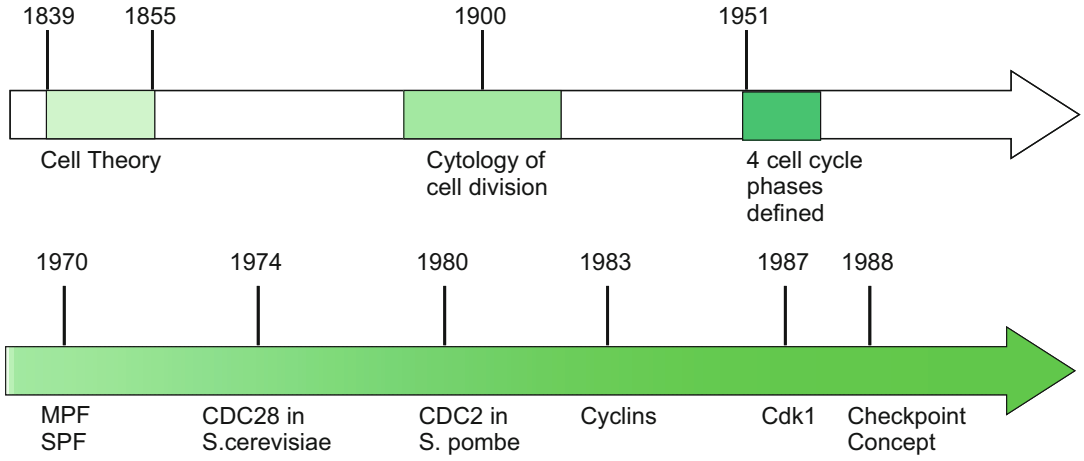

Fig. 2 Timeline of major discoveries in the early cell cycle research

morphological change outside of mitosis was the growth of the cell size. Interphase remained a black box and was initially recognized as only one phase. This changed with the discovery that DNA synthesis occurred during only a short period within the interphase [16]. This discovery splits the interphase into three phases: the first gap period between the formation of the cell and DNA synthesis, termed the Gap 1 or G1 phase; the period of DNA synthesis, termed the S phase; and the second gap period between DNA synthesis and mitosis, termed the Gap 2 or G2 phase.

Following the recognition of the four major cell cycle states, namely G1, S, G2, and M, the focus of cell cycle research shifted to understanding the transitions between these phases. A major task was identifying the factors driving these transitions. One such discovery was made in the early 1970s through the fusion of cells at different stages of the cell cycle. It was shown that G1 phase cells contained an S phase-promoting factor (SPF) that helped induce the onset of the S phase, while cells in the late G2 phase contained an M phase-promoting factor (MPF) that helped induce the onset of mitosis [17, 18].

There emerged a growing interest in purifying SPF and MPF for further study. Unfortunately, no biochemical method existed at the time that could accomplish this. Genetic approaches, however, were more fruitful. At the end of the 1960s, Leland Hartwell discovered the possibility of using genetic methods to study the cell cycle. He accomplished this through his experiments on *Saccharomyces cerevisiae*, a budding yeast that acted as a highly suitable model system for cell cycle research. In an elegant series of experiments in 1970–71, he used the temperature-sensitive lethal mutants of *S. cerevisiae* to isolate yeast cells that contained mutated variants of the genes responsible for cell cycle progression. This approach allowed him to successfully identify more than 100 genes

involved in cell cycle control, including those encoding SPF and MPF. Hartwell named these genes -Cdc-genes (cell division cycle genes) [19–21]. One particularly important cdc gene he identified was Cdc28, which controlled the first step of cell cycle progression in the G1 phase and was also known as "start".

In the middle of the 1970s, Paul Nurse followed Hartwell's approach of studying cell cycle regulation through genetic methods, this time using the fission yeast *Schizosaccharomyces pombe* as his model system. Through his research, Nurse discovered the gene Cdc2 in fission yeast, which functioned identically to the Cdc28 gene in budding yeast. He further found that Cdc2 played a key role in regulating the transition from the G2 phase to mitosis [22]. In 1987, Nurse isolated the mammalian version of the Cdc28 and Cdc2 gene, which he called Cdk1 due to it encoding a cyclin-dependent kinase (Cdk) protein. He found that the phosphorylation status of its catalytic subunit, p34cdk1, was closely related to cell cycle progression. When cells were stimulated to enter the G1 phase of the cycle, p34cdk1 is phosphorylated. The timing of the phosphorylation is right before the DNA synthesis in the S phase [23, 24]. Since then, half a dozen more Cdk proteins have been found in humans with similar roles in cell cycle regulation. It appears that what is accomplished by one protein (the product of Cdc28 or Cdc2) in yeast is actually accomplished by a group of proteins (Cdks) in mammalian cells.

In the early 1980s, Tim Hunt discovered the first cyclin molecule through his study of the sea urchin genus Arbacia. During embryological development, sea urchins undergo eight very rapid cell divisions; to sustain these cell divisions, continual protein synthesis is required. Hunt found that one specific protein was always destroyed each time the cells divided. He named this protein cyclin because he found that the intracellular level of this protein varied periodically during the cell cycle [25]. In the following years, more cyclins were identified in various species by Hunt and other groups. It was later shown that cyclins help control the progression of the cell cycle by binding to Cdk molecules, regulating their activity, and determining their substrate specificity [26]. It is now well understood that the eukaryotic cell cycle is controlled by the Cdk-Cyclin complex. In lower organisms, only one Cdk (Cdk1 or Cdc2) controls cell-cycle progression. However, in mammals, different Cdk-Cyclin complexes drive the cell cycle through sequential activation. In mammalian cells, progression through the G1 phase is driven by Cdk4/Cdk6-Cyclin D activation. The transition from the G1 to the S phase is regulated by the Cdk2-Cyclin E complex. Progression through S and G2 phases is controlled by Cdk2-Cyclin A complex. Finally, the entry into the M phase is driven by the formation and activation of Cdk1-Cyclin A/B complexes [27] (Fig. 3).

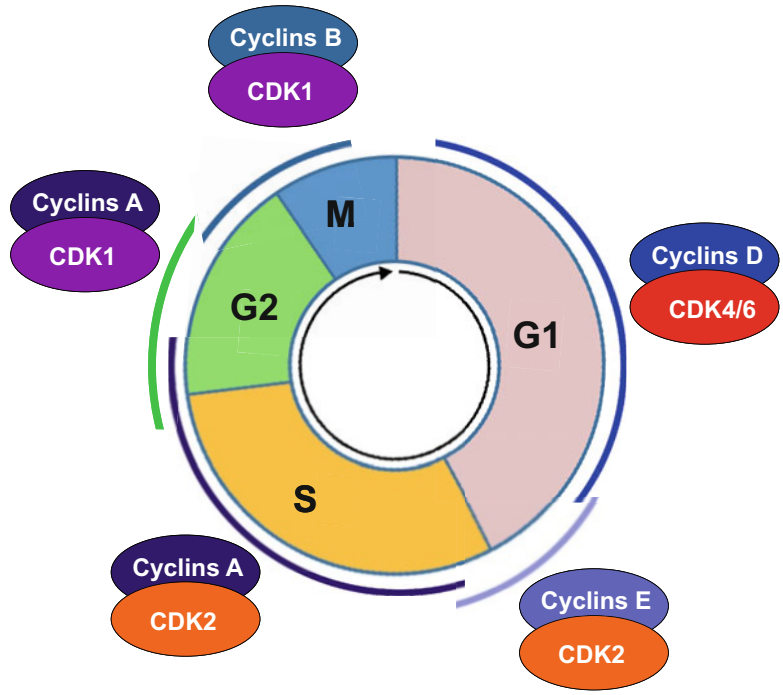

Fig. 3 Regulation of cell cycle progression by Cdks and Cyclins

Another important concept introduced during this period was the checkpoint. This concept was developed by Hartwell in the late 1980s after studying the sensitivity of yeast cells to irradiation [28, 29]. He observed that the cell cycle would be arrested at certain points after enough DNA damage took place; these points were referred to as checkpoints. Checkpoints would later be described as a surveillance mechanism used by cells to check the integrity and fidelity of the major events of the cell cycle. Examples of these major events include cell size growth, DNA replication and integrity, and accurate chromosome segregation [6].

The historical contributions of Leland H. Hartwell, Paul M. Nurse, and R. Timothy (Tim) Hunt earned them the 2001 Nobel Prize in Physiology or Medicine for their discovery of "key regulators of the cell cycle."

3 Cell Cycle Progression Through Various Phases

The cell cycle consists of the G1, S, G2, and M phases. In the G1 phase, the cell grows and becomes larger. The cell enters the S phase when it reaches a certain size. The S phase is the period during which DNA synthesis occurs, which is achieved through DNA replication. In the following G2 phase, the cell assesses for the proper completion of DNA replication and prepares for mitosis.

Chromosome segregation and cell division are completed in the M phase. The proper cell cycle progression from G1 to M ensures that each of the two daughter cells receives identical chromosomes from the parent cell. After cell division, the cell cycle is completed, and the new daughter cells are back in the G1 phase. Cells in the G1 phase can exit from the cell cycle and enter the G0 phase, a state of quiescence. The duration of cell cycle phases varies between 10 and 30 h in most mammalian cells, depending on the cell type. For a typical proliferating human cell, if we assume the total cycle time is 24 h, the duration of the G1, S, G2, and M phases are approximately 11, 8, 4, and 1 h, respectively. Cell cycle progression is mainly driven and regulated by two classes of proteins: Cdks and cyclins [30] (Fig. 3). Cdks are kinases that phosphorylate substrates within cells; however, they are inactive by themselves. Cyclins activate Cdks by binding to them to form cyclin-Cdk complexes. Cyclins also confer substrate specificity to the Cdk, thereby determining which substrates the Cdk phosphorylates. Thus, depending on the phase of the cell cycle, certain cyclins will bind to certain Cdks and drive them to phosphorylate substrates in a way that is appropriate for the given cell cycle phase. This phosphorylation can have varying effects on the substrate, including activation, inactivation, and localization. This hypothesis represents the classical model of cell-cycle regulation, and it has been established through extensive research in numerous eukaryotic organisms.

According to this model, Cdk4 and/or Cdk6 form complexes with D-type cyclins, which activate Cdk4/6 and initiate phosphorylation of the retinoblastoma protein (Rb) family in the early G1 phase [31, 32]. Rb phosphorylation stimulates the release of the transcription factor E2F, which in turn stimulates the transcription of early E2F-responsive genes required for the progression of the cell cycle [33, 34]. Early E2F-responsive genes include A- and E-type cyclins [31, 35]. In the late G1 phase, cyclin E binds to and activates Cdk2, which leads to full Rb phosphorylation and the further activation of E2F-mediated transcription [31, 32]. Together, the above events drive the passage of the cell through the restriction point at the boundary of the G1/S phase and initiate the S phase. At the onset of the S phase, A-type cyclins are synthesized and form complex with Cdk2, which phosphorylates proteins involved in DNA replication and drive the cell progression to the G2 phase [36, 37]. Cyclin A also associates with Cdk1 from the late S phase to the late G2 phase, which is involved in the activation and stabilization of the cyclin B/Cdk1 complex. Cyclin B/Cdk1 activity steadily increases in the G2 phase and peaks in the late G2 phase, driving the transition of the cell cycle from the G2 to the M phase. The Cyclin B/Cdk1 complex activity remains high in the early M phase and decreases in the late M phase, driving the completion of mitosis [38] (Fig. 3).

3.1 G1 Phase

Cells enter G1 from either the preceding M phase or from the G0 phase. The transition of cells between the G0 and G1 phase is determined by extracellular mitogenic signals [39, 40]. The G1 phase is the growth phase. While the biosynthetic activities of the cell are slowed down considerably in the M phase, they are resumed at a high rate in the G1 phase. These activities include synthesizing many proteins, amplifying organelles like ribosomes and mitochondria, and increasing cell size.

During the G1 phase, diverse signals including environmental cues, stress, and metabolic cues intervene to influence the cell's developmental program. These signals are integrated and interpreted by the cells. Based on these inputs, the cell decides whether to self-renew, differentiate, or die. To enter the S phase to begin self-renewal, all cells must fulfill one essential requirement: Cdk activation [40, 41].

3.2 S Phase

The S phase is characterized by DNA synthesis. In the S phase, the amount of DNA in each chromosome is doubled, resulting in a chromosome consisting of two identical sister chromatids. The S phase is also characterized by low levels of gene expression and protein synthesis. One notable exception is histone production, as most histones are produced in the S phase [42].

It is suggested that an intra-S phase checkpoint exists to control S phase progression. This intra-S phase checkpoint turns off Cdk2 in response to DNA damage and other replication stress, which blocks origin firing and therefore avoids replication of damaged DNA [43]. The S phase to the G2 phase transition is regulated by the active checkpoint kinase ATR (ataxia-telangiectasia and Rad3-related) [44].

3.3 G2 Phase

The G2 phase begins after the successful completion of the S phase and ends with the onset of mitosis. The major task for cells in G2 is to prepare themselves for mitosis. Consequently, the G2 phase is marked by significant protein/lipid synthesis and cell growth [45]. Protein synthesis inhibitors arrest cells at the G2 phase; however, a recent study suggests that this may be due to the inhibition of p38, and that protein synthesis is not absolutely required for mitosis entry [46]. It is also hypothesized that cell size controls the growth in the G2 phase, however, this is only demonstrated in fission yeast [47]. Another process that occurs during the G2 phase is DNA DSBs repair. During and after DNA replication, DNA double-strand breaks accumulate in the cell and need to be repaired before cell can move to pass the G2/M checkpoint [28, 48, 49].

Interestingly, some cell types, including certain cancer cells and Xenopus embryos, lack a G2 phase. In these cells, the cell cycle proceeds directly from the S phase to the M phase.

3.4 Mitosis and Cytokinesis

The M phase is comprised of mitosis, during which the cell's nucleus divides, and cytokinesis, during which the cell's cytoplasm divides to form two daughter cells. Mitosis is further divided into prophase, prometaphase, metaphase, anaphase, and telophase (Fig. 1). Prophase is characterized by chromatin/chromosome condensation, centrosome separation, and nuclear membrane breakdown. The migration of the centrosomes to two opposite poles is important for the formation of the bipolar mitotic spindle apparatus. Importantly, chromosome morphology changes dramatically in prophase. A recent detailed study showed that the interphase organization of chromosomes is rapidly lost in prophase in a condensin-dependent manner [50]. In early prophase, chromosomes become recognizable under a microscope as linearly organized structures [51]. Each sister chromatid can be seen as an array of loops radiating from an axial core that contains topoisomerase II alpha and condensin complexes [52]. The rise of cyclin B-Cdk1 activity is a defining molecular event of prophase [53].

The next phase is prometaphase, during which mitotic spindle microtubules attach to the kinetochores (disk-shaped protein structures) at the centromere of each chromosome [54]. The chromatids additionally shorten and become thicker to form fully condensed chromosomes.

During metaphase, the chromosomes are pulled back and forth by the kinetochore microtubules until they align along the metaphase plate at the cell equator. Achieving this configuration is key for faithful chromosome segregation. Here, the SAC checkpoint confirms whether the chromosomes are properly aligned at the metaphase plate, and if all kinetochores are attached to microtubules at opposite polls. If the checkpoint fails, mitosis halts.

If the cell passes the SAC checkpoint, it enters anaphase. The cohesion between the sister chromatids is dissolved, and the microtubules begin to pull the chromatids to the opposite poles. This involves two mechanistically distinct steps: anaphase A and anaphase B [55]. In anaphase A, the kinetochore microtubules shorten and cause the migration of each sister chromatid toward its respective pole. In anaphase B, the disjointed sister chromatids are further separated through elongation of the mitotic spindle in the midzone. These two steps are temporally separated in some organisms, while occur simultaneously in other organisms. In human mitotic cells, anaphase B usually starts 30–50s after the start of the anaphase A [56, 57].

The final stage of mitosis is telophase. The separated chromatids (now referred to as chromosomes) de-condense [55]. At the same time, nuclear membranes form around the separated chromosomes to divide the nuclear DNA from the cytoplasm [58].

Cytokinesis results in the physical separation of the cytoplasm of the parent cell into two daughter cells [59, 60]. The segregation of chromosomes and cytoplasm needs to be tightly coordinated to

generate offspring with the right complement of chromosomes [61]. Cell cytokinesis is initiated in anaphase, when lower Cdk1 activity causes the reorganization of the mitotic spindle and the stabilization of microtubules. The assembly of the central spindle is the key early event, which provides the template for the midbody and contributes to division plane specification. The division plane is positioned between the two sets of segregated chromosomes; the precise position of the plane is critical to prevent segregation errors. Cytokinetic furrow ingression of the attached plasma membrane is then initiated by the contraction of the actomyosin ring, which partitions the cytoplasm into two domains of emerging daughter cells. The last step of cytokinesis is abscission [62]. Abscission is the physical separation of the plasma membrane of the two daughter cells. During abscission, cells remove the cytoskeletal structures from the intercellular bridge, which is followed by constriction of the cell cortex and finally the division of the plasma membrane [63, 64].

4 Cell Cycle Synchronization

Most cellular events, including DNA duplication, gene transcription, protein translation, and post-translational modification of proteins, occur in a cell-cycle-dependent manner. To understand these cellular events and the underlying molecular mechanisms, it is desirable to have a population of cells that are traversing the cell cycle synchronously. This can be achieved through a process called cell synchronization, during which cultured cells at different stages of the cell cycle are brought to the same phase. Cell synchronization is a vital process in the study of cell cycle progression and regulation that allows population-wide data to be collected rather than relying solely on single-cell experiments [11–14].

Many methods have been developed to synchronize cells to the various phases of the cell cycle. These methods can be classified into two groups: synchronization methods using chemical inhibitors and synchronization methods without using chemical inhibitors. All these methods have their own merit and shortcomings, which are summarized in Fig. 4 and will be discussed in this section.

4.1 Cell Synchronization Without Using Chemical Inhibitors

Various methods have been developed for the purpose of synchronizing cells to specific cell cycle phases without using chemical inhibitors. In general, the advantage of these methods is that they avoid the side effects imposed by chemical inhibitors. However, they tend to have lower yield and less specificity.

4.1.1 Serum Starvation

It is well established that a cell will exit the cell cycle to enter the G0 phase in the absence of growth factors [4, 65]. Thus, serum deprivation will arrest and synchronize cells in the G0 phase. The

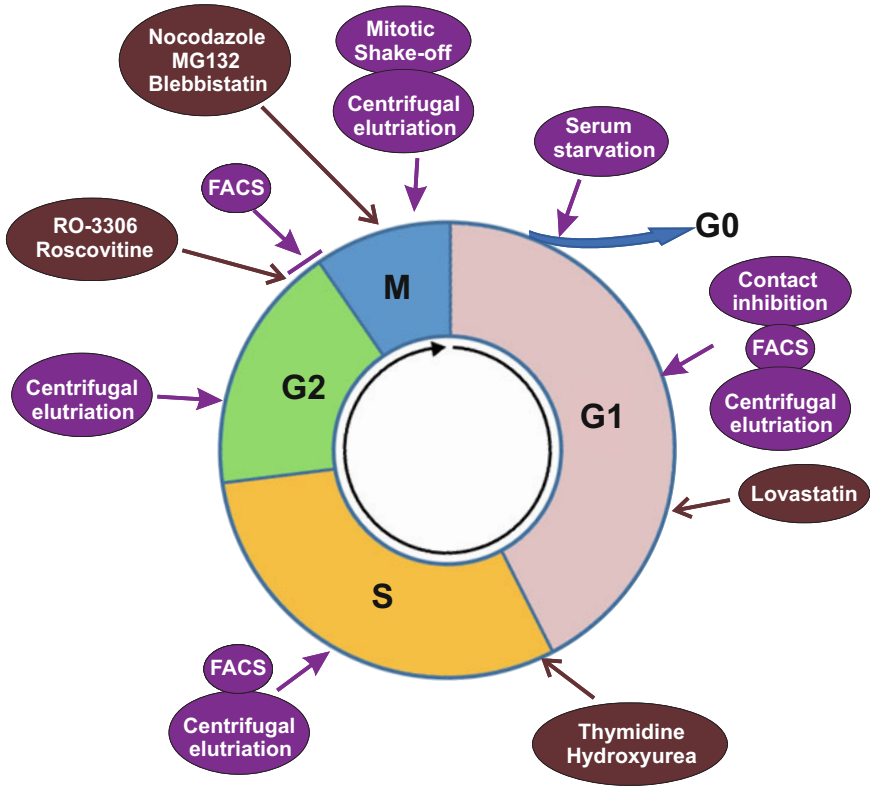

Fig. 4 Overview of the cell cycle phases and some synchronization methods. Cell synchronization methods without using chemical inhibitors are labeled purple. Cell synchronization by using chemical inhibitors labeled brown

re-addition of serum or growth factors will ideally cause the cells to return to the G1 phase and resume cell cycle progression together [11].

The effectiveness of this method is mostly dependent on the sensitivity of cells to serum withdrawal. This method is suitable for cultured normal cells but less so for transformed cells, as some transformed cells are able to continue the cell cycle in the absence of growth factor stimulation. It should also be noted that after the re-addition of serum, not all cells will return to the G1 phase. Thus, synchronization by serum starvation is highly dependent on the cell type [11, 66].

4.1.2 *Contact Inhibition*

When normal cells in culture reach a high density or full confluence, the amount of cell-to-cell contact is maximized. This triggers the arrest of the cell cycle in the early G1 phase for up to weeks at a time. This arrest is mediated by p27, a Cdk2 inhibitor [67, 68]. When the culture is split and replated at a lower density, the cells resume the cell cycle [11, 69]. Arrest by contact inhibition resembles quiescence; however, the former can occur in the

presence of growth stimulation, and arrest is in the early G1 phase as opposed to the G0 phase. Contact inhibition is likely the most important and physiologically relevant type of cell cycle arrest, as division of most cells in an organism is suppressed by contact inhibition.

However, not all cells display contact inhibition. There are two important physiological examples of this. Firstly, cancer cells frequently lack contact inhibition [69, 70]. Secondly, wounds can remove contact inhibition, with cells in the wounded area resuming the cell cycle to proliferate and fill the wound. Thus, when studying cancer cells or cells in wound repair, contact inhibition together with serum withdrawal may significantly improve the synchronization of these cells to the early G1 phase [11].

4.1.3 Mitotic Shake-off

Mitotic shake-off is a nondisruptive method of isolating mitotic cells [11, 71–74]. Cells round during mitosis and become only loosely attached to the plate, allowing them to be easily detached from the plate by shaking. Therefore, in a population of cells at different cell cycle phases, mitotic cells can be isolated from interphase cells by shaking the plate. The detached mitotic cells in the medium can then be collected by centrifugation.

One disadvantage of this method is that the mitotic period constitutes approximately 5 percent of the cell cycle, which means that only 5% of the asynchronized cell population is in mitosis at any given time. Consequently, the yield of mitotic cells will be very low, and it is often insufficient for many types of experiments. One way to increase the yield is to combine the shake-off protocol with serum deprivation. Following the re-addition of serum to serum-deprived cells, the cells will resume the cell cycle in a partially synchronized fashion. Thus, a higher proportion of cells will enter mitosis, and performing the mitotic shake will significantly increase the yield of mitotic cells [74].

4.1.4 Flow Cytometry and Cell Sorting After DNA Staining

Flow cytometry is a key technique in cell sorting. In flow cytometry, cells suspended in a fluid are injected into the flow cytometer instrument one cell at a time through a laser beam, and the resulting light scatter is measured by a detector. Each cell will have a unique light scatter depending on the physical and chemical properties of the cells, allowing for sorting. This technique can be used in combination with fluorescence-activated cell sorting (FACS), where cells are also tagged with fluorescent antibodies. Through FACS, a population of cells can be sorted by flow cytometry based on differences in light scatter (i.e., cell size) and/or fluorescence emission (i.e., DNA content).

FACS can be used to reliably sort out cells in the G1 phase based on cell size, as G1 cells are relatively small and roughly half the size of G2/M phase cells. Thus, FACS offers a fast, inexpensive, and nonhazardous method for synchronizing proliferating

mammalian cells to G1 [75]. However, it can only reliably sort out G1 phase cells, and the yield is often low [14].

FACS can also be used to sort out of cells in the G1, S, and G2/M phases based on DNA content. In this procedure, the most common fluorescent dye used to label cells is Hoechst 33342 due to its low side effect profile on living cells [76]. The biggest advantage of this method is that it can isolate cells synchronized in the G1, S, and G2/M phases from only a single sample. The downsides are that the fluorescent DNA dye affects cell metabolism and that the yield is often low [14].

4.1.5 Centrifugal Elutriation

Centrifugal elutriation is a most commonly used non-chemical method to synchronize cells to each phase of cell cycle [11, 77, 78]. In theory, cells in each phase of the cell cycle can be isolated based on size by centrifugal elutriation. For example, cells in the late G2 or M phase are twice as big as cells in the early G1 phase. The size of S phase cells is in between. The method of centrifugal elutriation consists of a specially designed centrifuge rotor in which the centrifugal force on the cell population is countered by medium flowing in the opposite direction.

Centrifugal elutriation offers significant biological advantages compared with other methods of cell-cycle synchronization. First, centrifugal elutriation can be used to synchronize almost all types of cells to each specific cell cycle phase, including both adherent and suspension cells, as well as both mammalian cells and unicellular model organisms. It has been used to isolate the following cells and unicellular organisms: Rat1 fibroblasts [79], primary diploid fibroblasts [79, 80], NOSE-1 epithelial cells [81], Swiss 3T3 cells [80, 81], NB41A3 neuroblastoma cells [82, 83], Jurkat leukemia cells [84], HT-29 adenocarcinoma cells [85], HeLa, U2OS, 293, Manca (B-cell lymphoma), Raji [86], fission yeast *Schizosaccharomyces pombe* [87, 88], budding yeast *Saccharomyces cerevisiae* [89], protozoan parasite *Giardia intestinalis* [90], parasitic kinetoplastid *Trypanosoma brucei* [91], and unicellular eukaryote *Tetrahymena thermophila* [78]. Second, this method causes the least amount of stress to cells. It does not require maintaining cells in stress-inducing environments, such as low-serum or high-density conditions. Third, centrifugal elutriation can yield a large population of phase-specific cells in a very rapid manner. Finally, centrifugal elutriation is highly reproducible. Once the parameters are established for a given cell type and cell-cycle position, it offers consistent results [11, 78].

Despite these advantages, centrifugal elutriation also has some drawbacks. Centrifugal elutriation setup requires expensive and specially designated equipment. It also requires preliminary experiments to determine the right parameters for different cell types. Moreover, adherent cells need to be released from the plate surface, which may cause some stress to the cells [14].

4.2 Cell Synchronization by Using Chemical Inhibitors

Cell synchronization through chemical inhibitors is a major approach used by many researchers. Each cell cycle phase has its own protein expression profile and regulation mechanisms, and through this different chemical inhibitors have been identified that can target each phase. Lovastatin, a reversible competitive inhibitor of 3-hydroxy-3-methylglutaryl-coenzyme A reductase, is a commonly used chemical inhibitor for the synchronization of cells to G1. Various DNA synthesis inhibitors, including thymidine and hydroxyurea, are widely used for synchronizing cells to the early S phase. CDK inhibitors, including RO-3306 and roscovitine, have been used to synchronize cells to the G2 phase. And microtubule inhibitors like nocodazole are frequently used to synchronize cells to prometaphase.

4.2.1 Synchronization of Cell Cycle to G1 Phase by Lovastatin

Synchronization by lovastatin efficiently arrests many cell types reversibly in the G1 phase of the cell cycle, especially some cancer cells like MCF-7 and MDA-MB-231 [92, 93]. Lovastatin is a reversible competitive inhibitor of 3-hydroxy-3-methylglutaryl-coenzyme A reductase, an enzyme that is vital in the production of mevalonic acid and later cholesterol. However, it is unclear how lovastatin induces G1 arrest. It appears that lovastatin inhibits the formation of an early intermediate in the pathway that is essential for progression through early G1 [92]. Lovastatin treatment also increases protein and mRNA levels of the cyclin-dependent kinase inhibitor p21WAF1/CIP1, increases the binding of p21 with Cdk2 [94], and decreases the activity of cyclin-dependent kinase 1 [14]. The downside of lovastatin use is that it may induce cell apoptosis, and it is not clear at which specific stage of G1 the cells are arrested.

4.2.2 Synchronization of Cell Cycle to Early S Phase by Double Thymidine Block

Thymidine is a DNA synthesis inhibitor that can arrest cells at the G1/S boundary, prior to DNA replication. When high concentrations of thymidine are added to the culture fluid, the excess thymidine blocks the enzyme ribonucleotide reductase, which is responsible for converting ribonucleotides into deoxyribonucleotides. As a result, the supply of deoxyribonucleotides falls and DNA synthesis stops [95, 96]. However, this thymidine block will arrest cells in the different stages of S phases immediately, resulting in a cell population at different stages of DNA duplication. A second thymidine block is needed to synchronize all the cells to the early stage of the S phase. The release of the first thymidine block will allow all the cells to resume DNA synthesis and progress out of the S phase. The second thymidine block then results in the synchronization of all cells to the early S phase when DNA duplication starts.

A double thymidine block is simple and cheap. It can be used for both adherent and suspended cell lines. However, it may induce replication stress and cause an imbalance in nucleotide pools [14].

While used less frequently, hydroxyurea is an alternative for synchronizing cells to the early S phase. Hydroxyurea inhibits production of dNTPs and subsequently DNA synthesis [97]. The inhibition can be easily reversed by washing, which makes it an ideal agent for cell synchronization.

4.2.3 Synchronization of Cell Cycle to G2 Phase by Inhibiting CDK1

CDK1 activity is essential for cell cycle progression from the G2 to M phase through the formation of the CDK1/cyclin B complex (also known as the maturation promoting factor) [4]. Inhibition of CDK1 activity can thus synchronize cells to the G2 phase. Two CDK1 inhibitors have been used for G2 phase synchronization: RO-3306 and Roscovitine.

RO-3306 is a reversible CDK1 inhibitor with high specificity for CDK1 vs. CDK2 (>10-fold). Treatment of cells with RO-3306 results in an effective late G2 phase arrest consistent with specific inhibition of CDK1 in the cellular context [98, 99]. In fact, the synchronization efficiency of cycling cells treated with 9 mM RO-3306 is over 95%. At the G2/M transition, CDK1/cyclin B levels are at their peak, and removing the inhibition of CDK1 should resume the cell cycle instantaneously. As a reversible CDK1 inhibitor, RO-3306 is thus an ideal agent for cell synchronization to the late G2 phase. However, several factors may influence the ability of RO-3306 to induce a clean G2 phase arrest, such as cell origin, compound concentration, and length of treatment. It should be noted that prolonged treatment can result in genome reduplication [98, 100].

Roscovitine inhibits CDKs by competing with ATP at the ATP binding sites of various CDKs, including CDK1, CDK2, CDK5, and CDK7. As a pan-CDK inhibitor, roscovitine can cause a reduction in retinoblastoma protein phosphorylation at multiple sites and cause cell cycle arrest in multiple different cell cycle phases [101]. Thus, to be used for G2 phase synchronization, roscovitine needs to be used together with another inhibitor. One established protocol is to first arrest the cells to the early S phase by hydroxyurea or a double thymidine block and allow them to progress into G2 before using roscovitine to arrest them in G2.

4.2.4 Synchronization of Cell Cycle to Mitosis by Nocodazole, MG132, and Blebbistatin

Mitosis involves a major reorganization of virtually all cell components and is the most dynamic and fragile period of the cell cycle. Indeed, mitosis is a frequent target for cancer therapy, and most cancer drugs are designed to specifically target mitotic cells [102]. The progression of the cell cycle through the mitotic subphases is tightly regulated by complicated molecular mechanisms. Synchronization of cells to the mitotic subphases is important for understanding these molecular mechanisms.

Nocodazole, a microtubule depolymerizing agent, is the most commonly used agent for inducing prometaphase arrest. It has a high affinity to tubulin, and it prevents tubulin-composed spindle microtubules from interacting properly with the kinetochores of chromosomes [103]. These chromosomes are therefore not brought to metaphase plate and cannot proceed past the spindle assembly checkpoint (SAC) [104]. Thus, nocodazole is an effective agent for arresting cells in early prometaphase. However, prolonged treatment can result in aneuploidy, cell death, or mitotic slippage [105].

MG132 is a potent, reversible, and cell-permeable proteasome inhibitor [106]. When used together with nocodazole, MG132 is able to arrest the cell cycle in metaphase [107]. The spindle assembly checkpoint (SAC) ensures that all chromosomes are properly aligned prior to commencing anaphase [108]. Upon satisfying the requirements of the SAC, the anaphase-promoting complex (APC) is turned on and initiates the proteasomal degradation of cyclin B and securin [109–111]. This proteasomal activity allows sister chromatids to separate and thus transitions the cell from metaphase to anaphase. To synchronize the cells to metaphase, the proteasome inhibitor MG132 is added to cells after the cells are released from the nocodazole-induced prometaphase inhibition. MG132 allows chromosomes to proceed past the SAC but prevents cells from proceeding into anaphase [107]. Chromosome and microtubule fluorescent staining have shown that MG132-treated oocytes are arrested at metaphase I. Intervention of proteasomal action with this inhibitor also results in an accumulation of cyclin B and elevated activity of CDK1 [112].

Blebbistatin is a specific inhibitor of nonmuscle myosin II that can help arrest cells in anaphase or telophase. Anaphase and telophase have traditionally been the most difficult phases to synchronize due to their short duration, and there are no known drugs that can completely block cells in anaphase or telophase. However, blebbistatin can be used to extend the duration of anaphase/telophase by inhibiting the ingression of the cleavage furrow, allowing easier synchronization. It has been shown that HeLa cells can be successfully synchronized to anaphase or telophase with blebbistatin in combination with nocodazole. In this procedure, cells are first arrested in the early S phase by a double thymidine block. After 9 h, the block is released, and the cells are treated with a low concentration of nocodazole for 5 h to synchronize the cells to prometaphase. The nocodazole block is then removed and 50 uM blebbistatin can be added after 20 or 50 min to synchronize the cells to anaphase or telophase, respectively [113].

References

1. Wolpert L (1995) Evolution of the cell theory. Philos Trans R Soc Lond Ser B Biol Sci 349(1329):227–233
2. Müller-Wille S (2010) Cell theory, specificity, and reproduction, 1837–1870. Stud Hist Phil Biol Biomed Sci 41(3):225–231
3. Ribatti D (2019) Rudolf Virchow, the founder of cellular pathology. Rom J Morphol Embryol = Revue Roumaine de Morphologie et Embryologie 60(4):1381–1382
4. Wang Z (2021) Regulation of cell cycle progression by growth factor-induced cell signaling. Cell 10(12):3327
5. Panagopoulos A, Altmeyer M (2021) The hammer and the dance of cell cycle control. Trends Biochem Sci 46(4):301–314
6. Barnum KJ, O'Connell MJ (2014) Cell cycle regulation by checkpoints. Methods Mol Biol 1170:29–40
7. Satyanarayana A, Kaldis P (2009) Mammalian cell-cycle regulation: several Cdks, numerous cyclins and diverse compensatory mechanisms. Oncogene 28(33):2925–2939
8. Gao X, Leone GW, Wang H (2020) Cyclin D-CDK4/6 functions in cancer. Adv Cancer Res 148:147–169
9. Jones SM, Kazlauskas A (2000) Connecting signaling and cell cycle progression in growth factor-stimulated cells. Oncogene 19(49): 5558–5567
10. Wee P, Wang Z (2017) Cell cycle synchronization of HeLa cells to assay EGFR pathway activation. *Methods Mol Biol* 1652:167–181
11. Davis PK, Ho A, Dowdy SF (2001) Biological methods for cell-cycle synchronization of mammalian cells. BioTechniques 30(6): 1322. -1326, 1328, 1330-1321
12. Cooper S (2003) Rethinking synchronization of mammalian cells for cell cycle analysis. Cell Mol Life Sci 60(6):1099–1106
13. Banfalvi G (2017) Overview of cell synchronization. *Methods Molecular Biol* 1524:3–27
14. Ligasová A, Koberna K (2021) Strengths and weaknesses of cell synchronization protocols based on inhibition of DNA synthesis. Int J Mol Sci 22(19):10759
15. Paweletz N (2001) Walther Flemming: pioneer of mitosis research. Nat Rev Mol Cell Biol 2(1):72–75
16. Howard A, Pelc SR (1951) Synthesis of nucleoprotein in bean root cells. Nature 167(4250):599–600
17. Rao PN, Johnson RT (1970) Mammalian cell fusion: studies on the regulation of DNA synthesis and mitosis. Nature 225(5228): 159–164
18. Johnson RT, Rao PN (1971) Nucleocytoplasmic interactions in the acheivement of nuclear synchrony in DNA synthesis and mitosis in multinucleate cells. Biol Rev Camb Philos Soc 46(1):97–155
19. Hartwell LH, Culotti J, Reid B (1970) Genetic control of the cell-division cycle in yeast. I. Detection of mutants. Proc Natl Acad Sci U S A 66(2):352–359
20. Hartwell LH, Culotti J, Pringle JR, Reid BJ (1974) Genetic control of the cell division cycle in yeast. Science 183(4120):46–51
21. Hartwell LH (1991) Twenty-five years of cell cycle genetics. Genetics 129(4):975–980
22. Nurse P, Thuriaux P (1980) Regulatory genes controlling mitosis in the fission yeast Schizosaccharomyces pombe. Genetics 96(3): 627–637
23. Lee MG, Nurse P (1987) Complementation used to clone a human homologue of the fission yeast cell cycle control gene cdc2. Nature 327(6117):31–35
24. Lee MG, Norbury CJ, Spurr NK, Nurse P (1988) Regulated expression and phosphorylation of a possible mammalian cell-cycle control protein. Nature 333(6174):676–679
25. Evans T, Rosenthal ET, Youngblom J, Distel D, Hunt T (1983) Cyclin: a protein specified by maternal mRNA in sea urchin eggs that is destroyed at each cleavage division. Cell 33(2):389–396
26. Pryor PR, Jackson L, Gray SR, Edeling MA, Thompson A, Sanderson CM, Evans PR, Owen DJ, Luzio JP (2008) Molecular basis for the sorting of the SNARE VAMP7 into endocytic clathrin-coated vesicles by the ArfGAP Hrb. Cell 134(5):817–827
27. Bashir T, Pagano M (2005) Cdk1: the dominant sibling of Cdk2. Nat Cell Biol 7(8): 779–781
28. Weinert TA, Hartwell LH (1988) The RAD9 gene controls the cell cycle response to DNA damage in Saccharomyces cerevisiae. *Science* 241(4863):317–322
29. Hartwell LH, Weinert TA (1989) Checkpoints: controls that ensure the order of cell cycle events. *Science* 246(4930):629–634
30. Morgan DO (1997) Cyclin-dependent kinases: engines, clocks, and microprocessors. Annu Rev Cell Dev Biol 13:261–291
31. Sherr CJ, Roberts JM (1999) CDK inhibitors: positive and negative regulators of G1-phase progression. Genes Dev 13(12):1501–1512

32. Sherr CJ, Roberts JM (2004) Living with or without cyclins and cyclin-dependent kinases. Genes Dev 18(22):2699–2711
33. Weinberg RA (1995) The retinoblastoma protein and cell cycle control. Cell 81(3): 323–330
34. Dyson N (1998) The regulation of E2F by pRB-family proteins. Genes Dev 12(15): 2245–2262
35. Lundberg AS, Weinberg RA (1998) Functional inactivation of the retinoblastoma protein requires sequential modification by at least two distinct cyclin-cdk complexes. Mol Cell Biol 18(2):753–761
36. Petersen BO, Lukas J, Sørensen CS, Bartek J, Helin K (1999) Phosphorylation of mammalian CDC6 by cyclin A/CDK2 regulates its subcellular localization. EMBO J 18(2): 396–410
37. Coverley D, Pelizon C, Trewick S, Laskey RA (2000) Chromatin-bound Cdc6 persists in S and G2 phases in human cells, while soluble Cdc6 is destroyed in a cyclin A-cdk2 dependent process. J Cell Sci 113(Pt 11): 1929–1938
38. Riabowol K, Draetta G, Brizuela L, Vandre D, Beach D (1989) The cdc2 kinase is a nuclear protein that is essential for mitosis in mammalian cells. Cell 57(3):393–401
39. Duan L, Raja SM, Chen G, Virmani S, Williams SH, Clubb RJ, Mukhopadhyay C, Rainey MA, Ying G, Dimri M et al (2011) Negative regulation of EGFR-Vav2 signaling axis by Cbl ubiquitin ligase controls EGF receptor-mediated epithelial cell adherens junction dynamics and cell migration. J Biol Chem 286(1):620–633
40. Limas JC, Cook JG (2019) Preparation for DNA replication: the key to a successful S phase. FEBS Lett 593(20):2853–2867
41. Massague J (2004) G1 cell-cycle control and cancer. Nature 432(7015):298–306
42. Nelson DM, Ye X, Hall C, Santos H, Ma T, Kao GD, Yen TJ, Harper JW, Adams PD (2002) Coupling of DNA synthesis and histone synthesis in S phase independent of cyclin/cdk2 activity. Mol Cell Biol 22(21): 7459–7472
43. Ciardo D, Goldar A, Marheineke K (2019) On the interplay of the DNA replication program and the intra-S phase checkpoint pathway. Genes 10(2):94
44. Saldivar JC, Hamperl S, Bocek MJ, Chung M, Bass TE, Cisneros-Soberanis F, Samejima K, Xie L, Paulson JR, Earnshaw WC et al (2018) An intrinsic S/G(2) checkpoint enforced by ATR. *Science* 361(6404):806–810
45. Hannen R, Selmansberger M, Hauswald M, Pagenstecher A, Nist A, Stiewe T, Acker T, Carl B, Nimsky C, Bartsch JW (2019) Comparative transcriptomic analysis of temozolomide resistant primary GBM stem-like cells and recurrent GBM identifies up-regulation of the carbonic anhydrase CA2 gene as resistance factor. Cancers 11(7):921
46. Lockhead S, Moskaleva A, Kamenz J, Chen Y, Kang M, Reddy AR, Santos SDM, Ferrell JE Jr (2020) The apparent requirement for protein synthesis during G2 phase is due to checkpoint activation. Cell Rep 32(2): 107901
47. Moseley JB, Mayeux A, Paoletti A, Nurse P (2009) A spatial gradient coordinates cell size and mitotic entry in fission yeast. Nature 459(7248):857–860
48. Burgoyne PS, Mahadevaiah SK, Turner JM (2007) The management of DNA double-strand breaks in mitotic G2, and in mammalian meiosis viewed from a mitotic G2 perspective. Bioessays 29(10):974–986
49. Zahnreich S, Weber B, Rösch G, Schindler D, Schmidberger H (2020) Compromised repair of radiation-induced DNA double-strand breaks in Fanconi anemia fibroblasts in G2. DNA Repair 96:102992
50. Gibcus JH, Samejima K, Goloborodko A, Samejima I, Naumova N, Nuebler J, Kanemaki MT, Xie L, Paulson JR, Earnshaw WC et al (2018) A pathway for mitotic chromosome formation. *Science* 359(6376): eaao6135
51. Liang Z, Zickler D, Prentiss M, Chang FS, Witz G, Maeshima K, Kleckner N (2015) Chromosomes progress to metaphase in multiple discrete steps via global compaction/expansion cycles. Cell 161(5):1124–1137
52. Samejima K, Samejima I, Vagnarelli P, Ogawa H, Vargiu G, Kelly DA, de Lima AF, Kerr A, Green LC, Hudson DF et al (2012) Mitotic chromosomes are compacted laterally by KIF4 and condensin and axially by topoisomerase IIα. J Cell Biol 199(5):755–770
53. Gavet O, Pines J (2010) Progressive activation of CyclinB1-Cdk1 coordinates entry to mitosis. Dev Cell 18(4):533–543
54. Santaguida S, Musacchio A (2009) The life and miracles of kinetochores. EMBO J 28(17):2511–2531
55. Vukušić K, Tolić IM (2021) Anaphase B: long-standing models meet new concepts. Semin Cell Dev Biol 117:127–139
56. Su KC, Barry Z, Schweizer N, Maiato H, Bathe M, Cheeseman IM (2016) A regulatory switch alters chromosome motions at the

metaphase-to-anaphase transition. Cell Rep 17(7):1728–1738

57. Vukušić K, Bua R, Tolić IM (2019) Force-generating mechanisms of anaphase in human cells. J Cell Sci 132(18):jcs231485
58. Afonso O, Matos I, Pereira AJ, Aguiar P, Lampson MA, Maiato H (2014) Feedback control of chromosome separation by a midzone Aurora B gradient. *Science* 345(6194): 332–336
59. Green RA, Paluch E, Oegema K (2012) Cytokinesis in animal cells. Annu Rev Cell Dev Biol 28:29–58
60. Fededa JP, Gerlich DW (2012) Molecular control of animal cell cytokinesis. Nat Cell Biol 14(5):440–447
61. Lens SMA, Medema RH (2019) Cytokinesis defects and cancer. Nat Rev Cancer 19(1): 32–45
62. Mierzwa B, Gerlich DW (2014) Cytokinetic abscission: molecular mechanisms and temporal control. Dev Cell 31(5):525–538
63. Gromley A, Yeaman C, Rosa J, Redick S, Chen CT, Mirabelle S, Guha M, Sillibourne J, Doxsey SJ (2005) Centriolin anchoring of exocyst and SNARE complexes at the midbody is required for secretory-vesicle-mediated abscission. Cell 123(1): 75–87
64. Schiel JA, Park K, Morphew MK, Reid E, Hoenger A, Prekeris R (2011) Endocytic membrane fusion and buckling-induced microtubule severing mediate cell abscission. J Cell Sci 124(Pt 9):1411–1424
65. Jones SM, Kazlauskas A (2001) Growth-factor-dependent mitogenesis requires two distinct phases of signalling. Nat Cell Biol 3(2):165–172
66. Murphy JS, D'Alisa R, Gershey EL, Landsberger FR (1978) Kinetics of desynchronization and distribution of generation times in synchronized cell populations. Proc Natl Acad Sci U S A 75(9):4404–4407
67. Polyak K, Kato JY, Solomon MJ, Sherr CJ, Massague J, Roberts JM, Koff A (1994) p27Kip1, a cyclin-Cdk inhibitor, links transforming growth factor-beta and contact inhibition to cell cycle arrest. Genes Dev 8(1): 9–22
68. Chen D, Walsh K, Wang J (2000) Regulation of cdk2 activity in endothelial cells that are inhibited from growth by cell contact. Arterioscler Thromb Vasc Biol 20(3):629–635
69. Leontieva OV, Demidenko ZN, Blagosklonny MV (2014) Contact inhibition and high cell density deactivate the mammalian target of rapamycin pathway, thus suppressing the senescence program. Proc Natl Acad Sci U S A 111(24):8832–8837
70. Abercrombie M (1979) Contact inhibition and malignancy. Nature 281(5729):259–262
71. Zwanenburg TS (1983) Standardized shake-off to synchronize cultured CHO cells. Mutat Res 120(2–3):151–159
72. Cao G, Liu LM, Cleary SF (1991) Modified method of mammalian cell synchronization improves yield and degree of synchronization. Exp Cell Res 193(2):405–410
73. Hulleman E, Bijvelt JJ, Verkleij AJ, Verrips CT, Boonstra J (1999) Integrin signaling at the M/G1 transition induces expression of cyclin E. Exp Cell Res 253(2):422–431
74. Wee P, Shi H, Jiang J, Wang Y, Wang Z (2015) EGF stimulates the activation of EGF receptors and the selective activation of major signaling pathways during mitosis. Cell Signal 27(3):638–651
75. Vecsler M, Lazar I, Tzur A (2013) Using standard optical flow cytometry for synchronizing proliferating cells in the G1 phase. PLoS One 8(12):e83935
76. Juan G, Hernando E, Cordon-Cardo C (2002) Separation of live cells in different phases of the cell cycle for gene expression analysis. Cytometry 49(4):170–175
77. Banfalvi G (2008) Cell cycle synchronization of animal cells and nuclei by centrifugal elutriation. Nat Protoc 3(4):663–673
78. Liu Y, Nan B, Niu J, Kapler GM, Gao S (2021) An optimized and versatile counter-flow centrifugal elutriation workflow to obtain synchronized eukaryotic cells. Front Cell Dev Biol 9:664418
79. Hengstschläger M, Knöfler M, Müllner EW, Ogris E, Wintersberger E, Wawra E (1994) Different regulation of thymidine kinase during the cell cycle of normal versus DNA tumor virus-transformed cells. J Biol Chem 269(19): 13836–13842
80. Hengstschläger M, Pusch O, Soucek T, Hengstschläger-Ottnad E, Bernaschek G (1997) Quality control of centrifugal elutriation for studies of cell cycle regulations. BioTechniques 23(2):232–234. 236-237
81. Vaughn JP, Cirisano FD, Huper G, Berchuck A, Futreal PA, Marks JR, Iglehart JD (1996) Cell cycle control of BRCA2. Cancer Res 56(20):4590–4594
82. Zurbriggen R, Dreyer JL (1996) The plasma membrane NADH-diaphorase is active during selective phases of the cell cycle in mouse neuroblastoma cell line NB41A3. Its relation to cell growth and differentiation. Biochim Biophys Acta 1312(3):215–222

83. Ly T, Endo A, Lamond AI (2015) Proteomic analysis of the response to cell cycle arrests in human myeloid leukemia cells. eLife 4: e04534
84. Lissy NA, Van Dyk LF, Becker-Hapak M, Vocero-Akbani A, Mendler JH, Dowdy SF (1998) TCR antigen-induced cell death occurs from a late G1 phase cell cycle check point. Immunity 8(1):57–65
85. Kim HD, Tomida A, Ogiso Y, Tsuruo T (1999) Glucose-regulated stresses cause degradation of DNA topoisomerase IIalpha by inducing nuclear proteasome during G1 cell cycle arrest in cancer cells. J Cell Physiol 180(1):97–104
86. Méndez J, Stillman B (2000) Chromatin association of human origin recognition complex, cdc6, and minichromosome maintenance proteins during the cell cycle: assembly of prereplication complexes in late mitosis. Mol Cell Biol 20(22):8602–8612
87. Willis N, Rhind N (2011) Studying G2 DNA damage checkpoints using the fission yeast Schizosaccharomyces pombe. *Methods Mol Biol* 782:1–12
88. Hagan IM, Grallert A, Simanis V (2016) Cell cycle synchronization of schizosaccharomyces pombe by centrifugal elutriation of small cells. Cold Spring Harb Protoc 2016(6):508–515
89. Rosebrock AP (2017) Synchronization of budding yeast by centrifugal elutriation. Cold Spring Harb Protoc 2017(1):53–62
90. Horlock-Roberts K, Reaume C, Dayer G, Ouellet C, Cook N, Yee J (2017) Drug-free approach to study the unusual cell cycle of giardia intestinalis. *mSphere* 2(5):e00384–16
91. Crozier TWM, Tinti M, Wheeler RJ, Ly T, Ferguson MAJ, Lamond AI (2018) Proteomic analysis of the cell cycle of procylic form Trypanosoma brucei. Mol Cell Proteomics 17(6):1184–1195
92. Keyomarsi K, Sandoval L, Band V, Pardee AB (1991) Synchronization of tumor and normal cells from G1 to multiple cell cycles by lovastatin. Cancer Res 51(13):3602–3609
93. Javanmoghadam-Kamrani S, Keyomarsi K (2008) Synchronization of the cell cycle using lovastatin. *Cell Cycle* 7(15):2434–2440
94. Lee SJ, Ha MJ, Lee J, Nguyen P, Choi YH, Pirnia F, Kang WK, Wang XF, Kim SJ, Trepel JB (1998) Inhibition of the 3-hydroxy-3-methylglutaryl-coenzyme a reductase pathway induces p53-independent transcriptional regulation of p21(WAF1/CIP1) in human prostate carcinoma cells. J Biol Chem 273(17):10618–10623
95. Bjursell G, Reichard P (1973) Effects of thymidine on deoxyribonucleoside triphosphate pools and deoxyribonucleic acid synthesis in Chinese hamster ovary cells. J Biol Chem 248(11):3904–3909
96. Schvartzman JB, Krimer DB, Van't Hof J (1984) The effects of different thymidine concentrations on DNA replication in pea-root cells synchronized by a protracted 5-fluorodeoxyuridine treatment. Exp Cell Res 150(2):379–389
97. Singh A, Xu YJ (2016) The cell killing mechanisms of hydroxyurea. Genes 7(11):99
98. Vassilev LT (2006) Cell cycle synchronization at the G2/M phase border by reversible inhibition of CDK1. *Cell Cycle* 5(22):2555–2556
99. Vassilev LT, Tovar C, Chen S, Knezevic D, Zhao X, Sun H, Heimbrook DC, Chen L (2006) Selective small-molecule inhibitor reveals critical mitotic functions of human CDK1. Proc Natl Acad Sci U S A 103(28): 10660–10665
100. Ma HT, Tsang YH, Marxer M, Poon RY (2009) Cyclin A2-cyclin-dependent kinase 2 cooperates with the PLK1-SCFbeta-TrCP1-EMI1-anaphase-promoting complex/cyclosome axis to promote genome reduplication in the absence of mitosis. Mol Cell Biol 29(24):6500–6514
101. Whittaker SR, Walton MI, Garrett MD, Workman P (2004) The cyclin-dependent kinase inhibitor CYC202 (R-roscovitine) inhibits retinoblastoma protein phosphorylation, causes loss of cyclin D1, and activates the mitogen-activated protein kinase pathway. Cancer Res 64(1):262–272
102. Chan KS, Koh CG, Li HY (2012) Mitosis-targeted anti-cancer therapies: where they stand. Cell Death Dis 3:e411
103. Lara-Gonzalez P, Westhorpe FG, Taylor SS (2012) The spindle assembly checkpoint. Curr Biol 22(22):R966–R980
104. Zieve GW, Turnbull D, Mullins JM, McIntosh JR (1980) Production of large numbers of mitotic mammalian cells by use of the reversible microtubule inhibitor nocodazole. Nocodazole accumulated mitotic cells. Exp Cell Res 126(2):397–405
105. Blagosklonny MV (2007) Mitotic arrest and cell fate: why and how mitotic inhibition of transcription drives mutually exclusive events. *Cell Cycle* 6(1):70–74
106. Lee DH, Goldberg AL (1998) Proteasome inhibitors: valuable new tools for cell biologists. Trends Cell Biol 8(10):397–403
107. Dulla K, Daub H, Hornberger R, Nigg EA, Korner R (2010) Quantitative site-specific

phosphorylation dynamics of human protein kinases during mitotic progression. Mol Cell Proteomics 9(6):1167–1181

108. Li R, Murray AW (1991) Feedback control of mitosis in budding yeast. Cell 66(3):519–531
109. Holloway SL, Glotzer M, King RW, Murray AW (1993) Anaphase is initiated by proteolysis rather than by the inactivation of maturation-promoting factor. Cell 73(7): 1393–1402
110. Hornig NC, Knowles PP, McDonald NQ, Uhlmann F (2002) The dual mechanism of separase regulation by securin. Curr Biol 12(12):973–982
111. Waizenegger I, Giménez-Abián JF, Wernic D, Peters JM (2002) Regulation of human separase by securin binding and autocleavage. Curr Biol 12(16):1368–1378
112. Josefsberg LB, Galiani D, Dantes A, Amsterdam A, Dekel N (2000) The proteasome is involved in the first metaphase-to-anaphase transition of meiosis in rat oocytes. Biol Reprod 62(5):1270–1277
113. Matsui Y, Nakayama Y, Okamoto M, Fukumoto Y, Yamaguchi N (2012) Enrichment of cell populations in metaphase, anaphase, and telophase by synchronization using nocodazole and blebbistatin: a novel method suitable for examining dynamic changes in proteins during mitotic progression. Eur J Cell Biol 91(5):413–419

Chapter 2

The Trypanosomatids Cell Cycle: A Brief Report

Arthur de Oliveira Passos, Luiz H. C. Assis, Yete G. Ferri, Vitor L. da Silva, Marcelo S. da Silva, and Maria Isabel N. Cano

Abstract

Trypanosomatids are protozoan parasites among which are the etiologic agents of various infectious diseases in humans, such as *Trypanosoma cruzi* (causative agent of Chagas disease), *Trypanosoma brucei* (causative agent of sleeping sickness), and species of the genus *Leishmania* (causative agents of leishmaniases). The cell cycle in these organisms presents a sequence of events conserved throughout evolution. However, these parasites also have unique characteristics that confer some peculiarities related to the cell cycle phases. This review compares general and peculiar aspects of the cell cycle in the replicative forms of trypanosomatids. Moreover, a brief discussion about the possible cross-talk between telomeres and the cell cycle is presented. Finally, we intend to open a discussion on how a profound understanding of the cell cycle would facilitate the search for potential targets for developing antiparasitic therapies that could help millions of people worldwide.

Key words Trypanosomatids, Cell cycle phases, DNA replication, Telomere maintenance, Organelle segregation, Synchronization

1 Introduction

Trypanosomatids (supergroup Excavata) are a group of single-celled eukaryotes, among which are the etiologic agents of some devastating neglected tropical diseases such as leishmaniases (caused by *Leishmania* spp.), Chagas disease (caused by *Trypanosoma cruzi*), and sleeping sickness (caused by *Trypanosoma brucei*). These diseases are vector-borne and have a widespread distribution across the globe, with a harsh incidence on East Africa, the Indian subcontinent, and Latin America, where approximately one million new diagnostics are expected yearly [1–3].

Leishmania spp., *T. cruzi*, and *T. brucei* present a heteroxenic life cycle, i.e., they have two hosts: a vertebrate (mammals) and an

Arthur de Oliveira Passos, Luiz H. C. Assis, Yete G. Ferri and Vitor L. da Silva have contributed equally to this chapter.

Zhixiang Wang (ed.), *Cell-Cycle Synchronization: Methods and Protocols*, Methods in Molecular Biology, vol. 2579,
https://doi.org/10.1007/978-1-0716-2736-5_2,

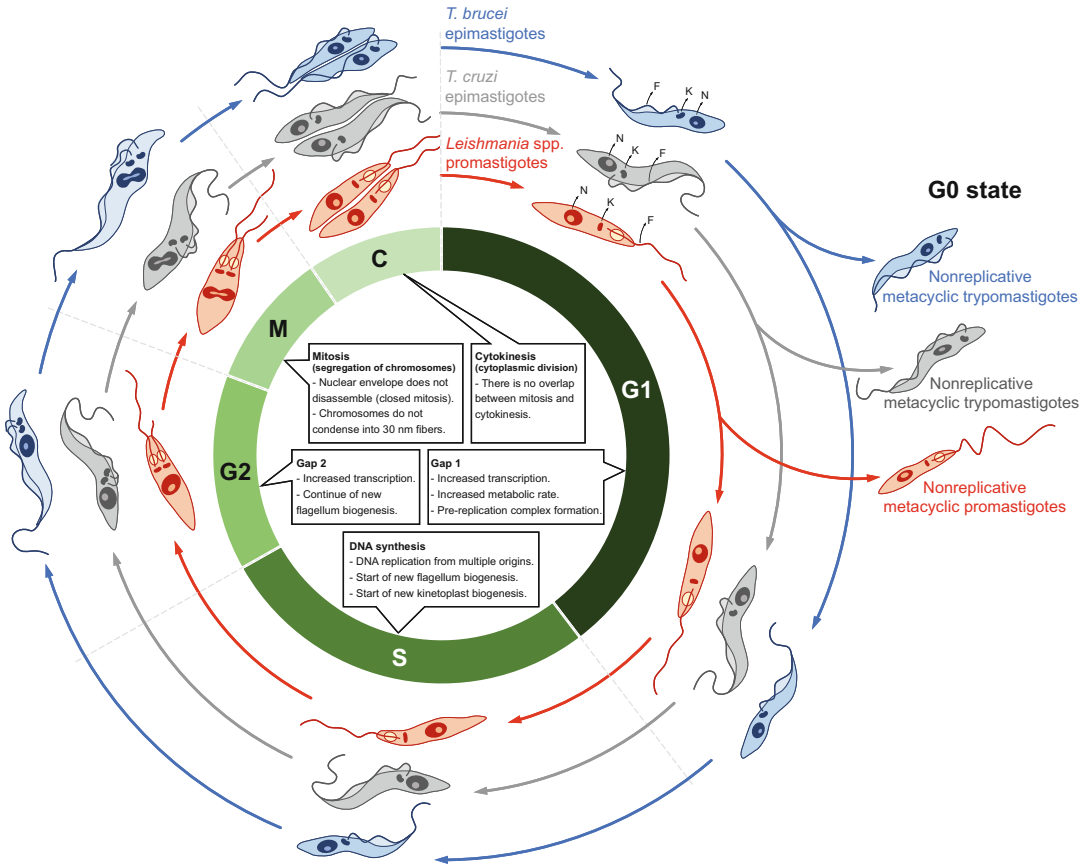

Fig. 1 Scheme showing the distinct morphological patterns of *Leishmania* spp. promastigotes (red), *T. cruzi* epimastigotes (gray), and *T. brucei* epimastigotes (blue) throughout the cell cycle. At the end of cell division, the resulting daughter cells can undergo environmental stimuli and differentiate into nonreplicative and infective (metacyclic) forms through a process called metacyclogenesis, which naturally occurs in the insect vector. The main events that occur in each cell cycle phase are mentioned. F – flagellum, K – kinetoplast, N – nucleus

invertebrate (insects) [4]. Interestingly, these parasites may assume different life forms as they transit between hosts. These life forms are classified according to the parasite morphology and can be grouped into proliferative (replicative) and transmissive (non-replicative) [4–6]. Due to this complexity, new advances in understanding and exploring the life cycle and/or the cell cycle of the proliferative forms could be used as a potential tool for the development of specific antiparasitic therapies, since these processes are related to infectivity and genome stability [7–11].

The cell cycle encompasses cell growth, reliable genome replication, and equitable segregation of chromosomes among daughter cells. For most eukaryotes (including trypanosomatids), the cell cycle follows a single pattern of organization consisting of the following phases: G1 (pre-DNA replication growth), S (DNA replication), G2 (post-DNA replication growth), mitosis (segregation of the replicated chromosomes), and cytokinesis (cytoplasmic division accomplishing the separation of the two daughter cells) [12, 13] (Fig. 1).

In trypanosomatids, as in other eukaryotes, the cell cycle must ensure a correct duplication and segregation of the organelles, especially the nucleus and kinetoplast (a network of circular DNA inside the single large mitochondrion presented by trypanosomatids). Here, we summarize relevant events related to the cell cycle in the replicative forms of trypanosomatids.

2 G0 State and G1 Phase

The G0 state describes a cellular stage outside the cell cycle, when the cell is not yet stimulated to initiate the cell division. Some authors consider the G0 state a "phase" of the cell cycle [14]. However, it is noteworthy that G0 comprises quiescent cells, i.e., cells that are not committed to genome replication and cell division [15]. Interestingly, the infective forms of most trypanosomatids remain at the G0 state (e.g., metacyclic promastigotes from *Leishmania* spp., and metacyclic trypomastigotes from *T. cruzi* and *T. brucei*) [16–19], suggesting that in these organisms, proliferation and infection are mutually exclusive events (Fig. 1).

In general, quiescent cells are stimulated to leave the G0 state, enter the G1 phase and initiate the cell cycle by cyclins and cyclin-dependent kinases (CDKs). At the end of the G1 phase, most eukaryotic cells reach a critical stage and overtake the "restriction point" to become irreversibly committed to cell division [12]. It is still unclear whether the trypanosomatids present a cell cycle restriction point like model eukaryotes.

For most trypanosomatids, the G1 phase corresponds to the larger proportion of the cell cycle, while the other phases vary slightly in duration [20, 21]. Also, there is an increase in the transcription rate and intense protein synthesis for factors related to DNA replication [22, 23]. Moreover, in the G1 phase occurs the establishment of a divergent pre-replication protein complex at specific sites on the chromosomes named replication origins, which can give rise to a replication bubble, i.e., two replication forks in bidirectional movements [23].

3 S Phase

The recruitment of specific protein complexes by the pre-replication complex located at the replication origins contributes to the so-called firing of replication origins. This phenomenon starts the S phase, which briefly consists of the reliable replication of DNA molecules [23]. Usually, eukaryotes have many replication origins per chromosome [13, 24]. However, in trypanosomatids, the number of replication origins per chromosome is an issue that generates debate. For instance, in *Leishmania*

spp. [25] and *T. brucei* [26], researchers used an approach called MFA-seq (Marker Frequency Analysis coupled with deep sequencing) to identify the number and position of the replication origins during the S phase. Subsequently, however, researchers used mathematical equations to reveal that the number of origins identified by MFA-seq was underestimated [13, 22]. The possible explanation for these discrepancies is that the MFA-seq approach is not sensitive enough to identify all replication origins [22]. Interestingly, another study described the presence of a stress-sensitive chromosome end-proximal replication activity outside the S phase [27]. Nevertheless, it is unclear whether this process is coupled with a replication fork, or it is a C-strand fill-in-like process, as already described in other eukaryotes [28, 29]. Further assays are needed to determine the real DNA replication dynamics during the S phase in trypanosomatids.

The beginning of flagellar duplication is another event that occurs during the S phase in trypanosomatids [30–32]. Also, *T. brucei*, *T. cruzi*, and most *Leishmania* spp. replicate and fully divide the kinetoplast during the nuclear S phase [13, 32, 33]. However, it is not yet fully understood how trypanosomatids regulate and restrict the division of their single-copy organelles (e.g., nucleus, kinetoplast/mitochondrion, flagellum, among others).

Interestingly, the S phase is usually the second cell cycle phase in trypanosomatids with the longest duration [20].

4 G2 Phase

In model eukaryotes, the G2 phase is characterized by duplicating centrioles and other cytoplasmic organelles [34]. In trypanosomatids, homologs of the proteins involved with centriole biogenesis described in model eukaryotes are associated with the basal body and flagellum biogenesis [35, 36]. Furthermore, based on studies with other organisms [37], we can infer that, in the G2 phase, most trypanosomatids increase the rate of transcription and resumption of intense protein synthesis, which is necessary for the completion of cell division. This entire process increases cell volume and size [30, 33] (Fig. 1).

Unlike model eukaryotes, where G2 is normally the shortest phase of the cell cycle, in trypanosomatids this phase varies considerably in terms of duration. For instance, in *L. amazonensis*, G2 and M have the same duration and are the shortest phases of the cycle. However, in *T. brucei* and *T. cruzi*, G2 is, respectively, the fourth- and third-longest phase of the cell cycle [20].

At the end of G2, if the cell does not present abnormalities related to DNA and exhibits an intracellular environment and size favorable to its division, it proceeds to the next phase, mitosis.

5 Mitosis and Cytokinesis Phases

During mitosis, trypanosomatids do not disassemble their nuclear envelope and perform a closed mitosis process organized by spindle pole body-like structures [38]. Moreover, trypanosomatids cannot condense their chromosomes into 30-nm fibers due to the absence of the N-terminal portion and globular domain of histone H1 and the lack of phosphorylation on serine 10 of histone H3 (H3S10) [39, 40].

In mammals, a curious feature worth being highlighted is that mitosis and cytokinesis overlap, since cytokinesis begins before the mitotic chromosome segregation is complete. Curiously, trypanosomatids seem not to strictly follow this premise. For instance, in *Leishmania* spp., once mitosis ends, the cell undergoes a rapid remodeling in shape, first growing in length and then in width prior to cytokinesis, which ends cell division, generating two daughter cells [5, 38] (Fig. 1).

Although challenging, all these peculiarities related to the cell cycle phases may provide new routes toward searching for suitable targets for parasite cell cycle interventions aiming at its elimination.

6 Cross-Talk Between Telomeres and the Cell Cycle

Telomeres are tandemly repeated non-coding DNA sequences associated with nucleoproteins that constitute the physical ends of eukaryotic linear chromosomes [41]. Curiously, telomeres shorten after each cell division due to the inability of DNA polymerase to complete replication in the lagging strand of linear chromosomes [42], leading to a progressive loss of telomeric repeats. When its length reaches critical levels, events such as early/unprogrammed cell senescence or even activation of local DNA damage repair are trigged. A holoenzyme named telomerase solves this problem in most organisms, including trypanosomatids, by adding telomeric repeats at the shortest telomeres. This specialized reverse transcriptase forms a ribonucleoprotein complex [43], whose regulation throughout the cell cycle is still a matter of debate [44–46].

Some studies in trypanosomatids have shown how telomere and telomerase dynamics correlate with the cell cycle [47–50]. In *L. amazonesis*, for instance, disturbance in telomere growth led to G2/M phase arrest [47]. Also, the influence of telomere growth/shortening during the cell cycle was demonstrated in studies involving proteins that regulate telomere size, such as the putative *TTAGGG repeat-binding factor* (TRF) [48, 49, 51]. For example, in *T. brucei*, induced expression of human TRF1 and knockdown of TbTRF promoted cell arrest in G1/S and G2/M, respectively

[48, 49]. These findings suggest that molecular mechanisms of the DNA/protein complexes involved in telomeres length control seem to be intrinsically linked to cell cycle progression in these organisms, perhaps through the generation of DNA damage or another unknown process that leads to cell cycle arrest. Thus, the development of new studies and techniques to understand how telomere length is regulated during the cell cycle and parasite life cycle is vital for uncovering the biology of these organisms that affect millions of people worldwide.

7 Cell Cycle Synchronization

Understanding the cell division cycle and the transformation processes across the life cycle has provided many insights about trypanosomatids cell biology and the importance of morphological changes for host-parasite interactions [9, 30, 52]. The characterization of cell cycle profile for different trypanosomatids species has been determined mainly through DNA monitoring and morphological analyses using exponentially growing procyclic forms. However, more accurate investigations of the cell cycle-dependent events require techniques that demand analyses of many cells (such as proteomic/transcriptomic approaches) and normally require cell synchronization, commonly using hydroxyurea (HU).

The mechanism of cell cycle synchronization using HU consists of inhibiting the activity of the enzyme ribonucleotide reductase responsible for converting ribonucleotides into deoxyribonucleotides [53]. This approach allows cells to be synchronized at the beginning of the S phase (G1/S transition) [54]. However, it is worth mentioning that prolonged treatment or a higher dosage of HU may lead to toxic effects for the cell. The lack of deoxyribonucleotides caused by HU treatment can lead cells to death due to the accumulation of DNA damage and oxidative stress [55, 56]. Thus, using this approach to investigate at the same time cell cycle synchronization and DNA repair pathways can lead to biased data. Furthermore, the association of this approach with proteomic analysis requires attention since proteins associated with DNA repair (and related pathways) can be shown as up- or downregulated. A more accurate alternative to non-synchronously investigating gene expression throughout the cell cycle in different life forms of trypanosomatids involves single-cell transcriptomics (scRNA-seq), which allows the identification of less prominent or transient changes to the transcriptome during parasitic differentiation [57].

8 Final Thoughts

A set of events referring to the replication and segregation of the kinetoplast deserve to be highlighted in the trypanosomatids cell cycle. The coordination of these events throughout the cell cycle does not follow their equivalents in model eukaryotes, where mitochondrial DNA replicates at any cell cycle stage [58, 59]. The nuclear and kinetoplast S phase occurs almost simultaneously, but the effective segregation of these organelles can occur at different periods according to the species analyzed. Previous studies have established a pattern of segregation for the kinetoplast relative to the nucleus in some species of trypanosomatids, specially *Leishmania* [30, 33, 60–62]. Together, these studies found out that some *Leishmania* spp. exhibit a nonfixed pattern of nucleus and kinetoplast segregation, theoretically presenting a loose control in the order of segregation of these organelles. In fact, when we compare the cell cycle among different *Leishmania* spp., the order and timing of the kinetoplast and nucleus division are not consensual and cannot be generalized [30, 33, 60–62].

For instance, *L. mexicana*, *L. major*, and *L. tarentolae* exhibit fixed patterns of kinetoplast and nucleus segregation. However, *L. mexicana* segregates its kinetoplast predominantly after the nucleus [33], while *L. major* and *L. tarentolae* do the opposite [60, 61]. A possible explanation for these different behaviors is that, although belonging to the same genus, these parasites show considerable phylogenetic distance [63]. In other words, this phylogenetic divergence may reflect possible species-specific differences relative to kinetoplast segregation, suggesting that some *Leishmania* spp. have less stringent control over the order of division of their DNA-containing organelles (nucleus and kinetoplast). More studies are needed to uncover the potential players involved in controlling cell division and organelle segregation, since some of them could be explored for precise interventions related to the parasite cell cycle.

Acknowledgments

The authors are grateful to Dr. Débora Andrade-Silva (São Paulo State University, Brazil) for her critical revision and valuable suggestions to improve the manuscript's writing.
This work was supported by São Paulo Research Foundation (FAPESP) under grants: 2018/04375-2 (MINC), and 2019/10753-2 and 2020/10277-3 (to MSdS). LHCA is a postdoctoral fellow from FAPESP (grant 2021/04253-7). AdOP, VLdS, and YGF are M.Sc. fellows from FAPESP (grants 2021/05861-0, 2020/16481-1, and 2020/16465-6, respectively).

References

1. Burza S, Croft SL, Boelaert M (2018) Leishmaniasis. Lancet 392(10151):951–970
2. Browne AJ, Guerra CA, Alves RV et al (2017) The contemporary distribution of Trypanosoma cruzi infection in humans, alternative hosts and vectors. Sci Data 4:170050
3. Franco JR, Simarro PP, Diarra A et al (2014) Epidemiology of human African trypanosomiasis. Clin Epidemiol 6:257–275
4. da Silva MS, Cano MIN (2017) Molecular and cellular biology of pathogenic Trypanosomatids. Bentham Science Publishers, Saif Zone Sharjah, United Arab Emirates
5. Wheeler RJ, Gluenz E, Gull K (2013) The limits on trypanosomatid morphological diversity. PLoS One 8(11):e79581
6. Abuchery BE, Black JA, da Silva MS (2022) Single-cell transcriptomics reveals hidden information in trypanosomatids. Trends Parasitol 38(1):4–6
7. Naula C, Parsons M, Mottram JC (2005) Protein kinases as drug targets in trypanosomes and *Leishmania*. Biochim Biophys Acta. 1754(1–2):151–159
8. Hammarton TC (2007) Cell cycle regulation in *Trypanosoma brucei*. Mol Biochem Parasitol 153:1–8
9. Wheeler RJ, Gull K, Sunter JD (2019) Coordination of the cell cycle in trypanosomes. Annu Rev Microbiol 73:133–154
10. de Castro Neto AL, da Silveira JF, Mortara RA (2021) Comparative analysis of virulence mechanisms of Trypanosomatids pathogenic to humans. Front Cell Infect Microbiol 11: 669079
11. Efstathiou A, Smirlis D (2021) *Leishmania* protein kinases: important regulators of the parasite life cycle and molecular targets for treating leishmaniasis. Microorganisms 9(4): 691
12. Matthews HK, Bertoli C, de Bruin RAM (2022) Cell cycle control in cancer. Nat Rev Mol Cell Biol 23(1):74–88
13. da Silva MS, Vitarelli MO, Souza BF et al (2020) Comparative analysis of the minimum number of replication origins in Trypanosomatids and yeasts. Genes 11:523
14. Cooper S (2021) The anti-G0 manifesto: should a problematic construct (G0) with no biological reality be removed from the cell cycle? Yes! BioEssays 43(3):e2000270
15. Tomura M, Sakaue-Sawano A, Mori Y et al (2013) Contrasting quiescent G0 phase with mitotic cell cycling in the mouse immune system. PLoS One 8(9):e73801
16. Gossage SM, Rogers ME, Bates PA (2003) Two separate growth phases during the development of *Leishmania* in sand flies: implications for understanding the life cycle. Int J Parasitol 33(10):1027–1034
17. Rittershaus ESC, Baek SH, Sassetti CM (2013) The normalcy of dormancy: common themes in microbial quiescence. Cell Host Microbe 13(6):643–651
18. Avila CC, Mule SN, Rosa-Fernandes L et al (2018) Proteome-wide analysis of *Trypanosoma cruzi* exponential and stationary growth phases reveals a subcellular compartment-specific regulation. Genes (Basel) 9(8):413
19. Briggs EM, Rojas F, McCulloch R et al (2021) Single-cell transcriptomic analysis of bloodstream *Trypanosoma brucei* reconstructs cell cycle progression and developmental quorum sensing. Nat Commun 121(12):1–15
20. da Silva MS, Muñoz PAM, Armelin HA et al (2017) Differences in the detection of BrdU/EdU incorporation assays Alter the calculation for G1, S, and G2 phases of the cell cycle in Trypanosomatids. J Eukaryot Microbiol 64: 756–770
21. Archer SK, Inchaustegui D, Queiroz R et al (2011) The cell cycle regulated transcriptome of *Trypanosoma brucei*. PLoS One 6(3): e18425
22. da Silva MS, Cayres-Silva GR, Vitarelli MO et al (2019) Transcription activity contributes to the firing of non-constitutive origins in African trypanosomes helping to maintain robustness in S-phase duration. Sci Rep 9:18512
23. da Silva MS, Pavani RS, Damasceno JD et al (2017) Nuclear DNA replication in Trypanosomatids: there are no easy methods for solving difficult problems. Trends Parasitol 33(11): 858–874
24. da Silva M (2020) Estimation of the minimum number of replication origins per chromosome in any organism. Bio Protoc 10(20):e3798
25. Marques CA, Dickens NJ, Paape D et al (2015) Genome-wide mapping reveals single-origin chromosome replication in *Leishmania*, a eukaryotic microbe. Genome Biol 16:230
26. Tiengwe C, Marcello L, Farr H et al (2012) Genome-wide analysis reveals extensive functional interaction between DNA replication initiation and transcription in the genome of *Trypanosoma brucei*. Cell Rep 2:185–197
27. Damasceno JD, Marques CA, Beraldi D et al (2020) Genome duplication in *Leishmania major* relies on persistent subtelomeric dna replication. elife 9:e58030

28. Ishikawa F (2013) Portrait of replication stress viewed from telomeres. Cancer Sci 104(7): 790–794
29. Feng X, Hsu SJ, Kasbek C et al (2017) CTC1-mediated C-strand fill-in is an essential step in telomere length maintenance. Nucleic Acids Res 45(8):4281–4293
30. da Silva MS, Monteiro JP, Nunes VS et al (2013) *Leishmania amazonensis* promastigotes present two distinct modes of nucleus and Kinetoplast segregation during cell cycle. PLoS One 8:e81397
31. Jones NG, Thomas EB, Brown E et al (2014) Regulators of *Trypanosoma brucei* cell cycle progression and differentiation identified using a Kinome-wide RNAi screen. PLoS Pathog 10(1):e1003886
32. Woodward R, Gull K (1990) Timing of nuclear and kinetoplast DNA replication and early morphological events in the cell cycle of *Trypanosoma brucei*. J Cell Sci 95:49–57
33. Wheeler RJ, Gluenz E, Gull K (2011) The cell cycle of Leishmania: morphogenetic events and their implications for parasite biology. Mol Microbiol 79:647–662
34. Harashima H, Dissmeyer N, Schnittger A (2013) Cell cycle control across the eukaryotic kingdom. Trends Cell Biol 23(7):345–356
35. Hu H, Liu Y, Zhou Q et al (2015) The centriole cartwheel protein SAS-6 in *Trypanosoma brucei* is required for probasal body biogenesis and flagellum assembly. Eukaryot Cell 14: 898–907
36. Wheeler RJ, Sunter JD, Gull K (2016) Flagellar pocket restructuring through the *Leishmania* life cycle involves a discrete flagellum attachment zone. J Cell Sci 129(4):854–867
37. Lodish H, Berk A, Zipursky S et al (2000) Overview of the cell cycle and its control. In: Molecular cell biology, section 13.1, Garland Science, New York, U.S.A
38. Campbell PC, De Graffenried CL (2020) Alternate histories of cytokinesis: lessons from the trypanosomatids. Mol Biol Cell 31(24): 2631–2639
39. Hecker H, Gander ES (1985) The compaction pattern of the chromatin of trypanosomes. Biol Cell 53:199–208
40. Hecker H, Betschart B, Bender K et al (1994) The chromatin of trypanosomes. Int J Parasitol 24(6):809–819
41. Blackburn EH (2005) Telomeres and telomerase: their mechanisms of action and the effects of altering their functions. FEBS Lett 579(4): 859–862
42. Harley CB, Futcher AB, Greider CW (1990) Telomeres shorten during ageing of human fibroblasts. Nature 345(6274):458–460
43. Greider CW, Blackburn EH (1987) The telomere terminal transferase of tetrahymena is a ribonucleoprotein enzyme with two kinds of primer specificity. Cell 51(6):887–898
44. Giardini MA, Segatto M, da Silva MS et al (2014) Telomere and telomerase biology. In: Progress in molecular biology and translational science, pp 1-40, Elsevier, Amsterdam, The Netherlands
45. Zhao YM, Li JY, Lan JP et al (2008) Cell cycle dependent telomere regulation by telomerase in human bone marrow mesenchymal stem cells. Biochem Biophys Res Commun 369(4): 1114–1119
46. Holt SE, Aisner DL, Shay JW et al (1997) Lack of cell cycle regulation of telomerase activity in human cells. Proc Natl Acad Sci U S A 94(20): 10687–10692
47. de Oliveira BCD, Shiburah ME, Paiva SC et al (2021) Possible involvement of Hsp90 in the regulation of telomere length and telomerase activity during the *Leishmania amazonensis* developmental cycle and population proliferation. Front Cell Dev Biol 9:713415
48. Muoz-Jordán JL, Cross GAM (2001) Telomere shortening and cell cycle arrest in *Trypanosoma brucei* expressing human telomeric repeat factor TRF1. Mol Biochem Parasitol 114(2):169–181
49. Li B, Espinal A, Cross GAM (2005) Trypanosome telomeres are protected by a homologue of mammalian TRF2. Mol Cell Biol 25(12): 5011–5021
50. da Silva MS, Segatto M, Pavani RS et al (2017) Consequences of acute oxidative stress in *Leishmania amazonensis*: from telomere shortening to the selection of the fittest parasites. Biochim Biophys Acta, Mol Cell Res 1864:138–150
51. da Silva MS, Perez AM, de Cássia V da Silveira R et al (2010) The *Leishmania amazonensis* TRF (TTAGGG repeat binding factor) homologue binds and co-localizes with telomeres. BMC Microbiol 10:136
52. Serafim TD, Coutinho-Abreu IV, Oliveira F et al (2018) Sequential blood meals promote *Leishmania* replication and reverse metacyclogenesis augmenting vector infectivity. Nat Microbiol 3(5):548–555
53. Timson J (1975) Hydroxyurea. Mutat Res 32(2):115–132
54. Ligasová A, Koberna K (2021) Strengths and weaknesses of cell synchronization protocols based on inhibition of dna synthesis. Int J Mol Sci 22(19):10759
55. Musiałek MW, Rybaczek D (2021) Hydroxyurea—the good, the bad and the ugly. Genes (Basel) 12(7):1096

56. Singh A, Xu YJ (2016) The cell killing mechanisms of hydroxyurea. Genes (Basel) 7(11):99
57. Abuchery BE, Black JA, da Silva MS (2021) Single-cell transcriptomics reveals hidden information in trypanosomatids. Trends Parasitol 38(1):4–6
58. Shlomai J (2005) The structure and replication of Kinetoplast DNA. Curr Mol Med 4(6): 623–647
59. Liu B, Liu Y, Motyka SA et al (2005) Fellowship of the rings: the replication of kinetoplast DNA. Trends Parasitol 21(8):363–369
60. Ambit A, Woods KL, Cull B et al (2011) Morphological events during the cell cycle of leishmania major. Eukaryot Cell 10:1429–1438
61. Simpson L, Braly P (1970) Synchronization of *Leishmania tarentolae* by hydroxyurea. J Protozool 17(4):511–517
62. Minocha N, Kumar D, Rajanala K et al (2011) Kinetoplast morphology and segregation pattern as a marker for cell cycle progression in *Leishmania donovani*. J Eukaryot Microbiol 58(3):249–253
63. Valdivia HO, Reis-Cunha JL, Rodrigues-Luiz GF et al (2015) Comparative genomic analysis of *Leishmania* (*Viannia*) *peruviana* and *Leishmania* (*Viannia*) *braziliensis*. BMC Genomics 16(1):715

Chapter 3

Cell Cycle-Related Clinical Applications

Md Gulam Musawwir Khan and Yi Wang

Abstract

The cell cycle is a highly regulated and orchestrated mechanism of life that ensures successive division of a cell and precise replication of cellular contents. Cyclins, cyclin-dependent kinases (CDKs), and CDK inhibitors are three of the most critical cell cycle regulatory proteins that enable the smooth progression of cells through the different phases of cell cycle before and after division. The alteration of cell cycle-related proteins causes aberration in the normal cell cycle process, which is one of the pivotal causes of cancer and other diseases. Targeting cell cycle components has proven to be a valuable therapeutic strategy and leads to the development of novel anticancer therapeutic. The purpose of this book chapter is to summarize the literature and discuss the clinical significance of cell cycle-related proteins in cancers and other diseases, with a focus on identifying potential targets as therapeutic interventions for cancer patients.

Key words Cell cycle, Cyclins, Cyclin-dependent kinases, Cancer, Stem cells, Senescence

1 Introduction

As a biological concept, the cell cycle refers to a series of tightly regulated events that result in cell division. A complex network of checks and balances ensures that these sequential events in the cell cycle, such as cell growth, the replication of genetic material and organelles, and their distribution into daughter cells are executed without error.

Given that individual cell cycle event occurs at a particular time and period, the cell cycle can be partitioned into four phases: G1 (preparatory phase for division), S (chromosome replication), G2 (preparatory phase for mitosis), and M (mitosis, when chromosomes are distributed to two progeny cells) (Fig. 1). The only cell cycle event that can be observed visually is mitosis since conventional microscopes can readily identify chromosomal condensation. However, the remainder of the cell cycle (interphase or intermitotic period) cannot be distinguished visually. Using autoradiography technology, Howard and Pelc first differentiated the different phases of the cell cycle in 1953, but with the advent of state-of-

Zhixiang Wang (ed.), *Cell-Cycle Synchronization: Methods and Protocols*, Methods in Molecular Biology, vol. 2579,
https://doi.org/10.1007/978-1-0716-2736-5_3,

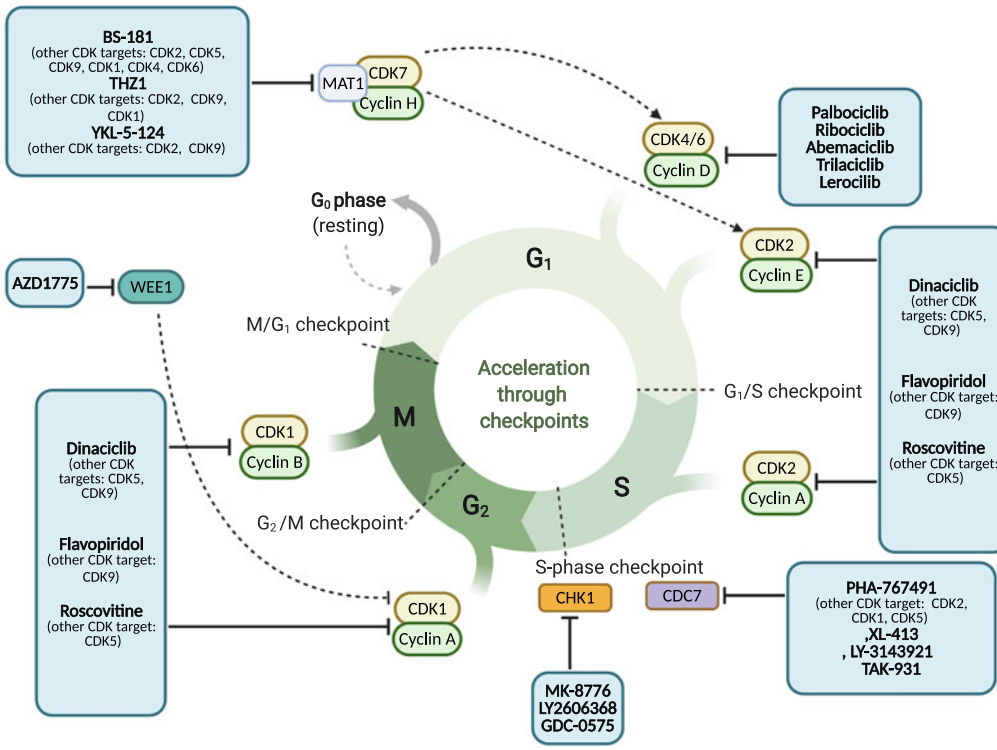

Fig. 1 Cell cycle inhibitors targeting CDKs and other regulatory proteins (including off-target CDKs)

the-art technology, a range of DNA synthesis markers (fluorescence or radiolabelling) have been developed. In different cellular contexts, cell cycle time might vary from several hours to 100 hours (for example, stem cells have a relatively longer cell cycle period). Intriguingly, the length of the G1 phase is responsible for the differences in cell cycle time among different types of cells as the lengths of the M (around 2 hours), S (6–8 hours), and G2 (3–4 hours) phases are relatively constant.

During the cell cycle process, periodic activation of cyclin-dependent kinases (Cdks) and their regulatory cyclin subunits plays a crucial role in maintaining unidirectional and synchronized progression. The cell cycle process is governed by several other regulatory proteins which include Rb (retinoblastoma) protein, transcription factors (e.g., E2Fs), CDK inhibitors (e.g., p16INK4 and $p21^{Waf1}$), CDC25 isoforms, p53 family proteins, and MDM2. Dysregulation of the cell cycle processes and its control mechanisms is frequently observed in many human cancers, resulting in aberrant activation of cell-cycle proteins. Oncogenesis occurs when mutations inside the cell-cycle machinery disrupt cell cycle

control, allowing continuous cell division and resulting in tumor development. Therefore, targeting cell-cycle proteins appears to be one of the most effective ways to stop tumor growth. In this book chapter, we discuss the current state of affairs regarding targeting cell cycle components as an effective therapeutic approach against cancer [1–3].

2 The Regulation of Cell Cycle

To generate two genetically identical progeny cells during cell division is an enormous undertaking, and several evolutionary conserved control mechanisms strictly regulate the cell cycle process. Three cell cycle checkpoints are implicated to ensure error-free cell division, including the G1/S checkpoint or restriction point, the G2/M DNA damage checkpoint, and the spindle assembly checkpoint (SAC). The cell cycle checkpoints serve as DNA surveillance systems to monitor and prevent genetic errors during cell division. As a result of various internal and external stimuli (e.g., radiation), these checkpoints can delay cell cycle progression to manage DNA repair and in case of irreparable DNA damage, execute cell death (or cell cycle exit) [4].

Growth factors (GF) and their receptors mostly receptor tyrosine kinases (RTKs) regulate cell cycle progression through various phases by activating signaling pathways.

The activation of RTks by GFs plays a pivotal role in controlling cell proliferation and cell cycle progression through the activation of several downstream signaling cascades and transcription factors. For instance, the Ras/Erk and PI3K/Akt signaling pathways are activated by EGFR and have a direct effect on cell cycle progression. These two GF-induced cell signaling pathways are involved mostly in the G1 phase to regulate the cell cycle progression through the restriction point. Since the late 1990s, evidence has also been emerging for the role of GF signaling in other phases of the cell cycle. In the event of irreversible genetic lesion caused by external or internal stimuli, DNA damage checkpoint can trigger p53-dependent pathways to execute cell cycle exit, leading to cellular quiescence, senescence, or programmed cell death [5].

According to recent studies, the control of the cell cycle can also be influenced by hypoxia sensing and downstream signaling pathways. In hypoxia, several transcription factors are activated, including HIFs, Myc, p53, AP-1, SP1, and NFκB, which all play a role in regulating gene expressions in the cell cycle, such as p21, p27, cyclin D1, A, and E. As well as transcriptional regulation, hypoxia-induced effects on the cell cycle are also governed by non-transcriptional mechanisms. For instance, in response to hypoxia, a direct interaction between HIF1α and Cdc6 can prevent replication, while PHD-mediated proline hydroxylation can regulate p53 stabilization and signaling via the AKT pathway [6].

Dysregulation of these cell cycle checkpoint controls and aberrant activation of signaling pathways can lead to hyperactivation of cell cycle components and compromise the ability of cells to exit the cell cycle. Consequently, uncontrolled cell division can contribute to the development of many cancers.

3 Clinical Applications of Cell Cycle

3.1 Cancer Therapy

The aberrant expression of cell cycle proteins and/or their regulators results in uncontrolled cell cycle progression, which is considered a hallmark of cancers. The cyclin-CDK kinases are promising targets for inhibiting cancers since they are frequently overexpressed and crucial to cancer cell proliferation, whereas individual cyclin and CDK are generally not essential for the proliferation of normal cells.

The TCGA genomic data revealed that genes encoding D-type cyclins (*CCND1*, *CCND2*, *CCND3*), CDK4, or CDK6 are highly expressed in a wide variety of tumor types, as well as overexpression of these proteins. CDK4/6 selective inhibitors palbociclib, ribociclib, and abemaciclib showed promising results in the treatment of many cancers and have been approved for use in clinics. Palbociclib and ribociclib inhibit CDK4 and CDK6 selectively by blocking RB phosphorylation and causing cell cycle arrest, while abemaciclib inhibits several other kinases as well. Two other CDK4/6 inhibitors, trilaciclib and lerociclib, are currently being evaluated in Phase I/II clinical trials and have shown efficacy as anti-neoplastic agents, particularly against lung and breast cancer.

It is noteworthy that only a few cancers show deregulation of CDK1 despite CDK1 being the only CDK vital for the whole cell cycle progression. The aberrant expression of B-type cyclins is usually associated with deregulated CDK1 activity rather than overexpression. Moreover, several studies in vivo have revealed that CDK1 plays a significant role in tumor formation and progression (e.g., liver cancer, colorectal cancer). Alternatively, CDK2 can be activated by forming complexes with cyclins of either E- or A-type. The role of CDK2 in cancer is still being debated; however, several in vitro and mouse cancer models have shown that CDK2 is required for tumorigenesis in ovarian cancer, B-cell lymphoma, and neuroblastoma. In addition, CDK2 overexpression contributes to the development of radioresistance in glioblastoma multiforme and drug resistance against CDK4/6 inhibitors in breast cancer. These findings explain why CDK2 is an important factor for specific cancer types. Dinaciclib, a potent small-molecule inhibitor, is currently being tested in Phase II/III clinical trials and showed increased potency against CDK1 and CDK2, although it acts as a pan-CDK inhibitor (inhibits CDK5 and CDK9). Another popular first-generation drug flavopiridol is also effective as a CDK1 and CDK2 inhibitor. Its preclinical and clinical trial results showed

promise, but it can target a diverse range of CDKs. CDK7, associated with cyclin H, is overexpressed in several cancers (squamous cell carcinoma and breast cancer) and offers another promising target for anticancer treatment. BS-181, THZ1, and YKL-5-124 are three general CDK7-specific inhibitors that have shown potential efficacy in some cancers and are now being tested in clinical trials for further insights.

Over the past decade, there has been an increase in interest in targeting other cell cycle proteins as therapeutic strategies against cancer. CHK1 (checkpoint protein kinase 1) and nuclear kinase WEE1 have been implicated in oncogenesis in many cancers (e.g., HCC and breast cancer). CHK1 inhibitors (MK-8776, LY2606368, GDC-0575) and WEE1 inhibitors (AZD1775) have been developed and tested in preclinical and clinical studies, and their preliminary results have demonstrated powerful anti-tumor activity against several cancers. Another cell cycle protein CDC7 has been reported to be overexpressed in a wide range of tumors and high expression of CDC7 is associated with tumor aggressiveness and poor clinical outcome. Several CDC7 inhibitors (e.g., PHA-767491, XL-413, LY-3143921, and TAK-931) are currently being evaluated in Phase I clinical trial. The primary outcome is inconclusive due to toxicity effects and other off-target kinases being affected. Figure 1 illustrates inhibitors targeting CDKs and other regulatory factors at different phases of the cell cycle.

The advent of modern technology allowed scientists to develop more potential and efficient cell cycle targeted therapies. Although it is still debatable whether selective CDK inhibitors are more effective than pan-CDK inhibitors, intense studies must be conducted to determine the drug resistance mechanisms of these cell-cycle inhibitors [1, 7].

Growing preclinical and clinical evidence indicate that cell-cycle inhibitors exert a range of immunostimulatory effects in addition to acting as anticancer agents. Depending on the context, immune cells are capable of exhibiting a variable response to CDK inhibitors. Both CDKs and cyclins also play a role in immune cell development, activation, and functions as well. CDK4/CDK6 inhibitor exerts immunostimulatory effects in several ways: (1) increased antigen presentation by tumor cells (1); the secretion of type III interferon during the reactivation of endogenous retroviruses (2); multiple pro-inflammatory cytokines and chemokines secretion resulting in senescence-associated secretory phenotypes (3); the activation of effector T cells (4); and/or inhibition of regulatory T cells (Treg). In response to CDK4/CDK6 inhibitors, malignant cells also employ multiple mechanisms (e.g., autophagy induction, PD-L1-dependent/independent immunoevation) to evade the antitumor immune responses and confer drug resistance. Therefore, novel cell-cycle targeted anticancer therapy must address the immunomodulatory effect in the clinical settings to overcome the drug resistance [8].

Autophagy, a self-degradation pathway in which cytoplasmic material is sequestered into the lysosome for degradation, is also suggested to regulate cell cycle components mutually. Under basal conditions, Aurora kinase and most CDKs inhibit autophagy, while in response to DNA damage, cyclin-dependent kinase inhibitors activate autophagy to prevent cell growth. Cell cycle proteins at different checkpoints (G0/G1 to S transition checkpoint, G2 to M transition checkpoint, and mitosis) are implicated in macroautophagy regulation primarily via activation of various signaling pathways. Conversely, selective autophagy regulates the cell cycle by degrading cell cycle proteins and signaling molecules via ubiquitin-proteosome system. Interestingly, autophagy serves as a double-edged sword in cancer; during tumor initiation, it suppresses tumor growth, while in fully developed tumors it promotes proliferation and growth. Therefore, the combination of selective autophagy and cell cycle-specific drugs appears as a promising strategy for treating cancer. CDK4/6 inhibitors demonstrated an unsatisfactory outcome for some patients because CDK4/6-cyclin D complexes failed to inhibit autophagy. In addition, combining the inhibition of autophagy and cell cycle checkpoint signals (ATM/ATR-CHK1) enhances cell death in cancer cells. Future research is needed to identify reliable biomarkers for combination therapies targeting the cell cycle and selective autophagy in cancer [9].

Cancer cells acquire resistance to chemotherapy via a variety of mechanisms, as is well known. Over the years, many studies have shown that cell cycle-related proteins are closely linked to chemotherapy resistance of tumor cells, and the overexpression of certain cell cycle proteins is associated with poor prognosis. In tumor cells, dysregulated cyclin E expression affects cell cycle regulation and confers resistance to chemotherapy. The overexpression of cyclin E is reported in many tumors including gastric cancer, HCC, pancreatic ductal adenocarcinoma, rectal cancer, metastatic colon cancer, and non-small cell lung cancer, and overexpression is often associated with poor outcomes. Consequently, many therapeutic approaches have been developed using cyclin E as a target to reverse or reduce chemotherapy resistance in cancer treatment. For instance, ganoderiol F, β-cryptoxanthin, and trifluoperazine (TFP) can downregulate the expression of cyclin E (as well as other cyclins) and mediate G0/G1 cell cycle arrest. Inhibiting CDK 2 and CCNE1/PIK3CA can also negatively affect cyclin E expression and reverse chemoresistance. Combining current chemotherapy with cyclin E inhibition may be a promising method for battling chemotherapy resistance. However, it requires further study in the laboratory and clinical settings [10].

In addition to chemoresistance, there have also been reports suggesting that cell cycle proteins are also involved in radioresistance, which poses a real challenge to radiation therapy treatment in

cancer. Recent evidence suggests that CDK2 promotes proliferation and induces radioresistance in glioblastoma [11]. It was also found that overexpression of cyclin B1 is associated with resistance to radiation therapy in head and neck squamous cell carcinomas [12]. Further in-depth investigations are required to identify the role of cell cycle components in radioresistance in different tumor contexts.

3.2 Cancer Biomarkers

Various components of the cell cycle genes are overexpressed in a wide variety of cancers. As we detailed in the earlier section, cyclin E plays an important role in the promotion of drug resistance and may indicate prognosis in a number of cancer types. Using immunohistochemistry, a recent study demonstrated that cyclin D1 is overexpressed in tumorous tissues of colon cancer patients compared to adjacent non-tumorous counterparts, suggesting that cyclin D1 might be a potential prognostic marker in colon cancer [13]. A TCGA-based genomic study examined the diagnostic and prognostic value of the expression of cell cycle genes in hepatocellular carcinoma (HCC) and concluded that BUB3, CDK1, and CHEK1 might serve as prognostic biomarkers in HCC [14]. By using genomics or proteomics data for cell cycle component expression patterns, it is now possible to identify patients with significantly better or worse survival rates, which may lead to more effective treatment and personalized medicine. Identifying potential biomarkers in cancers has often been limited by intra- or inter-heterogeneous tumors, as well as a wide spectrum of mutations – including those affecting cell cycle genes – across a wide range of tumor types. A recent study developed a cell cycle model system for breast cancer, using mass spectrometry and public data mining to identify potential biomarkers for aberrant cell proliferation, which can be explored further in a clinical settings [15].

Through the use of the genomic data from The Cancer Genome Atlas (TCGA) project, we can examine the expression profile of cell cycle genes and the possible relationship between overall survival, recurrence-free survival (RFS), and cell cycle gene expression across various cancer databases. Overexpression of cell cycle genes occurs in a range of cancers and may provide useful diagnostic and prognostic information [16, 17]. Several cell cycle-regulating genes and their prognostic relevance in various cancers are listed in Table 1.

3.3 Regulation of Stem Cells

In some mammalian stem cell types, such as pluripotent embryonic stem cells, certain mechanisms for controlling the cell cycle act in a distinct fashion. Compared to mouse embryonic fibroblasts (MEFs), murine embryonic stem cells (mESCs) divide rapidly since they have a shorter cell cycle and shorter G1 phase. A higher expression of cyclins E, A, and B is observed in mESCs as well as elevated Cdk1 and Cdk2 activity when compared to the somatic

Table1
Overexpression of cell cycle genes in cancers along with their potential as a prognostic marker [18]

Cell cycle genes	Upregulation in cancer[a] (compared to normal tissue)	Overall survival[b]
CDK1	BLCA BRCA COAD LUAD KIRC PRAD LUSC HNSC ESCA LIHC CESC READ UCEC GBM CHOL STAD	LUAD KIRC PAAD LGG KIRP LIHC PCPG ACC MESO KICH SKCM
CDK2	BLCA COAD LUSC HNSC KIRP ESCA LIHC CESC READ GBM STAD	PAAD LGG KIRP LIHC THYM ACC UVM MESO KICH SKCM
CDK4	BLCA COAD LUAD LUSC HNSC ESCA LIHC READ GBM CHOL STAD	KIRC LGG KIRP LIHC MESO KICH SKCM
CDK6	COAD LUSC HNSC GBM CHOL STAD	BLCA LUAD PAAD LGG UCEC SARC ACC MESO
CDK7	COAD ESCA LIHC CHOL STAD	PAAD PRAD LGG KIRP LIHC THYM GBM UCS KICH
WEE1	LUSC GBM	LGG HNSC READ ACC MESO LAML
CHEK1 (encode CHK1)	BLCA BRCA COAD LUAD LUSC HNSC ESCA LIHC CESC READ GBM UCEC CHOL STAD	LUAD PAAD LGG KIRP ESCA LIHC READ MESO KICH
CDC7	BLCA BRCA COAD LUAD KIRC LUSC HNSC KIRP ESCA LIHC CESC READ UCEC GBM CHOL STAD	KIRC HNSC LGG KIRP LIHC THYM ACC KICH
MNAT1 (encode MAT1)	COAD LUSC HNSC ESCA LIHC CESC CHOL STAD	KIRC LIHC PCPG

[a]*Abbreviation of* cancers; *BLCA* bladder urothelial carcinoma, *BRCA* breast invasive carcinoma, *COAD* colon adenocarcinoma, *LUAD* lung adenocarcinoma, *KIRC* kidney renal clear cell carcinoma, *PAAD* pancreatic carcinoma, *PRAD* prostate adenocarcinoma, *LGG* brain low-grade glioma, *LUSC* lung squamous cell carcinoma, *HNSC* head and neck squamous cell carcinoma, *KIRP* kidney renal papillary cell carcinoma, *ESCA* esophageal carcinoma, *OV* ovarian serous cystadenocarcinoma, *LIHC* liver hepatocellular carcinoma, *CESC* cervical squamous cell carcinoma, *READ* rectum adenocarcinoma, *UCEC* uterine corpus endometrial carcinoma, *THYM* thymoma, *THCA* thyroid carcinoma, *GBM* glioblastoma multiforme, *SARC* sarcoma, *PCPG* pheochromocytoma and paraganglioma, *ACC* adrenocortical carcinoma, *UVM* uveal melanoma, *MESO* mesothelioma, *UCS* uterine carcinosarcoma, *TGCT* testicular germ cell tumor, *CHOL* cholangiosarcoma, *KICH* kidney chromophobe, *DLBC* diffuse large B-cell lymphoma, *SKCM* skin cutaneous melanoma, *LAML* acute myeloid leukemia, *STAD* stomach adenocarcinoma; [b]Higher expression of cell cycle genes associated with poor overall survival)

counterparts. While the activity of all cell cycle kinases is high and constant throughout the cell cycle, cyclin B-Cdk1 maintains periodic activity despite being at higher levels than somatic cells. In ESC, KIP/CIP inhibitors are not expressed, which is thought to contribute to the high levels of Cdk1 and Cdk2 kinase activity. Thus, increased kinase activity induces hyperphosphorylation of RB1 and inhibits E2F activity. Additionally, cyclin D expression is low in mESCs. In contrast, hESCs show a slightly different pattern

of cell cycle organization, as they contain higher levels of D cyclins and KIP/CIP inhibitors, show a periodic fluctuation of CDK2 kinase activity, and have both hyper- and hypophosphorylated RB1. As we have seen, the distinct cell cycle organization seen in ESCs plays a direct role in maintaining pluripotent cells. Mechanistically, how cell cycle proteins are involved in these processes is not yet clear. Improving our understanding of stem cell self-renewal, differentiation, and reprogramming will likely have important implications for the future of regenerative medicine [19].

3.4 Aging and Senescence

Cellular senescence is one of the major causes of age-related diseases. Recent research suggests that cellular senescence is an intrinsic phenotype of cells caused by the coordination of cell expansion and cell cycle arrest. Normally, cellular senescence occurs in the G1 and possibly the G2 phase of the cell cycle. Several cell cycle components play critical roles in mediating cell cycle arrest in senescence. Activation of either one or both p53/p21^{WAF1}/CIP1 and p16INK4A/pRB tumor suppressor pathways is of particular importance in manifesting cell cycle arrest in senescence. The cyclin-dependent kinase inhibitors p21 and p16 are known to negatively regulate cell cycle progression and are therefore considered important mediators of senescence. Loss of cell cycle regulators is also known to confer senescence in cancer cells. The ablation of cyclin D1 in mice with Her2-driven mammary carcinomas or the ablation of Cdk4 in mice with Kras-driven lung cancers trigger senescence and prevent tumor growth. By gaining a deeper understanding of the cell cycle components that regulate senescence, new therapeutic approaches can be developed not only to treat cancer but also aging [1, 20].

3.5 Other Clinical Applications

Although the exact mechanisms responsible for the development of neurodegenerative diseases remain unclear, there is growing evidence that many neurodegenerative disorders are associated with DNA damage and abnormal cell cycle activity. In Alzheimer's disease (AD), an aberrant expression of cell cycle-related proteins, such as cell division cycle 2 (cdc2), CDK4, cyclin B1, and cyclin D, is associated with neuropathogenesis. Moreover, the cell cycle kinetics appears to be affected in familial AD brains; presenilin-1 (PSEN1) mutation may lead to the accumulation of cyclin D1 and neuronal apoptosis, thus aggravating neurodegeneration. In several neurodegenerative diseases, a portion of the neuron cells is arrested at the G2/M phase after successful DNA synthesis in the S phase, which is associated with a greater risk of neuronal cell death. The pathological accumulation of p25 in neurons may lead to hyperactivation of Cdk5, suggesting that Cdk5 is involved in neuronal cell cycle arrest. Additionally, Id1 plays an important role in cell cycle regulation in neuron cells, and its association with Ab triggers various neurotoxic mechanisms, including cell cycle reentry with

subsequent neuronal death. A better understanding of the role of cell cycle components in neurodegenerative disease may lead to the development of novel therapeutic interventions and prognostic markers [21].

Growing evidence suggests that cell cycle components play an important role in kidney disease. It appears that p21 is upregulated in the initial stages of renal damage in a p53-independent fashion and participates in the arrest of the G2 cell cycle. This damage-induced p21 expression prevents renal fibrosis progression and protects against kidney damage [22]. In acute kidney injury (AKI), cell cycle activation occurs and Cdk2 promotes injury, nephrotoxicity, and cytotoxicity while elevated p21 promotes cyto-protection [23]. Upon acute kidney stress, urinary tissue inhibitor of metalloproteinase-2 (TIMP-2) and insulin-like growth factor binding protein 7 (IGFBP7) are induced, resulting in the arrest of the G1 cell cycle which ultimately leads to AKI. Timp-2 and IGBFP7 showed promise in detecting AKI early as well as predicting the need for renal replacement therapy and mortality [24, 25].

4 Future Directions

For cells to grow and reproduce, the cell cycle is one of the most fundamental events. Cell cycle progression and arrest are strictly governed by the precise coordination of cell cycle-related proteins (cyclins CDKs and CDKIs) and their periodic activation at different cell cycle phases. One of the cardinal factors contributing to the development of cancers and other diseases is abnormal control of cell cycle dynamics. As knowledge about the role of cell cycle regulators in cancer has advanced dramatically over the past two decades, these molecules have been considered as potential cancer therapy targets. With the development of novel drugs and small molecular inhibitors targeting cell cycle-related proteins, cell cycle studies have moved from the laboratory to the clinic. This field of medicine is seeing successful clinical translation with the approval of a specific CDK4/6-selective inhibitor for cancer treatment. In addition, several CDK inhibitors and cell cycle-targeted therapeutics are being tested in preclinical and clinical trials, not just for cancer, but also for other diseases.

A growing concern regarding the toxicity, efficacy, and safety of first-generation drugs is limiting their use, which led to the development of many new drugs. Modern technology, specifically artificial intelligence and multi-omics approach, has contributed to the development of many cell cycle-targeted therapies with higher efficacy and lower toxicity. The computational cell cycle profiling and high-throughput screening of cell cycle inhibitors have recently been successfully implemented to screen approved drugs with repurposing potential, revealing new promise for future cancer therapeutics [26, 27].

References

1. Suski JM, Braun M, Strmiska V, Sicinski P (2021) Targeting cell-cycle machinery in cancer. Cancer Cell 39:759–778. https://doi.org/10.1016/j.ccell.2021.03.010
2. Hall EJ, Giaccia A (2019) Radiobiology for the radiologist, 8th edn. Chapter 4, pp 120–141
3. Khan MGM, Wang Y (2022) Advances in the current understanding of how low-dose radiation affects the cell cycle. Cell 11:356. https://doi.org/10.3390/cells11030356
4. Matthews HK, Bertoli C, de Bruin RAM (2022) Cell cycle control in cancer. Nat Rev Mol Cell Biol 23:74–88. https://doi.org/10.1038/s41580-021-00404-3
5. Wang Z (2021) Regulation of cell cycle progression by growth factor-induced cell signaling. Cell 10:doi:10.3390/cells10123327
6. Druker J, Wilson JW, Child F, Shakir D, Fasanya T, Rocha S (2021) Role of hypoxia in the control of the cell cycle. Int J Mol Sci 22: doi:10.3390/ijms22094874
7. Otto T, Sicinski P (2017) Cell cycle proteins as promising targets in cancer therapy. Nat Rev Cancer 17:93–115. https://doi.org/10.1038/nrc.2016.138
8. Petroni G, Formenti SC, Chen-Kiang S, Galluzzi L (2020) Immunomodulation by anticancer cell cycle inhibitors. Nat Rev Immunol 20:669–679. https://doi.org/10.1038/s41577-020-0300-y
9. Zheng K, He Z, Kitazato K, Wang Y (2019) Selective autophagy regulates cell cycle in cancer therapy. Theranostics 9:104–125. https://doi.org/10.7150/thno.30308
10. Pang W, Li Y, Guo W, Shen H (2020) Cyclin E: a potential treatment target to reverse cancer Chemoresistance by regulating the cell cycle. Am J Transl Res 12:5170–5187
11. Wang J, Yang T, Xu G, Liu H, Ren C, Xie W, Wang M (2016) Cyclin-dependent kinase 2 promotes tumor proliferation and induces radio resistance in glioblastoma. Transl Oncol 9:548–556. https://doi.org/10.1016/j.tranon.2016.08.007
12. Hassan KA, Ang KK, El-Naggar AK, Story MD, Lee JI, Liu D, Hong WK, Mao L (2002) Cyclin B1 overexpression and resistance to radiotherapy in head and neck squamous cell carcinoma. Cancer Res 62:6414–6417
13. Palaiologos P, Chrysikos D, Theocharis S, Kouraklis G (2019) The prognostic value of G1 cyclins, P21 and Rb protein in patients with colon cancer. Anticancer Res 39:6291–6297. https://doi.org/10.21873/anticanres.13839
14. Liping X, Jia L, Qi C, Liang Y, Dongen L, Jianshuai J (2020) Cell cycle genes are potential diagnostic and prognostic biomarkers in hepatocellular carcinoma. Biomed Res Int 2020:6206157. https://doi.org/10.1155/2020/6206157
15. Lazar IM, Hoeschele I, de Morais J, Tenga MJ (2017) Cell cycle model system for advancing cancer biomarker research. Sci Rep 7:17989. https://doi.org/10.1038/s41598-017-17845-6
16. Gao J, Aksoy BA, Dogrusoz U, Dresdner G, Gross B, Sumer SO, Sun Y, Jacobsen A, Sinha R, Larsson E et al (2013) Integrative analysis of complex cancer genomics and clinical profiles using the CBioPortal. Sci Signal 6: pl1. https://doi.org/10.1126/scisignal.2004088
17. Cerami E, Gao J, Dogrusoz U, Gross BE, Sumer SO, Aksoy BA, Jacobsen A, Byrne CJ, Heuer ML, Larsson E et al (2012) The CBio cancer genomics portal: an open platform for exploring multidimensional cancer genomics data. Cancer Discov 2:401–404. https://doi.org/10.1158/2159-8290.CD-12-0095
18. Chandrashekar DS, Bashel B, Balasubramanya SAH, Creighton CJ, Ponce-Rodriguez I, Chakravarthi BVSK, Varambally S (2017) UALCAN: a portal for facilitating tumor subgroup gene expression and survival analyses. Neoplasia 19. https://doi.org/10.1016/j.neo.2017.05.002
19. Liu L, Michowski W, Kolodziejczyk A, Sicinski P (2019) The cell cycle in stem cell proliferation, pluripotency and differentiation. Nat Cell Biol 21:1060–1067. https://doi.org/10.1038/s41556-019-0384-4
20. Kumari R, Jat P (2021) Mechanisms of cellular senescence: cell cycle arrest and senescence associated secretory phenotype. Front Cell Dev Biol 9:645593. https://doi.org/10.3389/fcell.2021.645593
21. Chen S-D, Yang J-L, Lin Y-C, Chao A-C, Yang D-I (2020) Emerging roles of inhibitor of Differentiation-1 in Alzheimer's disease: cell cycle reentry and beyond. Cells 9. https://doi.org/10.3390/cells9071746
22. Koyano T, Namba M, Kobayashi T, Nakakuni K, Nakano D, Fukushima M, Nishiyama A, Matsuyama M (2019) The P21 dependent G2 arrest of the cell cycle in epithelial tubular cells links to the early stage of renal fibrosis. Sci Rep 9:12059. https://doi.org/10.1038/s41598-019-48557-8

23. Price PM, Safirstein RL, Megyesi J (2009) The cell cycle and acute kidney injury. Kidney Int 76:604–613. https://doi.org/10.1038/ki.2009.224
24. Jia H-M, Huang L-F, Zheng Y, Li W-X (2017) Prognostic value of cell cycle arrest biomarkers in patients at high risk for acute kidney injury: a systematic review and meta-analysis. Nephrology (Carlton, Vic.) 22:831–837. https://doi.org/10.1111/nep.13095
25. Ortega LM, Heung M (2018) The use of cell cycle arrest biomarkers in the early detection of acute kidney injury. Is this the new renal troponin? Nefrologia 38:361–367. https://doi.org/10.1016/j.nefro.2017.11.013
26. Hoose SA, Duran C, Malik I, Eslamfam S, Shasserre SC, Downing SS, Hoover EM, Dowd KE, Smith R, Polymenis M (2012) Systematic analysis of cell cycle effects of common drugs leads to the discovery of a suppressive interaction between gemfibrozil and fluoxetine. PLoS One 7:e36503. https://doi.org/10.1371/journal.pone.0036503
27. Lo Y-C, Senese S, France B, Gholkar AA, Damoiseaux R, Torres JZ (2017) Computational cell cycle profiling of cancer cells for prioritizing FDA-approved drugs with repurposing potential. Sci Rep 7:11261. https://doi.org/10.1038/s41598-017-11508-2

Chapter 4

Flow Cytometry and Cell Cycle Analysis: An Overview

Aja M. Rieger

Abstract

Cell cycle analysis is one of the earliest applications in flow cytometry and continues to be highly used to this day. Since the first reported method of Feulgen-DNA staining, cell cycle analysis has continued to grow and mature. With the recent advances in DNA dyes, understanding of additional cell cycle phase markers, and new technologies, cell cycle analysis continues to be a dynamic field within the flow cytometry community. This chapter will give an overview of the current state of cell cycle analysis by flow cytometry.

Key words Cell cycle, Flow cytometry, DNA content, DNA content dyes

1 Introduction

The measurement of DNA content as a single parameter is one of the earliest applications of flow cytometry [1] and continues to be highly used to this day. It is one of the fundamental techniques in studying cell growth, differentiation, senescence, and apoptosis [2]. The first reported DNA content analysis method, the Feulgen-DNA staining method, was first reported in 1969 [3]. Since that time, numerous fluorescent DNA dyes have been developed, and, in conjunction with other proliferation-related markers, can provide a highly detailed multivariate analysis of cell cycle.

In classic univariate analysis of DNA content, the identification of the major cell cycle phases are determined based on DNA content: G0/G1 (characterized by 2 n DNA content), S phase (characterized by 2 n – 4 n DNA content), and G2/M (characterized by 4 n DNA content) [4]. While DNA content analysis can provide useful information on cell cycle population distributions, no information on kinetics (i.e., time to progress between stages) or quiescence cannot be determined. For these features, analysis of cell cycle can be further enhanced by a multiparametric approach that incorporates analysis of other hallmark features of the cell cycle,

Zhixiang Wang (ed.), *Cell-Cycle Synchronization: Methods and Protocols*, Methods in Molecular Biology, vol. 2579,
https://doi.org/10.1007/978-1-0716-2736-5_4,

including the incorporation of thymidine analogs, cyclin expression, and histone phosphorylation.

2 DNA Content Dyes

The commonly used DNA content dyes are listed in Table 1.

2.1 Propidium Iodide (PI)

The Feulgen-DNA staining procedure was improved upon in the early 1970s by the use of propidium iodide [4–6]. To this day, propidium iodide staining is the standard to which all dyes are compared. PI is a cell impermeant dye that intercalates into nucleic acid with little or no sequence preference. PI can intercalate into both DNA and RNA [7], necessitating the need for RNAse addition during cell cycle protocols. PI can be excited by the UV, 488 nm, 532 nm, or 561 nm lasers, making it accessible for use on most standard flow cytometry platforms.

2.2 4-6-Diamidino-2-Phenylindole (DAPI)

DAPI was first introduced to the flow cytometry scene in 1977 [8] and quickly became a favorite for cell cycle analysis. DAPI binds to the minor grooves of DNA in A-T-rich regions. Due to the higher selectivity for DNA [9], RNAse treatment is not needed in cell cycle analysis with DAPI. Compared with nine other DNA dyes used in flow cytometry, it was found that DAPI had the least impact on the composition and structure of nuclear chromatin [10]. DAPI is also commonly the best performer in cell cycle analysis in terms of CV, generally having the highest resolution of DNA content histograms with the lowest CV values among the common dyes [4, 11, 12]. DAPI is excited in the UV range of light, with very limited excitation from the 405 nm laser, which can limit the use of this dye as UV lasers are not common on all flow cytometers.

2.3 Hoescht

Hoescht 33342 was the first DNA binding dye that is cell-permeant to be used in the analysis of cell cycle and sorting of live cells based on DNA content [13]. Either Hoescht 33342 or Hoescht 33258 can be used for live-cell DNA content analysis; however, Hoescht 33,42 permeates cells more quickly so is more commonly used [14]. Like DAPI, Hoescht binds to the minor groove of DNA in A-T rich regions and is excited in the UV range of light, which may also limit its usage, depending on cytometer configuration.

2.4 DRAQ5

DRAQ5 is a more recently developed live-cell DNA content stain, and the first developed that does not rely on the use of a UV laser [4, 15]. DRAQ5 is excited optimally by 568 nm, 633 nm, or 647 nm lasers and emits in the far red range, making it usable on most standard flow cytometry platforms. It rapidly permeates cells and stains in a reproducible manner and does not require the use of RNAse [15]. DRAQ5 provides resolution of cell cycle phases

Table 1
Summary of DNA content dyes

Reagent	Excitation (max)	Emission (max)	Live cells	Requires fixation	Requires RNAse
Propidium iodide	535	617		x	x
DAPI	345	455		x	
Hoescht 33 342	350	461	x		
DRAQ5	647	681	x		
Vybrant DyeCycle Violet	369	437	x		
Vybrant DyeCycle Green	506	534	x		
Vybrant DyeCycle Orange	519	563	x		
Vybrant DyeCycle Ruby	638	686	x		
SYTOX Blue	444	480		x	x
SYTOX Green	504	523		x	x
SYTOX Orange	547	570		x	x
SYTOX AADvanced	546	647		x	x
SYTOX Red	640	658		x	x
FxCycle Violet	358	461		x	x
FxCycle Far Red	640	658		x	x

similar to those provided by PI, though with slightly higher CV values [15, 16]. However, it is important to note that DRAQ5 is part of a class of compounds with defined cytotoxic mechanisms (the anthraquinones) [15], so the long-term viability of cells stained with DRAQ5 is limited [4].

2.5 Vybrant DyeCycle

The Vybrant DyeCycle family of dyes are DNA-selective, cell membrane-permeant dyes; as such, they can be used on live cells and require no fixation, permeabilization, or addition of RNAse [17]. These dyes show enhanced fluorescence when bound to DNA [17]. Vybrant DyeCycle dyes can be combined with other viability dyes, antibody staining, and apoptotic markers [17]. Importantly, because DyeCycle stains allow the resolution of cell cycle information in viable cells, researchers have the ability to sort cells based on position in the cell cycle. These dyes are available in a range of colors and use commonly available excitation sources and emission filters: Vybrant DyeCycle Violet stain (excitation/emission maxima

~396/437 nm), Vybrant DyeCycle Green stain (excitation/emission maxima ~506/534 nm), Vybrant DyeCycle Orange stain (excitation/emission maxima ~519/563 nm), and Vybrant DyeCycle Ruby stain (excitation/emission maxima ~638/686 nm). Vybrant DyeCycle dyes have been shown to have low toxicity to cells [17].

2.6 SYTOX Dyes

SYTOX cell stains are a cell impermeant DNA dye; as such they have been largely used as cell viability dyes. However, recent studies have shown that SYTOX Green outperforms PI in a standard ethanol fixation protocol for analyzing cell cycle in *Saccharomyces cerevisiae* [18]. Specifically, it has been shown that SYTOX-stained cells have a decreased sensitivity to variances in experimental conditions compared to PI-stained cells, improved coefficients of variation (CVs), and a better correlation between DNA content and fluorescence [18].

2.7 FxCycle

FxCycle stains (FxCycle Violet and FxCycle Far Red) are DNA content dyes for cell cycle analysis on fixed cells. FxCycle Violet preferentially binds dsDNA, while FxCycle Far Red binds both DNA and RNA thus requiring RNAse addition to staining protocols. FxCycle dyes can be easily multiplexed with other stains and show similar results when compared to PI [19].

3 Going Beyond Single-Parameter DNA Content Analysis

DNA content analysis provides a static snapshot of the cell population but cannot discriminate between cells having the same DNA content such as quiescent (G0) cells versus G1 or G2 versus M cells [4] and provides no information on kinetics. For these types of studies, additional markers are needed.

3.1 Uptake of Thymidine Analogs

Dividing cells undergo DNA synthesis within the S-phase of the cell cycle. During DNA synthesis, analogs of thymidine may be inserted into replicating DNA, thereby identifying cells that have progressed through the S phase of the cell cycle during the labeling period [20]. In cell cycle analysis, this is most commonly 5-bromo-2-deoxyuridine (BrdU) or the more recent 5-ethynyl-2-′-deoxyuridine (EdU) [20]. In BrdU assays, DNA must be partially denatured by either strong acid or heat [4, 21]. This step is critical as a balance must be made between intact DNA (stainable by PI) and denatured DNA (single-stranded and accessible to BrdU antibody) in order for the staining to be successful [22]. This denaturation step also results in cell and tissue disruption, as well as the degradation of proteins and nucleic acids, limiting the utility of BrdU as a probe where other protein content or molecular analysis is required [20].

EdU, like BrdU, is also incorporated into replicating DNA during the S-phase of the cell cycle. However, unlike BrdU, EdU can be detected in intact double-stranded DNA (no denaturation step required) following its incorporation into DNA [20]. Using "click" chemistry and small-sized fluorescent azides, detection of EdU in intact DNA is quick and highly sensitive [20, 23, 24]. Finally, because partial DNA denaturation is not required, EdU can be complexed with other protein content or molecular analysis.

3.2 Protein Markers of Cell Cycle Progression

In order to further analyze cell cycle phases with the same DNA content (G0 vs G1; G2 vs M), additional protein markers are needed. Ki-67 and proliferating cell nuclear antigen (PCNA) are commonly used to identify proliferating cells from resting cells [2]. Ki-67 is highly expressed in proliferating cells (maximally in G2 and early M phase), is rapidly degraded during anaphase and telophase, and is rarely expressed in the G0 phase [25]. PCNA marks proliferating cells and is most highly expressed in S-phase cells [26].

To further dissect cell cycle phases, the expression of cyclin proteins is commonly used. Cyclins are a key part of cell cycle progression [27] and, during undisrupted growth, are expressed in discrete parts of the cell cycle. Of particular interest are Cyclins D, E, A, and B. Cyclin D1 is expressed by a fraction of G1 cells – specifically cells entering and progressing through S [22, 28]. Cyclin E is most highly expressed by the cells entering S, with levels dropping as cells progress through S-phase [22, 28]. Cyclin A is expressed by cells in S-phase, with the highest expression in G2 cells; mitotic cells (post-prometaphase) are negative for Cyclin A [22, 28]. Finally, Cyclin B1 is expressed by late S cells, with the highest levels in G2 and M [22, 28]. When combined with DNA content analysis it is possible to discriminate between cells having the same DNA content: G2 and M cells (based on differences in Cyclin A content), G2 diploid and G1 tetraploid cells (based on differences in expression of Cyclins E and/or B1), and G0 from G1 cells (expression of D-type Cyclins or Cyclin E) [28]. Finally, phospho-Histone H3 is commonly used to mark cells undergoing mitosis and can be used to differentiate from G2 cells [29, 30].

4 Additional Modes of Flow Cytometric Analysis

Standard flow cytometers have been used for decades in cell cycle analysis. In this section, we will look closer at three other types of cytometric analysis that have been recently adopted in the cell cycle analysis field.

4.1 Flow Cytometry with Acoustic Focusing

Acoustic flow cytometry is largely the same as standard flow cytometry, with a slight difference in how the cells are focused within the fluidics. Acoustic cytometry uses ultrasonic waves in addition to hydrodynamic focusing to position cells or particles in a flowing stream for analysis [31, 32]. Because of this, cells are precisely positioned into a single, focused line in the central axis, enabling tight focus at the point of laser interrogation. The dual focusing of cells may help reduce coincidence (2 cells passing through the laser simultaneously), which can be particularly detrimental in the analysis of cell cycle. Acoustic focusing may also help tighten CVs, especially at higher run speeds (CV generally below 3%) [33, 34].

4.2 Imaging Flow Cytometry

Standard flow cytometric approaches, while high throughput, lack the spatial resolution of microscopy approaches to analyze cell cycle, where nuclear morphology can be studied. With imaging flow cytometry, a recent technological advance that combines fluorescence microscopy with flow cytometry, you gain conventional flow cytometry's high-throughput speed with the spatial resolution of microscopy [35]. On an imaging flow cytometry platform, an image is captured of each cell on a CCD detector allowing for the measurement of not only fluorescence intensities but also the spatial image of the fluorescence together with brightfield and darkfield images of each cell in a population [35, 36]. Using an imaging flow cytometry approach, cells can be classified into cell cycle phases based on DNA content (similar to flow cytometry); however, from there, cells can be further subdivided based on nuclear morphology, allowing for dissection of, for example, mitotic cells into cells in prophase, metaphase, anaphase, or telophase [37]. Imaging flow cytometry has been successfully applied not only in the analysis of cell cycle in mammalian cells, but also in the analysis of cell cycle in budding yeast [38]. Most recently, a method using imaging flow cytometry has been described that allows for a "label-free" approach for analyzing cell cycle [36]. In this method, a cell's DNA content and mitotic phase can be determined based solely on the features extracted from the brightfield and darkfield images (no DNA content dyes added) and a machine learning approach [36].

4.3 Mass Cytometry

In mass cytometry, antibodies are tagged with metal isotopes rather than fluorescent molecules, and the subsequent read-out is done by time-of-flight mass spectrometry. Mass cytometry has allowed researchers to multiplex a much larger number of parameters in a single sample. As such, with mass cytometry, researchers are able to combine cell cycle measurements with an extensive immunophenotypic characterization of stem cells which has not been technically feasible using fluorescence-based flow cytometry

[39]. However, because of how the signals are detected, the standard DNA content dyes used in flow cytometry cannot be used in mass cytometry. In mass cytometry, the assessment of DNA content is measured using an iridium-labeled intercalator that has much poorer resolution than corresponding measurements of DNA-specific fluorescent dyes [39–41]. Due to this poor resolution, the study of cell cycle by mass cytometry relies on a panel of markers to distinguish between the different phases. The most recent published panel recommends the following markers as a minimum panel: Ir-intercalator (DNA content), IdU (S phase), anti-pS28HistoneH3 (mitosis), anti-CDT1 (G1 phase), and anti-Geminin (non-G1 phases), with the addition of anti-pS780RB1 (late G1) and anti-PLK1 (late G2) to discriminate between late G1 and late G2 [40]. Other potential markers include: p-Rb (S807/811) (G0/G1 phase), Cyclin B1 (G2 phase), p-HH3 (S28) (M phase), Ki-67 (confirm G0/G1 resolution), Cyclin A (confirm G0/G1, G2 resolution), Cyclin E (confirm G0/G1, G2 resolution), and pCDK1 (Y15) (confirm M phase, G2 resolution) [41]. In addition, markers can be added to analyze apoptosis (e.g., cleaved-PARP or cleaved-Caspase 3) or for DNA damage (e.g., p-H2AX (S139)) [41].

5 Additional Suggestions for Acquisition and Analysis of Cell Cycle Samples

In statistics, the coefficient of variation (CV) is a standardized measure of the dispersion of a probability or frequency distribution and is often expressed as a percentage [42]. CV is defined as the ratio of the standard deviation to the mean (StDev/mean) [43], and is widely used in flow cytometry for quality control checks, DNA content analysis, and proliferation analysis. Maintaining a low CV of the G0/G1 peak is critical to the success of DNA content analysis as this will impact your ability to properly discriminate between G0/G1 and S phase cells [44]. In each of the following sections, we will provide suggestions that can be incorporated into your workflow to help minimize CV values and improve your resolution.

5.1 Titrate Your Reagents

Titration of reagents is a standard best practice in flow cytometry and is necessary for all cell cycle experiments. Untitrated stains can lead to poor identification of cell cycle stages, high CVs, increased background, or insufficient separation of populations. In addition to this, if you are working with a cell-permeant dye on live cells, adding too much dye can adversely affect your cell viability, affecting your cell cycle measurements. As such, titration of DNA content dyes is a critical step for cell cycle analysis by flow cytometry.

5.2 Fixatives, Permeabilization, and Multiplexing

An important consideration in developing a cell cycle protocol with fixed cells is whether to only fix or fix and permeabilize. Original, PI-based cell cycle protocols have used 70% ethanol as a standard fixative. Ethanol fixation is known to result in low CVs; however, dehydrating fixatives like ethanol can limit downstream multiplexing. When ethanol fixes cells, it denatures and precipitates proteins – so any surface staining done with protein-based fluorescent molecules will be lost, antigens may become hidden and no longer be able to be bound by antibodies, and signals from fluorescent proteins such as GFP can be destroyed [44]. It is also important to note that dehydrating fixatives can increase cell clumping due to protein coagulation [44].

Cross-linking agents such as formaldehyde are also a common fixative used in flow cytometry. Cross-linking fixatives will not affect the structure of proteins as greatly as dehydrating fixatives do, so will better enable multiplexing with your DNA content analysis. However, because cross-linking fixatives will also cross-link chromatin, so dye staining of DNA is generally worse [22, 44] and the CVs of your samples will generally be much higher [22].

Finally, permeabilization agents such as Triton-X, NP-40, or saponin will all disrupt cellular membranes. The addition of permeabilization agents after fixation with either dehydrating or cross-linking fixatives can improve the resolution of cell cycle phases by improving access of dye to DNA [44]. With this in mind, it is important to test any fixatives or permeabilization agents to ensure that they are compatible with your experimental design and are having the least impact on DNA content resolution possible. For general strategies on cell fixation, permeabilization, and stoichiometry of antigen detection, Jacobberger provides an excellent reference [45].

5.3 Run on Low Speed

The fluidics system is the heart of the flow cytometer and is responsible for the transportation of cells/particles through the instrument [31, 32, 44]. Flow cytometers generally have different "speeds" at which samples can be run. As the speed at which a sample is being run is increased, the amount of force the sample core exerts on the sheath fluid increases, resulting in a widening of the sample core (Fig. 1). This widening of the sample core results in an increase in coincidence (the chance that more than 1 cell will pass by the laser at the same time) [32] and can also result in a decrease in the resolution of fluorescence signals. In DNA content analysis, changes in sample speed can have detrimental effects on the CV, with higher sample speeds resulting in widening of the CVs. This is largely due to the changes in signal resolution that occur as the sample core stream widens. As such, it is recommended that cell cycle samples be run on the lowest sample speed setting on a flow cytometer [44]. One caveat to this occurs with the use of acoustic focusing – because acoustic focusing keeps cells centered in

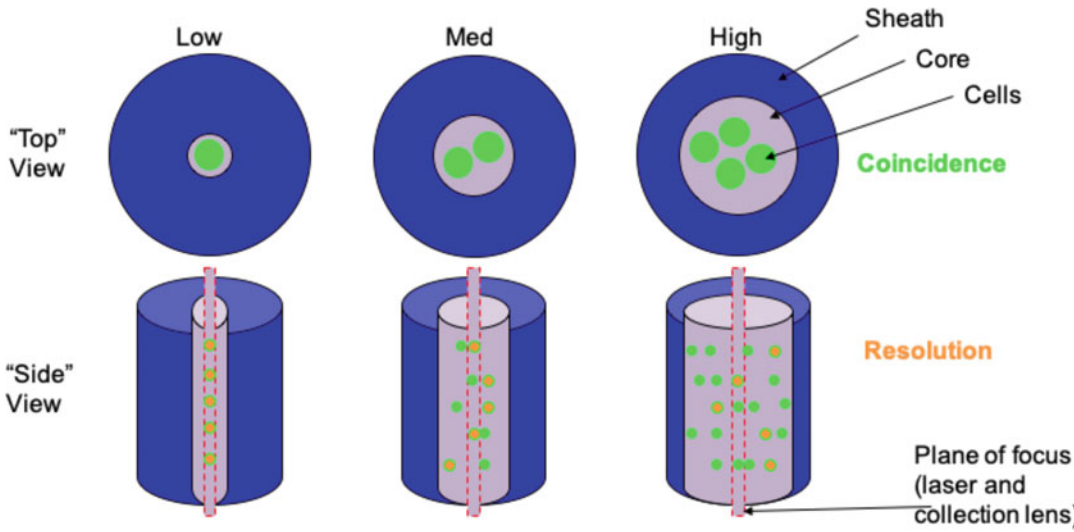

Fig. 1 Depiction of the effect of different fluidics speeds on sample acquisition. Increasing the speed of sample acquisition on a flow cytometer results in a widening of the sample core within the sheath fluid (depicted by the grey circle). Widening of the sample core increases the likelihood of more than one cell/particle passing through at a time (coincidence) and can impact the resolution of fluorescence signals

the core sample stream, regardless of how wide the core sample stream is, a higher fluidics rate can be used on these instruments while still maintaining a low CV [44].

5.4 Acquire Enough Events

Like all flow cytometric assays, it is critical to ensure that enough cells have been acquired in order to properly analyze the data. With cell cycle analysis, it is recommended that a minimum of 10,000–20,000 relevant events be acquired [44], though your assay will almost certainly be improved by acquiring more events. When creating your instrument acquisition settings, it is important that this count excludes debris, doublets, and dead cells; your event count should only be counting the cells you will be using in the DNA content analysis.

5.5 Use Modeling Software for Analysis

This last suggestion will not affect your CV but will affect the accuracy of your reported results. While G0/G1, S, and G2/M have a very distinct profile on a histogram plot, gating these areas with standard linear gates will result in inaccurate reporting of the phases. As such mathematical models have been created to attempt to deconvolute the peaks and provide a more objective approach to cell cycle analysis [44]. Commonly used software with cell cycle mathematical models include ModFit LT (Verity Software House), FlowJo (BD Biosciences), and Multicycle AV (Phoenix Flow Systems).

6 Discussion and Conclusions

Cell cycle analysis is, and will remain, a major technique in flow cytometry. Over the last years, the addition of multivariate analysis of cell cycle by flow cytometry has increased the power of this technique. With the ever-changing landscape of molecular probes for the analysis of the function/activity of individual proteins becoming available and novel DNA content dyes, multiparameter cytometry offers a unique opportunity to dissect the cell cycle in various biological systems and will continue to be an essential method, complementing other biochemical and molecular biology approaches.

References

1. Shankey TV, Rabinovitch PS, Bagwell B et al (1993) Guidelines for the implementation of clinical DNA cytometry. Breast Cancer Res Treat 28:61–68
2. Kim KH, Sederstrom JM (2015) Assaying cell cycle status using flow cytometry. Curr Protoc Mol Biol 111:28.6.1–28.6.11
3. Van Dilla MA, Trujillo TT, Mullaney PF et al (1969) Cell microfluorometry: a method for rapid fluorescence measurement. Science 163: 1213–1214
4. Darzynkiewicz Z, Crissman H, Jacobberger JW (2004) Cytometry of the cell cycle: cycling through history. Cytom Part J Int Soc Anal Cytol 58:21–32
5. Crissman HA, Steinkamp JA (1973) Rapid, simultaneous measurement of DNA, protein, and cell volume in single cells from large mammalian cell populations. J Cell Biol 59: 766–771
6. Krishan A (1975) Rapid flow cytofluorometric analysis of mammalian cell cycle by propidium iodide staining. J Cell Biol 66:188–193
7. Rosenberg M, Azevedo NF, Ivask A (2019) Propidium iodide staining underestimates viability of adherent bacterial cells. Sci Rep 9:6483
8. Stöhr M, Eipel H, Goerttler K et al (1977) Extended application of flow microfluorometry by means of dual laser excitation. Histochemistry 51:305–313
9. Kapuściński J, Yanagi K (1979) Selective staining by 4′, 6-diamidine-2-phenylindole of nanogram quantities of DNA in the presence of RNA on gels. Nucleic Acids Res 6:3535–3542
10. Darzynkiewicz Z, Traganos F, Kapuscinski J et al (1984) Accessibility of DNA in situ to various fluorochromes: relationship to chromatin changes during erythroid differentiation of friend leukemia cells. Cytometry 5: 355–363
11. Lewalski H, Otto FJ, Kranert T et al (1993) Flow cytometric detection of unbalanced ram spermatozoa from heterozygous 1;20 translocation carriers. Cytogenet Cell Genet 64: 286–291
12. Otto F, Tsou KC (1985) A comparative study of DAPI, DIPI, and Hoechst 33258 and 33342 as chromosomal DNA stains. Stain Technol 60:7–11
13. Arndt-Jovin DJ, Jovin TM (1977) Analysis and sorting of living cells according to deoxyribonucleic acid content. J Histochem Cytochem Off J Histochem Soc 25:585–589
14. Bucevičius J, Lukinavičius G, Gerasimaitė R (2018) The use of Hoechst dyes for DNA staining and beyond. Chemosensors 6:18
15. Smith PJ, Wiltshire M, Davies S et al (1999) A novel cell permeant and far red-fluorescing DNA probe, DRAQ5, for blood cell discrimination by flow cytometry. J Immunol Methods 229:131–139
16. Yuan CM, Douglas-Nikitin VK, Ahrens KP et al (2004) DRAQ5-based DNA content analysis of hematolymphoid cell subpopulations discriminated by surface antigens and light scatter properties. Cytometry B Clin Cytom 58:47–52
17. Bradford JA, Whitney P, Huang T et al (2006) Novel Vybrant® DyeCycle ™ stains provide cell cycle analysis in live cells using flow cytometry with violet, blue, and green excitation. Blood 108:4234
18. Haase SB (2004) Cell cycle analysis of budding yeast using SYTOX Green. Curr Protoc Cytom Chapter 7:Unit 7.23

19. Tembhare P, Badrinath Y, Ghogale S et al (2016) A novel and easy FxCycle™ violet based flow cytometric method for simultaneous assessment of DNA ploidy and six-color immunophenotyping. Cytometry A 89: 281–291
20. Cavanagh BL, Walker T, Norazit A et al (2011) Thymidine analogues for tracking DNA synthesis. Molecules 16:7980–7993
21. Gratzner HG (1982) Monoclonal antibody to 5-bromo- and 5-iododeoxyuridine: a new reagent for detection of DNA replication. Science 218:474–475
22. Darzynkiewicz Z, Huang X, Zhao H (2017) Analysis of cellular DNA content by flow cytometry. Curr Protoc Immunol 119: 5.7.1–5.7.20
23. Salic A, Mitchison TJ (2008) A chemical method for fast and sensitive detection of DNA synthesis in vivo. Proc Natl Acad Sci U S A 105:2415–2420
24. Buck SB, Bradford J, Gee KR et al (2008) Detection of S-phase cell cycle progression using 5-ethynyl-2′-deoxyuridine incorporation with click chemistry, an alternative to using 5-bromo-2′-deoxyuridine antibodies. BioTechniques 44:927–929
25. Gerdes J, Lemke H, Baisch H et al (1984) Cell cycle analysis of a cell proliferation-associated human nuclear antigen defined by the monoclonal antibody Ki-67. J Immunol Baltim Md 1950 133:1710–1715
26. Gerdes J, Schwab U, Lemke H et al (1983) Production of a mouse monoclonal antibody reactive with a human nuclear antigen associated with cell proliferation. Int J Cancer 31: 13–20
27. Sherr CJ (2000) The Pezcoller lecture: cancer cell cycles revisited. Cancer Res 60:3689–3695
28. Darzynkiewicz Z, Gong J, Juan G et al (1996) Cytometry of cyclin proteins. Cytometry 25: 1–13
29. Davidson EJ, Morris LS, Scott IS et al (2003) Minichromosome maintenance (Mcm) proteins, cyclin B1 and D1, phosphohistone H3 and in situ DNA replication for functional analysis of vulval intraepithelial neoplasia. Br J Cancer 88:257–262
30. Juan G, Traganos F, James WM et al (1998) Histone H3 phosphorylation and expression of cyclins A and B1 measured in individual cells during their progression through G2 and mitosis. Cytometry 32:71–77
31. Ward MD, Kaduchak G (2018) Fundamentals of acoustic cytometry. Curr Protoc Cytom 84:e36
32. Suthanthiraraj PPA, Graves SW (2013) Fluidics. Curr Protoc Cytom Editor Board J Paul Robinson Manag Ed Al 0 1:Unit-1.2
33. Flegel K, Sun D, Grushko O et al (2013) Live cell cycle analysis of drosophila tissues using the attune acoustic focusing cytometer and vybrant DyeCycle Violet DNA stain. J Vis Exp 75: e50239
34. Mori R, Matsuya Y, Yoshii Y et al (2018) Estimation of the radiation-induced DNA double-strand breaks number by considering cell cycle and absorbed dose per cell nucleus. J Radiat Res (Tokyo) 59:253–260
35. Basiji DA, Ortyn WE, Liang L et al (2007) Cellular image analysis and imaging by flow cytometry. Clin Lab Med 27:653–670
36. Blasi T, Hennig H, Summers HD et al (2016) Label-free cell cycle analysis for high-throughput imaging flow cytometry. Nat Commun 7:10256
37. Filby A, Perucha E, Summers H et al (2011) An imaging flow cytometric method for measuring cell division history and molecular symmetry during mitosis. Cytometry A 79A:496–506
38. Patterson JO, Swaffer M, Filby A (2015) An imaging flow cytometry-based approach to analyse the fission yeast cell cycle in fixed cells. Methods 82:74–84
39. Behbehani GK, Bendall SC, Clutter MR et al (2012) Single-cell mass cytometry adapted to measurements of the cell cycle. Cytom Part J Int Soc Anal Cytol 81:552–566
40. Rein ID, Notø HØ, Bostad M et al (2020) Cell cycle analysis and relevance for single-cell gating in mass cytometry. Cytom Part J Int Soc Anal Cytol 97:832–844
41. Behbehani GK (2018) Cell cycle analysis by mass cytometry. Methods Mol Biol Clifton NJ 1686:105–124
42. Everitt B (1998) The Cambridge dictionary of statistics. Cambridge University Press, Cambridge, New York, Melbourne, Madrid, Cape Town, Singapore, São Paulo, Delhi, Dubai, Tokyo Cambridge University Press, The Edinburgh Building, Cambridge CB2 8RU, UK
43. Misra RK, Easton MDL (1999) Comment on analyzing flow cytometric data for comparison of mean values of the coefficient of variation of the G1 peak. Cytometry 36:112–116
44. Cossarizza A, Chang H-D, Radbruch A et al (2019) Guidelines for the use of flow cytometry and cell sorting in immunological studies (second edition). Eur J Immunol 49: 1457–1973
45. Jacobberger JW (2001) Chapter 13 stoichiometry of immunocytochemical staining reactions, Methods in cell biology, Academic Press, 63, Part A, 271–298, ISSN 0091-679X, ISBN 9780125441667, https://doi.org/10.1016/S0091-679X(01)63017-6

Part II

Methods for Cell Cycle Synchronization of Mammalian Cells

Chapter 5

Synchronization of Cultured Cells to G1, S, G2, and M Phases by Double Thymidine Block

Richard C. Wang and Zhixiang Wang

Abstract

The typical cell cycle in eukaryotes is composed of four phases including the G1, S, G2, and M phases. G1, S, and G2 together are called interphase. Cell synchronization is a process that brings cultured cells at different stages of the cell cycle to the same phase. For many experiments, it is desirable to have a population of cells that are traversing the cell cycle synchronously, as it allows population-wide data to be collected rather than relying solely on single-cell experiments. While there are various drugs that can be used to arrest the cell at each specific phase of the cell cycle, they may cause undesired side effects. Here, we describe a protocol to synchronize cells to each cell cycle phase by using only one chemical: thymidine. Non-synchronized cells are synchronized to early S phase by a double thymidine block. The release of the double thymidine block allows the cells to progress through the cell cycle in a synchronized pace. By collecting the cells at various time intervals following the release of double thymidine block, we are able to harvest cells synchronized to the G2, M, and G1 phases. This synchronization can be assessed by various methods, including flow cytometry to examine the DNA content, Western blotting to examine the expression of various cell phase-specific markers, and microscopy to examine the morphology of the chromosome.

Key words Cell cycle, Synchronization, Interphase, Mitosis, G1 phase, S phase, G2 phase, Flow cytometry, Wester blotting, Microscopy

1 Introduction

Cells divide and produce two new daughter cells by completing a round of cell cycle. The typical cell cycle in cultured eukaryotic cells is composed of four phases including the G1, S, G2, and M phases. G1, S, and G2 together are called interphase. The M phase is comprised of mitosis, in which the cell's nucleus divides, and cytokinesis, in which the cell's cytoplasm divides to form two daughter cells. Mitosis is further divided into five subphases including prophase, prometaphase, metaphase, anaphase, and telophase. Each phase of cell cycle progression is reliant on the proper completion

Zhixiang Wang (ed.), *Cell-Cycle Synchronization: Methods and Protocols*, Methods in Molecular Biology, vol. 2579,
https://doi.org/10.1007/978-1-0716-2736-5_5,

of the previous cell cycle phase. A cell can also exit from the cell cycle to enter the G0 phase, a state of quiescence [1, 2].

For many experiments, it is desirable to have a population of cells that are traversing the cell cycle synchronously. This can be achieved through a process called cell synchronization, during which cultured cells at different stages of the cell cycle are brought to the same phase. Cell synchronization is a vital process in the study of cell cycle progression and regulation that allows population-wide data to be collected rather than relying solely on single-cell experiments.

Many methods have been developed to synchronize cells to the various phases of the cell cycle. In general, better synchronization is achieved by using specific chemical inhibitors to arrest the cells to the specific phase of the cell cycle. However, these chemical inhibitors may also cause undesired side effects to the cells. Thus, it would be ideal to achieve a high level of synchronization with as few chemical inhibitors as possible. A double thymidine block without using other chemical inhibitors is one of the best methods in this regard [3].

Thymidine is a DNA synthesis inhibitor that can arrest cells at the G1/S boundary, prior to DNA replication. When high concentrations of thymidine are added to the culture fluid, the excess thymidine blocks the enzyme ribonucleotide reductase, which is responsible for converting ribonucleotides into deoxyribonucleotides. As a result, the supply of deoxyribonucleotides falls and DNA synthesis stops [4, 5]. However, this thymidine block will arrest cells in the different stages of S phases immediately, resulting in a cell population at different stages of DNA duplication. A second thymidine block is needed to synchronize all the cells to the early stage of the S phase. The release of the first thymidine block will allow all the cells to resume DNA synthesis and progress out of the S phase. The second thymidine block then results in the synchronization of all cells to the early S phase when DNA duplication starts.

Following the release of the second thymidine block, the cells synchronized to the early S phase will progress through the various cell cycle phases including G2, M, and G1 in a largely synchronized fashion. By collecting the cells at different time intervals following the double thymidine release, we can obtain cells largely synchronized at these different phases.

Here, we describe a protocol to synchronize the cells to G1, S, G2, and M phases with a double thymidine block and release (Fig. 1). The synchronization was assessed by various methods including image flow cytometry to examine the DNA content and chromosome morphology and by Western blot to examine the expression of protein markers specific for each cell cycle phase. The HeLa cell line is the most commonly used mammalian model system for cell cycle research [3, 6]. Its entire cell cycle lasts approximately 24 hours, with the G1, S, G2, and M phases lasting approximately 11, 10, 2, and 1 hours, respectively.

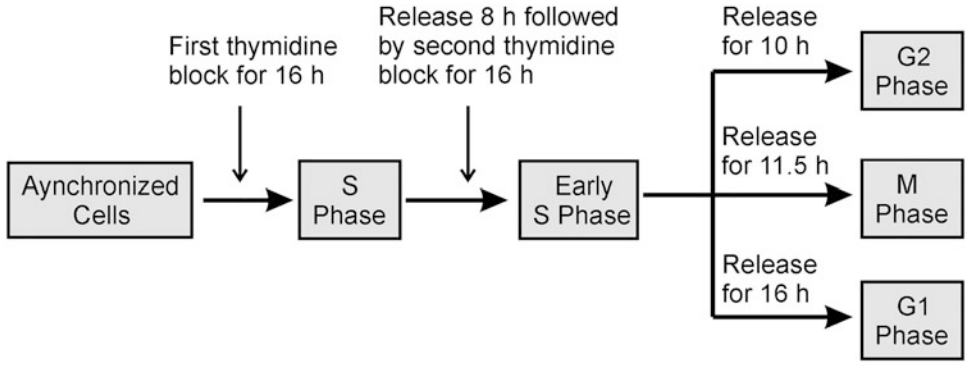

Fig. 1 Flow chart to show the steps of cell synchronization to various interphases

2 Materials

2.1 Solutions, Reagents, and Chemicals

1. Growth Medium: Dulbecco's modified Eagle's medium (DMEM) in 10% FBS (Hyclone) and 1× Antibiotic Antimycotic Solution.
2. PBS: 1× Phosphate Buffered Saline sterilized by autoclaving.
3. Thymidine stock: 200 mM in PBS. Dissolve completely and filter sterilize. Store at 4 °C. Working Concentration: 2 mM.
4. Trypsin: 0.25% Trypsin, 0.03% EDTA (ethylenediaminetetraacetic acid).
5. TBS: Tris Buffered Saline sterilized by autoclaving.
6. Cell lysis buffer A: 50 mM Tris–HCl (pH 7.5), 0.25% Chap. Add fresh: Protease Inhibitor Mix (0.03%), Na_3VO_4 (0.01%) (inhibits protein phosphotyrosyl phosphatases).
7. Cell lysis buffer B: 500 mM Tris–HCl (pH 7.5), 10% Nonidet P-40.
8. Protease Inhibitor Mix: 0.1 mM AEBSF, 10 μg/mL Aprotinin, 1 μM Pepstatin in 100% EtOH.
9. SDS Loading Buffer (4×): 200 mM Tris–Cl (pH 6.8), 400 mM DTT, 8% SDS, 0.4% bromophenol blue, 40% glycerol.
10. 5% separating gel: In 15 mL tube add 0.625 mL acrylamide/bis-acrylamide 40% solution to 3.125 mL double-distilled water (ddH2O), 1.25 mL 1.5 M Tris–HCl buffer with pH 8.8 (lower gel buffer), 25 μL ammonium persulfate (APS), and 2.5 μL tetramethylethylenediamine (TEMED).
11. 4% stacking gel: In 15 mL tube add 250 μL acrylamide/bis-acrylamide 40% solution to 1.6 mL ddH_2O, 625 μL 0.5 M Tris–HCl buffer with pH 6.8 (higher gel buffer), 25 μL 10% SDS solution, 12.5 μL APS, and 2.5 μL TEMED.
12. 70% Ethanol.
13. Pre-stained molecular weight protein ladder.

14. Running buffer: dilute 10× Tris-Glycine-SDS buffer solution from Bio Basic Canada Inc. to 1× buffer solution which contains 0.025 M Tris Base, 0.192 M Glycin, and 0.1% SDS.
15. Transfer buffer: to prepare 500 mL transfer buffer add 400 mL ddH_2O to 2.91 g Tris (48 mM), 1.47 g glycine (39 mM), 1.88 mL 10% SDS solution, and 100 mL methanol.
16. Antibodies to cyclin A, B, D, E, and p-Histone 3 Ser10.
17. HRP-conjugated secondary antibodies.
18. DRAQ5 (Biostatus): 0.5 mM.
19. Flow Cytometry Blocking Buffer: TBS, 0.01% Triton X-100, 4% BSA.
20. Ribonuclease (RNase) buffer with 100 μg/mL concentration of RNase A: add 10 μL Triton X-100 10% and 10 μL RNase A solution from 10 mg/mL stock solution to 1 mL 1× PBS.
21. Propidium iodide (PI) solution with 50 μg/mL concentration of PI: add 10 μL Triton X-100 10% and 50 μL PI solution from 1 mg/mL stock solution to 1 mL 1× PBS.
22. Methanol.
23. Permeabilization solution (0.2% Triton X in PBS).
24. DAPI (4′,6-Diamidine-2′-phenylindole dihydrochloride) stock: 30 μM in PBS. Working Concentration: 300 nM.
25. Mounting Medium: n-Propyl Gallate in 10 mL boiled 50% glycerol.

2.2 Equipment

1. Standard Tissue Culture Equipment.
2. Optical microscope.
3. Cell Culture Dishes: 100-mm.
4. Cell Culture Plate: 24-well plate.
5. Centrifuge for 15 mL centrifuge tubes that can reach 1000 × g at 4 °C.
6. Microcentrifuge that can reach 14,000 × g at 4 °C.
7. Heated water bath.
8. Spectrophotometer.
9. Standard gel electrophoresis equipment.
10. Standard protein transfer equipment.
11. Standard X-ray film processing equipment.
12. Glass slides.
13. Coverslips.
14. Fluorescence microscope.
15. Flow cytometer.

2.3 Cell Lines

1. Hela cells.

3 Methods

3.1 S Phase Synchronization: Double Thymidine Block

The double thymidine block is a highly effective and widely used protocol for the synchronization of cells to the early S phase (*see* **Note 1**). Excess thymidine inhibits the formation of dCTP, an essential precursor of DNA, and thus halts DNA replication [4]. Care should be taken to keep thymidine incubation times consistent.

1. Seed 2.0×10^6 HeLa cells in 100-mm plates with 8 mL cell culture medium.
2. Grow HeLa cells overnight to ~40% confluency.
3. Aspirate the medium and add 5 mL growth media with 500 μL 200 mM thymidine (final concentration of 2 mM).
4. Incubate for 16h.
5. Aspirate the medium and release cells from the S-phase block by washing cells with 15 mL PBS three times.
6. Add 8 mL growth medium.
7. Incubate for 8h.
8. Aspirate the medium and add 5 mL growth media with 500 μL 200 mM thymidine (final concentration of 2 μM).
9. Incubate for 16h

3.2 Synchronization of Cells to G2, M, and G1 Cells by Releasing Cells from Double Thymidine Block

Cells are synchronized to the early S phase following the double thymidine block. Removing thymidine from the growth medium will allow the cells to resume the cell cycle in a largely synchronized fashion. The duration of a typical cell cycle for a Hela cell is approximately 23 hours. The duration for G1, S, G2, and M phases is 10.5, 9, 2.5, and 1 hours, respectively. Following the release of the thymidine block, the cells will begin DNA synthesis. The cells will stay in the S phase for approximately 8 hours, be in the G2 phase between approximately the 9th–11th hours, be in the M phase between approximately the 11th–12th hours, and be in the G1 phase between approximately the 12th–22nd hours.

1. Aspirate the medium and release cells from the S-phase block by washing cells with 15 mL PBS three times.
2. Add 8 mL growth medium.
3. Culture the cells for 5 hours to collect cells in the S phase.
4. Alternatively, culture the cells for 9 hours to collect cells in the G2 phase.

5. Alternatively, culture the cells for 11 hours to collect cells in the M phase (*see* **Note 2**).
6. Alternatively, culture the cells for 15 hours to collect the cells in the G1 phase.

3.3 Validation of Synchronization by Western Blot

Probing with cell cycle markers by Western blotting is necessary to provide confidence that samples are in the cell cycle stage they are claimed to be. Table 1 shows the expression of the proteins throughout the cell cycle of HeLa cells that can be used as markers of synchronization. A popular family of cell cycle markers include the cyclin proteins, since specific cyclins are produced and degraded at specific phases of the cell cycle to drive cell cycle progression [7, 8]. All interphase cells will be negative for p-Histone 3 Ser10, while all M phase cells will be positive for p-Histone 3 Ser10. Among the interphase cells, G1 cells will have maximal levels of Cyclin D but no Cyclin A (*see* **Note 3**), S phase cells will have the highest level of Cyclin E, but no Cyclin D [9], and G2 phase cells will have the highest level of Cyclin A and B but no Cyclin D and E [9–11].

3.3.1 Protein Isolation

1. Synchronize the cells to each phase as described above.
2. Aspirate and wash cells with PBS. Aspirate as much PBS as possible.
3. Add 500 μL Cell Lysis Buffer A.
4. Put dish on ice and scrape cells using cell scraper.
5. Transfer scraped cells to a microcentrifuge tube and incubate on ice for 5 mins from the addition of Cell Lysis Buffer A.
6. Add 60 μL Cell Lysis Buffer B.
7. Incubate for 15 mins on a rotator at 4 °C.
8. Centrifuge at 14,000 × g at 4 °C for 15 mins.
9. Collect supernatant immediately and store at −80 °C until ready for use.

3.3.2 Protein Quantification

1. Prepare protein standard solutions with different concentrations and protein samples in separate tubes according to Table 1.
2. Incubate the tubes at room temperature for 5 minutes.
3. Measure the absorbance of each protein standard solution and protein sample at 595 nm wavelength and write down the absorbance in the last row of Table 1.
4. Draw the standard curve by plotting the concentrations of each protein standard solutions against their absorbance.
5. Use the standard curve to calculate the concentrations of protein samples.

Table 1
Preparation of protein standard solutions with different concentrations and protein samples for protein quantification

Groups	PSS1	PSS2	PSS3	PSS4	PSS5	PSS6	PSS7	PS
Distilled water	18 μL	15 μL	12 μL	9 μL	6 μL	3 μL	0 μL	18 μL
Protein extraction buffer	2 μL	2 μL	2 μL	2 μL	2 μL	2 μL	2 μL	–
BSA (1×)	0 μL	3 μL	6 μL	9 μL	12 μL	15 μL	18 μL	2 μL
Bradford (1×)	1000 μL	1000 μL	1000 μL	1000 μL	1000 μL	1000 μL	1000 μL	1000 μL
Concentration (mg/mL)	0	4.44	8.88	13.32	17.76	22.2	26.64	?
Absorbance	?	?	?	?	?	?	?	?

PSS protein standard solution, *PS* protein sample

3.3.3 Western Blot

1. SDS Loading Buffer (4×) to each protein sample at a 1:3 ratio.
2. Incubate the protein samples in a 90–100 °C water bath for 5 minutes (*see* **Note 4**).
3. Load 10–50 μg total protein sample to each well of 5% acrylamide gel.
4. Adjust the power supply at 100 V and run the electrophoresis for 185 minutes.
5. Put the gel in transfer buffer and incubate it at room temperature with gentle shaking for 15 minutes.
6. Prepare the protein transfer sandwich by putting the gel on the nitrocellulose paper and between two sets of filter papers.
7. Use the semi-dry transfer system at 15 V for 120 minutes to transfer proteins onto the nitrocellulose paper (*see* **Note 5**).
8. Incubate the membrane containing transferred proteins in blocking buffer at room temperature with gentle shaking for 1 hour.
9. Dilute the primary antibodies (A-10 and A-2) in the blocking buffer at a 1:1000 ratio.
10. Incubate the membrane with the primary antibody solution at 4 °C overnight.
11. Remove the primary antibody solution and wash the membrane three times, 10 minutes per wash, in TBST at room temperature with gentle shaking.
12. Dilute the HRP-conjugated mouse secondary antibody in the diluted blocking buffer at a 1:2000 ratio.
13. Incubate the membrane with the secondary antibody solution at room temperature for 1 hour.

Table 2
Expression of various cyclins throughout the cell cycle in HeLa GFP-H2B cells

	Cyclin D	Cyclin E	Cyclin A	Cyclin B	p-Histone 3 Ser10
G0/early G1	–	–	–	–	–
Late G1	++	+	–	–	–
Early S-phase	–	++	+	–	–
Late G2	–	–	++	++	–
Prometaphase	–	–	++	++	++
Metaphase	–	–	+	++	++
Ana/telophase	–	–	–	–	++

14. Remove the secondary antibody solution and wash the membrane three times, 10 minutes per wash, in TBST at room temperature with gentle shaking.
15. Incubate the membrane with ECL substrate solution for 5 minutes at room temperature with gentle shaking and then detect the protein bands on X-ray film.

Table 2 lays out the expression of cell cycle markers that can be used to validate the synchronization methods.

3.4 Validation of Synchronization by Flow Cytometry

Flow cytometry analysis can be used to measure DNA content. G0/G1 cells have 2 N DNA, S-phase cells have 2-4 N DNA, and G2/M cells have 4 N DNA.

1. After completing cell cycle arrest, aspirate media and wash with PBS once. Add 0.8 mL of Trypsin and incubate in an incubator for 2.5 min. Add 4.2 mL PBS and detach cells off the plate by pipetting repeatedly. Collect cells in a pre-cooled 15 mL tube. Centrifuge cells at 1000 × g for 5 min. Aspirate liquid and resuspend cells in 0.5 mL PBS. Transfer cells to 4.5 mL of ice-cold 100% MeOH.
2. Fix cells for 20 min at −20 °C (*see* **Note 6**).
3. Centrifuge cells at 1000 × g for 5 min. Aspirate liquid and resuspend cells in 1 mL Flow Cytometry Blocking Buffer. Incubate for 10 min on ice.
4. Discard the supernatant and add 1 mL Ribonuclease (RNase) buffer to each tube and resuspend the cells gently by pipetting up and down (*see* **Note 7**).
5. Incubate the cells on ice for 30 min.
6. Centrifuge the cells at 1300–1500 rpm for 5 min.

Table 3
The synchronization of cells to various phases of cell cycle including S, G2, M, and G1 phases

	DNA (2 N)	DNA (2-4 N)	DNA (4 N)	DNA (2 N)
Asynchronous cells		38%	15%	42%
Double thymidine block (G1/S boundary)	**92%**	7%	1%	
Release for 5 h (S phase)	14%	**78%**	8%	
Release for 9 h (G2 phase)	7%	11%	**82%**	
Release for 11 h (M phase)		5%	**80%**	15%
Release for 15 h (G1 phase)		6%	4%	**90%**

7. Discard the supernatant and add 1 mL PI solution to each tube and resuspend the cells gently by pipetting up and down.
8. Incubate the cells on ice for 5–10 min.
9. Centrifuge cells at 1000 × g for 5 min. Aspirate liquid and wash cells with 1 mL ice-cold PBS. Repeat washing step.
10. Centrifuge cells at 1000 × g for 5 min. Aspirate liquid and resuspend cells well in 200 μL PBS with 2 μL 0.5 mM DRAQ5 (final concentration of 5 μM). Add cells to flow cytometry tube and incubate for 15 min at room temperature while protecting from light.
11. Run samples by flow cytometry analysis.
12. Use DNA content to distinguish between 2 N, 2-4 N, and 4 N, for G0/G1, S-phase, and G2 respectively.

A typical result of flow cytometry assessment of cell cycle synchronization is shown in Table 3.

3.5 Validation of Synchronization by Microscopy

Both G2 and M phase cells have the same DNA content of 4 N and thus cannot be distinguished by flow cytometry. Microscopic examination of the chromosome morphology is needed to determine if the cells are synchronized to the G2 and/or M phase.

1. Seed 5×10^4 HeLa cells on each coverslip in a 24-well plate with 0.5 mL growth medium.
2. Perform cell synchronization method of choice. Adapt protocols from 150-mm or 100-mm dishes to a 24-well plate.
3. Wash cells once with PBS. Aspirate PBS.
4. Fix cells by adding 0.5 mL ice-cold MeOH. Fix for 20 min at −20 °C.
5. Wash cells once with PBS. Aspirate PBS.
6. Add 500 μL PBS with 1:100 DAPI. Incubate for 10 min on ice, protected from light (*see* **Note 8**).

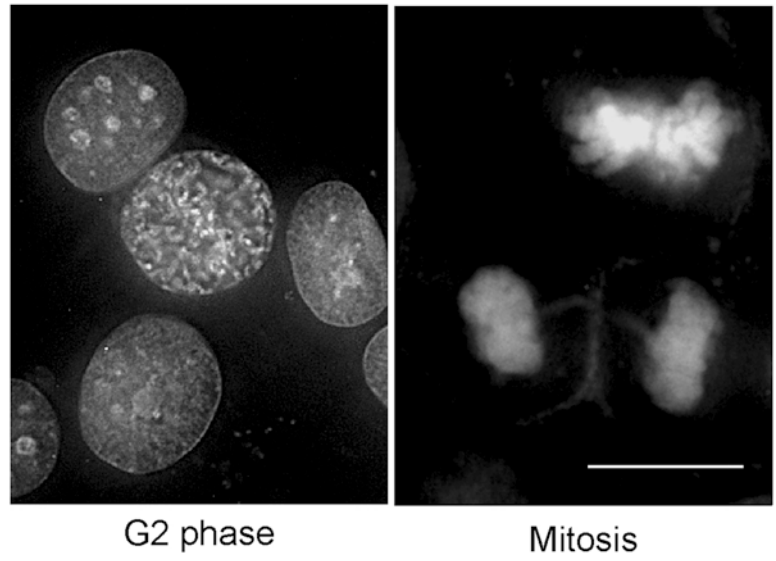

Fig. 2 Assessment of cell synchronization by fluorescence microscope. (**a**) Cells in the G2 phase. (**b**) Cells in mitosis. Size bar = 10 μm

7. Aspirate and wash twice with PBS.
8. Mount cells onto glass slide with 2.8 μL mounting medium.
9. Seal edges with nail polish.
10. Visualize cells by fluorescence for Dapi.

Figure 2 shows the typic chromosome morphology of cells in interphase and in the various stages of mitosis.

4 Notes

1. S-phase synchronization can also be performed using DNA replication inhibitors, such as the DNA polymerase inhibitor aphidocolin (5 μg/mL) [12] and hydroxyurea (1.0–2.5 mM) [13].
2. As the M phase is quite short, it is important to determine the specific time window for harvesting the mitotic cells following the release of double thymidine block. This can be achieved by running a few trials to collect cells every 30 min between the 10th–12th hours following the double thymidine block release.
3. Cyclin D1 expression can vary highly in other tumor cell lines, especially if they have perturbations in the Ras or Rb pathways.
4. Alternatively, cells don't need to be fixed but instead permeabilized with detergents and/or hypotonic solutions. This method provides more accurate estimates of DNA content compared to the measurement of fixed cells. However, fixation

will allow the cells to be stored in the fixative for extended periods and be transported while in the fixative. Thus, fixation allows one to prepare and collect cells independently of the timing of their analysis.

5. PI also binds to RNA strongly, which will interfere with the calculation of DNA contents. RNase treatment is necessary to reduce the interference of RNA. Alternatively, DAPI can be used to replace PI. Although DAPI also binds to RNA, the fluorescence of RNA-binding DAPI is not strong, and thus RNase treatment is not necessary [14].
6. DAPI can be replaced by other fluorescent dyes. Hoechst 33342 and Hoechst 34580 are most commonly used, especially in live imaging.

References

1. Panagopoulos A, Altmeyer M (2021) The hammer and the dance of cell cycle control. Trends Biochem Sci 46(4):301–314
2. Wang Z (2021) Regulation of cell cycle progression by growth factor-induced cell signaling. Cell 10(12):3327
3. Chen G, Deng X (2018) Cell synchronization by double thymidine block. Bio Protoc 8(17): e2994
4. Bjursell G, Reichard P (1973) Effects of thymidine on deoxyribonucleoside triphosphate pools and deoxyribonucleic acid synthesis in Chinese hamster ovary cells. J Biol Chem 248(11):3904–3909
5. Schvartzman JB, Krimer DB, Van't Hof J (1984) The effects of different thymidine concentrations on DNA replication in pea-root cells synchronized by a protracted 5-fluorodeoxyuridine treatment. Exp Cell Res 150(2):379–389
6. Wee P, Shi H, Jiang J, Wang Y, Wang Z (2015) EGF stimulates the activation of EGF receptors and the selective activation of major signaling pathways during mitosis. Cell Signal 27(3): 638–651
7. Darzynkiewicz Z, Gong J, Juan G, Ardelt B, Traganos F (1996) Cytometry of cyclin proteins. Cytometry 25(1):1–13
8. Pozarowski P, Darzynkiewicz Z (2004) Analysis of cell cycle by flow cytometry. Methods Mol Biol (Clifton, NJ) 281:301–311
9. Dulić V, Lees E, Reed SI (1992) Association of human cyclin E with a periodic G1-S phase protein kinase. Science (New York, NY) 257(5078):1958–1961
10. Pines J, Hunter T (1990) Human cyclin A is adenovirus E1A-associated protein p60 and behaves differently from cyclin B. Nature 346(6286):760–763
11. Kraft C, Herzog F, Gieffers C, Mechtler K, Hagting A, Pines J, Peters JM (2003) Mitotic regulation of the human anaphase-promoting complex by phosphorylation. EMBO J 22(24): 6598–6609
12. Pedrali-Noy G, Spadari S, Miller-Faurès A, Miller AO, Kruppa J, Koch G (1980) Synchronization of HeLa cell cultures by inhibition of DNA polymerase alpha with aphidicolin. Nucleic Acids Res 8(2):377–387
13. Pfeiffer SE, Tolmach LJ (1967) Inhibition of DNA synthesis in HeLa cells by hydroxyurea. Cancer Res 27(1):124–129
14. Darzynkiewicz Z, Juan G (2001) DNA content measurement for DNA ploidy and cell cycle analysis. Curr Protoc Cytom Chapter 7:Unit 7.5

Chapter 6

Cell Synchronization Techniques for Studying Mitosis

Joanne D. Hadfield, Sargun Sokhi, and Gordon K. Chan

Abstract

Cell synchronization allows the examination of cell cycle progression. Nocodazole and other microtubule poisons have been used extensively to interfere with microtubule function and arrest cells in mitosis. Since microtubules are important for many cellular functions, alternative cell cycle synchronization techniques independent of microtubule inhibition are also used for synchronizing cells in mitosis. Here we describe using nocodazole, STLC, and combining thymidine block with MG132 to synchronize cells in mitosis. These inhibitors are reversible and mitotic cells can be released into the G1 phase synchronously. These techniques can be applied to both Western blot and timelapse imaging to study mitotic progression.

Key words Cell cycle synchronization, Mitotic arrest, Double thymidine block, Timelapse imaging, Nocodazole, MG132, STLC

1 Introduction

Mammalian cell cycle is a complex circuit of growth and division which involves sequential activity of various regulatory protein complexes [1]. The cell cycle phases G1, S, and G2 together termed as interphase are succeeded by mitosis and cytokinesis consisting of accurate chromosome segregation which culminates in the production of two genetically identical daughter cells. The progression through the phases of the cell cycle is tightly coupled to transient factors and regulatory complexes which experience fluctuations in their levels reflecting association with a particular cell cycle phase [2]. At any time in the growing cell cultures, a population of cells is asynchronous meaning that they are dividing independently of each other's phase. To study cell cycle-regulated events or factors whose levels are dependent on cell cycle phases, a synchronized population of cells is needed. Synchronization, which can be achieved through various techniques, yields a homogenous population of cells which

The authors "Joanne D. Hadfield" and "Sargun Sokhi" contributed equally to this chapter.

Zhixiang Wang (ed.), *Cell-Cycle Synchronization: Methods and Protocols*, Methods in Molecular Biology, vol. 2579,
https://doi.org/10.1007/978-1-0716-2736-5_6,

advance through the cell cycle in a uniform manner. Although several methods have been developed that can successfully compile a homogenous population in different phases of the cell cycle, this chapter will focus on methodologies to enrich mitotic cell population. Mitosis is an important event in the cell cycle and errors during mitosis and its deregulation can potentially have serious impact on disease [3, 4]. Given the short duration of mitosis, it becomes tricky to accumulate cells for examination. Here, we provide various protocols (Fig. 1) to generate a synchronized mitotic cell population by (1) addition of excess nutrients (thymidine block) followed by chemical blockade, (2) reversible chemical treatment (Nocodazole, STLC, MG132), and (3) based on morphological differences (mitotic shake-off).

1.1 Enrichment of Mitotic Cells by Thymidine Block Followed by MG132 Treatment

Often a homogenous cell population can start to lose synchrony progressively at later time points in the cell cycle [5]. Hence, synchronizing cells in more than one phase of the cell cycle provides a way to increase the yield and purity of mitotic cells. Here, we describe a protocol to enrich mitotic cells using MG132 chemical blockade following the release of cells in the G1/S phase by thymidine block (Fig. 2). To trap the cells in the G1/S phase, excess thymidine can be added which results in the inhibition of DNA synthesis [6, 7]. The addition of high concentrations of thymidine to the cultures results in the allosteric inhibition of ribonucleotide reductase, causing an imbalance in the dNTP pool, leading to the inhibition of DNA replication. Hence, thymidine block can be used to synchronize cells at the G1/S boundary. Following the release from the block, cells synchronously progress through S-phase to other phases. To get a more synchronized G1/S-phase population, a double thymidine block can be used. A double thymidine block as described in the methods involves the release of cells from a single thymidine block and then trapping the cells again with a second round of excess thymidine treatment. On the other hand, MG132 (carbobenzoxy-Leu-Leu-leucinal) is an inhibitor of the 26S proteosome complex which has been shown to induce G2/M arrest in HeLa and colon cancer cell lines [8–10]. Following 8-h release from a single thymidine block, cells treated with MG132 for 2 h resulted in a population enriched in mitotic cells (Fig. 2). This protocol can be used to analyze a cell cycle event that has a narrow window of action and requires high degree of synchrony. However, it is essential to take into consideration the doubling time of the cell line while using this procedure as the protocol listed below is based on a 24-h doubling time frame.

1.2 Enrichment of Mitotic Cells Using Reversible Chemical Inhibitors

Chemical inhibitors can be used to reversibly arrest the cells at a particular cell cycle phase. Nocodazole is a spindle toxin which disrupts the assembly/disassembly dynamics of microtubule formation during mitosis [11, 12]. The metaphase to anaphase transition in mitosis is guarded by the mitotic checkpoint [13]. The mitotic

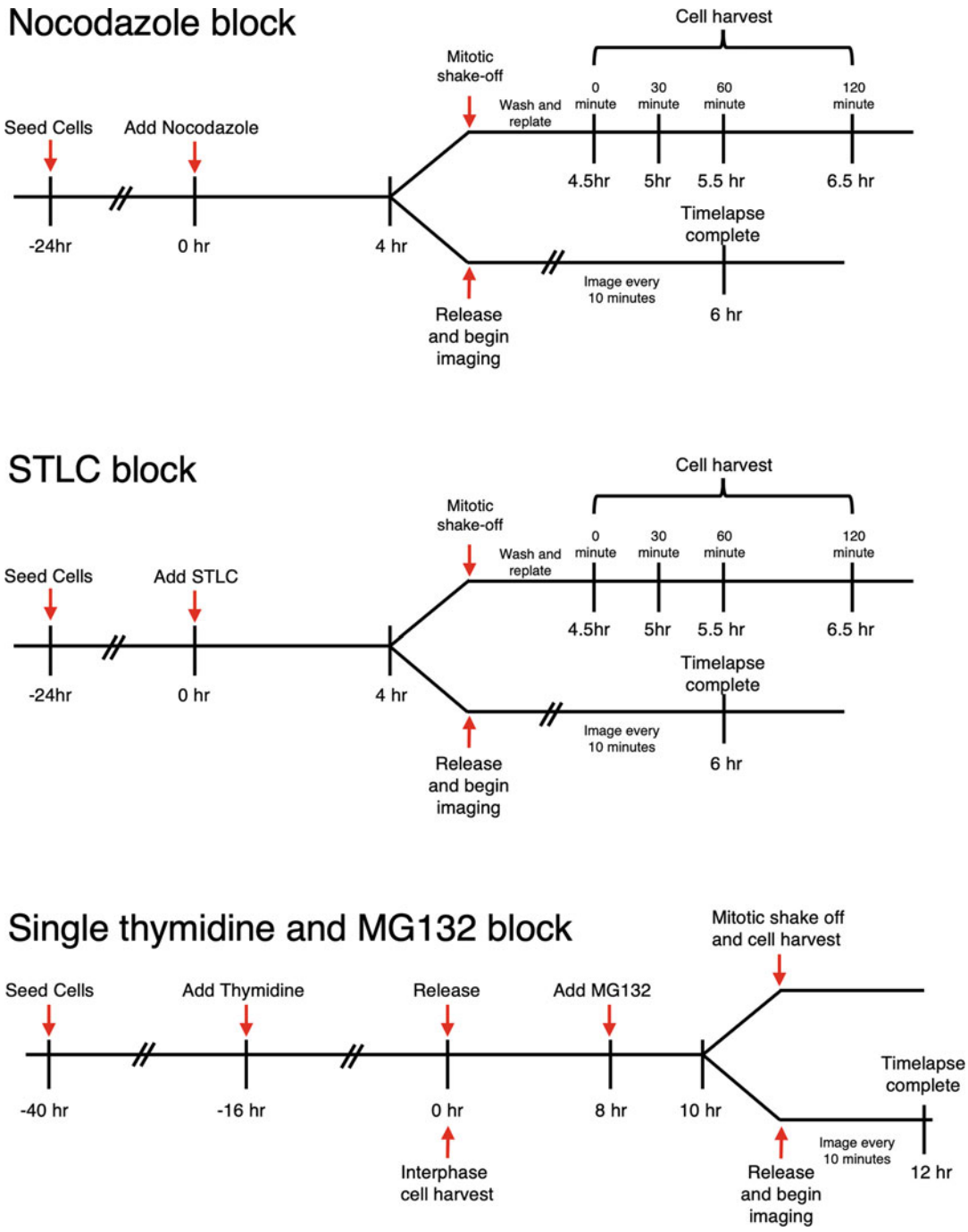

Fig. 1 Experimental flowcharts. Timing relative to the first addition of inhibitors is shown under each flowchart (scales are not proportional). *Nocodazole block*: Cells were seeded 24 h prior to treatment. Following 4-h of nocodazole treatment, mitotic cells were harvested via mitotic shake-off, washed and replated for 0-, 30-, 60-, and 120-min time points. For imaging, cells were released following 4-h treatment and imaged every 10 min for 2 h. *STLC block*: Cells were seeded 24 h prior to treatment. Following 4-h treatment, mitotic cells were removed via mitotic shake-off, washed and replated for 0-, 30-, 60-, and 120-min time points. For imaging, cells were released following 4-h treatment and imaged every 10 min for 2 h. *Single thymidine and MG132 block*: Cells were seeded 24 h prior to addition of thymidine. Cells were released after 16 h and

checkpoint is a failsafe mechanism that inhibits premature segregation and arrests the cell cycle in the presence of even a single unaligned chromosome. Hence, microtubule poisons like nocodazole, which interfere with spindle formation and chromosome alignment, can be used to activate the checkpoint machinery to trap the cells in a prometaphase arrest [5]. Several other microtubule poisons like colcemid can be used to induce a prometaphase arrest but recovery from nocodazole block is more rapid and reversible [11]. As with all the chemical inhibitors, a possible disadvantage is toxicities associated with high concentrations of the drug close to its effective concentration [12, 14]. Therefore, we provide a protocol with optimal nocodazole concentration with a short incubation period to minimize the disruption of normal cell-cycle regulatory events. Here, we treated the cells with 200 ng/μL nocodazole for 4 h prior to release (Fig. 3). Alternatively, STLC (S-Trityl-L-cysteine) which is a reversible inhibitor of human kinesin Eg5 can be used to arrest cells in mitosis [14, 15]. Eg5 is a member of Kinesin-5 family and is responsible for the formation of bipolar spindles. Upon inhibition of Eg5 with STLC, a prometaphase arrest is induced with cells exhibiting monoastral spindles and non-separation of duplicated centrosomes [10]. For the protocol described below, asynchronous cell population was treated with 2.5 μM 4 h prior to release from STLC after which arrested cells exited mitosis normally (Fig. 4). Post release from nocodazole or STLC block, mitotic cells were collected by mitotic shake-off which is one of the oldest methods for collecting mitotic cell population. Mitotic shake-off allows the collection of mitotic cells based on their morphology [16]. As the cells progress through mitosis, they become rounded and weakly adherent with the culture vessel. Hence, this simple morphological difference was exploited to enrich a mitotic cell population and these cells were then re-plated and collected at specified time points.

To validate the degree of synchronization and progression of cell cycle, we performed immunoblotting to determine the fluctuations in the levels of periodic (Cyclin B1, Spindly) and invariable proteins (FNTB, Cdk1) (Figs. 2a, 3a, and 4a). Time-lapse microscopy was used to monitor the progression of cells post synchronization to analyze the time required to complete mitosis and characterize cell cycle features (Figs. 2c, 3c, and 4c).

Fig. 1 (continued) interphase extracts were made. After 8-h release, MG132 was added for 2 h. Mitotic extracts were made using mitotic shake-off. For imaging, cells were released following the 2-h MG132 treatment and imaged every 10 min for 2 h

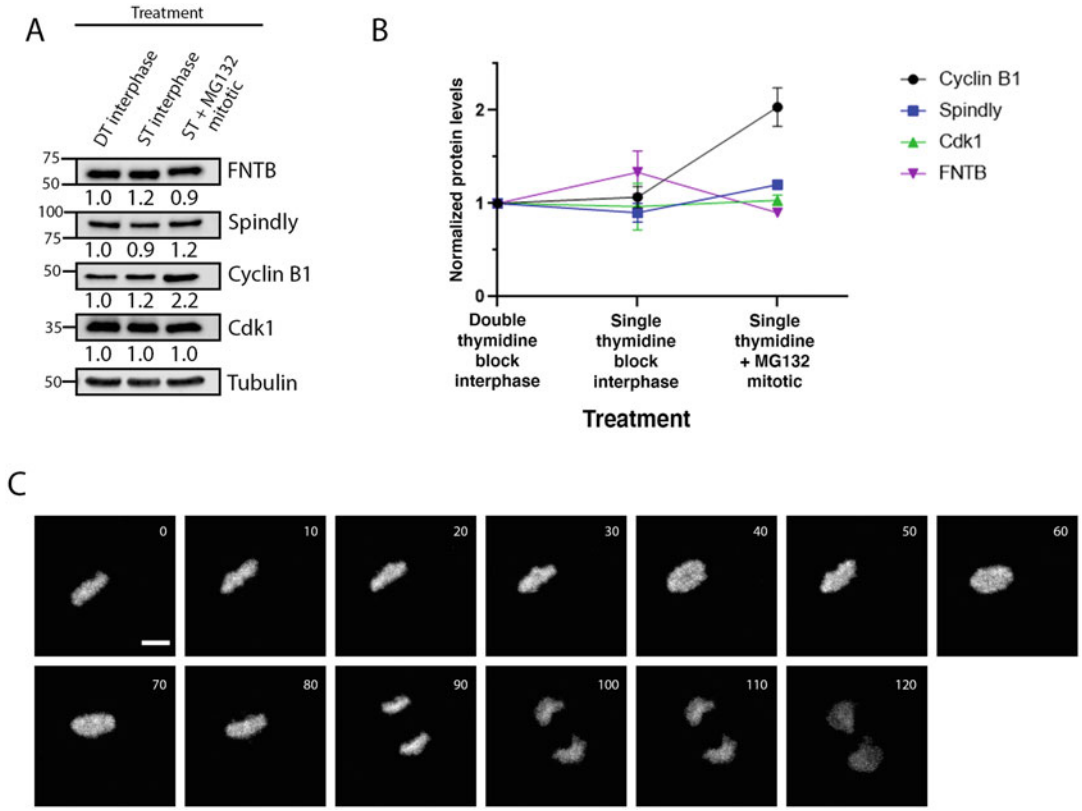

Fig. 2 Mitotic arrest by single thymidine block and MG132 treatment. (**a**) Western blot showing interphase and mitotic levels of FNTB, Spindly, Cyclin B, Cdk1, and Tubulin. Cells were treated with 2 mM thymidine for 16 h, released into fresh media for 8 h and then treated with 12.5 μM MG132 for 2 h. Mitotic cells were then collected by mitotic shake-off. Double thymidine (DT) and single thymidine (ST) blocked interphase cell extracts were made after thymidine block release. Protein levels were normalized to the Tubulin control. Quantification is shown below each blot. (**b**) Graph shows quantification of protein levels in double and single thymidine blocked interphase cells and MG132 blocked mitotic cells. (**c**) Images from timelapse microscopy. Cells were treated with 2 mM thymidine for 16 h, released into fresh media for 8 h and then treated with 12.5 μM MG132 for 2 h, then released and imaged every 10 min for 2 h. End of mitosis was determined when chromosomes separated in anaphase. Elapsed time shown in upper right corner. Scale bar 10 μm

2 Materials

2.1 Cell Culture

HeLa cells stably expressing mCherry-H2B and GFP-tubulin were previously described [17]. Cells were tested for *Mycoplasma* contamination by DAPI staining and confocal imaging. HeLa cells were grown as a monolayer in high-glucose DMEM supplemented with 2 mmol/L L-glutamine and 5% (vol/vol) FBS.

1. High glucose DMEM, Thermo Scientific #12430062.
2. Phosphate buffered saline (PBS): 1.37 M NaCl, 27 mM KCl, 100 mM Na_2HPO_4, and 18 mM KH_2PO_4.

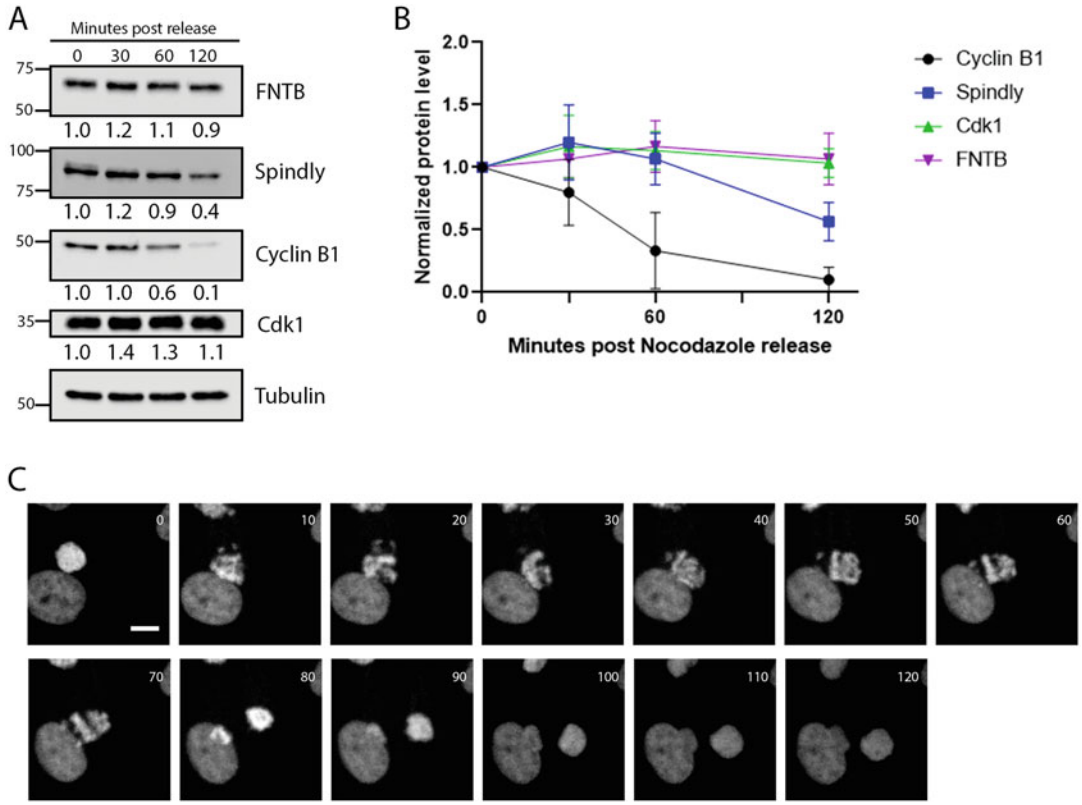

Fig. 3 Mitotic arrest by nocodazole treatment. (**a**) Western blot showing mitotic and post-mitotic levels of FNTB, Spindly, Cyclin B, Cdk1, and Tubulin. Cells were treated with 200 ng/mL nocodazole for 4 h and mitotic cells were collected by mitotic shake--off. Mitotic cells were replated for 30-, 60-, and 120-min time points. Extracts were collected at 0-, 30-, 60-, and 120-min post-release. Protein levels are normalized to the Tubulin control. Quantification is shown relative to time point zero. (**b**) Graph shows quantification of protein levels at 0, 30, 60, and 120 min. Protein levels were normalized to time point 0 min. (**c**) Images from timelapse microscopy. Cells were treated with 200 ng/mL Nocodazole for 4 h, then released and imaged every 10 min for 2 h. End of mitosis was determined when chromosomes separated in anaphase. Elapsed time shown in upper right corner. Scale bar 10 μm

3. Trypsin, Gibco, LS15400054.
4. 35 mm glass-bottomed plates, Matek, P35G-1.5-14-C.
5. 10 cm plates, Sarstedt, 83.3902.
6. 15 mL falcon tubes, Fischer, #14955238.
7. 50 mL falcon tubes, Fischer, #14955240.
8. 1.7 mL Eppendorf tubes, VWR #14955240.

2.2 Lysates

1. RIPA buffer, Thermo Scientific, #89900.
2. Protease inhibitor cocktail, EDTA-free, 100× in DMSO, Bimake #B14001.

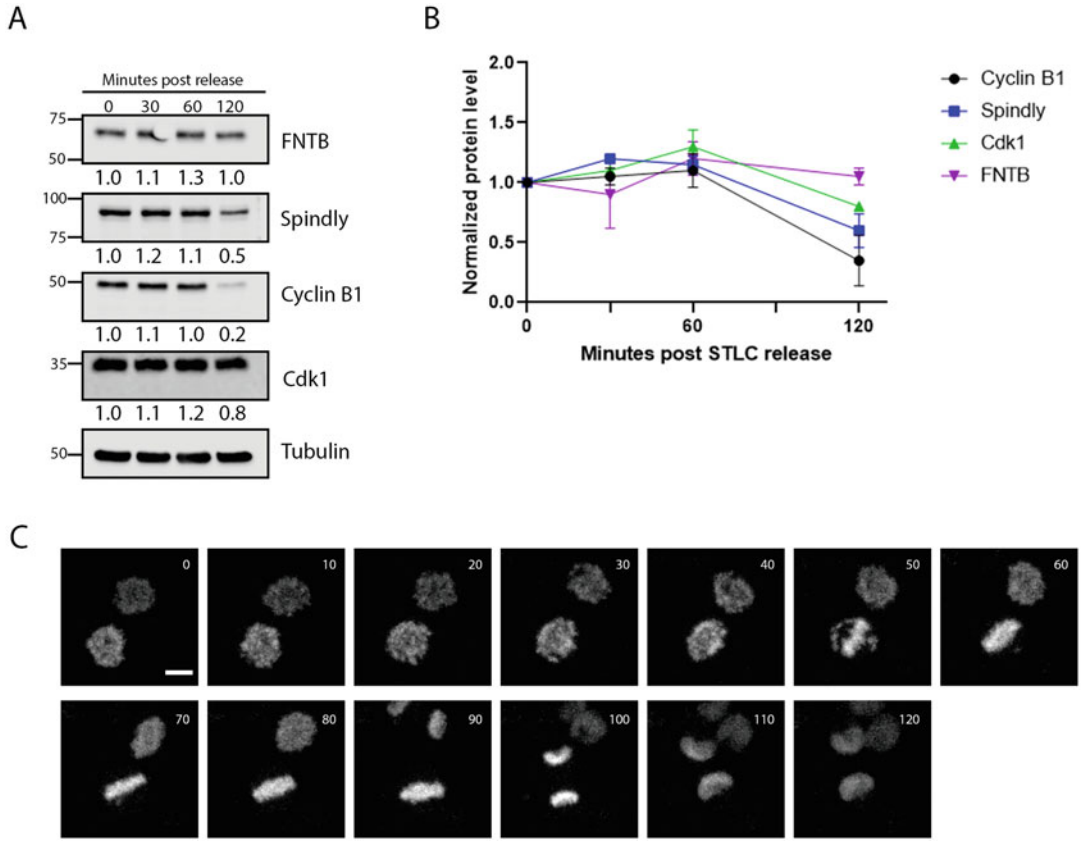

Fig. 4 Mitotic arrest by STLC treatment. (**a**) Western blot showing mitotic and post-mitotic levels of FNTB, Spindly, Cyclin B, Cdk1, and Tubulin. Cells were treated with 2.5 μM STLC for 4 h and mitotic cells were collected by mitotic shake-off. Mitotic cells were replated. Extracts were collected at 0-, 30-, 60-, and 120-min post release. Protein levels were normalized to Tubulin control. Quantification is shown (below each panel) relative to time point zero. (**b**) Graph shows quantification of protein levels at 0, 30, 60, and 120 min. Protein levels are normalized to time point 0 min. (**c**) Images from timelapse microscopy. Cells were treated with 2.5 μM STLC for 4 h, then released and imaged every 10 min for 2 h. End of mitosis was determined when chromosomes separated in anaphase. Elapsed time shown in upper right corner. Scale bar 10 μm

2.3 Western Blotting

1. Nitrocellulose membrane 0.45 μm, Bio-Rad #1620115.
2. Trans-Blot Turbo Transfer System, Bio-Rad #1704150.
3. Bio-Rad Trans-Blot Turbo transfer system 5× transfer buffer, Bio-Rad #1704270 20% 5× transfer buffer, 20% Methanol, 60% water.
4. Bio-Rad Trans-Blot Turbo mini size transfer stack, Bio-Rad #1704270.
5. Methanol.
6. Tris-buffered saline (TBS: 10×), 1.5 M NaCl, 0.1 M Tris-HCl, pH 7.4.

7. TBS containing 0.01% Tween-20 (TBS-T).
8. Blocking solution: 5% milk in TBS-T, store at 4 °C.
9. Mini PROTEAN glass plates, Bio-Rad #1653308.
10. 2× laemmli sample buffer containing 5% 2-Mercaptoethanol, Bio-Rad #1610737.
11. 0.5 mL Axygen tubes, Fisher Scientific #14222292.
12. Pierce BCA assay, ThermoFisher Scientific 23227.
13. PageRuler Plus Prestained protein ladder, ThermoFisher Scientific 26619.

2.4 Primary Antibodies

Protein	Species	Dilution	Company and catalogue number
Farnesyltransferase B	Rabbit	1:25000	Abcam, ab109625
hSpindly	Rat	1:1000	Moudgil et al. [17]
Tubulin	Mouse	1:10000	Sigma T5168
Cyclin B1	Rabbit	1:500	Santa Cruz, SC-752
CDK1 (Cdc2 p34)	Mouse	1:1000	Santa Cruz, SC-54

2.5 Secondary Antibodies

Fluorophore	Species	Dilution	Company and catalog number
Alexa Fluor 680	Rat	1:1000	Thermo Fisher Scientific, A21096
Alexa Fluor 680	Rabbit	1:1000	Thermo Fisher Scientific, A21109
Alexa Fluor 800	Rabbit	1:1000	Thermo Fisher Scientific, A32735
Alexa Fluor 680	Mouse	1:1000	Thermo Fisher Scientific, A21057
Alexa Fluor 800	Mouse	1:1000	Thermo Fisher Scientific, A32730

2.6 Spinning Disk Confocal Imaging

Live cell timelapse imaging on the spinning disk confocal microscope was performed as described previously [18].

1. Ultraview ERS Rapid confocal imager (PerkinElmer) on an Axiovert 200M Inverted Microscope (Carl Zeiss) and a CMOS camera (ORCAFlash4.0, Hamamatsu) using the 40× 1.3 oil objective lens. Cells were incubated at 37 °C and 5% CO_2 for the duration of imaging.
2. Images were captured at a 10-min interval for 2 h using the Volocity software.
3. The 561 nm laser was set to 2.5% power and 200 ms exposure time.
4. Movie files were exported as OMETIFF files and further processed in Photoshop v6.0 (Adobe).

2.7 Small Molecule Inhibitors

1. Nocodazole, 200 μg/mL stock, DMSO, Selleckchem # S2775.
2. Thymidine, 100 mM stock, PBS, Sigma #T1895-10G.
3. STLC, 9.7 mM stock, DMSO, Sigma # 164739.
4. MG132, 10 mM stock, DMSO, Calbiochem #474790.

3 Methods

3.1 Nocodazole Block

1. Plate HeLa cells with high glucose DMEM with 5% FBS.
   (a) 2×10^6 cells per 10 cm dish for Western blot extracts. 4 10 cm plates per time point, if doing 0, 30 min, 60 min, and 120 min seed 16 10 cm plates.
   (b) 2.5×10^5 cells in a Matek dish for imaging.
2. Incubate cells at 37 °C overnight.
3. Add nocodazole to a final concentration of 200 ng/μL, incubate in a tissue culture incubator at 37 °C for 4 h.

3.1.1 Western Blot

1. Remove mitotic cells by mitotic shake-off, collect media with mitotic cells in a 50 mL falcon tube. Wash dish with 5 mL of PBS to remove any remaining mitotic cells, add to 15 mL falcon tube with media. Combine 4 plates per tube.
2. Spin down media with mitotic cells: 5 min, 450 × *g* at 4 °C.
3. Remove media and resuspend pellet with 5 mL PBS.
4. Spin down PBS with mitotic cells, 5 min, 450 × *g* at 4 °C.
5. Resuspend cells in 10 mL fresh prewarmed media and replate for 30-, 60-, and 120-min time points.
6. Resuspend cells in 0 timepoint tube with RIPA buffer + Proteasome inhibitor, transfer to 1.7 mL Eppendorf tube and incubate on ice for 10 min.
7. Spin down lysate at 14,000 rpm for 12 min at 4 °C.
8. Aliquot soluble protein and discard cell debris pellet.
9. For 30- and 60-min time points collect all cells that are in suspension and adherent to the dish. Once cells are collected repeat **steps 6–8** for each time point.
10. For the 120-min time point, collect only adherent cells. Remove media, wash with 5 mL PBS, remove PBS and incubate cells with trypsin. Neutralize trypsin with media and add to 15 mL falcon tube. Follow **steps 6–8** with these cells.
11. Quantitate protein with BCA assay to load 20 μg protein per sample.
12. Run samples using a 10% SDS-PAGE gel, for 45 min at 200 V.

13. Transfer for 12 min at 25 V and 2.5 mA on the trans turbo blot system.
14. Block membrane in 5% milk in TBS-T for 2 h at room temperature.
15. Incubate with primary antibody, shaking overnight at 4 °C.
16. Remove primary antibody, wash for 5 min, 3 times with TBS-T.
17. Incubate with secondary antibody for 2 h at room temperature, shaking.
18. Remove secondary antibody, wash for 5 min, 3 times with TBS-T.
19. Image blot with Odessey IR imager system.
20. Quantify protein levels using Image Studio light V5.2 and standardize to Tubulin and then normalize to 0 time point.

3.1.2 Imaging

1. Wash 3 times with 2 mL prewarmed PBS, add 2 mL fresh pre-warmed media.
2. Image every 10 min for 2 h.

3.2 STLC Block

1. Plate HeLa cells with high glucose DMEM with 10% FBS.
   (a) 2×10^6 cells per 10 cm dish for Western blot extracts. 4 10 cm plates per time point, if doing 0, 30 min, 60 min, and 120 min seed 16 10 cm plates.
   (b) 2.5×10^5 cells in a Matek dish for imaging.
2. Incubate cells at 37 °C overnight.
3. Add STLC to a final concentration of 2.5 μM, incubate in a tissue culture incubator at 37 °C for 4 h.

3.2.1 Western Blot

1. Remove mitotic cells by mitotic shake-off, collect media with mitotic cells in a falcon tube. Wash dish with 5 mL of PBS to remove any remaining mitotic cells, add to 50 mL falcon tube with media. Combine 4 plates per tube.
2. Spin down media with mitotic cells: 5 min, 450 × *g* at 4 °C.
3. Remove media and resuspend pellet with 5 mL PBS.
4. Spin down PBS with mitotic cells, 5 min, 450 × *g* at 4 °C.
5. Resuspend cells in 10 mL fresh prewarmed media and replate for 30-, 60-, and 120-min time points.
6. Resuspend cells in 0 timepoint tube with RIPA buffer + Proteasome inhibitor, transfer to 1.7 mL Eppendorf tube and incubate on ice for 10 min.
7. Spin down lysate at 14,000 rpm for 12 min at 4 °C.

8. Aliquot soluble protein and discard cell debris pellet.
9. For 30- and 60-min time points collect all cells that are in suspension and adherent to the dish. Once cells are collected repeat **steps 6–8** for each time point.
10. For the 120-min time point, collect only adherent cells. Remove media, wash with 5 mL PBS, remove PBS and incubate cells with trypsin. Neutralize trypsin with media and add to a falcon tube. Follow **steps 6–8** with these cells.
11. Quantitate protein with BCA assay to load 20 μg protein per sample.
12. Run samples using a 10% SDS-PAGE gel, for 45 min at 200 V.
13. Transfer 12 min 25 V, 2.5 mA on the trans turbo blot system.
14. Block membrane in 5% milk in TBS-T for 2 h.
15. Incubate with primary antibody, shaking overnight at 4 °C.
16. Remove primary antibody, wash for 5 min, 3 times with TBS-T.
17. Incubate with secondary antibody for 2 h at room temperature, shaking.
18. Remove secondary antibody, wash for 5 min, 3 times with TBS-T.
19. Image blot with Odessey IR imager system.
20. Quantify protein levels using Image Studio light V5.2 and standardize to Tubulin and then normalize to 0 time point.

3.2.2 Imaging

1. Wash 3 times with 2 mL prewarmed PBS, add 2 mL fresh pre-warmed media.
2. Image every 10 min for 2 h.

3.3 Single Thymidine Block + MG132

1. Plate HeLa cells with high glucose DMEM with 10% FBS.
   (a) 2×10^6 cells per 10 cm dish for Western blot extracts.
   (b) 2.5×10^5 cells in a Matek dish for imaging.
2. Incubate cells at 37 °C overnight.
3. Add thymidine to a final concentration of 2 mM, incubate in a tissue culture incubator at 37 °C for 16 h overnight.
4. Release cells by removing media, washing 3 times with 8 mL of prewarmed PBS and add 10 mL fresh pre-warmed media.
5. Collect interphase cell extracts from one released dish.
6. Incubate cells at 37 °C for 8 h.
7. Add MG132 to a final concentration of 12.5 μM to thymidine-released plates. Incubate cells for 2 h at 37 °C.

3.3.1 Double Thymidine Block

Cells were synchronized in the G1/S phase by double thymidine block as previously described [19]. Cells were treated with 2 mM thymidine for 16 h with 8 h release interval between thymidine treatments. Following the 8-h release in **step 6** above, 2 mM thymidine is added for a second block for a further 16 h and then released.

3.3.2 Western Blot

1. Remove mitotic cells from the interphase plate and collect attached interphase cells.
2. Remove mitotic cells by mitotic shake-off, collect media with mitotic cells in a falcon tube. Wash dish with 5 mL of PBS to remove any remaining mitotic cells, add to 50 mL falcon tube with media. Combine 4 plates per tube.
3. Spin down media with mitotic cells: 5 min, 450 × *g* at 4 °C.
4. Remove media and resuspend pellet with 5 mL PBS.
5. Spin down PBS with mitotic cells, 5 min, 450 × *g* at 4 °C.
6. Resuspend cell pellet with RIPA buffer + Proteasome inhibitor, incubate on ice for 10 min.
7. Spin down samples, 14,000 rpm for 12 min at 4 °C.
8. Aliquot soluble protein and discard cell debris pellet.
9. Quantitate protein with BCA assay to load 20 μg protein per sample.
10. Run samples using a 10% SDS-PAGE gel, for 45 min at 200 V.
11. Transfer 12 min 25 V, 2.5 mA on trans turbo blot system.
12. Block membrane in 5% milk for 2 h.
13. Incubate with primary antibody, shaking overnight at 4 °C.
14. Remove primary antibody, wash for 5 min, 3 times with TBS-T.
15. Incubate with secondary antibody for 2 h at room temperature, shaking.
16. Remove secondary antibody, wash for 5 min, 3 times with TBS-T.
17. Image blot with Odessey IR imager system.
18. Quantify protein levels using Image Studio light V5.2 and standardize to Tubulin and then normalize to interphase cells.

3.3.3 Imaging

1. Wash 3 times with 2 mL prewarmed PBS, add 2 mL fresh pre-warmed media.
2. Image every 10 min for 2 h.

4 Notes

4.1 Cell Culture

1. Ensure dish is not more than 80% confluent before adding compounds.
2. Need at least 4 dishes per time point. If there is not enough protein for your needs, increase to 5–6 10 cm dishes per time point.

4.2 Western Blot

1. If having issues with visualizing protein levels using IR dye conjugated secondary, use HRP-linked secondary antibodies.

4.3 Imaging

1. Ensure the microscope is turned on a minimum 1 h before imaging for system to warm up at the appropriate temperature.
2. Place Matek dish in the chamber on the microscope for 1 h prior to beginning imaging to allow dish to be at correct temperature for system.
3. If cells are not exiting mitosis and arresting at metaphase, there is most likely phototoxicity, reduce laser lower and/or exposure time.
4. If possible, use red fluorescent proteins instead of green which can cause less toxicity.

Acknowledgments

We thank Drs. Guobin Sun and Xuejun Sun for help with live cell timelapse microscopy at the Cross Cancer Institute Cell Imaging Facility. SS is supported by an Alberta Cancer Foundation Antoine Noujaim Scholarship. The Chan laboratory was funded by NSERC (RGPIN-2016-06466) and CIHR (PJT-159585).

References

1. Weinberg RA (2014) The biology of cancer, 2nd edn. Garland Science, Taylor & Francis Group, New York
2. Lemmens B, Lindqvist A (2019) DNA replication and mitotic entry: a brake model for cell cycle progression. J Cell Biol 218(12): 3892–3902. https://doi.org/10.1083/jcb.201909032
3. Crasta K, Ganem NJ, Dagher R, Lantermann AB, Ivanova EV, Pan Y, Nezi L, Protopopov A, Chowdhury D, Pellman D (2012) DNA breaks and chromosome pulverization from errors in mitosis. Nature 482(7383):53–58. https://doi.org/10.1038/nature10802
4. Kubara PM, Kerneis-Golsteyn S, Studeny A, Lanser BB, Meijer L, Golsteyn RM (2012) Human cells enter mitosis with damaged DNA after treatment with pharmacological concentrations of genotoxic agents. Biochem J 446(3):373–381. https://doi.org/10.1042/BJ20120385
5. Ma HT, Poon RY (2017) Synchronization of HeLa cells. Methods Mol Biol 1524:189–201. https://doi.org/10.1007/978-1-4939-6603-5_12
6. Bjursell G, Reichard P (1973) Effects of thymidine on deoxyribonucleoside triphosphate pools and deoxyribonucleic acid synthesis in Chinese hamster ovary cells. J Biol Chem 248(11):3904–3909
7. Thomas DB, Lingwood CA (1975) A model of cell cycle control: effects of thymidine on synchronous cell cultures. Cell 5(1):37–42. https://doi.org/10.1016/0092-8674(75)90089-6

8. Wu WK, Wu YC, Yu L, Li ZJ, Sung JJ, Cho CH (2008) Induction of autophagy by proteasome inhibitor is associated with proliferative arrest in colon cancer cells. Biochem Biophys Res Commun 374(2):258–263. https://doi.org/10.1016/j.bbrc.2008.07.031
9. Han YH, Park WH (2010) MG132 as a proteasome inhibitor induces cell growth inhibition and cell death in A549 lung cancer cells via influencing reactive oxygen species and GSH level. Hum Exp Toxicol 29(7):607–614. https://doi.org/10.1177/0960327109358733
10. Famulski JK, Vos LJ, Rattner JB, Chan GK (2011) Dynein/dynactin-mediated transport of kinetochore components off kinetochores and onto spindle poles induced by nordihydroguaiaretic acid. PLoS One 6(1):e16494. https://doi.org/10.1371/journal.pone.0016494
11. Zieve GW, Turnbull D, Mullins JM, McIntosh JR (1980) Production of large numbers of mitotic mammalian cells by use of the reversible microtubule inhibitor nocodazole. Nocodazole accumulated mitotic cells. Exp Cell Res 126(2):397–405. https://doi.org/10.1016/0014-4827(80)90279-7
12. Matsui Y, Nakayama Y, Okamoto M, Fukumoto Y, Yamaguchi N (2012) Enrichment of cell populations in metaphase, anaphase, and telophase by synchronization using nocodazole and blebbistatin: a novel method suitable for examining dynamic changes in proteins during mitotic progression. Eur J Cell Biol 91(5):413–419. https://doi.org/10.1016/j.ejcb.2011.12.008
13. Barnum KJ, O'Connell MJ (2014) Cell cycle regulation by checkpoints. Methods Mol Biol 1170:29–40. https://doi.org/10.1007/978-1-4939-0888-2_2
14. Surani AA, Colombo SL, Barlow G, Foulds GA, Montiel-Duarte C (2021) Optimizing cell synchronization using nocodazole or double thymidine block. Methods Mol Biol 2329:111–121. https://doi.org/10.1007/978-1-0716-1538-6_9
15. Skoufias DA, DeBonis S, Saoudi Y, Lebeau L, Crevel I, Cross R, Wade RH, Hackney D, Kozielski F (2006) S-trityl-L-cysteine is a reversible, tight binding inhibitor of the human kinesin Eg5 that specifically blocks mitotic progression. J Biol Chem 281(26):17559–17569. https://doi.org/10.1074/jbc.M511735200
16. Tobey RA, Anderson EC, Petersen DF (1967) Properties of mitotic cells prepared by mechanically shaking monolayer cultures of Chinese hamster cells. J Cell Physiol 70(1):63–68. https://doi.org/10.1002/jcp.1040700109
17. Moudgil DK, Westcott N, Famulski JK, Patel K, Macdonald D, Hang H, Chan GK (2015) A novel role of farnesylation in targeting a mitotic checkpoint protein, human Spindly, to kinetochores. J Cell Biol 208(7):881–896. https://doi.org/10.1083/jcb.201412085
18. Lewis CW, Bukhari AB, Xiao EJ, Choi WS, Smith JD, Homola E, Mackey JR, Campbell SD, Gamper AM, Chan GK (2019) Upregulation of Myt1 promotes acquired resistance of cancer cells to Wee1 inhibition. Cancer Res. https://doi.org/10.1158/0008-5472.CAN-19-1961
19. Lewis CW, Jin Z, Macdonald D, Wei W, Qian XJ, Choi WS, He R, Sun X, Chan G (2017) Prolonged mitotic arrest induced by Wee1 inhibition sensitizes breast cancer cells to paclitaxel. Oncotarget 8(43):73705–73722. https://doi.org/10.18632/oncotarget.17848

Chapter 7

Synchronization of HeLa Cells to Various Interphases Including G1, S, and G2 Phases

Ping Wee, Richard C. Wang, and Zhixiang Wang

Abstract

The typical cell cycle in eukaryotes is composed of four phases including the G1, S, G2, and M phases. G1, S, and G2 together are called interphase. Cell synchronization is a process that brings cultured cells at different stages of the cell cycle to the same phase, which allows the study of phase-specific cellular events. While interphase cells can be easily distinguished from mitotic cells by examining their chromosome morphology, it is much more difficult to separate and distinguish the interphases from each other. Here, we describe drug-derived protocols for synchronizing HeLa cells to various interphases of the cell cycle: G1 phase, S phase, and G2 phase. G1 phase synchronization is achieved through serum starvation, S phase synchronization is achieved through a double thymidine block, and G2 phase synchronization is achieved through the release of the double thymidine block followed by roscovitine treatment. Successful synchronization can be assessed using flow cytometry to examine the DNA content and Western blot to examine the expression of various cyclins.

Key words Cell cycle, synchronization, interphase, mitosis, G1 phase, S phase, G2 phase, flow cytometry, Western blot

1 Introduction

The cell cycle is the series of events that drive a cell to divide and produce two new daughter cells. The typical cell cycle in eukaryotes is composed of four phases including the G1, S, G2, and M phases. G1, S, and G2 together are called interphase. Cells in the G1 can exit from the cell cycle and enter the G0 phase, a state of quiescence [1, 2]. Cell cycle progression is mediated by cyclin-dependent kinases (CDKs) and their regulatory cyclin subunits. CDKs, such as CDK4/6, CDK2, and CDK1 (also known as CDC2), are serine/threonine kinases with a wide variety of substrates. CDKs are mainly activated through binding to their cyclin partners, whose expressions rise and fall throughout the cell cycle to mediate the temporal activation of each CDK. Various cell cycle checkpoints exist to ensure that critical processes are engaged prior to progression to

Zhixiang Wang (ed.), *Cell-Cycle Synchronization: Methods and Protocols*, Methods in Molecular Biology, vol. 2579,
https://doi.org/10.1007/978-1-0716-2736-5_7,

the next phase. There are three major cell cycle checkpoints: the G1/S checkpoint (also referred as restriction point), the G2/M DNA damage checkpoint, and the spindle assembly checkpoint (SAC) [2–5].

Cell synchronization is a process that brings cultured cells at different stages of the cell cycle to the same phase. Cell synchronization is a vital process in the study of cell cycle progression and regulation. It allows population-wide data to be collected rather than relying solely on single-cell experiments.

Synchronization in mitosis can be achieved with relative ease. There are many different agents that can arrest cells in the different subphases of mitosis. It is also easier to confirm successful mitotic synchronization, as there are dramatic morphological differences between mitotic cells and interphase cells, as well as between the different subphases of mitosis. In contrast, the differences between the interphases are not morphologically obvious, and the synchronization of cells to the various interphases is technically different.

The most commonly used method to synchronize cells to the G1 phase is serum starvation. A double thymidine block is the most established method to synchronize cells to the early S phase, which is also a starting point for synchronizing cells to the other phases of the cell cycle, including G2 [6]. Thymidine is a DNA synthesis inhibitor that arrests cells that are at any stage of the S phase (DNA replication) [7, 8]. However, a single thymidine block results in cells being blocked at different stages of the S phase. A more uniform synchronization can be achieved by releasing this first thymidine block, which allows cells to resume DNA synthesis and S phase progression, and then applying a second thymidine block. This results in the synchronization of all cells to the early S phase [9]. Following the release of the second thymidine block, the cells synchronized to the early S phase will progress through the remaining cell cycle phases together. Using specific chemical inhibitors, these cells can then be synchronized to other phases of the cell cycle. For example, synchronization in G2 can be accomplished using the CDK inhibitor roscovitine, while addition of nocodazole will synchronize the cells to mitosis [10].

Here, we describe drug-derived protocols for synchronizing HeLa cells to various specific interphases of the cell cycle: G1 phase, S phase, and G2 phase (Fig. 1). This synchronization can be assessed by various methods, including flow cytometry to examine the DNA content and Western blot to examine the expression of various cyclins. The HeLa cell line is the most commonly used mammalian model system for cell cycle research. Its entire cell cycle lasts approximately 24 h, with the G1, S, G2, and M phases lasting approximately 11, 10, 2, and 1 h, respectively.

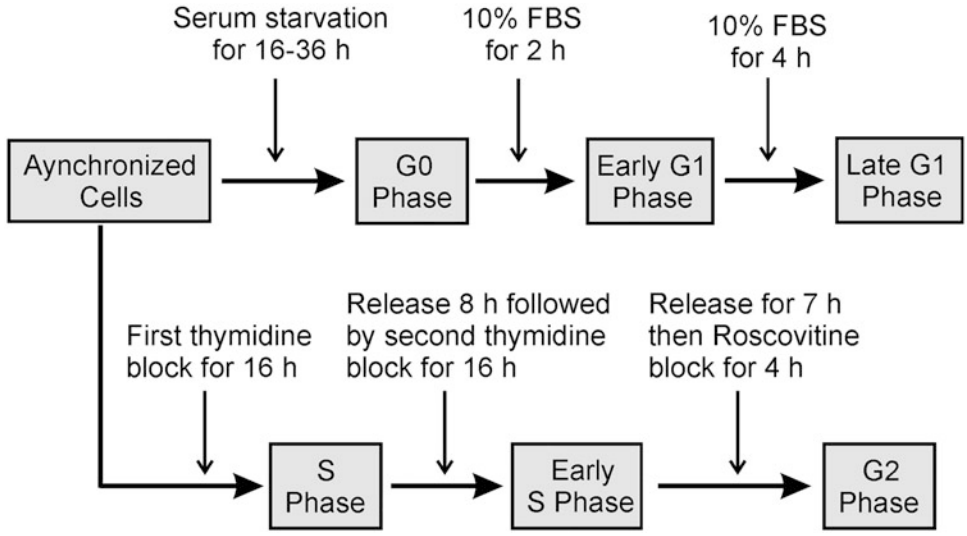

Fig. 1 Flow chart to show the steps of cell synchronization to various interphases

2 Materials

2.1 Solutions, Reagents, and Chemicals

1. Growth Medium: Dulbecco's modified Eagle's medium (DMEM) in 10% FBS (Hyclone) and 1× Antibiotic Antimycotic Solution.
2. PBS: 1× Phosphate Buffered Saline sterilized by autoclaving.
3. Thymidine stock: 200 mM in PBS. Dissolve completely and filter sterilize. Store at 4 °C. Working Concentration: 2 mM.
4. Roscovitine stock: 100 mM Roscovitine in DMSO. Store at −20 °C. Working Concentration: 50 μM.
5. Trypsin: 0.25% Trypsin, 0.03% EDTA (ethylenediaminetetraacetic acid).
6. TBS: Tris Buffered Saline sterilized by autoclaving.
7. Cell lysis buffer A: 50 mM Tris–HCl (pH 7.5), 0.25% Chap. Add fresh: Protease Inhibitor Mix (0.03%), Na_3VO_4 (0.01%) (inhibits protein phosphotyrosyl phosphatases).
8. Cell lysis buffer B: 500 mM Tris–HCl (pH 7.5), 10% Nonidet P-40.
9. Protease Inhibitor Mix: 0.1 mM AEBSF, 10 μg/mL Aprotinin, 1 μM Pepstatin in 100% EtOH.
10. SDS Loading Buffer (4×): 200 mM Tris–Cl (pH 6.8), 400 mM DTT, 8% SDS, 0.4% bromophenol blue, 40% glycerol.
11. 5% separating gel: In 15 mL tube add 0.625 mL acrylamide/bis-acrylamide 40% solution to 3.125 mL double-distilled

water (ddH_2O), 1.25 mL 1.5 M Tris-HCl buffer with pH 8.8 (lower gel buffer), 25 μL ammonium persulfate (APS), and 2.5 μL tetramethylethylenediamine (TEMED).

12. 4% stacking gel: In 15 mL tube add 250 μL acrylamide/bis-acrylamide 40% solution to 1.6 mL ddH_2O, 625 μL 0.5 M Tris–HCl buffer with pH 6.8 (higher gel buffer), 25 μL 10% SDS solution, 12.5 μL APS, and 2.5 μL TEMED.
13. 70% Ethanol.
14. Pre-stained molecular weight protein ladder.
15. Running buffer: dilute 10× Tris-Glycine-SDS buffer solution from Bio Basic Canada Inc. to 1× buffer solution which contains 0.025 M Tris Base, 0.192 M Glycin, and 0.1% SDS.
16. Transfer buffer: to prepare 500 mL transfer buffer add 400 mL ddH_2O to 2.91 g Tris (48 mM), 1.47 g glycine (39 mM), 1.88 mL 10% SDS solution and 100 mL methanol.
17. Antibodies to cyclin A, B, D, E.
18. HRP-conjugated secondary antibodies.
19. DRAQ5 (Biostatus): 0.5 mM.
20. Flow Cytometry Blocking Buffer: TBS, 0.01% Triton X-100, 4% BSA.
21. Ribonuclease (RNase) buffer with 100 μg/mL concentration of RNase A: add 10 μL Triton X-100 10% and 10 μL RNase A solution from 10 mg/mL stock solution to 1 mL 1× PBS.
22. Propidium iodide (PI) solution with 50 μg/mL concentration of PI: add 10 μL Triton X-100 10% and 50 μL PI solution from 1 mg/mL stock solution to 1 mL 1× PBS.

2.2 Equipment

1. Standard Tissue Culture Equipment.
2. Optical microscope.
3. Cell Culture Dishes: 100-mm.
4. Cell Culture Plate: 24-well plate.
5. Centrifuge for 15 mL centrifuge tubes that can reach 1,000 × g at 4 °C.
6. Microcentrifuge that can reach 14,000 × g at 4 °C.
7. Heated water bath.
8. Spectrophotometer.
9. Standard gel electrophoresis equipment.
10. Standard protein transfer equipment.
11. Standard X-ray film processing equipment.
12. Flow Cytometer.

2.3 Cell Lines

1. HeLa cell line stably expressing H2B-GFP (HeLa H2B-GFP). The HeLa H2B stable cell line is a generous gift from Dr. Wahl (The Salk Institute for Biological Studies)

3 Methods

3.1 G0/G1 Synchronization

G0/G1 synchronization is performed by serum starvation (*see* **Note 1**).

1. Seed 2.0 × 10^6 HeLa cells in 100-mm plates with 8 mL cell culture medium.
2. Culture cells at 37 °C with 5% CO_2.
3. Grow HeLa cells overnight to ~40% confluency.
4. Aspirate the medium and add 8 mL Serum-Starvation medium (*see* **Note 2**).
5. Culture the cells for 24 h to synchronize the cells to the G0 phase (*see* **Note 3**).
6. Aspirate the medium and add 8 mL growth medium for 2 h to drive the cells to re-enter the G1 phase (early G1 phase).
7. Alternatively, allow the cells to be incubated in growth medium for additional 4 h to harvest cells in the late G1 phase.

3.2 S phase Synchronization: Double Thymidine Block

The double thymidine block is a highly effective and widely used protocol for the synchronization of cells to the early S phase (*see* **Note 4**). Excess thymidine inhibits the formation of dCTP, an essential precursor of DNA, and thus halts DNA replication [7]. Importantly, it has been reported that excess thymidine does not block cells at the G1/S border, but that it instead considerably slows down the rate of DNA synthesis and the progression through the S phase [11]. Care should be taken to keep thymidine incubation times consistent.

1. Seed 2.0 × 10^6 HeLa cells in 100-mm plates with 8 mL cell culture medium.
2. Grow HeLa cells overnight to ~40% confluency.
3. Aspirate the medium and add 5 mL growth media with 500 μL 200 mM thymidine (final concentration of 2 mM).
4. Incubate for 16 h.
5. Aspirate the medium and release cells from the S-phase block by washing cells with 15 mL PBS three times.
6. Add 8 mL growth medium.
7. Incubate for 8 h.
8. Aspirate the medium and add 5 mL growth media with 500 μL 200 mM thymidine (final concentration of 2 μM).
9. Incubate for 16 h.

3.3 Late G2 Synchronization: Roscovitine

Roscovitine inhibits CDKs by competing with ATP at the ATP binding sites of various CDKs, including CDK1, CDK2, CDK5, and CDK7 [12]. Here, we release cells from the S phase block and allow them to progress into G2 before using roscovitine to prevent the activation of the CDK1/cyclin B1 complex (also known as maturation promoting factor) [10]. This prevents the cells from entering mitosis and therefore arrests them in late G2 (*see* **Note 5**).

1. Perform S-phase synchronization by double thymidine block (*see* **Note 6**).
2. Release cells from S-phase block by washing cells with 15 mL PBS three times.
3. Add 8 mL growth medium.
4. Incubate for 7 h.
5. Aspirate and add 5 mL of warm DMEM with 2.5 μL 100 mM roscovitine (final concentration of 50 μM).
6. Incubate for 4 h.

3.4 Validation of Synchronization by Western Blot

Probing with cell cycle markers by Western blot is necessary to provide confidence that samples are in the cell cycle stage they are claimed to be. Table 1 shows the expression of proteins throughout the cell cycle of HeLa cells that can be used as markers of synchronization. A popular family of cell cycle markers include the cyclin proteins, since specific cyclins are produced and degraded at specific phases of the cell cycle to drive cell cycle progression [13, 14]. G0 cells will be negative for all cyclin proteins. G1 cells will have maximal levels of Cyclin D (*see* **Note 7**). S phase cells will have the highest level of Cyclin E [15]. G2 phase cells will have the highest level of Cyclin A [15–17].

3.4.1 Protein Isolation

1. Synchronize the cells to each phase as described above.
2. Aspirate and wash cells with PBS. Aspirate as much PBS as possible.
3. Add 500 μL Cell Lysis Buffer A.
4. Put dish on ice and scrape cells using cell scraper.
5. Transfer scraped cells to a microcentrifuge tube and incubate on ice for 5 mins from the addition of Cell Lysis Buffer A.
6. Add 60 μL Cell Lysis Buffer B.
7. Incubate for 15 mins on a rotator at 4 °C.
8. Centrifuge at 14,000 × g at 4 °C for 15 mins.
9. Collect supernatant immediately and store at −80 °C until ready for use.

Table 1
Preparation of protein standard solutions with different concentrations and protein samples for protein quantification

Groups	PSS1	PSS2	PSS3	PSS4	PSS5	PSS6	PSS7	PS
Distilled water	18 μL	15 μL	12 μL	9 μL	6 μL	3 μL	0 μL	18 μL
Protein extraction buffer	2 μL	2 μL	2 μL	2 μL	2 μL	2 μL	2 μL	–
BSA (1×)	0 μL	3 μL	6 μL	9 μL	12 μL	15 μL	18 μL	2 μL
Bradford (1×)	1000 μL	1000 μL	1000 μL	1000 μL	1000 μL	1000 μL	1000 μL	1000 μL
Concentration (mg/mL)	0	4.44	8.88	13.32	17.76	22.2	26.64	?
Absorbance	?	?	?	?	?	?	?	?

PSS protein standard solution, *PS* protein sample

3.4.2 Protein Quantification

1. Prepare protein standard solutions with different concentrations and protein samples in separate tubes according to Table 1.
2. Incubate the tubes at room temperature for 5 mins.
3. Measure the absorbance of each protein standard solution and protein sample at 595 nm wavelength and write down the absorbance in the last row of Table 1.
4. Draw the standard curve by plotting the concentrations of each protein standard solutions against their absorbance.
5. Use the standard curve to calculate the concentrations of protein samples.

3.4.3 Western Blot

1. SDS Loading Buffer (4×) to each protein sample at a 1:3 ratio.
2. Incubate the protein samples in a 90–100 °C water bath for 5 mins (*see* **Note 8**).
3. Load 10–50 μg total protein sample to each well of 5 percent acrylamide gel.
4. Adjust the power supply at 100 V and run the electrophoresis for 185 mins.
5. Put the gel in transfer buffer and incubate it at room temperature with gentle shaking for 15 mins.
6. Prepare the protein transfer sandwich by putting the gel on the nitrocellulose paper and between two sets of filter papers.
7. Use the semi-dry transfer system at 15 V for 120 mins to transfer proteins onto the nitrocellulose paper (*see* **Note 9**).

Table 2
Expression of various cyclins throughout the cell cycle in HeLa GFP-H2B cells

	Cyclin D	Cyclin E	Cyclin A	Cyclin B
G0/early G1	−	−	−	−
Late G1	++	+	−	−
Early S-phase	−	++	+	−
Late G2	−	−	++	++

8. Incubate the membrane containing transferred proteins in blocking buffer at room temperature with gentle shaking for 1 h.
9. Dilute the primary antibodies (A-10 and A-2) in the blocking buffer at a 1:1000 ratio.
10. Incubate the membrane with the primary antibody solution at 4 °C for overnight.
11. Remove the primary antibody solution and wash the membrane three times, 10 mins per wash, in TBST at room temperature with gentle shaking.
12. Dilute the HRP-conjugated mouse secondary antibody in the diluted blocking buffer at a 1:2000 ratio.
13. Incubate the membrane with the secondary antibody solution at room temperature for 1 h.
14. Remove the secondary antibody solution and wash the membrane three times, 10 mins per wash, in TBST at room temperature with gentle shaking.
15. Incubate the membrane with ECL substrate solution for 5 mins at room temperature with gentle shaking and then detect the protein bands on X-ray film.

Table 2 lays out the expression of cell cycle markers that can be used to validate the synchronization methods.

3.5 Validation of Synchronization by Flow Cytometry

Flow cytometry analysis can be used to measure DNA content and validate successful interphase synchronization. G0/G1 cells have 2 N DNA, S-phase cells have 2-4 N DNA, and G2/M cells have 4 N DNA.

1. After completing cell cycle arrest, aspirate media and wash the cells with PBS once. Add 0.8 mL of Trypsin and incubate the cells in an incubator for 2.5 min. Add 4.2 mL PBS and detach cells by pipetting repeatedly. Collect cells in a pre-cooled 15 mL tube. Centrifuge cells at 1000 × g for 5 min. Aspirate liquid and resuspend cells in 0.5 mL PBS. Transfer cells to 4.5 mL of ice-cold 10% MeOH.

2. Fix cells for 20 min at −20 °C.
3. Centrifuge cells at 1000 × g for 5 min. Aspirate liquid and resuspend cells in 1 mL Flow Cytometry Blocking Buffer. Incubate for 10 min on ice.
4. Discard the supernatant and add 1 mL Ribonuclease (RNase) buffer to each tube and resuspend the cells gently by pipetting up and down.
5. Incubate the cells on ice for 30 min.
6. Centrifuge the cells at 1300–1500 rpm for 5 min.
7. Discard the supernatant and add 1 mL PI solution to each tube and resuspend the cells gently by pipetting up and down.
8. Incubate the cells on ice for 5–10 min.
9. Centrifuge cells at 1000 × g for 5 min. Aspirate liquid and wash cells with 1 mL ice-cold PBS. Repeat washing step.
10. Centrifuge cells at 1000 × g for 5 min. Aspirate liquid and resuspend cells well in 200 μL PBS with 2 μL 0.5 mM DRAQ5 (final concentration of 5 μM). Add cells to flow cytometry tube and incubate for 15 min at room temperature while protecting from light.
11. Run samples by flow cytometry analysis.
12. Use DNA content to distinguish between 2 N, 2–4 N, and 4 N, for G0/G1, S-phase, and G2 respectively.

A typic result of flow cytometry assessment of cell cycle synchronization is shown in Fig. 2.

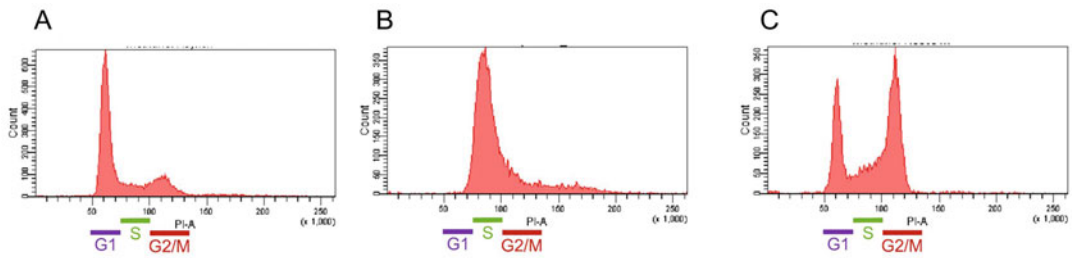

D

	G0/G1 Phase	S Phase	G2/M Phase
Asynchronous	50	37	13
Serum Starvation	70	11	19
Double Thymidine	2	75	23
Roscovitine	32	28	40

Fig. 2 Assessment of cell synchronization by flow cytometry. (**a**) Asynchronized Hela GFP-H2B cells. (**b**) Hela GFP-H2B cells synchronized to S phase. (**c**) Hela GFP-H2B cells synchronized to G2 phase. (**d**) Percentage of Hela GFP-H2B cells in various cell phases following the synchronization

4 Notes

1. G1 synchronization can also be performed with lovastatin (20 μM) for early G1 arrest [18], or mimosine (400 μM) [19], actinomycin D (0.1 μg/mL), or cycloheximide (10 μg/mL) [20] for late G1 arrest. Other cell types may be synchronized to G0 by serum starvation or contact inhibition. HeLa cells do not properly undergo G0 synchronization by serum starvation due to their p53 inactivation.
2. Depending on the cell type and specific clone of the cultured cells, the time for serum starvation may vary from 16 h to 36 h.
3. If cells become unhealthy due to serum starvation, 0.5% FBS could be included in the culture medium.
4. S phase synchronization can also be performed using DNA replication inhibitors, such as the DNA polymerase inhibitor aphidocolin (5 μg/mL) [21] or hydroxyurea (1.0–2.5 mM) [22].
5. G2 synchronization has also been performed with the reversible CDK inhibitor RO-3306 (9 μM), which specifically inhibits CDK1/Cyclin B1 activity [23, 24].
6. For G2 and mitotic synchronization, a prior single thymidine block may be sufficient, rather than a double thymidine block. This may also help minimize potential side effects.
7. Cyclin D1 expression can vary highly in other tumor cell lines, especially if they have perturbations in the Ras or Rb pathways.
8. Do not put the heated protein samples in too cold environment immediately. Leave them at room temperature for 2 mins in order to cool down slowly.
9. Running the semi-dry transfer device for a long time increases the transfer buffer temperature and causes buffer evaporation. To avoid any possible damages to proteins, gel, and nitrocellulose paper, saturate the protein transfer sandwich with transfer buffer.

References

1. Panagopoulos A, Altmeyer M (2021) The hammer and the dance of cell cycle control. Trends Biochem Sci 46(4):301–314
2. Wang Z (2021) Regulation of cell cycle progression by growth factor-induced cell signaling. Cell 10(12):3327
3. Barnum KJ, O'Connell MJ (2014) Cell cycle regulation by checkpoints. Methods Mol Biol (Clifton, NJ) 1170:29–40
4. Satyanarayana A, Kaldis P (2009) Mammalian cell-cycle regulation: several Cdks, numerous cyclins and diverse compensatory mechanisms. Oncogene 28(33):2925–2939
5. Gao X, Leone GW, Wang H (2020) Cyclin D-CDK4/6 functions in cancer. Adv Cancer Res 148:147–169
6. Ma HT, Poon RY (2011) Synchronization of HeLa cells. Methods Mol Biol (Clifton, NJ) 761:151–161

7. Bjursell G, Reichard P (1973) Effects of thymidine on deoxyribonucleoside triphosphate pools and deoxyribonucleic acid synthesis in Chinese hamster ovary cells. J Biol Chem 248(11):3904–3909
8. Schvartzman JB, Krimer DB, Van't Hof J (1984) The effects of different thymidine concentrations on DNA replication in pea-root cells synchronized by a protracted 5-fluorodeoxyuridine treatment. Exp Cell Res 150(2):379–389
9. Chen G, Deng X (2018) Cell synchronization by double thymidine block. Bio Protoc 8(17): e2994
10. Maurer M, Komina O, Wesierska-Gadek J (2009) Roscovitine differentially affects asynchronously growing and synchronized human MCF-7 breast cancer cells. Ann N Y Acad Sci 1171:250–256
11. Bostock CJ, Prescott DM, Kirkpatrick JB (1971) An evaluation of the double thymidine block for synchronizing mammalian cells at the G1-S border. Exp Cell Res 68(1):163–168
12. Whittaker SR, Walton MI, Garrett MD, Workman P (2004) The cyclin-dependent kinase inhibitor CYC202 (R-roscovitine) inhibits retinoblastoma protein phosphorylation, causes loss of cyclin D1, and activates the mitogen-activated protein kinase pathway. Cancer Res 64(1):262–272
13. Darzynkiewicz Z, Gong J, Juan G, Ardelt B, Traganos F (1996) Cytometry of cyclin proteins. Cytometry 25(1):1–13
14. Pozarowski P, Darzynkiewicz Z (2004) Analysis of cell cycle by flow cytometry. Methods Mol Biol (Clifton, NJ) 281:301–311
15. Dulić V, Lees E, Reed SI (1992) Association of human cyclin E with a periodic G1-S phase protein kinase. Science (New York, NY) 257(5078):1958–1961
16. Kraft C, Herzog F, Gieffers C, Mechtler K, Hagting A, Pines J, Peters JM (2003) Mitotic regulation of the human anaphase-promoting complex by phosphorylation. EMBO J 22(24): 6598–6609
17. Pines J, Hunter T (1990) Human cyclin a is adenovirus E1A-associated protein p60 and behaves differently from cyclin B. Nature 346(6286):760–763
18. Keyomarsi K, Sandoval L, Band V, Pardee AB (1991) Synchronization of tumor and normal cells from G1 to multiple cell cycles by lovastatin. Cancer Res 51(13):3602–3609
19. Park SY, Im JS, Park SR, Kim SE, Wang HJ, Lee JK (2012) Mimosine arrests the cell cycle prior to the onset of DNA replication by preventing the binding of human Ctf4/And-1 to chromatin via Hif-1α activation in HeLa cells. Cell Cycle (Georgetown, Tex) 11(4):761–766
20. Kim JH, Gelbard AS, Djordjevic B, Kim SH, Perez AG (1968) Action of daunomycin on the nucleic acid metabolism and viability of HeLa cells. Cancer Res 28(12):2437–2442
21. Pedrali-Noy G, Spadari S, Miller-Faurès A, Miller AO, Kruppa J, Koch G (1980) Synchronization of HeLa cell cultures by inhibition of DNA polymerase alpha with aphidicolin. Nucleic Acids Res 8(2):377–387
22. Pfeiffer SE, Tolmach LJ (1967) Inhibition of DNA synthesis in HeLa cells by hydroxyurea. Cancer Res 27(1):124–129
23. Vassilev LT, Tovar C, Chen S, Knezevic D, Zhao X, Sun H, Heimbrook DC, Chen L (2006) Selective small-molecule inhibitor reveals critical mitotic functions of human CDK1. Proc Natl Acad Sci U S A 103(28): 10660–10665
24. Dulla K, Daub H, Hornberger R, Nigg EA, Korner R (2010) Quantitative site-specific phosphorylation dynamics of human protein kinases during mitotic progression. Mol Cell Proteomics 9(6):1167–1181

Chapter 8

Synchronization of HeLa Cells to Mitotic Subphases

Ping Wee, Richard C. Wang, and Zhixiang Wang

Abstract

The cell cycle is a series of events leading to cell replication. When plated at low cell densities in serum-containing medium, cultured cells start to proliferate, moving through the four phases of the cell cycle: G1, S, G2, and M. Mitosis is the most dynamic period of the cell cycle, involving a major reorganization of virtually all cell components. Mitosis is further divided into prophase, prometaphase, metaphase, anaphase, and telophase, which can be easily distinguished from one another by protein markers and/or comparing their chromosome morphology under fluorescence microscope. The progression of the cell cycle through these mitotic subphases is tightly regulated by complicated molecular mechanisms. Synchronization of cells to the mitotic subphases is important for understanding these molecular mechanisms. Here, we describe a protocol to synchronize Hela cells to prometaphase, metaphase, and anaphase/telophase. In this protocol, Hela cells are first synchronized to the early S phase by a double thymidine block. Following the release of the block, the cells are treated with nocodazole, MG132, and blebbistatin to arrest them at prometaphase, metaphase, and anaphase/telophase, respectively. Successful synchronization is assessed using Western blot and fluorescence microscopy.

Key words Cell cycle, Synchronization, Mitosis, Prometaphase, Metaphase, Anaphase, Telophase, Fluorescence microscopy, Western blot

1 Introduction

The cell cycle is a series of events leading to cell replication. When plated at low cell densities in serum-containing medium, cultured cells start to proliferate, moving through the four phases of the cell cycle: G1, S, G2, and M. Growth factors regulate cell cycle progression, especially the G1-S progression. Growth factors must be present until the restriction point (R point) in the G1 phase to stimulate entry into the cell cycle and proliferation. After the R point, growth factors are no longer required to complete the other stages of the cell cycle [1–3].

The M phase is comprised of mitosis, in which the cell's nucleus divides, and cytokinesis, in which the cell's cytoplasm divides to form two daughter cells. Mitosis is the most dynamic period of the

Zhixiang Wang (ed.), *Cell-Cycle Synchronization: Methods and Protocols*, Methods in Molecular Biology, vol. 2579,
https://doi.org/10.1007/978-1-0716-2736-5_8,

cell cycle, involving a major reorganization of virtually all cell components. Mitosis is the most fragile period of the cell cycle. Therefore, most cancer drugs are designed to specifically target mitotic cells [4].

Mitosis is further divided into prophase, prometaphase, metaphase, anaphase, and telophase. Prophase is characterized by chromatin/chromosome condensation, centrosome separation, and nuclear membrane breakdown. This is followed by prometaphase, during which mitotic spindle microtubules attach to the kinetochores at the centromere of each chromosome. During metaphase, the sister chromatids are pulled back and forth by the kinetochore microtubules until they align along the equatorial plane. The next step is anaphase, which involves two mechanistically distinct steps: anaphase A and anaphase B. In anaphase A, the kinetochore microtubules shorten and cause the migration of each sister chromatid toward its respective pole. In anaphase B, the disjointed sister chromatids are further separated through elongation of the mitotic spindle in the midzone. In the final stage of mitosis, telophase, nuclear envelopes reform around the separated chromatids (now referred to as chromosomes) and chromosome de-condensation occurs [5, 6]. These mitotic subphases can be easily distinguished from one another by protein markers and/or comparing their chromosome morphology under fluorescence microscope. The progression of the cell cycle through these mitotic subphases is tightly regulated by complicated molecular mechanisms. Synchronization of cells to the mitotic subphases is important for understanding these molecular mechanisms. Here, we describe a protocol to synchronize Hela cells to prometaphase, metaphase, and anaphase/telophase (Fig. 1). In this protocol, Hela cells are first synchronized to the early S phase by a double thymidine block. Following the release of the block for 9 h, the cells are treated with nocodazole for 5 h to synchronize the cells to prometaphase. From here, the cells can be synchronized to either metaphase or anaphase/telophase. To synchronize the cells to metaphase, the cells are released from nocodazole inhibition and immediately treated with MG132 for 70 min. To synchronize the cells to anaphase/telophase, the cells are released from nocodazole inhibition and, after 20 min, treated with blebbistatin for 40 min. Successful synchronization to the different phases is assessed using fluorescence microscopy and Western blot.

2 Materials

2.1 Solutions, Reagents, and Chemicals

1. Growth Medium: Dulbecco's modified Eagle's medium (DMEM) in 10% FBS (Hyclone) and 1× Antibiotic Antimycotic Solution.

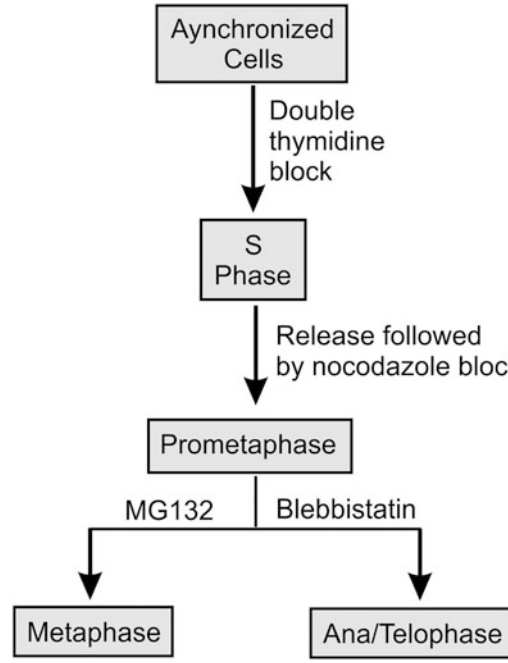

Fig. 1 Flow chart to show the steps of cell synchronization to various mitotic subphases

2. PBS: 1× Phosphate Buffered Saline sterilized by autoclaving.
3. Thymidine stock (Sigma): 200 mM in PBS. Dissolve completely and filter sterilize. Store at 4 °C. Working Concentration: 2 mM.
4. Nocodazole stock: 1 mg/mL in DMSO. Store at −20 °C. Working Concentration: 20 ng/mL.
5. MG132 stock: 25 mM in DMSO. Store at −20 °C. Working Concentration: 25 μM.
6. (S)-(-)-Blebbistatin stock: 5 mM in DMSO. Store at −20 °C. Working Concentration: 50 μM.
7. Trypsin: 0.25% Trypsin, 0.03% EDTA (ethylenediaminetetraacetic acid).
8. TBS: Tris Buffered Saline sterilized by autoclaving.
9. Cell lysis buffer A: 50 mM Tris-HCl (pH 7.5), 0.25% Chap. Add fresh: Protease Inhibitor Mix (0.03%), Na_3VO_4 (0.01%) (inhibits protein phosphotyrosyl phosphatases).
10. Cell lysis buffer B: 500 mM Tris-HCl (pH 7.5), 10% Nonidet P-40.
11. Protease Inhibitor Mix: 0.1 mM AEBSF, 10 μg/mL Aprotinin, 1 μM Pepstatin in 100% EtOH.

12. SDS Loading Buffer (4×): 200 mM Tris-Cl (pH 6.8), 400 mM DTT, 8% SDS, 0.4% bromophenol blue, 40% glycerol.
13. 5% separating gel: In 15 ml tube add 0.625 ml acrylamide/bis-acrylamide 40% solution to 3.125 ml double-distilled water (ddH_2O), 1.25 ml 1.5 M Tris-HCl buffer with pH 8.8 (lower gel buffer), 25 μl ammonium persulfate (APS), and 2.5 μl tetramethylethylenediamine (TEMED).
14. 4% stacking gel: In 15 ml tube add 250 μl acrylamide/bis-acrylamide 40% solution to 1.6 ml ddH_2O, 625 μl 0.5 M Tris-HCl buffer with pH 6.8 (higher gel buffer), 25 μl 10% SDS solution, 12.5 μl APS, and 2.5 μl TEMED.
15. 70% Ethanol.
16. Pre-stained molecular weight protein ladder.
17. Running buffer: dilute 10× Tris-Glycine-SDS buffer solution from Bio Basic Canada Inc. to 1× buffer solution which contains 0.025 M Tris Base, 0.192 M Glycin, and 0.1% SDS.
18. Transfer buffer: to prepare 500 ml transfer buffer add 400 ml ddH_2O to 2.91 g Tris (48 mM), 1.47 g glycine (39 mM), 1.88 ml 10% SDS solution, and 100 ml methanol.
19. Antibodies to cyclin A, B, p-Histone 3 Ser10, Securin, and p-BubR1 Ser676.
20. HRP-conjugated secondary antibodies.
21. Methanol.
22. Permeabilization solution (0.2% Triton X in PBS).
23. DAPI (4′,6-Diamidine-2′-phenylindole dihydrochloride) stock: 30 μM in PBS. Working Concentration: 300 nM.
24. Mounting Medium: n-Propyl Gallate in 10 mL boiled 50% glycerol.

2.2 Equipment

1. Standard Tissue Culture Equipment.
2. Optical microscope.
3. Cell Culture Dishes: 100-mm.
4. Cell Culture Plate: 24-well plate.
5. Centrifuge for 15 mL centrifuge tubes that can reach 1000 × *g* at 4 °C.
6. Glass slides.
7. Coverslips.
8. Fluorescence microscope.
9. Microcentrifuge that can reach 14,000 × *g* at 4 °C.
10. Heated water bath.
11. Spectrophotometer.

12. Standard gel electrophoresis equipment.
13. Standard protein transfer equipment.
14. Standard X-ray film processing equipment.

2.3 Cell Lines

1. HeLa cell line stably expressing H2B-GFP (HeLa H2B-GFP). The HeLa H2B stable cell line is a generous gift from Dr. Wahl (The Salk Institute for Biological Studies).

3 Methods

3.1 Synchronization of Cells to Prometaphase by Nocodazole

The microtubule depolymerizing agent nocodazole may be the most commonly used agent for inducing prometaphase arrest. It has a high affinity to tubulin, and it prevents tubulin-composed spindle microtubules from interacting properly with the kinetochores of chromosomes [7]. These chromosomes are therefore not brought to metaphase plate and cannot proceed past the spindle assembly checkpoint (SAC) [8] (*see* **Note 1**). Thus, nocodazole is an effective agent for arresting cells in early prometaphase. The following protocol for prometaphase synchronization is performed in two 150-mm culture dishes simultaneously to match the yield of interphase cells collected from one 100-mm dish. Notably, achieving a cell confluency of ~70% is ideal for later isolating synchronized cells using the mitotic shake-off method for assessment of synchronization by Western blot (described in Subheading 3.4).

1. Seed 5.0×10^6 HeLa cells in each 150-mm plate with 20 mL cell culture medium.
2. Grow HeLa cells overnight to ~40% confluency.
3. Aspirate the medium and add 10 mL growth media with 100 μL 200 mM thymidine (final concentration of 2 mM).
4. Incubate for 16 h.
5. Release cells from the S-phase block by aspirating the medium and washing cells with 30 mL PBS three times.
6. Add 10 mL growth medium.
7. Incubate for 8 h.

   Steps 8–11 is the repeat of **Steps 3–6**: thymidine block and release (*see* **Note 2**).
8. Aspirate the medium and add 10 mL growth media with 100 μL 200 mM thymidine (final concentration of 2 mM).
9. Incubate for 16 h.
10. Release cells from the S-phase block by aspirating the medium and washing cells with 30 mL PBS three times.
11. Add 10 mL growth medium.

12. Incubate for 9 h.
13. Aspirate and add 10 mL warm DMEM with 2 μL of 100 μg/mL nocodazole (final concentration of 20 ng/mL).
14. Incubate for 5 h.

3.2 Synchronization of Cells to Metaphase by MG132

The spindle assembly checkpoint (SAC) ensures all chromosomes are properly aligned prior to commencing anaphase [9]. Upon satisfying the requirements of the SAC, the anaphase-promoting complex (APC) is turned on and initiates the proteasomal degradation of cyclin B and securin [10–12]. This proteasomal activity allows sister chromatids to separate and thus transitions the cell from metaphase to anaphase. To synchronize the cells to metaphase, the proteasome inhibitor MG132 is added to cells after the cells are released from the nocodazole-induced prometaphase inhibition. MG132 allows chromosomes to proceed past the SAC but prevents cells from proceeding into anaphase [13].

1. Perform prometaphase synchronization as described above (Subheading 3.1).
2. Release cells from prometaphase arrest by washing cells with 30 mL PBS three times.
3. Add 10 mL warm DMEM with 10 μL of 25 mM MG132 (final concentration of 25 μM) to each dish.
4. Incubate for 70 min.

3.3 Anaphase/Telophase Synchronization: Blebbistatin

Anaphase/telophase are the most difficult phases to synchronize due in part to their short duration (20–30 min). There are no drugs known to completely block cells in anaphase or telophase. However, the myosin II inhibitor blebbistatin may be used to extend the duration of anaphase and telophase [14] (*see* **Note 3**).

1. Perform prometaphase synchronization as described above (Subheading 3.1).
2. Release cells from prometaphase arrest by washing cells with 30 mL PBS three times.
3. Add 10 mL warm DMEM to each dish.
4. Incubate for 20 min.
5. Add 100 μL 5 mM blebbistatin (final concentration of 50 μM).
6. Incubate for 40–55 min.

3.4 Validation of Synchronization by Western Blot

Probing with cell cycle markers by Western blot is necessary to provide confidence that samples are in the cell cycle stage they are claimed to be. Mitotic cells can first be distinguished from interphase cells by the presence of p-Histone 3 Ser10. Cells in different mitotic subphases can then be distinguished from one another using other protein markers. Metaphase cells can be distinguished

Table 1
Preparation of protein standard solutions with different concentrations and protein samples for protein quantification

Groups	PSS1	PSS2	PSS3	PSS4	PSS5	PSS6	PSS7	PS
Distilled water	18 μl	15 μl	12 μl	9 μl	6 μl	3 μl	0 μl	18 μl
Protein extraction buffer	2 μl	2 μl	2 μl	2 μl	2 μl	2 μl	2 μl	–
BSA (1×)	0 μl	3 μl	6 μl	9 μl	12 μl	15 μl	18 μl	2 μl
Bradford (1×)	1000 μl	1000 μl	1000 μl	1000 μl	1000 μl	1000 μl	1000 μl	1000 μl
Concentration (mg/ml)	0	4.44	8.88	13.32	17.76	22.2	26.64	?
Absorbance	?	?	?	?	?	?	?	?

PSS protein standard solution, *PS* protein sample

by their positive staining for p-BubR1 Ser676 [15]. Anaphase/telophase cells can be distinguished by their negative Securin, Cyclin B1, and Cyclin A staining [15, 16]. Table 1 shows the expression of these protein markers throughout the mitosis of HeLa cells.

To perform a Western blot, we need to first collect the synchronized mitotic cells to prepare cell lysates. Here, we describe the mitotic shake-off method used to isolate cells synchronized in prometaphase (Subheading 3.1), metaphase (Subheading 3.2), and anaphase/telophase (Subheading 3.3) for the purpose of Western blot analysis.

3.4.1 Protein Isolation

1. Synchronize the cells to each phase as described above.
2. Aspirate media and add 6 mL cold DMEM to each dish.
3. Perform mitotic shake-off. Place dishes on ice and knock the dishes to the sidewall of the ice bucket for 5 min (*see* **Note 4**). Care should be taken to keep consistency in the force used to shake the plates between different samples.
4. Transfer cells to a 15 mL centrifuge tube.
5. Centrifuge cells at 1000 × *g* for 5 min.
6. Add 6 mL ice-cold PBS to each dish and shake gently until centrifugation is complete.
7. Aspirate media from centrifuge tube. Add remaining cells from dishes to the centrifuge tube.
8. Centrifuge cells at 1000 × *g* for 5 min.
9. Aspirate media from the centrifuge tube.
10. Add 500 μL Cell Lysis Buffer A to cells. Transfer cells to a microcentrifuge tube and incubate on ice for 5 min.
11. Add 60 μL Cell Lysis Buffer B.

12. Incubate for 15 min on a rotator at 4 °C.
13. Centrifuge at 14,000 × *g* at 4 °C for 15 min.
14. Collect supernatant immediately and store at −80 °C until ready for use.

3.4.2 Protein Quantification

1. Prepare protein standard solutions with different concentrations and protein samples in separate tubes according to Table 1.
2. Incubate the tubes at room temperature for 5 min.
3. Measure the absorbance of each protein standard solution and protein sample at 595 nm wavelength and write down the absorbance in the last row of Table 1.
4. Draw the standard curve by plotting the concentrations of each protein standard solutions against their absorbance.
5. Use the standard curve to calculate the concentrations of protein samples.

3.4.3 Western Blot

1. SDS Loading Buffer (4×) to each protein sample at a 1:3 ratio.
2. Incubate the protein samples in 90–100 °C water bath for 5 min (*see* **Note 5**).
3. Load 10–50 μg total protein sample to each well of 5% acrylamide gel.
4. Adjust the power supply at 100 V and run the electrophoresis for 185 min.
5. Put the gel in transfer buffer and incubate it at room temperature with gentle shaking for 15 min.
6. Prepare the protein transfer sandwich by putting the gel on the nitrocellulose paper and between two sets of filter papers.
7. Use the semi-dry transfer system at 15 V for 120 min to transfer proteins onto the nitrocellulose paper (*see* **Note 6**).
8. Incubate the membrane containing transferred proteins in blocking buffer at room temperature with gentle shaking for 1 h.
9. Dilute the primary antibodies (A-10 and A-2) in the blocking buffer at a 1:1000 ratio.
10. Incubate the membrane with the primary antibody solution at 4 °C overnight.
11. Remove the primary antibody solution and wash the membrane three times, 10 min per wash, in TBST at room temperature with gentle shaking.
12. Dilute the HRP-conjugated mouse secondary antibody in the diluted blocking buffer at a 1:2000 ratio.

Table 2
Expression of protein markers throughout mitotic subphases in HeLa cells

	Cyclin A	Cyclin B	p-Histone 3 Ser10	Securin	p-BubR1 Ser676
Prometaphase	++	++	++	++	−
Metaphase	+	++	++	++	++
Ana/telophase	−	−	++	−	−

13. Incubate the membrane with the secondary antibody solution at room temperature for 1 h.
14. Remove the secondary antibody solution and wash the membrane three times, 10 min per wash, in TBST at room temperature with gentle shaking.
15. Incubate the membrane with ECL substrate solution for 5 min at room temperature with gentle shaking and then detect the protein bands on X-ray film.

Table 2 lays out the expression of cell cycle markers that can be used to validate the synchronization methods.

3.5 Validation of Synchronization by Fluorescence Microscopy

As previously described, each mitotic subphase is associated with its own chromosome morphology. Therefore, successful synchronization to the different subphases of mitosis can also be confirmed by looking at their chromosome morphology under fluorescence microscope. This is most easily accomplished if the synchronization treatments described in the previous sections are done with cells seeded in 24-well plates, which can be fixed and examined. For Hela H2B-GFP cells, the chromosomes should appear green due to H2B-GFP. For other cells, a simple protocol for staining chromosome with Dapi in 24-well plates is also provided.

1. Seed 5×10^4 HeLa cells on each coverslip in a 24-well plate with 0.5 mL growth medium.
2. Perform cell synchronization method of choice. Adapt protocols from 150-mm or 100-mm dishes to a 24-well plate.
3. Wash cells once with PBS. Aspirate PBS.
4. Fix cells by adding 0.5 mL ice-cold MeOH. Fix for 20 min at −20 °C.
5. Wash cells once with PBS. Aspirate PBS.
6. Permeabilize the cells with the Permeabilization solution.
7. Add 500 μL PBS with 1:100 DAPI. Incubate on ice for 10 min, protected from light (*see* **Note 7**).
8. Aspirate and wash twice with PBS.
9. Mount cells onto glass slide with 2.8 μL mounting medium.

10. Seal edges with nail polish.
11. Visualize cells by fluorescence for GFP (for Hela H2B-GFP cells) or Dapi (for other cells) (*see* **Note 8**). The rate of synchronization can be calculated by counting the number of cells in interphase, prophase, prometaphase, metaphase, anaphase, and telophase, as well as any morphologically abnormal cells.

The following is a guide we use to identify each mitotic stage, as well as the sub-stages often found in the literature. Prophase is the period when the chromosomes begin to condense, but a nuclear shape is still largely maintained since the nuclear envelope is still intact. Prometaphase is a long period of transition between prophase and metaphase and begins after the nuclear envelope has broken down [17] and the nucleolus has disappeared [18]. During early prometaphase, the chromosomes appear disorganized. In late prometaphase, all sister chromatids are attached to spindle microtubules in a bi-oriented fashion towards the metaphase plate. Metaphase starts when the duplicated chromosomes are aligned along the metaphase plate in the middle of the cell. In anaphase, the chromatids have started separating, with the degree of separation increasing with the progression of anaphase until the cell membrane begins to pinch slightly and the chromosomes have almost reached their respective poles. Telophase begins when the chromosomes have been pulled to the opposite poles of the cell. In late telophase, the chromosomes have despiralized and the nuclear envelop has reformed [3, 19] (*see* **Note 9**).

As revealed by fluorescence microscopy, cells in this protocol were highly synchronized to the various mitotic subphases, including prometaphase, metaphase, and anaphase/telophase (Fig. 2).

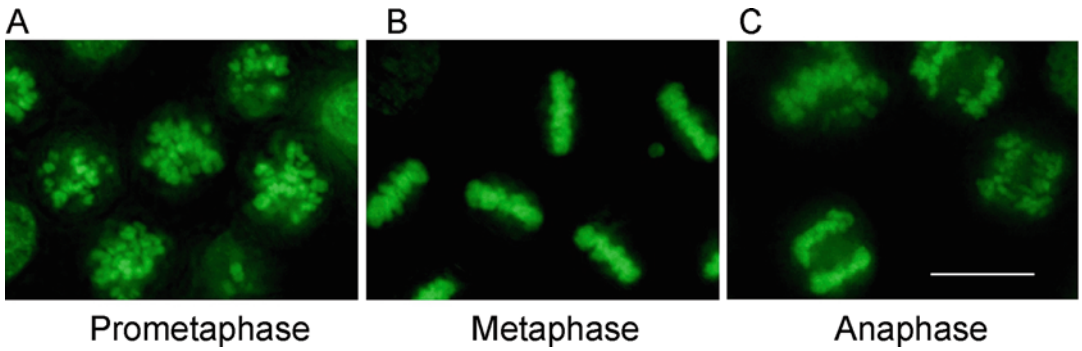

Fig. 2 Assessment of cell synchronization by fluorescence microscopy. (**a**) Hela GFP-H2B cell synchronized to prometaphase. (**b**) Hela GFP-H2B cells synchronized to metaphase. (**c**) Hela GFP-H2B cells synchronized to anaphase/telophase. Size bar = 10 μm

4 Notes

1. Since it destabilizes spindle microtubules, nocodazole treatment leads to many unattached kinetochores, and thus synchronizes cells to early prometaphase [7]. This is different from paclitaxel (Taxol) treatment, which does not prevent the attachment of microtubules to kinetochores but instead stabilizes spindle microtubules and prevents them from moving chromosomes to the central metaphase plate. Thus, Taxol treatment synchronizes cells to late prometaphase. Mitotic synchronization can also be achieved using vinca alkaloids, including colchicine and colcemid.
2. For G2 and mitotic synchronization, a prior single thymidine block may be sufficient, rather than a double thymidine block. This may also help minimize potential side effects.
3. Blebbistatin inhibits the ingression of the cleavage furrow. Thus, the anaphase/telophase synchronization protocol can be further tweaked to increase the number of anaphase cells or telophase cells by increasing or decreasing the duration of blebbistatin treatment.
4. Mitotic shake-off is performed on ice in order to slow intracellular signaling. We compress the ice in the bucket to make a smoother shaking surface.
5. Do not put the heated protein samples in too cold environment immediately. Leave them at room temperature for 2 min in order to cool down slowly.
6. Running the semi-dry transfer device for a long time increases the transfer buffer temperature and causes buffer evaporation. To avoid any possible damages to proteins, gel, and nitrocellulose paper, saturate the protein transfer sandwich with transfer buffer.
7. For HeLa H2B-GFP cells, this step can be omitted as chromatin/chromosomes stain green by GFP under fluorescence microscope.
8. Validation of synchronization may also be performed by live imaging fluorescence microscopy using HeLa H2B-GFP cells. However, the user must be certain that the conditions in the microscope's growth chamber completely reflect the conditions of the incubator.
9. Other markers may be used to better differentiate between mitotic stages. For example, prophase may be more easily visualized by translocation of CDK1/Cyclin B1 to the nucleus. Tubulin staining can help differentiate early anaphase cells from prometaphase cells.

References

1. Jones SM, Kazlauskas A (2001) Growth factor-dependent signaling and cell cycle progression. FEBS Lett 490(3):110–116
2. Massague J (2004) G1 cell-cycle control and cancer. Nature 432(7015):298–306
3. Wang Z (2021) Regulation of cell cycle progression by growth factor-induced cell signaling. Cell 10(12):3327
4. Chan KS, Koh CG, Li HY (2012) Mitosis-targeted anti-cancer therapies: where they stand. Cell Death Dis 3:e411
5. Afonso O, Matos I, Pereira AJ, Aguiar P, Lampson MA, Maiato H (2014) Feedback control of chromosome separation by a midzone Aurora B gradient. Science (New York, NY) 345(6194):332–336
6. Vukušić K, Tolić IM (2021) Long-standing models meet new concepts. Semin Cell Dev Biol 117:127–139
7. Lara-Gonzalez P, Westhorpe FG, Taylor SS (2012) The spindle assembly checkpoint. Curr Biol 22(22):R966–R980
8. Zieve GW, Turnbull D, Mullins JM, McIntosh JR (1980) Production of large numbers of mitotic mammalian cells by use of the reversible microtubule inhibitor nocodazole. Nocodazole accumulated mitotic cells. Exp Cell Res 126(2):397–405
9. Li R, Murray AW (1991) Feedback control of mitosis in budding yeast. Cell 66(3):519–531
10. Holloway SL, Glotzer M, King RW, Murray AW (1993) Anaphase is initiated by proteolysis rather than by the inactivation of maturation-promoting factor. Cell 73(7):1393–1402
11. Hornig NC, Knowles PP, McDonald NQ, Uhlmann F (2002) The dual mechanism of separase regulation by securin. Curr Biol 12(12):973–982
12. Waizenegger I, Giménez-Abián JF, Wernic D, Peters JM (2002) Regulation of human separase by securin binding and autocleavage. Curr Biol 12(16):1368–1378
13. Dulla K, Daub H, Hornberger R, Nigg EA, Korner R (2010) Quantitative site-specific phosphorylation dynamics of human protein kinases during mitotic progression. Mol Cell Proteomics 9(6):1167–1181
14. Matsui Y, Nakayama Y, Okamoto M, Fukumoto Y, Yamaguchi N (2012) Enrichment of cell populations in metaphase, anaphase, and telophase by synchronization using nocodazole and blebbistatin: a novel method suitable for examining dynamic changes in proteins during mitotic progression. Eur J Cell Biol 91(5):413–419
15. Elowe S, Hümmer S, Uldschmid A, Li X, Nigg EA (2007) Tension-sensitive Plk1 phosphorylation on BubR1 regulates the stability of kinetochore microtubule interactions. Genes Dev 21(17):2205–2219
16. Widrow RJ, Laird CD (2000) Enrichment for submitotic cell populations using flow cytometry. Cytometry 39(2):126–130
17. Güttinger S, Laurell E, Kutay U (2009) Orchestrating nuclear envelope disassembly and reassembly during mitosis. Nat Rev Mol Cell Biol 10(3):178–191
18. Gavet O, Pines J (2010) Progressive activation of CyclinB1-Cdk1 coordinates entry to mitosis. Dev Cell 18(4):533–543
19. Eggert US, Mitchison TJ, Field CM (2006) Animal cytokinesis: from parts list to mechanisms. Annu Rev Biochem 75:543–566

Chapter 9

Cell Cycle Synchronization of Primary and Cultured Articular Chondrocytes

Loraine L. Y. Chiu, Omar D. Subedar, and Stephen D. Waldman

Abstract

Cell cycle synchronization allows cells in a culture, originally at different stages of the cell cycle, to be brought to the same phase. It is normally performed by applying cell cycle arresting chemical agents to cells cultured in monolayer. While effective, isolated chondrocytes tend to dedifferentiate when cultured in monolayer and typically require 3D culturing methods to ensure phenotypic stability. Here, we describe both the conventional cell cycle synchronization method for cells in monolayer culture and an adapted method of synchronizing primary chondrocytes directly during the cell isolation process to limit potential dedifferentiation. Different methods including serum-starvation and treatment with thymidine, nocodazole, aphidicolin, and RO-3306 can synchronize the chondrocytes at different discrete phases. A cell purity of more than 90% in the S phase can be achieved with simultaneous cell isolation and synchronization using double thymidine treatment, generating a population of synchronized chondrocytes that show increased matrix synthesis when subsequently cultured in 3D.

Key words Cell cycle, Synchronization, Articular chondrocytes, Primary cells, Cell monolayers

1 Introduction

Damage to the articular cartilage tissue, due to injury, disease, or deterioration, leads to joint pain and loss of mobility [1–3]. Autologous osteochondral transfer [4] and cell transplantation [5, 6] are common current articular cartilage repair strategies; however, these approaches are limited respectively by donor site morbidity and low cell retention at the defect site. Cartilage tissue engineering provides an alternative treatment option, involving the in vitro development of replacement cartilage tissue to be used for articular cartilage repair.

The in vitro generation of engineered cartilage tissues of appropriate size, thickness, biochemical composition, and functional properties remains a challenge. Various strategies, such as the use of growth factors and mechanical stimulation [7–14], have been investigated to enhance the deposition of cartilaginous extracellular

Zhixiang Wang (ed.), *Cell-Cycle Synchronization: Methods and Protocols*, Methods in Molecular Biology, vol. 2579,
https://doi.org/10.1007/978-1-0716-2736-5_9,

matrix and in turn functional properties of engineered cartilage tissues. However, the population of isolated chondrocytes is a nonhomogeneous one. Particularly, there are differences in the progression of individual chondrocytes through the cell cycle [15], which affects both their macromolecular biosynthesis [16–18] and responses to stimuli [19–21]. Cell cycle synchronization can be used as a means to create a homogeneous cell population at a discrete cell cycle phase that is most sensitive to the applied tissue engineering stimuli.

Commonly used cell cycle synchronization methods involve the application of cell cycle arresting chemical agents in monolayer culture, which results in undesired dedifferentiation in the case of chondrocytes [22]. Here, we describe the conventional cell cycle synchronization procedure for cell monolayers [23–27] and present an adapted method to synchronize primary chondrocytes during the process of cell isolation, thereby eliminating the need for monolayer culture [28]. In this method, different treatments such as serum-starvation, thymidine, nocodazole, aphidicolin, and RO-3306 can be applied simultaneously with the cell isolation process to synchronize primary articular chondrocytes at different cell cycle phases. Specifically, we have shown that the double thymidine treatment can yield more than 90% chondrocytes in the S phase, and that these synchronized chondrocytes show increased glycosaminoglycan and collagen II deposition compared to unsynchronized chondrocytes [28].

2 Materials

2.1 Tissue Harvest

1. Metacarpophalangeal joints of cows: obtained from a local abattoir immediately after slaughter (*see* **Note 1**).
2. Scalpel handle (no. 3) and blade (no. 11).
3. Petri dishes: 100 mm.
4. Ham's F12 media: Ham's F12 with 25 mM (4-(2-hydroxyethyl)-1-piperazineethanesulfonic acid) in deionized water, pH 7.4, sterile filtered. Store at 4 °C. Warm to 37 °C in a water bath before use.
5. Antibiotic-antimycotic.
6. Complete media: Ham's F12 media with 10% fetal bovine serum (FBS) and 1% antibiotic-antimycotic. Store at 4 °C. Warm to 37 °C in a water bath before use.

2.2 Cell Isolation and Synchronization

1. Protease solution: 0.5% w/v protease in Ham's F12 media (*see* **Note 2**).
2. Collagenase A solution: 0.15% w/v collagenase A in Ham's F12 media (*see* **Note 3**).

3. Aphidicolin-supplemented collagenase solution: 5 μg/mL aphidicolin in Collagenase A solution with 10% FBS (*see* **Note 3**).
4. Thymidine-supplemented complete media: 10 mM thymidine in complete media (*see* **Note 4**).
5. Thymidine-supplemented collagenase solution:10 mM thymidine in Collagenase A solution with 10% FBS (*see* **Note 3**).
6. Nocodazole-supplemented collagenase solution: 100 ng/mL nocodazole in Collagenase A solution with 10% FBS (*see* **Note 3**).
7. RO-3306-supplemented collagenase solution: 10 μM RO-3306 in Collagenase A solution with 10% FBS (*see* **Note 3**).
8. Cell strainer: 70 μm.
9. Phosphate buffered saline (PBS): 1× PBS powder dissolved in deionized water.
10. Alginic acid solution: 1.25% w/v alginic acid in PBS with 20 mM HEPES and 150 mM sodium chloride, pH 7.4, sterile filtered.
11. Calcium chloride bath: 102 mM calcium chloride in PBS with 10 mM HEPES, pH 7.4, sterile filtered.
12. Forceps: autoclave sterilized.
13. Ascorbic acid: 50 mg/mL l-ascorbic acid in PBS, aliquoted in black Eppendorf tubes. Store at −20 °C (*see* **Note 5**).
14. Growth media: Complete media supplemented with 100 μg/mL ascorbic acid (*see* **Note 6**).

2.3 Cell Monolayer Culture

1. Tissue culture flask: T75 flask.
2. Centrifuge tubes: 50 mL.
3. Trypsin: 10× trypsin-EDTA solution.

2.4 Cell Recovery and Flow Cytometry

1. Calcium chelating solution: 55 mM ethylenediaminetetraacetic acid (EDTA) in PBS.
2. Trypan blue solution: 0.4% trypan blue.
3. Ethanol: 80% ethanol in deionized water.
4. Triton-x100 solution: 10% Triton-x100 in PBS.
5. Propidium iodide: Abcam, ab139418.

3 Methods

3.1 Synchronization of Cultured Articular Chondrocytes in Monolayer

Harvest articular cartilage explants and digest in protease and collagenase solutions to isolate chondrocytes. Seed and culture isolated cells in tissue culture flasks. Synchronize the chondrocytes by applying thymidine treatment to the cell monolayers. Recover the chondrocytes using trypsin. All steps should be performed under aseptic conditions using a Class II biological safety cabinet.

1. Harvest articular cartilage explants (~10–15 full-thickness slices using a scalpel, no bone) from the articular surfaces of the metacarpophalangeal joints of cows (obtained from a local abattoir) under sterile conditions. Place cartilage explants (<5 mm × 5 mm × 1 mm) into a 100 mm Petri dish containing 20 mL Ham's F12 media with 1% antibiotic-antimycotic.
2. Digest cartilage explants with protease solution by aspirating the media and adding 20 mL protease solution. Incubate for 1 h at 37 °C and 5% CO_2.
3. Aspirate the protease solution and add 20 mL collagenase A solution. Incubate for 12 h at 37 °C and 5% CO_2.
4. Pipette the cell digest up and down. Incubate for 1 h at 37 °C and 5% CO_2.
5. Put the cell digest through a 70 μm cell strainer into a 50 mL centrifuge tube.
6. Wash cells by centrifuging them at 700 × *g* for 7 min and resuspending them in 20 mL Ham's F12 media. Repeat.
7. Count cells using a hemacytometer and the trypan blue exclusion method [29].
8. Centrifuge cells at 700 × *g* for 7 min. Resuspend cells in complete media and seed 500,000 cells in 15 mL complete media in a tissue culture flask. Incubate at 37 °C and 5% CO_2 overnight.
9. Apply different cell synchronization methods as follows (*see* **Note 7**):
   (a) Serum starvation for synchronization in the G_0/G_1 phase [23]: Remove media from the flask and wash with pre-warmed PBS. Add 15 mL Ham's F12 media to the flask. Incubate at 37 °C and 5% CO_2 for 18 h to synchronize cells at the G_0/G_1 phase. Remove media and wash cells with 15 mL pre-warmed PBS.
   (b) Aphidicolin treatment for synchronization in the S phase [24]: Remove media from the flask and add 15 mL 5 μg/mL aphidicolin in complete media to the flask. Incubate at 37 °C and 5% CO_2 for 24 h to synchronize cells at the S phase. Remove aphidicolin and wash cells with 15 mL pre-warmed PBS.

(c) Double thymidine treatment for synchronization in the S phase [25]: Remove media from the flask and add 15 mL 2 mM thymidine in complete media to the flask. Incubate at 37 °C and 5% CO_2 for 18 h. Remove thymidine and wash cells with 15 mL pre-warmed PBS. Remove PBS and add 15 mL complete media. Incubate at 37 °C and 5% CO_2 for 9 h. Remove complete media and add 15 mL 2 mM thymidine in complete media. Incubate at 37 °C and 5% CO_2 for 18 h to synchronize cells at the G_1/S boundary. Release cells by removing thymidine and washing with pre-warmed PBS.

(d) Thymidine-nocodazole treatment for synchronization in the G_2/M phase [26]: Remove media from the flask and add 15 mL 2 mM thymidine in complete media to the flask. Incubate at 37 °C and 5% CO_2 for 20 h. Remove thymidine and wash cells with 15 mL pre-warmed PBS. Remove PBS and add 15 mL complete media. Incubate at 37 °C and 5% CO_2 for 5 h. Remove complete media and add 15 mL 50 ng/mL nocodazole in complete media. Incubate at 37 °C and 5% CO_2 for 10 h to synchronize cells at the G_2/M boundary. Release cells by removing nocodazole and washing with pre-warmed PBS.

(e) Thymidine-RO-3306 treatment for synchronization in the G_2/M phase [27]: Remove media from the flask and add 15 mL 2 mM thymidine in complete media to the flask. Incubate at 37 °C and 5% CO_2 for 24 h. Remove thymidine and wash cells with 15 mL pre-warmed PBS. Remove PBS and add 15 mL complete media. Incubate at 37 °C and 5% CO_2 for 5 h. Remove complete media and add 15 mL 10 μM RO-3306 in complete media. Incubate at 37 °C and 5% CO_2 for 12 h to synchronize cells at the G_2/M boundary. Release cells by removing RO-3306 and washing with pre-warmed PBS.

10. Remove PBS and add 15 mL growth media.
11. For subsequent flow cytometry analyses (Subheading 3.3), lift cells from the flask surface by removing growth media and incubating cells with 3 mL trypsin at 37 °C and 5% CO_2 for 5 min. Neutralize trypsin by adding 7 mL complete media. Transfer cell suspension to a centrifuge tube. Centrifuge cells at 700 × *g* for 7 min and resuspend them in Ham's F12 media.

3.2 Simultaneous Isolation and Synchronization of Primary Articular Chondrocytes

Harvest articular cartilage explants and digest in combination with various cell synchronization treatments to obtain chondrocytes to be subsequently encapsulated in alginate beads. Culture cell-encapsulated alginate beads and then dissociate them to recover the chondrocytes. All steps should be performed under aseptic conditions using a Class II biological safety cabinet.

1. Harvest articular cartilage explants (~10–15 full-thickness slices using a scalpel, no bone) from the articular surfaces of the metacarpophalangeal joints of cows (obtained from a local abattoir) under sterile conditions. Place cartilage explants (<5 mm × 5 mm × 1 mm) into a 100 mm Petri dish containing 20 mL Ham's F12 media with 1% antibiotic-antimycotic.
2. Apply different cell synchronization methods as follows:
   (a) Serum starvation for synchronization in the G_0/G_1 phase [23]: Digest cartilage explants with protease solution by aspirating the media and adding 20 mL protease solution. Incubate for 1 h at 37 °C and 5% CO_2. Aspirate the protease solution and add 20 mL collagenase A solution. Incubate for 12 h at 37 °C and 5% CO_2.
   (b) Aphidicolin treatment for synchronization in the S phase [30]: Serum starve cells by incubating cartilage explants in 20 mL Ham's F12 media for 47 h at 37 °C and 5% CO_2. Then, incubate in 20 mL protease solution for 1 h at 37 °C and 5% CO_2, followed by a wash with Ham's F12 media. Digest and treat explants with aphidicolin-supplemented collagenase solution for 24 h at 37 °C and 5% CO_2.
   (c) Double thymidine treatment for synchronization in the S phase [31]: Block cells by incubating cartilage explants in 20 mL thymidine-supplemented complete media for 24 h at 37 °C and 5% CO_2, followed by a wash with 5 mL Ham's F12 media. Release cells from the thymidine block by incubating in 20 mL Ham's F12 media at 37 °C and 5% CO_2 for 8 h. Aspirate the media and replace with 20 mL protease solution for 1 h at 37 °C and 5% CO_2, followed by a wash with 5 mL Ham's F12 media. Block the cells again by incubating explants in thymidine-supplemented collagenase solution for 12 h at 37 °C and 5% CO_2.
   (d) Thymidine-nocodazole treatment for synchronization in the G_2/M phase [32]: Block cells by incubating cartilage explants in 20 mL thymidine-supplemented complete media for 24 h at 37 °C and 5% CO_2, followed by a wash with 5 mL Ham's F12 media. Release cells from the thymidine block by incubating in 20 mL Ham's F12 media at 37 °C and 5% CO_2 for 2 h. Aspirate the media and replace with 20 mL protease solution for 1 h at 37 °C and 5% CO_2, followed by a wash with 5 mL Ham's F12 media. Block the cells again by incubating explants in nocodazole-supplemented collagenase solution for 12 h at 37 °C and 5% CO_2.

(e) Thymidine-RO-3306 treatment for synchronization in the G_2/M phase [33]: Block cells by incubating cartilage explants in 20 mL thymidine-supplemented complete media for 24 h at 37 °C and 5% CO_2, followed by a wash with 5 mL Ham's F12 media. Release cells from the thymidine block by incubating in 20 mL Ham's F12 media at 37 °C and 5% CO_2 for 5 h. Aspirate the media and replace with 20 mL protease solution for 1 h at 37 °C and 5% CO_2, followed by a wash with 5 mL Ham's F12 media. Block the cells again by incubating explants in RO-3306-supplemented collagenase solution for 12 h at 37 °C and 5% CO_2.

3. Pipette the cell digest up and down. Incubate for 1 h at 37 °C and 5% CO_2.
4. Put the cell digest through a 70 μm cell strainer into a 50 mL centrifuge tube.
5. Wash cells by centrifuging them at 700 × *g* for 7 min and resuspending them in 20 mL Ham's F12 media. Repeat.
6. Count cells using a hemacytometer and the trypan blue exclusion method [29].
7. Centrifuge cells at 700 × *g* for 7 min. Resuspend cells in complete media to create a high-density cell suspension of 20×10^6 chondrocytes/mL.
8. Encapsulate isolated cells in alginate beads by first mixing the cell suspension with equal part (by volume) of sterile-filtered alginic acid solution at room temperature. Then, create cell-encapsulated alginate beads by dropping 30 μL cell-alginate solution in a calcium chloride bath. After 10 min, extract polymerized cell encapsulated alginate beads using forceps. Place them into individual wells of a 24-well plate containing 1 mL growth media.
9. Cultivate in 1 mL growth media at 37 °C with 5% CO_2 and 95% humidity for a maximum of 4 weeks. Change culture media every 48 h.
   (a) To determine cell viability and purity immediately after synchronization (Fig. 1, Table 1), proceed to **Step 10** without further cultivation.
   (b) To determine the percentage of cells within each cell cycle phase at different timepoints after synchronization (Table 2), cultivate cell encapsulated alginate beads for 0, 12, 24, 36, and 48 h and then proceed to **Step 10**.
   (c) To determine the effect of synchronization on extracellular matrix production and accumulation (Fig. 2), cultivate cell encapsulated alginate beads for 2 or 4 weeks and then proceed with safranin O staining and collagen II immunostaining as described in [28].

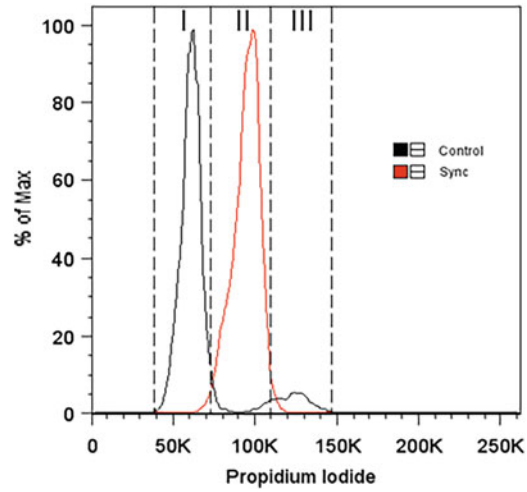

Fig. 1 Representative emission spectra of control and synchronized chondrocyte populations stained with propidium iodide, with an overlay of cell cycle gating. Chondrocytes were simultaneously isolated and synchronized using the double thymidine method. Staining regions for nuclei in the G0-G1 phase, S phase, and G2-M phase are indicated by I, II, and III, respectively. (Reproduced from Subedar et al. [28]. Copyright © 2019 (SAGE Publishing))

Table 1
Viability and purity of chondrocyte populations subjected to different cell cycle synchronization methods simultaneously with cell isolation

Synchronization method	Cell viability (%)	Phase of interest	Cell purity (% cells in phase of interest)
Serum starvation	97.5 ± 0.1	G_0/G_1	83.3 ± 0.7
Aphidicolin	89.3 ± 0.2	S	81.0 ± 2.5
Double thymidine	95.2 ± 0.1	S	92.7 ± 0.3
Thymidine-nocodazole	42.8 ± 0.5	G_2/M	77.3 ± 5.8
Thymidine-RO-3306	85.9 ± 0.4	G_2/M	6.6 ± 0.4

Reproduced from Subedar et al. [28]. Copyright © 2019 (SAGE Publishing)

10. For subsequent flow cytometry analyses (Subheading 3.3), recover the cells from encapsulation by dissociating the cell encapsulated alginate beads at 37 °C under light agitation at 120 rpm in the calcium chelating solution for 15 min.
11. Determine cell viability using the trypan blue exclusion method [29].

Table 2
Percentage of cells within each phase of the cell cycle at different timepoints after synchronization

Experimental group	% DNA content in cell cycle phase		
	G_0/G_1	S	G_2/M
0-h	1.1 ± 0.2	92.7 ± 0.3	6.1 ± 0.5
12-h	61.1 ± 0.3	26.6 ± 0.2	12.3 ± 0.4
24-h	54.9 ± 0.1	38.1 ± 0.5	6.9 ± 0.4
36-h	24.7 ± 0.3	72.8 ± 0.5	2.5 ± 0.1
48-h	2.9 ± 0.5	81.6 ± 3.0	15.4 ± 2.5

Reproduced from Subedar et al. [28]. Copyright © 2019 (SAGE Publishing)
Synchronization was performed using simultaneous cell isolation and synchronization with the double thymidine method

3.3 Flow Cytometry

Stain cells with propidium iodide to provide a measure of DNA content. Assess cell cycle phase synchrony by flow cytometry and gating of cells in the target cell cycle phase.

1. Pelletize trypsinized cells (from Subheading 3.1) or dissociated cells (from Subheading 3.2) by centrifugation at 700 × *g* for 10 min. Resuspend cells in Ham's F12 media.
2. Add 1 mL cell suspension dropwise to 4.5 mL cold ethanol. Vortex cells and leave on ice for 30 min for fixation (*see* **Note 8**).
3. Pelletize cells by centrifugation at 1000 × *g* for 5 min. Resuspend cells in 5 mL PBS.
4. Permeabilize cells using 100 μL Triton-x100 solution.
5. Stain cells with 100 μL propidium iodide dye solution.
6. Perform flow cytometric analysis using BD Aria analytical cytometer (or equivalent) by exciting the propidium iodide bound to DNA with a 488 nm laser and detecting emission with the 664/22 bandpass filter.
7. Perform data analysis with FlowJo software (or equivalent). Analyze the emission spectra of the stained cells to determine DNA content. Use unsynchronized control cell populations to establish the staining region of cells in the G_0/G_1 phase. Determine cells that fluoresce with twice the intensity to be in the G_2/M phase. Determine cells distributed between the G_0/G_1 and G_2/M peaks to be in the S phase.

Figure 1 shows representative emission spectra of stained cells that were simultaneously isolated and synchronized using double thymidine treatment [28]. Table 1 shows representative results of

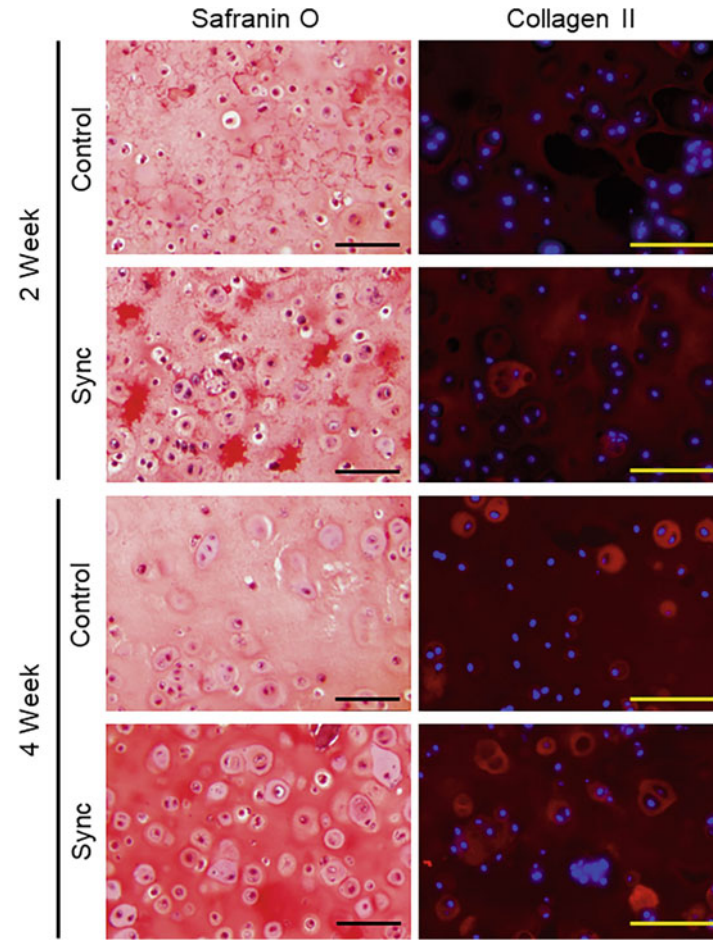

Fig. 2 Increased extracellular matrix accumulation in tissue-engineered cartilage constructs developed with synchronized chondrocytes and grown for 2 or 4 weeks. Representative images of Safranin O staining (Safranin O staining of sulfated proteoglycans in red) and collagen II immunofluorescence staining (collagen II staining in red, DAPI counterstaining of nuclei in blue). Chondrocytes were simultaneously isolated and synchronized using the double thymidine method. (Reproduced from Subedar et al. [28]. Copyright © 2019 (SAGE Publishing))

cell cycle synchronization using simultaneous isolation and synchronization with various treatment methods [28]. Double thymidine treatment shows the best results in terms of both cell viability and purity, while thymidine-nocodazole and thymidine-RO-3306 treatments are examples of unsuccessful cell cycle synchronization due to a low cell viability and an extremely low percentage of cells in the phase of interest respectively. Table 2 shows the percentage of cells in each cell cycle phase at different time points after synchronization for chondrocytes simultaneously isolated and synchronized using double thymidine treatment [28].

Constructs developed with chondrocytes that were simultaneously isolated and synchronized using double thymidine treatment had increased accumulation of sulfated proteoglycan and collagen II (Fig. 2), despite a loss of cell cycle synchronization only 12 h after synchronization (Table 2) [28]. Thus, the short-term cell cycle synchronization of chondrocytes has a long-term effect on the resulting tissue-engineered cartilage constructs.

4 Notes

1. The age of the animals may affect the results. Cows under the age of 18 months were used with this protocol.
2. Protease solution should be made fresh and sterile filtered on the day of usage.
3. All collagenase solutions should be made fresh and sterile filtered on the day of usage.
4. Thymidine-supplemented complete media should be made fresh by adding the appropriate amount of thymidine to prepared complete media and sterile filtered on the day of usage.
5. Avoid freeze-thaw for ascorbic acid aliquots.
6. Growth media should be made fresh by adding the appropriate amount of ascorbic acid to prepared complete media immediately before use for every change of culture medium, as ascorbic acid has a short half-life.
7. The treatment concentrations and durations for serum starvation, aphidicolin, double thymidine, thymidine-nocodazole, and thymidine-RO-3306 methods have not yet been optimized for chondrocyte monolayers.
8. Vortexing the cells and leaving them on ice will prevent cell aggregation.

References

1. Hunziker EB (2002) Articular cartilage repair: basic science and clinical progress. A review of the current status and prospects. Osteoarthr Cartil 10:432–463. https://doi.org/10.1053/joca.2002.0801
2. Tiku ML, Sabaawy HE (2015) Cartilage regeneration for treatment of osteoarthritis: a paradigm for nonsurgical intervention. Ther Adv Musculoskelet Dis 7:76–87. https://doi.org/10.1177/1759720X15576866
3. Vos T, Allen C, Arora M et al (2016) Global, regional, and national incidence, prevalence, and years lived with disability for 310 diseases and injuries, 1990–2015: a systematic analysis for the Global Burden of Disease Study 2015. Lancet 388:1545–1602. https://doi.org/10.1016/S0140-6736(16)31678-6
4. Redman S, Oldfield S, Archer C (2005) Current strategies for articular cartilage repair. Eur Cells Mater 9:23–32. https://doi.org/10.22203/eCM.v009a04
5. Vasiliadis HS, Wasiak J (2010) Autologous chondrocyte implantation for full thickness articular cartilage defects of the knee. Cochrane Database of Systematic Reviews, In

6. Brittberg M, Lindahl A, Nilsson A et al (1994) Treatment of deep cartilage defects in the knee with autologous chondrocyte transplantation. N Engl J Med 331:889–895. https://doi.org/10.1056/NEJM199410063311401
7. Mauck RL, Nicoll SB, Seyhan SL et al (2003) Synergistic action of growth factors and dynamic loading for articular cartilage tissue engineering. Tissue Eng 9:597–611. https://doi.org/10.1089/107632703768247304
8. Jonnalagadda US, Hill M, Messaoudi W et al (2018) Acoustically modulated biomechanical stimulation for human cartilage tissue engineering. Lab Chip 18:473–485. https://doi.org/10.1039/c7lc01195d
9. Kaupp JA, Weber JF, Waldman SD (2012) Mechanical stimulation of chondrocyte-agarose hydrogels. J Vis Exp. https://doi.org/10.3791/4229
10. Meinert C, Schrobback K, Hutmacher DW, Klein TJ (2017) A novel bioreactor system for biaxial mechanical loading enhances the properties of tissue-engineered human cartilage. Sci Rep 7:16997. https://doi.org/10.1038/s41598-017-16523-x
11. Waldman SD, Couto DC, Grynpas MD et al (2006) A single application of cyclic loading can accelerate matrix deposition and enhance the properties of tissue-engineered cartilage. Osteoarthr Cartil 14:323–330. https://doi.org/10.1016/j.joca.2005.10.007
12. Waldman SD, Spiteri CG, Grynpas MD et al (2004) Long-term intermittent compressive stimulation improves the composition and mechanical properties of tissue-engineered cartilage. Tissue Eng 10:1323–1331. https://doi.org/10.1089/ten.2004.10.1323
13. Weber JF, Chiu LLY, Balko S, Waldman SD (2019) Stochastic resonance with dynamic compression improves the growth of adult chondrocytes in agarose gel constructs. Ann Biomed Eng 47:243–256. https://doi.org/10.1007/s10439-018-02123-x
14. Li S, Glynne-Jones P, Andriotis OG et al (2014) Application of an acoustofluidic perfusion bioreactor for cartilage tissue engineering. Lab Chip 14:4475–4485. https://doi.org/10.1039/c4lc00956h
15. Barradas OP, Jandt U, Becker M et al (2015) Synchronized mammalian cell culture: Part I – a physical strategy for synchronized cultivation under physiological conditions. Biotechnol Prog 31:165–174. https://doi.org/10.1002/btpr.1944
16. Stubblefield E, Klevecz R, Deaven L (1967) Synchronized mammalian cell cultures. I. Cell replication cycle and macromolecular synthesis following brief colcemid arrest of mitosis. J Cell Physiol 69:345–353. https://doi.org/10.1002/jcp.1040690311
17. Tseu I, Ridsdale R, Liu J et al (2002) Cell cycle regulation of pulmonary phosphatidylcholine synthesis. Am J Respir Cell Mol Biol 26:506–515. https://doi.org/10.1165/ajrcmb.26.4.4702
18. Kwok ACM (2003) Cellulose synthesis is coupled to cell cycle progression at G1 in the dinoflagellate Crypthecodinium cohnii. Plant Physiol 131:1681–1691. https://doi.org/10.1104/pp.102.018945
19. Beaumont KA, Hill DS, Daignault SM et al (2016) Cell cycle phase-specific drug resistance as an escape mechanism of melanoma cells. J Invest Dermatol 136:1479–1489. https://doi.org/10.1016/j.jid.2016.02.805
20. Murray D, Meyn RE (1986) Cell cycle-dependent cytotoxicity of alkylating agents: determination of nitrogen mustard-induced DNA cross-links and their repair in Chinese hamster ovary cells synchronized by centrifugal elutriation. Cancer Res 46:2324–2329
21. Fan P, Zhang Y, Guo X et al (2017) Cell-cycle-specific cellular responses to sonoporation. Theranostics 7:4894–4908. https://doi.org/10.7150/THNO.20820
22. Takigawa M, Shirai E, Fukuo K et al (1987) Chondrocytes dedifferentiated by serial monolayer culture form cartilage nodules in nude mice. Bone Min 2:449–462
23. Chen M, Huang J, Yang X et al (2012) Serum starvation induced cell cycle synchronization facilitates human somatic cells reprogramming. PLoS One 7:e28203. https://doi.org/10.1371/journal.pone.0028203
24. Szczepański K, Kwapiszewska K, Hołyst R (2019) Stability of cytoplasmic nanoviscosity during cell cycle of HeLa cells synchronized with Aphidicolin. Sci Rep 9:16486. https://doi.org/10.1038/s41598-019-52758-6
25. Chen G, Deng X (2018) Cell synchronization by double thymidine block. Bio-Protocol 8:e2994. https://doi.org/10.21769/bioprotoc.2994
26. Apraiz A, Mitxelena J, Zubiaga A (2017) Studying cell cycle-regulated gene expression by two complementary cell synchronization protocols. J Vis Exp 124:e55745. https://doi.org/10.3791/55745
27. Hayashi Y, Fujimura A, Kato K et al (2018) Nucleolar integrity during interphase supports faithful Cdk1 activation and mitotic entry. Sci Adv 4:eaap7777. https://doi.org/10.1126/sciadv.aap7777

28. Subedar OD, Chiu LLY, Waldman SD (2019) Cell cycle synchronization of primary articular chondrocytes enhances Chondrogenesis. Cartilage. https://doi.org/10.1177/1947603519841677
29. Strober W (2015) Trypan blue exclusion test of cell viability. Curr Protoc Immunol 111:A3.B.1–A3.B.3. https://doi.org/10.1002/0471142735.ima03bs111
30. Pedrali-Noy G, Spadari S, Miller-Faurès A et al (1980) Synchronization of HeLa cell cultures by inhibition of DNA polymerase alpha with aphidicolin. Nucleic Acids Res 8:377–387. https://doi.org/10.1093/nar/8.2.377
31. Roberts EC, Shapiro PS, Nahreini TS et al (2002) Distinct cell cycle timing requirements for extracellular signal-regulated kinase and phosphoinositide 3-kinase signaling pathways in somatic cell mitosis. Mol Cell Biol 22:7226–7241. https://doi.org/10.1128/MCB.22.20.7226-7241.2002
32. Jackman J, O'Connor PM (2001) Methods for synchronizing cells at specific stages of the cell cycle. Curr Protoc Cell Biol. https://doi.org/10.1002/0471143030.cb0803s00
33. Vassilev LT (2006) Cell cycle synchronization at the G2/M phase border by reversible inhibition of CDK1. Cell Cycle 5:2555–2556

Part III

Methods for Cell Cycle Synchronization of Unicellular Organisms

Chapter 10

Synchronization of *Leishmania amazonensis* Cell Cycle Using Hydroxyurea

Beatriz C. D. de Oliveira, Luiz H. C. Assis, Mark E. Shiburah, Stephany C. Paiva, Veronica S. Fontes, Leilane S. de Oliveira, Vitor L. da Silva, Marcelo S. da Silva, and Maria Isabel N. Cano

Abstract

Leishmania spp. comprises a group of protozoan parasites that affect millions of people around the world. Understanding the main cell cycle-dependent events could provide an important route for developing specific therapies since some factors involved in cell cycle control may have low similarity relative to their homologs in mammals. Furthermore, accurate cell cycle-dependent analyses often require many cells, which can be achieved through cell cycle synchronization. Here, we described a useful method to synchronize procyclic promastigote forms of *Leishmania amazonensis* using hydroxyurea (HU) and the analysis of its DNA content profile. This approach can be extended to other trypanosomatids, such as *Trypanosoma cruzi* or *Trypanosoma brucei*, and provides an effective method for arresting more than 80% of cells at the G1/S phase transition.

Key words *Leishmania amazonensis*, Cell cycle synchronization, Hydroxyurea, DNA content profile

1 Introduction

Leishmania genus comprises more than 20 species of single-celled protozoan parasites, most of them showing human and veterinary medical importance. They are the causative agents of leishmaniasis, a neglected tropical disease with a large spectrum of clinical manifestations that affect millions worldwide [1, 2]. The parasite presents three main life forms in its developmental cycle: amastigotes (proliferative), procyclic promastigotes (proliferative), and metacyclic promastigotes (quiescent) [3, 4]. Procyclic and metacyclic promastigotes are both flagellates. They grow and suffer morphological transformations inside the gastric apparatus of the phlebotomine (insect vector). They can also be maintained in axenic cultures under controlled conditions, facilitating laboratory manipulation. Metacyclics are preadapted to infect the mammalian host.

Zhixiang Wang (ed.), *Cell-Cycle Synchronization: Methods and Protocols*, Methods in Molecular Biology, vol. 2579,
https://doi.org/10.1007/978-1-0716-2736-5_10,

Inside the macrophage parasitophorous vacuole, they can transform into amastigotes, the proliferative and intracellular forms with no apparent flagellum [4]. All three parasite life forms present two DNA-containing organelles, the nucleus and a unique mitochondrion that contains many copies of kinetoplast DNA (kDNA) [1]. Understanding the cell division cycle and the transformation processes across the life cycle has provided many insights about *Leishmania's* cell biology and the importance of morphological changes for host-parasite interactions [5–7]. The characterization of the cell cycle profile of different *Leishmania* species has been determined mainly through exponentially growing procyclic promastigotes. The cell cycle phases duration of procyclic promastigotes and some important features, such as the organelles segregation order and daughter flagellum appearance, show slight variation among *Leishmania* species, with few exceptions determined predominantly through microscopic analysis of individual cells [5, 6, 8, 9]. However, analyses of cell cycle-dependent events through techniques such as proteomic/transcriptomic that require analyses of a large number of cells are arduous tasks and require cell synchronization (commonly using hydroxyurea – HU).

The mechanism of action of cell cycle synchronization using HU consists of inhibiting the activity of the enzyme ribonucleotide reductase, which is responsible for converting ribonucleotides into deoxyribonucleotides. This approach allows cells to be synchronized at the beginning of the S phase of the cell cycle (G1/S transition). *Leishmania tarentolae* was the first species to have its cell cycle division described after cell synchronization with hydroxyurea (HU) [10]. More recently, our group used a similar approach in procyclic promastigotes of *Leishmania amazonensis*, and we were able to successfully synchronize more than 80% of the population [6]. Furthermore, *L. infantum* and *L. major* procyclic promastigotes can also be synchronized using HU [11, 12]. Here, we describe the steps of a straightforward method for synchronizing in vitro procyclic promastigote forms of *L. amazonensis*.

2 Materials

2.1 Cell Culture and Counting

1. General supplies: Cell culture flasks, biological oxygen demand chamber (BOD), Neubauer chamber (or cell counter), biological safety cabinet.
2. M199 complete medium (adapted from Kapler et al., 1990): Add about 800 mL distilled water to a 1 L beaker. Weigh 9.9 g M199 medium, 0.35 g of sodium bicarbonate, 136 mg of streptomycin, 60 mg of penicillin, and transfer to the beaker. Mix well using a magnetic stirrer. Then, add 40 mL of 1 M HEPES pH 7.5, 10 mL of 10 mM adenine, 1 mL of 0.1%

Biotin (diluted in 95% ethanol). Mix and adjust the pH to 7.5. Transfer to a graduated cylinder, add 100 mL of heat-inactivated fetal bovine serum (FBS) and bring up the volume to 1 L with distilled water. Finally, filter the mixture using a 0.2 μm MCE (mixed cellulose esters) membrane in a sterile environment (e.g., biological safety cabinet). Store it in a sterile bottle at 4 °C.

3. PBS (140 mM NaCl, 2.7 mM KCl, 10 mM Na_2HPO_4, and 2 mM KH_2PO_4, pH 7.4). Weigh 4.1 g NaCl, 0.1 g KCl, 0.71 g of Na_2HPO_4, 0.14 g of KH_2PO_4, and transfer to 1 L beaker. Add about 400 mL distilled water, mix well using a magnetic stirrer, and adjust the pH to 7.4. Transfer to a graduated cylinder, bring up the volume to 500 mL with distilled water, and autoclave. Store at room temperature and use it only in sterile environments to avoid contamination.
4. 1% (v/v) formaldehyde diluted in PBS: dilute formaldehyde in PBS to a final concentration of 1%. Store at 4 °C.

2.2 Hydroxyurea Treatment

1. M199 complete medium: *see* **item 2** in Subheading 2.1.
2. PBS: *see* **item 3** in Subheading 2.1.
3. Hydroxyurea (HU) stock solution (500 mM Hydroxyurea). Add about 500 μL distilled water to a 1.5 mL microtube. Weigh 3.8 g HU and transfer to a microtube. Solubilize using a vortex and bring up the volume to 1 mL with distilled water. Filter the solution using a sterile 0.2 μm syringe filter in a sterile environment (e.g., biosafety cabinet) and store at 4 °C (*see* **Note 1**).

2.3 Sample Preparation for Flow Cytometry

1. PBS: *see* **item 3** in Subheading 2.1.
2. Ice-cold methanol anhydrous 99.8%.
3. PI staining solution: 10 μg/mL propidium iodide and 10 μg/mL RNase A (DNase free) diluted in PBS. Prepare 100 μL for each sample.

2.4 Flow Cytometry Data Collection and Analysis

1. For data collection, it was used BD Accuri™ C6 Flow Cytometer.
2. For data analysis, it was used FlowJo software.

3 Methods

3.1 Cell Culture: Starting, Counting, and Passage

3.1.1 L. amazonensis Procyclic Promastigote Axenic Culture

1. Allow the M199 complete medium to warm up to room temperature (~20–30 min) inside the biological safety cabinet.
2. Allow your stock of cells frozen at −80 °C to thaw or take a 1 mL sample from an exponentially growing culture (Fig. 1) to make a 1:5 dilution in a new M199 complete medium.

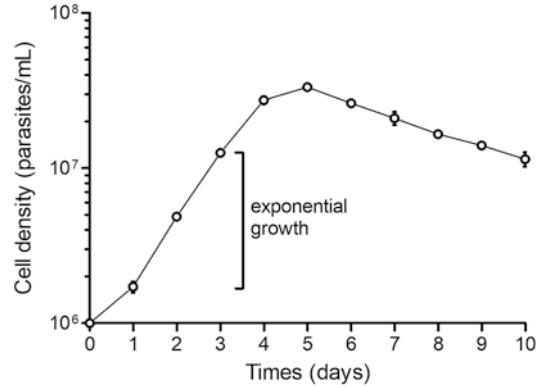

Fig. 1 Growth curve of *L. amazonensis* procyclic promastigotes. The curve was obtained by counting cells growing in M199 complete medium every 24 h for ten days. As shown in the graph obtained using GraphPad Prism, cell density increases exponentially (exponential phase) for ~3–4 days in culture before reaching a stationary phase of growth (approximately after five days in culture)

3. Pipette the necessary amount of M199 complete medium into a 25 cm^3 culture flask. Afterward, transfer the cells to the culture flask and incubate them inside the biological oxygen demand chamber (BOD) at 26 °C in a vertical position.
4. Let the cells grow for ~3–4 days.

3.1.2 Counting and Maintaining the Cells in Culture

1. Take the flask containing the cells to the biological safety cabinet and procedure as described right above. Afterward, dilute the cells 1:10 for counting by adding 10 μL of culture in a 600 μL microtube containing 90 μL of 1% (v/v) formaldehyde. Pipette up and down to mix well.
2. Count the cells using a Neubauer chamber or a cell counter. If you use a Neubauer chamber, apply 10 μL of the cell dilution in each chamber slot. Wait ~1–2 min for the cell fixation.
3. Prepare a new culture flask containing 5 mL of M199 complete medium.
4. Transfer from the old culture to the new flask the equivalent to 1.0×10^6 cells/mL.
5. Incubate the flask at 26 °C.

3.2 Growth Curve

Count the cells every day until they reach the stationary phase (Fig. 1).

1. During a passage procedure, prepare triplicates (three culture flasks) of each cell lineage to be analyzed, starting with 1.0×10^6 cells/mL.
2. Count the cells as specified in Subheading 3.1.2 daily, preferably simultaneously every day.

3.3 Cell Synchronization

Carry out all procedures at room temperature unless otherwise specified:

1. Synchronize the *Leishmania* promastigotes in exponential growth (10 mL containing 1×10^7cells/mL) by adding HU stock solution to a final concentration of 5 mM. Incubate for 14 h. The volume of HU required must be estimated according to the volume of the culture used. For instance, to the 10 mL, it will be necessary to use 100 μL of HU stock solution.
2. After this incubation period (14 h), collect 1 mL of the synchronized culture by centrifugation (2300*g* for 5 min) at 4 °C. Wash the collected sample twice with 1 mL PBS, and resuspend the parasites (pellet) in 300 μL PBS. Add 700 μL anhydrous methanol (99.8%) to the resuspended pellet (for fixation and permeabilization) and store it at 4 °C overnight.
3. Centrifuge the remaining parasites (2300*g* for 5 min) at room temperature, discard the supernatant (medium containing HU), and resuspend the parasites (pellet) in fresh M199 complete medium (the same volume discarded) previously incubated at 27 °C. At this moment, parasites will be released from synchronization.
4. For cell cycle monitoring and DNA content analysis, approximately 1 mL (1.10^7 cells) must be collected hourly by centrifugation (2300*g* for 5 min) at 4 °C, for the next 8 h. Each collected sample must be prepared as described in **step 2** of the present section.
5. The next day, centrifuge each collected sample (5000*g* for 5 min) at 4 °C, wash twice with 1.5 mL PBS, and resuspend the parasites (pellet) in 500 μL PBS for subsequent analysis of DNA content by flow cytometry.

3.4 DNA Content Analysis

3.4.1 Preparation of Cells to Flow Cytometer Analysis

1. Harvest approximately 5×10^6 cells by centrifuging at 2300*g* for 5 min at 4 °C (*see* **Note 2**).
2. Discard the supernatant and wash the cells by resuspending them with 1 ml of PBS 1×.
3. Centrifuge again at 2300*g* for 5 min at 4 °C. Repeat **steps 2** and **3**.
4. Discard the supernatant and resuspend the cells in 98.2 μL of PBS (*see* **Note 3**).
5. Add 901,8 μL of cold methanol 99.8% (*see* **Note 4**).
6. Incubate at −20 °C for at least 20 min (*see* **Note 5**).
7. Centrifuge at 2300*g* for 5 min at 4 °C (*see* **Note 6**).
8. Discard the supernatant and add 100 μL of PI staining solution to each sample (*see* **Note 7**).

9. Incubate at 37 °C for 30–40 min (*see* **Note 8**).
10. Proceed to analyze by setting the parameters of the acquisition of the Flow Cytometer to a threshold of 50,000 FSC, the flow rate at medium, and acquire no less than 20,000 events (*see* **Note 9**).

The cell preparation for DNA content analysis was standardized following some parameters described in [13].

3.4.2 Data Analysis in FlowJo

1. Export the data from the cytometer in format .fcs files and open it in FlowJo (File > open > select the document).
2. Open a pseudocolor plot FSC-A × SSC-A by double-clicking in the file.
3. Create a gate selecting the population of interest by clicking in the toolbar and choosing a polygon (Fig. 2a).
4. Open a new pseudocolor FSC-A x FSC-H of the previous gate and regulate the value of the X and Y-axis in a way to better visualize the target data. Generate a new gate selecting the population of interest excluding the doublets (Fig. 2b).
5. Open the new population of the last gate, choosing FL2-A/PE-A × FL2-H/PE-H (this is the channel of PI reading).
6. Create a new gate selecting the population at the more concentrated area (Fig. 2c) and open a new graph choosing FL2-A/PE-A × Histogram to obtain the DNA content histograms (Fig. 2d).
7. For the cell synchronization analysis, overlap the DNA content histograms obtained from the analysis of each cell sample every hour (from 0 to −8 h) after HU release. As a result, most cells right after HU release (0 h) should show an arrest at G1/G0, confirming they are synchronized (Fig. 3).

4 Notes

1. Prolonged treatment or a higher dosage of Hydroxyurea (HU) may lead to toxic effects for the cell. The lack of deoxyribonucleotides caused by HU treatment (or even the action of HU per se) can lead cells to death due to accumulated DNA damage and oxidative stress [14]. Thus, using this protocol for the simultaneous investigation of repair pathways can lead to biased data. Furthermore, the association of this protocol with proteomic analysis requires attention since proteins associated with DNA repair (and related pathways) can be shown as up- or downregulated.
2. It is recommended to use at least 5×10^6 cells or a higher number for better results once cells can be lost during washes.

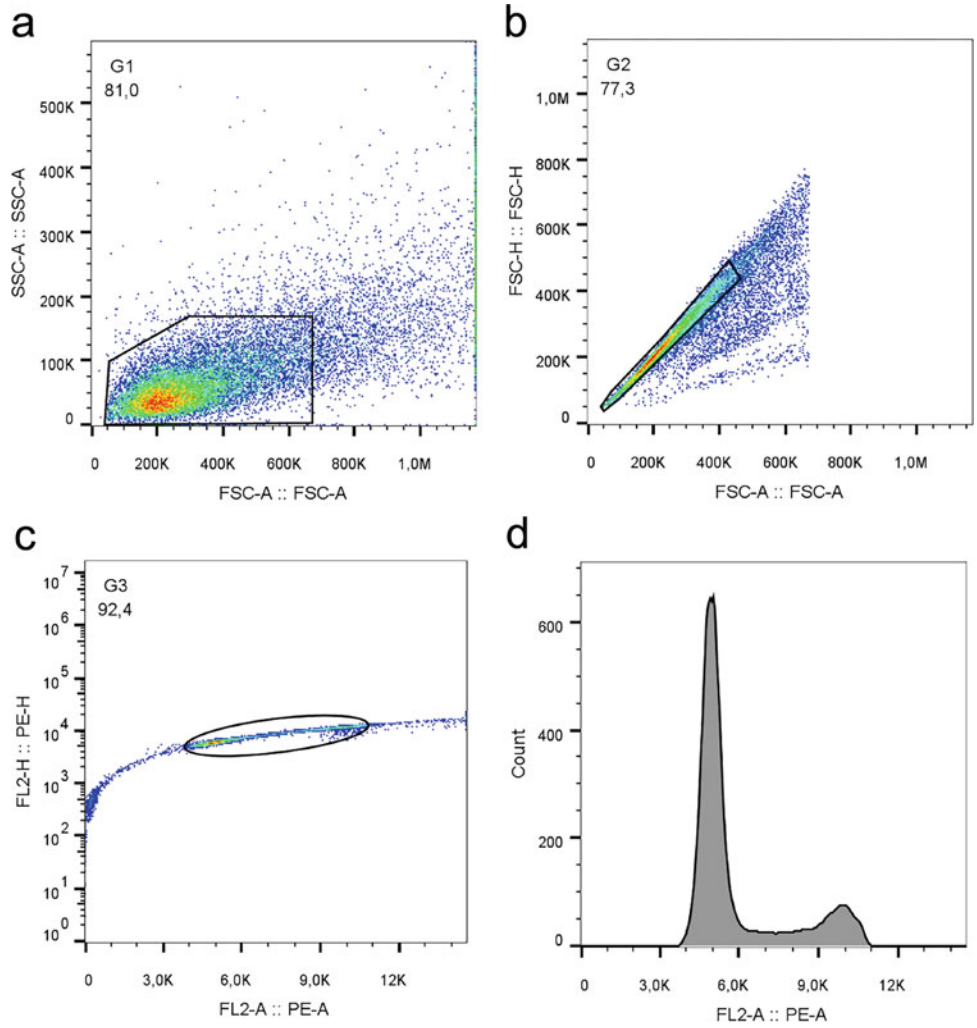

Fig. 2 Data analysis using FlowJo: (**a**) gating the population of interest, (**b**) creation of new gate in FSC-A x FSC-H graph, (**c**) new gate after the selection of the population at the more concentrated area, (**d**) new FL2-A/PE-A x histogram

3. Always resuspend the cells first in PBS. Otherwise, it will form cell aggregates which will be difficult to dissociate.
4. The final concentration of methanol should be 90%.
5. In this step, the cells can be kept at −20 °C for posterior use.
6. Attention when discarding the supernatant. In this step, methanol leaves the cells very loose, and most of the cells don't form a pellet at the bottom of the tube. Instead, they stick on the wall.
7. The addition of PI staining solution must be done in the dark. From this step onwards, the samples must be protected from light since PI is light-sensitive.

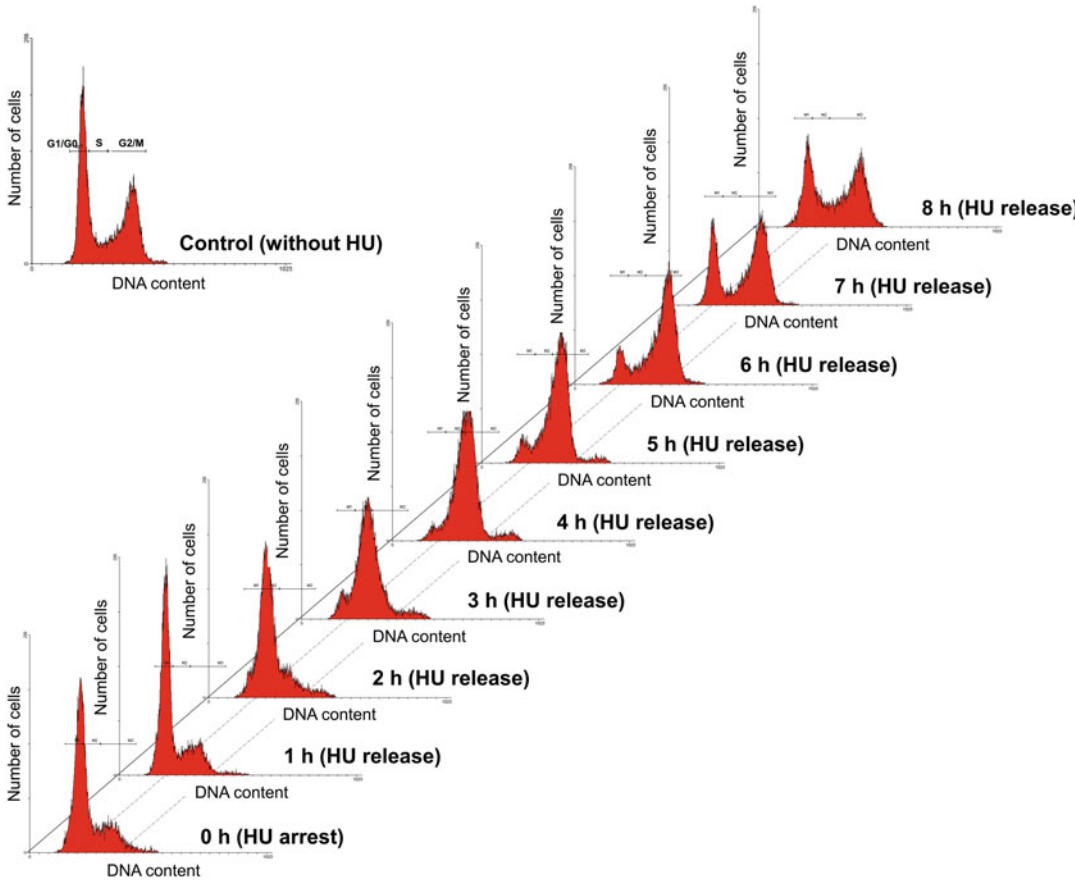

Fig. 3 Overlap of the DNA content histograms generated from the kinetic established after HU release. The progression of the peak through the X-axis (DNA content) over time demonstrates synchronization efficiency

8. After this step, the samples can be kept at 4 °C to be analyzed posteriorly. However, better results can be obtained when analyzed immediately.
9. It is recommended to analyze 20,000 events or more to obtain results statistically acceptable.

Acknowledgments

This work was supported by São Paulo Research Foundation (FAPESP) under grants: 2018/04375-2 (MICANO) and 2019/10753-2 and 2020/10277-3 (to MSdS). LHCA is a postdoctoral fellow from FAPESP (grant 2021/04253-7), BCDO and MES are doctoral fellows from FAPESP (grants 2019/25985-6 and 2020/00316-1), SCP is a master fellow from CAPES (Coordenação de Aperfeiçoamento de Pessoal de Nível Superior-Brazil), and VSF

and VLdS are undergraduate fellows from FAPESP (grants 2020/08162-3 and 2020/16481-1).

References

1. Alvar J, Vélez ID, Bern C, Herrero M, Desjeux P et al (2012) Leishmaniasis worldwide and global estimates of its incidence. PLoS One 7(5):e35671. https://doi.org/10.1371/journal.pone.0035671
2. WHO (2020) Leishmaniasis, WHO, World Health Organization. https://www.who.int/healthtopics/leishmaniasis#tab=tab_1
3. Gossage SM, Rogers ME, Bates PA (2003) Two separate growth phases during the development of *Leishmania* in sand flies: implications for understanding the life cycle. Int J Parasitol 33(10):1027–1034. https://doi.org/10.1016/S0020-7519(03)00142-5
4. Inbar E, Hughitt VK, Dilon LAL et al (2017) The transcriptome of *Leishmania major* developmental stages in their natural sanf fly vector. J Clinic Microbiol 8(2):e00029–e00017. https://doi.org/10.1128/mBio.00029-17
5. Wheeler RJ, Gluenz E, Gull K (2011) The cell cycle of *Leishmania*: morphogenetic events and their implications for parasite biology. Mol Microbiol 79(3):647–662. https://doi.org/10.1111/j.1365-2958.2010.07479.x
6. da Silva MS, Monteiro JP, Nunes VS, Vasconcelos EJ, Perez AM, Freitas-Júnior LH et al (2013) *Leishmania amazonensis* promastigotes present two distinct modes of nucleus and kinetoplast segregation during cell cycle. PLoS One 8(11):e81397. https://doi.org/10.1371/journal.pone.0081397
7. Serafim TD, Coutinho-Abreu IV, Oliveira F et al (2018) Sequential blood meals promote *Leishmania* replication and reverse metacyclogenesis augmenting vector infectivity. Nature Microbiol 3(5):548–555. https://doi.org/10.1038/s41564-018-0125-7
8. Ambit A, Woods KL, Cull B et al (2011) Morphological events during the cell cycle of *Leishmania major*. Eukaryot Cell 10(11):1429–1438. https://doi.org/10.1128/EC.05118-11
9. Minocha N, Kumar D, Rajanala K et al (2011) Kinetoplast morphology and segregation pattern as a marker for cell cycle progression in *Leishmania donovani*. J Eukaryot Microbiol 58(3):249–253. https://doi.org/10.1111/j.1550-7408.2011.00539.x
10. Simpson L, Braly P (1970) Synchronization of *Leishmania tarentolae* by hydroxyurea. J Protozool 17:511–517. https://doi.org/10.1111/j.1550-7408.1970.tb04719.x
11. Taladriz S, Hanke T, Ramiro MJ et al (2001) Nuclear DNA polymerase beta from *Leishmania infantum*. Cloning, molecular analysis and developmental regulation. Nucleic Acids Res 29(18):3822–3834. https://doi.org/10.1093/nar/29.18.3822
12. Zick A, Onn I, Bezalel R et al (2005) Assigning functions to genes: identification of S-phase expressed genes in *Leishmania major* based on post-transcriptional control elements. Nucleic Acids Res 33(13):4235–4242. https://doi.org/10.1093/nar/gki742
13. Barak E, Amin-Spector S, Gerliak E et al (2005) Differentiation of *Leishmania donovani* in host-free system: analysis of signal perception and response. Mol Biochem Parasitol 141(1):99–108. https://doi.org/10.1016/j.molbiopara.2005.02.004
14. Musiałek MW, Rybaczek D (2021) Hydroxyurea – the good, the bad and the ugly. Genes 12(7):1096. https://doi.org/10.3390/genes12071096

Chapter 11

Synchronization of *Trypanosoma brucei* by Counter-Flow Centrifugal Elutriation

Corinna Benz and Michael D. Urbaniak

Abstract

Centrifugal counter-flow elutriation is a non-invasive technique that separates cells based on their hydrodynamic volume in a specialized centrifugation chamber that allows the application of a counter-flow of buffer to oppose sedimentation. Here, we report a centrifugal counter-flow elutriation protocol for *Trypanosoma brucei* cells that is able to rapidly isolate highly enriched G1 subpopulations (>95%) of synchronized cells. The cells obtained are viable and proliferate without lag, allowing subsequent cell cycle phases to be obtained by continued culture. The synchronized cell cultures obtained by this process have uniform DNA content, a narrow size distribution, undergo synchronous division, and maintain synchrony into subsequent cell cycles.

Key words *Trypanosoma brucei*, Cell cycle, Elutriation, Synchronization, Flow cytometry

1 Introduction

Trypanosoma brucei is the best characterized of the kinetoplastid group of unicellular eukaryotes which includes several members of clinical and veterinary importance [1]. In common with all eukaryotes, the cell cycle of *T. brucei* is highly organized and tightly controlled, reflecting the need to coordinate not only nuclear division but also the division and segregation of the mitochondrial kinetoplast DNA [2, 3]. The genome organization of *T. brucei* is atypical, with a paucity of transcription factor-mediated regulation of gene expression, making them an excellent model system for studying post-transcriptional regulation [4].

A reliable and high-quality method for cell cycle synchronization is an invaluable tool to study cell cycle regulation in any organism. Centrifugal counter-flow elutriation separates cells based on their hydrodynamic volume in a specialized centrifugation chamber and has been successfully applied to obtain cell-cycle synchronized population of many different eukaryotic cells

Zhixiang Wang (ed.), *Cell-Cycle Synchronization: Methods and Protocols*, Methods in Molecular Biology, vol. 2579,
https://doi.org/10.1007/978-1-0716-2736-5_11,

[5, 6]. The elutriation chamber allows the application of a counter-flow of buffer to oppose the sedimentation caused by centrifugation, and the balance of these opposing forces keeps cells in suspension within the chamber. While centrifugal force increases uniformly with distance from the center of the rotor, the diamond shape of the elutriation chamber is such that the flow rate decreases to a minimum at the widest point of the chamber and then rapidly increases as the chamber narrows (Fig. 1). The rotor is kept at a constant centrifugal speed, and a low flow rate of the elutriation buffer is used to load cells into the chamber where they are retained below the widest part of the chamber. Incremental increases in the flow rate force the cells higher up the chamber, and those that pass above the widest part of the chamber are rapidly eluted. The force experienced due to the flow of buffer is inversely proportional to the cells' hydrodynamic volume, resulting in smaller cells eluting at a lower flow rate than larger cells. The resolution of the separation achieved is such that smaller cells earlier in the cell cycle are eluted prior to larger cells which are later in the cell cycle.

We have optimized a centrifugal counter-flow elutriation protocol for *Trypanosoma brucei* cells that is able to rapidly and directly isolate highly enriched G1 sub-populations (>95%) of synchronized cells [7]. The cells obtained are viable and proliferate without lag when placed back into cell culture, allowing subsequent cell cycle phases to be accessed. The protocol isolates sub-populations of G1 phase cells that are indistinguishable by flow cytometry but progress synchronously through the cell cycle with distinct temporal profiles post-elutriation (Fig. 2). We have confirmed the high quality of the synchronized cell cultures [8, 9] obtained by demonstrating that cell populations have uniform DNA content, a narrow size distribution, undergo synchronous division, and maintain synchrony into subsequent cell cycles [7]. The procedure is able to separate up to 3×10^9 cells in under an hour, and is compatible with metabolic labeling techniques such as SILAC, facilitating proteomic studies of cell cycle regulation [10].

2 Materials

2.1 Cell Culture

1. HMI-11T: To 450 mL HMI-9 (custom synthesis) add the following ingredients in order with stirring: 1 g Sodium bicarbonate, 50 mL fetal calf serum, 5 mL 100× L-glutamine and 5 mL 100× Penicillin-Streptomycin (*see* **Note 1**). Adjust to pH 7.3–7.4, filter-sterilize and incubate at 37 °C for >24 h prior to use to check for the absence of microbial growth.
2. SDM-79: To 425 mL SDM-79 (custom synthesis), add the following ingredients in order with stirring: 375 μL Hemin stock (10 mg/mL in 0.1 M NaOH), 1 g Sodium bicarbonate,

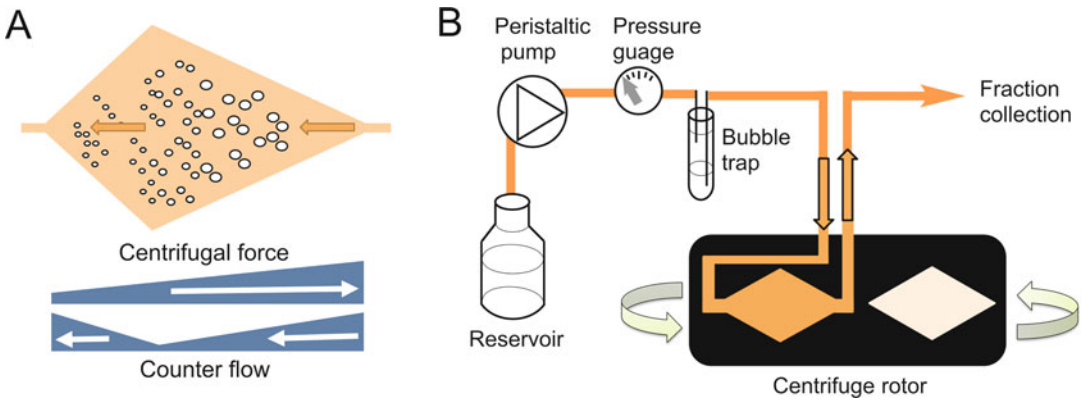

Fig. 1 Schematic of counter flow centrifugal elutriation. (**a**) Cells in the elutriation chamber experience a centrifugal force and an opposing force due to the counter flow of fluid. (**b**) The elutriation chamber is centrifuged at a constant speed with a continuous flow of buffer. Cells are introduced and retained in the chamber at low flow rate, and sequential increases in the flow rate forces the cells to elute from the chamber in size order, with smallest cells eluting first

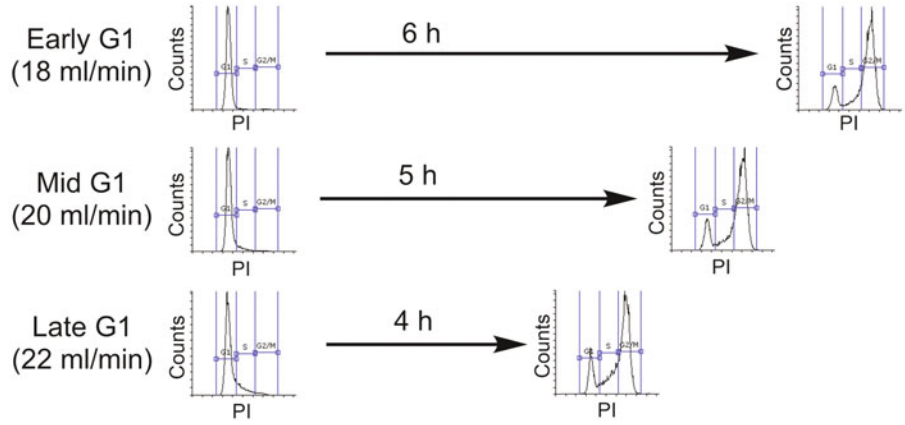

Fig. 2 Isolation of distinct populations of G1 phase cells. Early eluting G1 synchronized Pcf *T. brucei* cells are initially indistinguishable by flow cytometry of PI stained cells but progress through the cell cycle with a temporally distinct profile, reaching a highly enriched G2/M state at a different time post-elutriation

75 mL heat-inactivated fetal calf serum, 5 mL 100× L-glutamine and 5 mL 100× Penicillin-Streptomycin (*see* **Note 1**). Adjust to pH 7.3–7.4, filter-sterilize and incubate at 28 °C for >24 h prior to use to check for absence of microbial growth.

3. Culture flasks (25 and 150 cm^2 surface area) and roller bottles (for bloodstream forms (Bsf)), nontreated.

2.2 Centrifugal Counter-Flow Elutriation

1. High-speed centrifuge compatible with an elutriation rotor (e.g., Beckmann Coulter Avanti J-26S XP).

2. Elutriation rotor (e.g., Beckmann Coulter JE 5.0 with elutriation chamber) (*see* **Note 2**).
3. Peristaltic pump with an in-line pressure gauge and bubble trap.
4. Phosphate buffered saline (PBS): 137 mM NaCl, 2.7 mM KCl, 10 mM Na_2HPO_4, 1.5 mM KH_2PO_4.
5. Elutriation buffer (EB), 1 L: PBS with 25% SDM-79 for procyclic forms (Pcf), PBS with 25% HMI-11T and 10 g/L glucose for Bsf. Filter-sterilize both buffers using a 0.2 μM filter, degas in an ultrasonic bath for 15 min and pre-warm to the appropriate temperature (28 °C for Pcf and 37 °C for Bsf).
6. 50 mL conical tubes.
7. Culture flasks (75 and 150 cm^2 surface area).
8. Culture medium (SDM-79 or HMI-11T).
9. Ethanol, 500 mL.
10. Double distilled water (ddH_2O), 500 mL.

2.3 Flow Cytometry for Cell Cycle Analysis

1. 1.5 mL microcentrifuge tubes.
2. 70% methanol in PBS.
3. Propidium iodide stock solution (10 mg/mL).
4. RNaseA solution (10 mg/mL).

2.4 DAPI-Staining for Cell Cycle Analysis

1. Glass slides and coverslips.
2. Methanol.
3. Fluoroshield™ with DAPI (Sigma) or similar.

3 Methods

3.1 Cell Culture

1. Culture Bsf in HMI-11T at 37 °C, 5% CO_2, 100% humidity or Pcf in SDM-79 at 28 °C. Harvest a maximum of 3×10^9 (Pcf) or 1×10^9 (Bsf) during logarithmic growth (*see* **Note 3**).

3.2 Centrifugal Counter-Flow Elutriation

1. Harvest cells by centrifugation at 1000 × *g* for 10 min at room temperature (RT). During the centrifugation, begin to prepare the elutriation centrifuge (**step 3**).
2. Remove the supernatant and resuspend cell pellets in 20 mL of the appropriate EB for Bsf or Pcf, combining them in one conical tube (*see* **Note 4**).
3. Prepare the elutriation centrifuge: Prior to starting the centrifuge, replace storage solution within the tubes (70% ethanol) first with ddH_2O, and then with 1 × PBS and finally the appropriate EB for Bsf or Pcf (with pump speed set to 25 mL/min) (*see* **Note 5**).

4. Reduce the pump speed to 8 mL/min (Bsf) or 10 mL/min (Pcf) while pumping the respective EB through the system and perform short spins (1 min at 1000 rpm) to remove bubbles from the system.
5. Once all bubbles are removed, bring the centrifuge slowly up to speed (final speed: 5000 rpm; increase by increments of 1000 rpm per min).
6. Load cells in EB at 8 mL/ min (Bsf) or 10 mL/min (Pcf) for approximately 10 min (*see* **Note 6**). Monitor the in-line pressure gauge for evidence of blockage in the fluid systems (*see* **Note 7**).
7. For Bsf cells only: Increase pump speed to 11 mL/min for about 4 min before starting to collect fractions (*see* **Note 8**).
8. Collect 100 mL (Bsf) or 150 mL (Pcf) fractions (*see* **Note 9**) in conical tubes at increasing pump speeds: 13, 15, and 17 mL/ min (Bsf) or 15, 18, 20, and 22 mL/min (Pcf) (*see* **Note 10**).
9. Harvest cells at 1000 × *g* at RT, resuspend in appropriate amounts of culture medium and combine cells from the same fraction in an appropriately sized culture flask (*see* **Note 11**).
10. Take samples for cell cycle analysis by flow cytometry and DAPI staining, microscopy, western blots, and proteomics (as required by the experimental design) and process accordingly.
11. Incubate cultures at 37 °C (Bsf) or 28 °C (Pcf) for up to 12 h (Bsf) or 24 h (Pcf) (*see* **Note 12**) and remove samples at regular intervals or at a specific time point according to experimental design (*see* **Note 13**).
12. Clean elutriation rotor: Pump out EB and wash through with 1 × PBS, followed by ddH_2O and finally 70% ethanol for storage.

3.3 Flow Cytometry for Cell Cycle Analysis

1. Harvest 1–2 × 10^6 cells in microcentrifuge tubes at 2500 × *g* for 3 min.
2. Remove supernatant and resuspend in 1 mL of 70% methanol in PBS (*see* **Note 14**).
3. Store at 4 °C until ready to analyze (*see* **Note 15**).
4. Once ready to analyze, centrifuge samples at 2500 × *g* for 3 min.
5. Remove supernatant and resuspend in PBS.
6. Centrifuge samples at 2500 × *g* for 3 min.
7. Remove supernatant and resuspend in 1 mL PBS with propidium iodide (10 μg/mL) and RNaseA (10 μg/mL).
8. Incubate at 37 °C for 45 min.
9. Analyze by flow cytometry (*see* **Note 16**).

3.4 DAPI-Staining for Cell Cycle Analysis by Microscopy

1. Harvest 1–2 $\times$ 10^6 cells in microcentrifuge tubes at 2500 $\times$ *g* for 3 min.
2. Remove the supernatant leaving about 50 μL behind.
3. Resuspend the cells in leftover medium.
4. Spread the cell suspension on a glass slide.
5. Air-dry slide for approximately 5–10 min.
6. Incubate at −20 °C in methanol until ready to analyze.
7. Once ready to analyze, remove slides from freezer and let them air-dry for approximately 5–10 min.
8. Rehydrate slides in PBS for 5 min.
9. Apply DAPI-containing solution and coverslip and seal with nail polish (*see* **Note 17**).
10. Analyze on fluorescent microscope: Count at least 200 cells per time point and score them according to cell cycle stage (*see* **Note 18**).

4 Notes

1. Addition of penicillin-streptomycin should be avoided for routine cell culture, but is recommended for elutriation when synchronized cells are placed back into culture as typically cells are loaded and collected in open systems for convenience. Sterility can be achieved using a suitably modified system.
2. Elutriation chambers are available in different shapes and volumes; we found the 4 mL standard elutriation chamber (Beckmann Coulter) to be the most useful for elutriation of both Bsf and Pcf parasites.
3. Bsf trypanosomes grow faster the bigger the available surface area within a given culture flask; since roller bottles provide a large surface area as well as constant mixing, they were chosen to grow Bsf cells in larger volumes as required for elutriation. A specialized roller bottle incubator can be used if available but can be emulated by placing a roller mixer into an existing Bsf incubator.
4. Ensure that cells are completely resuspended. Any aggregation or clumps will adversely affect the volume-based separation and can cause blocking of the fluid system.
5. The total volume to be pumped through the system should be $\geq$100 mL per buffer. Pump speeds given here are based on our experimental set up using the 4 mL standard elutriation chamber (Beckmann Coulter), and may have to be adjusted to achieve optimum performance if different equipment is used.

6. A specialized elutriation centrifuge has a small window in the lid through which the elutriation chamber can be observed during the run by suitably adjusting the strobe backlight. You will observe cells slowly filling up the elutriation chamber during the loading stage, and once an equilibrium is reached and you can see a clear upper boundary forming, proceed with **step** 7.
7. Blockage of the fluidic system, evidenced by a rapid spike in pressure, is catastrophic and the pump must be switched off immediately and the centrifuge run aborted to prevent damage to the equipment and avoid potential harm to the user.
8. This will ensure that any cellular debris is removed before collecting the first fraction to be analyzed. The 15 mL/min fraction serves the same purpose for Pcf.
9. All three 50 mL fractions taken at the same pump speed contain relevant amounts of Pcf cells, while the third 50 mL fraction for Bsf contains only negligible amounts of cells. Hence we decided to collect fractions of 100 mL only for Bsf.
10. The first fraction is typically discarded as it contains few cells and debris, and the subsequent fractions are highly enriched for G1 cells. Once the relevant fractions to be analyzed are collected, a final 100 mL (Bsf) or 150 mL (Pcf) fraction at a pump speed of 35 mL/min is collected to remove all remaining cells from the chamber.
11. It is important to count the harvested cells at this point and resuspend them in a volume of culture medium equivalent to a logarithmically growing culture. This is especially relevant for Bsf cells which are more susceptible to density-dependent effects on growth, metabolism, and gene expression.
12. Pcf trypanosomes can divide synchronously for up to three cell cycles post-elutriation while Bsf generally cells lose synchronicity after passage through more than one cell cycle. Samples for quantitative analysis are best taken from the first cycle post-elutriation since synchronicity is gradually lost over time in both life stages.
13. To monitor progression of the cell cycle post-elutriation over time, take hourly samples for flow cytometry (essential) and DAPI staining (optional).
14. Some trypanosome cell lines appear to be more prone to aggregation in flow cytometry, which can be reduced by the addition of 0.1% TX-100 in the PBS wash step. As an alternative to methanol fixation, 0.8% formaldehyde may be used when monitoring endogenously expressed fluorophores to reduce fluorescence quenching.

15. Flow cytometry samples should be kept at 4 °C at least overnight and up to a maximum of 3–4 weeks prior to analysis.
16. Collect 50,000 events per time point and sample and analyze percentage of cells in the respective cell cycle stage using an appropriate flow cytometry analysis software (e.g., Flowing, FlowJo) using doublet discrimination.
17. As an alternative to Fluoroshield™ with DAPI, 50 μL of a 1 μg/mL solution of DAPI in PBS can be used.
18. *T. brucei* cell cycle stages can be easily determined by counting the number of kinetoplasts (concatenated mitochondrial DNA) and nuclei per cell. A cell in the G1 phase will have one nucleus and one kinetoplast (1N1K). Kinetoplast S phase commences prior to nuclear S phase, so the next cell cycle stage that can be observed is a cell with one nucleus and a dividing kinetoplast (1N1Kd). Cells in nuclear S phase will have one nucleus and 2 kinetoplasts (1N2K), and following mitosis cells with two nuclei and two kinetoplasts (2N2K) will emerge.

References

1. World Health Organisation (2001) African trypanosomiasis. Fact sheet number 259 ed., WHO Publications, Geneva
2. McKean PG (2003) Coordination of cell cycle and cytokinesis in Trypanosoma brucei. Curr Opin Microbiol 6(6):600–607
3. Li Z (2012) Regulation of the cell division cycle in Trypanosoma brucei. Eukaryot Cell 11(10):1180–1190
4. Clayton C (2019) Regulation of gene expression in trypanosomatids: living with polycistronic transcription. Open Biol 9(6):190072
5. Lindbergh CA (1932) A method for washing corpuscles in suspension. Science 75(1946): 415–546
6. Lindahl PE (1948) Principle of a counterstreaming centrifuge for the separation of particles of different sizes. Nature 161:648–649
7. Benz C et al (2017) Cell cycle synchronisation of Trypanosoma brucei by centrifugal counterflow elutriation reveals the timing of nuclear and kinetoplast DNA replication. Sci Rep 7(1):17599
8. Cooper S (2003) Rethinking synchronization of mammalian cells for cell cycle analysis. Cell Mol Life Sci 60:1099–1106
9. Cooper S (2004) Is whole-culture synchronization biology's perpetual-motion machine? Trends Biotechnol 22:266–269
10. Benz C, Urbaniak MD (2019) Organising the cell cycle in the absence of transcriptional control: dynamic phosphorylation co-ordinates the Trypanosoma brucei cell cycle post-transcriptionally. PLoS Pathog 15(12): e1008129

Chapter 12

Synchronization of *Saccharomyces cerevisiae* Cells for Analysis of Progression Through the Cell Cycle

Brianna L. Greenwood and David T. Stuart

Abstract

The cell division cycle is a fundamental process required for proliferation of all living organisms. The eukaryotic cell cycle follows a basic template with an ordered series of events beginning with G1 (Gap1) phase, followed successively by S (Synthesis) phase, G2 (Gap 2) phase, and M-phase (Mitosis). The process is tightly regulated in response to signals from both the internal and external milieu. The budding yeast *S. cerevisiae* is an outstanding model for the study of the cell cycle and its regulatory process. The basic events and regulatory processes of the *S. cerevisiae* cell cycle are highly conserved with other eukaryotes. The organism grows rapidly in simple medium, has a sequenced annotated genome, well-established genetics, and is amenable to analysis by proteomics and microscopy. Additionally, a range of tools and techniques are available to generate cultures of *S. cerevisiae* that are homogenously arrested or captured at specific phases of the cell cycle and upon release from that arrest these can be used to monitor cell cycle events as the cells synchronously proceed through a division cycle. In this chapter, we describe a series of commonly used techniques that are used to generate synchronized populations of *S. cerevisiae* and provide an overview of methods that can be used to monitor the progression of the cells through the cell division cycle.

Key words Yeast, Cell cycle, Synchronization, *cdc* mutants, α-factor, Hydroxyurea, Nocodazole, Block-release, Centrifugal elutriation

1 Introduction

The eukaryotic cell division cycle is a highly regulated process that allows a growing cell to divide with high fidelity yielding two viable daughter cells. This is achieved by cells progressing through G1-phase where cell growth and protein synthetic capacity are monitored at a restriction point and if conditions are appropriate the cell will transition to S-phase where the chromosomal DNA is duplicated. Checkpoints monitor the fidelity of DNA replication and when this process has been completed, the duplicated chromosomes align in the nucleus in the G2-phase. Further checkpoints monitor chromosome capture by mitotic spindles prior to chromosome and nuclear division during mitosis. Finally, the cell

Zhixiang Wang (ed.), *Cell-Cycle Synchronization: Methods and Protocols*, Methods in Molecular Biology, vol. 2579,
https://doi.org/10.1007/978-1-0716-2736-5_12,

undergoes cytokinesis to complete division [1, 2]. Ordered progress through this series of events is maintained through a combination of dependent events and checkpoints [2, 3]. The cell division cycle is highly orchestrated and conserved among eukaryotes but malleable and is subject to modification to achieve some developmental goals [4–7].

The budding yeast *Saccharomyces cerevisiae* has a long history as a model for the processes of eukaryotic biology [8]. The organism has an expansive array of genetic tools as well as a sequenced and well-annotated genome which adds to the value of the mutant strains, plasmids, and techniques available for experimental applications [9]. The cells can be maintained stably as haploids or diploids which potentiates the power of genetic applications available. Additionally, *S. cerevisiae* is amenable to sophisticated proteomic and cytological applications that benefit from the ability to easily delete genes, create mutants, and introduce genes encoding epitope-tagged proteins and proteins tagged with fluorescent reporter genes [10].

Owing to its rapid doubling time, ability to be propagated in simple media, amenability to genetic analysis, and ease of genetic manipulation *S. cerevisiae* has been a powerful model for understanding the regulation of the cell cycle [3]. *S. cerevisiae* cells divide by a process of budding and this benefits investigators as the cells display distinct morphological changes as they progress through key phases of the cell cycle (*see* Fig. 1). An additional aspect of the budding process is that cell division is asymmetric. Upon cytokinesis the growing bud (daughter cell) separates and is smaller than mother cell [11, 12]. This makes it possible to distinguish between mother and daughter. Immediately following cytokinesis both mother and daughter enter G1-phase as round unbudded cells with a 1 N DNA content (*see* Fig. 1). Transition from G1-phase into the cells cycle requires that the cells grow in size and protein synthetic capacity, as the mother cell is larger than the daughter, the mother cell achieves minimum size faster and thus transitions into S-phase and forms a new bud faster than the daughter cell [13]. As the cells enter S-phase the bud grows in size and DNA content increases to greater than 1 N (*see* Fig. 1). Following the completion of DNA replication the cells enter G2-phase with a larger sized bud and 2 N DNA content (*see* Fig. 1). Bud growth continues until the cells enter M-phase and undergo cytokinesis. Thus, it is possible to distinguish different cell cycle phases in *S. cerevisiae* based on the morphology of the cells [14].

Many of the key regulators of the eukaryotic cell cycle were first discovered and characterized through genetic screens with *S. cerevisiae* that identified the *cdc* (Cell Division Cycle) mutants [15]. These conditional mutants were and still are powerful tools for analysis of the cell division cycle owing to the ability to reversibly arrest a population of cells uniformly at specific phases of the cell

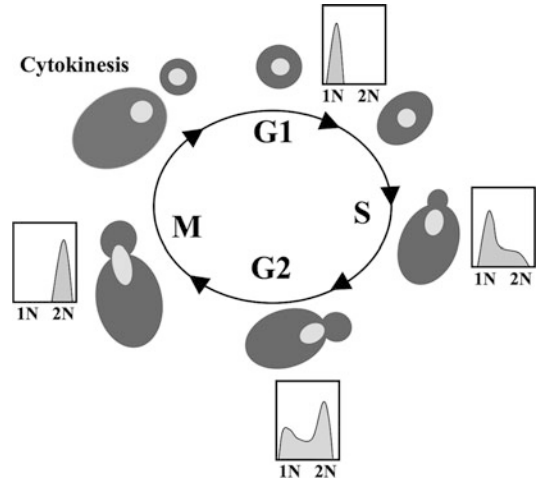

Fig. 1 *S. cerevisiae* cell cycle. *S. cerevisiae* divide by budding and so the morphology of the cells provides an indication of their position in the cell cycle. The yeast cells are depicted as grey ovals and the nucleus in white. Asymmetric cell division results in a daughter cell that is smaller than the mother at cytokinesis. The G1-phase cells are round and unbudded with a 1 N DNA content as determined by flow cytometry. As the G1-phase cells grow in size and progress toward S-phase a small bud forms and DNA content increases to greater than 1 N. The cells complete S-phase and the nucleus moves toward the site of bud growth. The cells reach G2-phase and move into M-phase as large budded cells with a 2 N DNA content. The nucleus with replicated DNA is stretched between the bud and mother prior to the completion of anaphase. Upon the completion of nuclear division, the cells proceed with cytokinesis to begin the cycle over again

cycle and then release them to synchronously to complete the division cycle. There are *cdc* mutants that produce cell cycle arrest in G1-phase (*cdc28, cdc 36, cdc37, cdc39*). S-phase (*cdc2, cdc6, cdc7, cdc8, cdc9*), metaphase (cdc16, cdc23, cdc20), and anaphase/telophase (*cdc5, cdc14, cdc14*). Various other *cdc* mutants lead to the arrest of specific processes such as budding (*cdc24*) or cytokinesis (*cdc3, cdc10, cdc11, cdc12*) [15].

In addition to the *cdc* mutant strains, a variety of tools and techniques are available to produce synchronized populations of *S. cerevisiae* and monitor those populations as they uniformly proceed through the cell cycle [16]. In this chapter, we describe a series of protocols that have been widely employed by researchers to synchronize cell populations at various stages of the cell cycle using drugs, including α-factor (Protocol 3.4.1), hydroxyurea (Protocol 3.4.2), nocodazole (Protocol 3.4.3), depletion of cyclins, that are required for transit through the G1-S boundary (Protocol 3.4.4) or Cdc20 required for completion of G2-M phase (Protocol 3.4.5), and arrest mediated by temperature shift with *cdc* mutants (Protocol 3.4.6). Additionally, we describe the process of

centrifugal elutriation to select G1-phase cells from an asynchronous population (Protocol 3.5.1). General techniques for growth, and analysis of *S. cerevisiae* including detailed descriptions of growth medium preparation have been described elsewhere [17].

2 Materials

2.1 Yeast Media

1. YEPD: 10 g yeast extract, 20 g bacto-peptone, 20 g glucose, 10 mg adenine in 1 liter distilled water.
2. YEP-Raff: 10 g yeast extract, 20 g bacto-peptone, 20 g raffinose, 10 mg adenine in 1 liter distilled water.
3. YEP-Raff-Gal: 10 g yeast extract, 20 g bacto-peptone, 10 g raffinose, 10 g galactose, 10 mg adenine in 1 liter distilled water.
4. YEP-Suc: 10 g yeast extract, 20 g bacto-peptone, 20 g sucrose, 10 mg adenine in 1 liter distilled water.
5. YEP-Glyc: 10 g yeast extract, 20 g bacto-peptone, 30 g glycerol, 10 g galactose, 10 mg adenine in 1 liter distilled water.
6. Synthetic Defined medium, SD: 1.7 g yeast nitrogen base w/o ammonium sulfate w/o amino acids, 5 g ammonium sulfate, 20 g glucose, in 1 liter distilled water.
7. SD -Met medium: SD medium supplemented with 2.0 g/L –Met drop out mix.
8. -Met drop out mix: 2 g each of: alanine, arginine, asparagine, aspartic acid, cysteine, glutamine, glutamic acid, glycine, histidine, isoleucine, lysine, phenylalanine, proline, serine, threonine, tryptophan, tyrosine, uracil, valine, 4 g of leucine.
9. Methionine stock: 25 mg/mL in H_2O, filter sterilized.
10. Water bath or Incubator.
11. Culture tubes.
12. Erlenmeyer and Fernbach flasks are typically employed for yeast culture as they allow for good aeration of the culture.
13. Centrifuge tubes.
14. Centrifuge bottles (*see* **Note 1**).
15. Spectrophotometer with cuvettes.
16. Sonicator with microtip probe.
17. Optical light Microscope.
18. Slides and coverslips.
19. Hand held counters.
20. Ethanol.
21. 37% Formaldehyde.
22. Alpha-factor stock 1 mg/mL in H_2O stored at −20 °C.

23. Hydroxyurea stored at 4 °C. Use at 200–400 mM final concentration in yeast medium.
24. Nocodazole stock 5 mg/mL in DMSO, store at −20 °C. Use at 15 μg/mL final concentration in yeast medium.
25. DAPI (4′,6-diamidino-2-phenylindole) 50 ng/mL in water.
26. Propidium iodide staining solution. 180 mM Tris base, 190 mM NaCl, 55 mM $MgCl_2$, 75 μM Propidium iodide pH 7.5 (*see* **Note 2**).
27. 5 mL round bottom 12 × 75 mm polystyrene tubes for flow cytometry.
28. Pronase E stock: 0.1 mg/mL in H_2O, store at −20 °C.
29. DNase-free RNAse A (*see* **Note 3**).
30. Pepsin 5 mg/mL prepared fresh (5 mL H_2O, 25 μL conc. HCl, 25 mg pepsin).
31. FACS Calibur Flow cytometer (Becton-Dickinson Immunocytometry Systems).
32. Centrifugal elutriator system (*see* **Note 4**).
33. Z2 channelyzer (*see* **Note 5**).

3 Methods

3.1 Growth of S. cerevisiae

Liquid cultures of *S. cerevisiae* are used for synchronization experiments. Cells are typically cultured in Erlenmeyer flasks as these provide a large surface area for oxygen transfer that is essential for optimal growth of the culture. Baffled flasks will provide the most aeration and allow for optimal growth. Culture volume should be 1/10– /5th of flask volume for best growth. Determination of cell culture density is a key parameter when performing an experiment involving analysis of cell cycle progression. Cell density and nutrient availability influence the rate of active cycling and unfettered cell cycle progression will occur when cells are in early log phase ~1×10^7 cells/mL. As culture density increases beyond 5×10^7 cells/mL the rate of progression through the cell cycle will slow and larger numbers of cells will begin to accumulate in G1-phase. Additionally, since cell density and medium composition influence the rate of cell cycle progression it is important that the rate of cell doubling in the conditions to be used in the experiment is determined in advance.

3.1.1 Monitoring Cell Density

1. Culture cells in the desired medium (*see* **Note 6**).
2. Place 1 mL of the culture medium in a 1 mL cuvette to use as a blank. Read to optical density of the medium at 600 nm (OD_{600}) and zero the absorbance of spectrophotometer.

3. Prepare 1:10, 1:100 dilutions of the culture in the growth medium and read the OD_{600} value. For reliability OD_{600} readings less than 1.0 should be used to determine culture density.
4. While there is some variation from strain to strain an OD_{600} reading of 1.0 corresponds to approximately 2.0×10^7 cells/mL (*see* **Note 7**).

3.1.2 Counting Cells with Hemocytometer

1. Place coverslip on the counting chamber of a glass hemocytometer.
2. Disperse the cell culture by mixing.
3. Pipette 10 μL of culture under the coverslip using the grooved sample slot.
4. Allow the cells to settle for 1 min.
5. Using the 40× objective of an optical microscope focus on the grid pattern.
6. Count all the cells in the four large corner squares and the center square.
7. Cells/mL = (# cells counted × # squares counted) × 10^4. This should be multiplied by any dilution made to the cells before counting.

3.2 Monitoring Synchrony

Any experiment that makes use of a synchronized cell culture requires that one or more parameters be monitored to determine cell cycle position of the population and to follow progression through the cell cycle. The morphology of *S. cerevisiae* changes as the cells proceed through cycle from unbudded G1-phase cells to large budded M-phase cells (Fig. 1). Thus, simple microscopic examination of cell morphology can inform the degree of synchronization (Protocol 3.2.1). The percent of cells in the culture that display a bud is the budding index. Analysis of DNA content by flow cytometry provides another indicator of cell cycle position with information distinct from that which can be obtained from the budding index in the culture (Protocol 3.2.2). Finally, the nuclear morphology of the cells can be observed to define cell cycle position and is particularly informative in the case of mutants that display defects in M-phase or cytokinesis (Protocol 3.2.3).

3.2.1 Determining the Percent of Budded Cells

1. Take 500 μL of culture to a microfuge tube.
2. Add 50 μL of 37% formaldehyde to fix cells.
3. Sonicate 1 × 10 seconds with microtip probe to disrupt clumps and separate cells that have completed cytokinesis.
4. Pipette 10 μL of the culture to a microscope slide and cover with a coverslip.
5. Examine the culture using a light microscope through a 40× objective.

6. Count at least 200 cells/sample recording the cells as unbudded, small budded, large budded.
7. Calculate the percentage of each class of cells in the sample.

3.2.2 Analysis of DNA Content by Flow Cytometry

1. Collect 5 mL samples of culture into 15 mL screw cap tubes at the desired time points.
2. Collect the cells by centrifugation at 3000 × g for 3–5 minutes. Pour or aspirate off the medium. Fix the cells by resuspending in 1 mL of 70% ethanol. The cells should be fixed at least overnight and may be stored for up to one week at 4 °C.
3. Transfer the fixed cells to a microfuge tube and recover by centrifugation at 14000 × g for 30 seconds in a microfuge. Aspirate off the medium.
4. Rehydrate the cells by resuspending in 1 mL of 50 mM Tris–HCl.
5. Recover the cells by centrifugation at 14000 × g for 30 seconds in a microfuge. Aspirate off the Tris–HCl buffer.
6. Resuspend the cell pellet in 1 mL of a freshly made solution of 50 mM Tris–HCl, 1 mg/mL DNase-free RNase A (*see* **Note 3**).
7. Ensure that the cells are well dispersed in the RNase solution and incubate at 37 °C for at least 2 hours, overnight is even better.
8. Recover the cells by centrifugation at 14000 × g for 30 seconds in a microfuge. Aspirate off the RNase solution.
9. Resuspend the cells in 200 µL of pepsin solution.
10. Incubate the cells for 60 minutes at 37 °C. Do not over digest.
11. Neutralize the samples by adding 1 mL of 50 mM Tris–HCl pH 8.0.
12. Recover the cells by centrifugation at 14000 × g for 30 seconds in a microfuge. Aspirate off the pepsin and buffer solution.
13. Resuspend the cell pellet in 500 µL of propidium iodide staining solution (*see* **Note 2**).
14. Stain the cells overnight at 4 °C. These samples are stable for up to 2 weeks.
15. Immediately before analysis vortex the samples to mix the cells well and take 50 µL of each sample to 2.5 mL of Tris–HCl pH 8.0 in a 5 mL polystyrene round bottom tube 12 × 75 mm.
16. Vortex the samples and then sonicate each sample with a microtip equipped sonicator at full power to break apart clumps of cells.
17. The samples are now ready to proceed to analysis by flow cytometry.

3.2.3 Analysis of Nuclear Morphology by DAPI (4′,6-Diamidino-2-Phenylindole) Staining

1. Collect 0.5 mL samples of cell culture at the desired time points in a 1.5 mL microfuge tube and pellet the cells by centrifugation at 14000 × g for 30 seconds in a microcentrifuge. Aspirate off the medium.
2. Resuspend the cell pellet in 200 μL of 70% ethanol and fix the cells at 4 °C (*see* **Note 8**).
3. To visualize nuclei recover the cells from ethanol by centrifugation at 14000 × g for 30 seconds and aspirate off the ethanol.
4. Rehydrate the cells in 100 μL of 50 mM Tris–HCl.
5. Spot 5 μL of 100 ng/mL DAPI on a microscope slide and mix in 5 μL of the fixed cells.
6. Cells can now be examined under fluorescence microscopy to examine nuclear morphology and determine the timing of the nuclear divisions.

3.3 Synchronization of S. cerevisiae Cell Cultures

S. cerevisiae is a hardy and robust organism with a fully sequenced genome and the organism is amenable to genetic manipulation. These properties allow a wide range of tools and methods to be applied to achieve synchronous cultures for the analysis of cell cycle progression. Two general processes can be employed to achieve synchronous cell cultures. The simplest process involves applying a condition or chemical agent that blocks cell cycle progression and forces the culture to accumulate at a uniform cell cycle position. Removal of the arresting agent allows the cells to proceed to the subsequent stage of the cell cycle as a uniform population. These block and release processes also referred to as induced synchrony are relatively simple to apply and allow for large numbers of cells to be analyzed. These are particularly beneficial for biochemical studies where substantial amounts of protein or RNA may be required. A potential disadvantage to the block and release protocols is that they are generally more perturbing to the cells physiology as they uncouple the normal linkage between cell growth and division, can lead to toxicity, and can introduce confounding factors like heat shock response and side effects from the drug treatments applied.

A second approach to producing synchronized cultures of *S. cerevisiae* is selection synchrony. These processes involve fractionating an asynchronous culture to collect cells that are at specific phase of the cell cycle. Selection synchrony is distinct from induced synchrony in that no chemical or conditions force the cells to accumulate. Thus, a significant benefit of selection procedures is that they do not perturb the cells much or disturb the natural coordination between cell size, growth, and division. While selection synchrony has benefits for investigation of an unperturbed cell cycle it is limited by the requirement for specialized equipment and by the relatively small numbers of cells that can be isolated for analysis.

3.4 Induced Synchronization Block and Release Protocols

Induced synchronization procedures result in an asynchronous culture of cells accumulating at a single position in the cell cycle. This leads to a population that is synchronized with respect to the cell cycle but is nonuniform in size as arrested cells continue to grow while arrested. The cell cycle can be investigated both at the arrest points and following release from the arrest as the population synchronously moves through a cell cycle. Included in this chapter are induced synchronization protocols for G1-phase arrest with mating pheromone (Protocol 3.4.1), S-phase arrest using hydroxyurea (Protocol 3.4.2), and M-phase arrest using nocodazole (Protocol 3.4.3). Methods to achieve a synchronized population in G1-phase by reversible depletion of Cln1 Cln2 Cln3 (Protocol 3.4.4), and arrest in G2/M by reversible depletion of Cdc20 (Protocol 3.4.5). Protocols to achieved reversible arrest using thermosensitive *cdc* mutants is also included (Protocol 3.4.6).

3.4.1 Pheromone-Mediated Arrest and Release

Haploid *MAT*a *S. cerevisiae* are naturally subject to a transient G1-phase arrest in response to the 13 amino acid α-factor peptide secreted by haploid *MAT*α cells. In the presence of *MAT*α cells the arrested *MAT*a haploid will form a mating projection taking on a morphology referred to as "shmooing" and fuse with the *MAT*α haploid to form a *MAT*a/*MAT*α diploid that does not respond to mating pheromone [18]. Synthetic α-factor effectively arrests *MAT*a cells as a homogeneous population in G1-phase with a shmoo morphology (*see* Fig. 2a). Removal of the α-factor from the medium leads to synchronous progression out of G1-phase and through the cell cycle.

1. Culture cells in YEPD medium at 30 °C until a density of 2–5 $\times$ 10^6 cells/mL is achieved (*see* **Note 9**).
2. Collect the cells by centrifugation at 4000 $\times$ g 3–5 minutes, wash with pre-warm YEPD, resuspend in YEPD at a density of 0.5 $\times$ 10^7 cells/mL (*see* **Note 10**).
3. Alternatively, cells can be collected by filtration (*see* **Note 11**).
4. Add synthetic α-factor to final conc of 5 μg/mL for *BAR1* strains or 50 ng/mL for *bar1* strains from a 5 mg/mL stock of peptide (*see* **Note 12**).
5. Incubate the culture at 30 °C for 2–3 hours with agitation (*see* **Note 13**).
6. When greater than 95% of cells are unbudded or display shmoo morphology the arrest is complete (*see* **Note 14**).
7. Releasing cells from the arrest can be achieved in several ways. Cells can be collected by centrifugation at 4000 $\times$ g for 3–5 min, washed with prewarmed YEPD and resuspended in prewarmed YEPD at a density of 0.5–1.0 $\times$ 10^7 cells/mL.

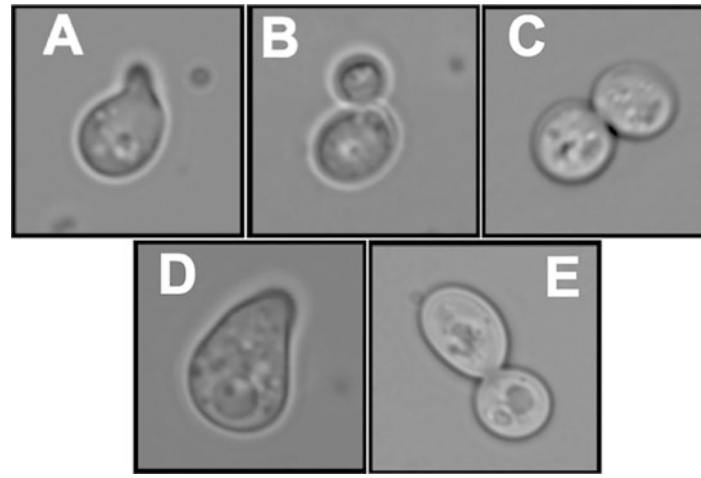

Fig. 2 Phenotypes of arrested cells. (**a**) *MATa, bar1Δ* cells that have been arrested by treatment with 50 ng/mL α-factor display a shmoo morphology. (**b**) Treatment with hydroxyurea arrests cells in S-phase with medium-sized buds. (**c**) Nocodazole treatment leads to an arrest in the G2/M phase and cells accumulate with large buds displaying a dumbbell morphology. (**d**) At the non-permissive temperature *cdc28–13* strains accumulate as unbudded cells. (**e**) At the non-permissive temperature *cdc15–2* mutants accumulate with a dumbbell morphology similar to the arrest displayed by nocodazole treatment

Alternatively, cells can be collected by filtration on nylon membranes, washed and resuspended in fresh prewarmed medium at a density of 0.5–1 × 10^7 cells/mL (*see* **Note 11**). Synchrony of release is improved by addition of pronase to a final concentration of 50 μg/mL to degrade any residual α-factor (*see* **Note 11**).

8. Remove cell samples at time 0 for processing (*see* **Note 15**).
9. Collect samples every 10–15 minutes to monitor progression through the cell cycle (*see* **Note 16**).

3.4.2 Hydroxyurea-Induced S-Phase Arrest and Release

Hydroxyurea is an inhibitor of ribonucleotide reductase that acts by quenching a tyrosyl radical required for catalytic activity [19]. Inactivation of ribonucleotide reductase leads to a depletion of dNTPs thus inhibiting progression of DNA replication, inducing an S-phase arrest [20]. Upon treatment with an arresting concentration of hydroxyurea, cells in the culture will accumulate with a small- to medium-sized bud morphology (*see* Fig. 2b) and DNA content greater between 1 N and 2 N.

1. Culture cells in YEPD medium at 30 °C until a density of 2–5 × 10^6 cells/mL is achieved (*see* **Note 9**).
2. Add hydroxyurea powder to a final conc of 0.2 M (*see* **Note 17**).

3. Incubate the culture at 30 °C with agitation for ~2–3 hours (*see* **Note 13**).
4. When greater than 95% of cells display small-medium size budded morphology the cells are arrested. Cell number will increase as cells complete division and arrest. There should be no increase in cell number past 2 hours but cells will continue to increase in size (*see* **Note 14**).
5. Release the cells from arrest. This can be achieved by collecting the cells by centrifugation (4000 × g for 3–5 min), washing 2× with prewarmed medium and resuspending the cells in prewarmed medium at a density of 0.5–1.0 × 10^7 cells/mL. Alternatively, the cells can be collected from the culture by filtration on membranes washed with prewarmed medium and resuspended in prewarmed medium at a density of ~0.5–1 × 10^7 cells/mL (*see* **Note 11**).
6. Remove cell samples at time 0 (*see* **Note 15**).
7. Collect samples every 10–15 minutes to monitor progression through the cell cycle (*see* **Note 16**).

3.4.3 Nocodazole-Induced G2/M-Phase Arrest and Release

Nocodazole inhibits microtubule polymerization by binding tubulin and thus disrupts formation of the metaphase spindles leading to cell cycle arrest at G2/M-phase [21]. At this phase of the cell cycle *S. cerevisiae* arrest with large budded phenotype referred to as dumbbell morphology (*see* Fig. 2c), 2 N DNA content and a nucleus stretched between the mother and bud.

1. Culture cells in YEPD medium at 30 °C until a density of 2–5 × 10^6 cells/mL is achieved (*see* **Note 9**).
2. Add nocodazole to a final conc of 15 μg/mL (*see* **Note 18**).
3. Incubate the culture at 30 °C with agitation for ~2–3 hours.
4. When greater than 95% of cells display large budded morphology the G2/M-phase arrest is complete (*see* **Note 19**).
5. Release the cells from arrest. This can be achieved by collecting the cells by centrifugation (4000 × g for 3–5 min), washing 2× with prewarmed medium and resuspending the cells in prewarmed medium at a density of 0.5–1.0 × 10^7 cells/mL. Alternatively, the cells can be collected from the culture by filtration on membranes washed with prewarmed medium and resuspended in prewarmed medium at a density of ~0.5–1 × 10^7 cells/mL (*see* **Note 11**).
6. Remove cell samples at time 0 (*see* **Note 15**).
7. Collect samples every 10–15 minutes to monitor progression through the cell cycle (see **Note 16**).

3.4.4 G1-Phase Arrest Induced by Cyclin Depletion

Cell cycle arrest can be achieved by depletion of proteins that perform a function required for progression from one cell cycle phase to the next. This is most effectively applied to proteins that are highly unstable and so can be rapidly degraded leading to a uniform arrest of the culture. The G1 cyclins encoded by *CLN1, CLN2,* and *CLN3* are essential to progress from G1 into S-phase. Any single *CLN* gene is sufficient for viability but inactivation of all three leads to an arrest in the G1-phase as round unbudded cells [22]. Placing one *CLN* gene under the control of a regulatable promoter and deletion of the other two *CLN* genes allows regulated reversible arrest in the G1-phase [22]. Upon induction of *CLN* expression from the regulatable promoter cells will synchronously transit the G1- to S-phase boundary and proceed through the cell cycle [23, 24]. This strategy can be employed with anyone of the *CLN1, CLN2,* or *CLN3* genes under the control of a regulatable promoter but *CLN3* is reported to be the most unstable of the three proteins ensuring rapid arrest of the cells following inactivation of the promoter [25, 26].

1. Culture *cln1 cln2 cln3 MET3-CLN3* or *GAL1-CLN3* cells in medium that allows expression of the *CLN3* gene, either medium lacking methionine (SD – Met) to induce the *MET3* promoter (*see* **Note 20**) or YEP 1% Raff 1% Gal medium to induce the *GAL1* promoter (*see* **Note 21**).
2. When cells achieve a density of 0.5–1.0 × 10^7 cells/mL extinguish expression of the inducible *CLN* gene. *MET3-CLN3* can be shut-off by addition of methionine to the medium to a final concentration of 4 mM, *GAL1-CLN3* can be inactivated through collecting the cells by filtration onto nylon membranes, washing with prewarmed YEP-1% Raff and resuspending in prewarmed YEP-1% Raff at a density of 0.5–1.0 × 10^7 cells/mL (*see* **Note 11**). Alternatively, the cells can be collected by centrifugation at 4000 × g for 3–5 min, washing 2× with YEP-1% Raff and resuspending the culture in prewarmed YEP-1% Raff at a density of 0.5–1.0 × 10^7 cells/mL.
3. Incubate the culture at 30 °C with agitation for 3 hours, when greater than 95% of the cells have accumulated as round unbudded cells the arrest is complete.
4. A *cln1 cln2 GAL1-CLN3* culture can be released from arrest by addition of galactose to the medium to a final concentration of 1%. A *cln1 cln2 MET3-CLN3* culture is released from arrest by collecting the cells by filtration washing with prewarmed synthetic medium lacking methionine and resuspending the cells in prewarmed SD-Met medium to a final density of 0.5–1.0 × 10^7 cells/mL (*see* **Note 11**). Alternatively, the arrested *cln1 cln2 MET3-CLN3* cells can be collected by centrifugation at 4000 × g for 3–5 min, washing in prewarmed synthetic

medium lacking methionine and resuspending in prewarmed SD – Met medium at a density of 0.5–1.0 × 10^7 cells/mL.

5. Remove cell samples at time 0 (*see* **Note 15**).
6. Collect samples every 10–15 minutes to monitor progression through the cell cycle (*see* **Note 16**).

3.4.5 Metaphase Arrest Achieved by Depletion of Cdc20

Cdc20 is an essential activator of the Anaphase Promoting Complex (APC) required for transition through metaphase and completion of mitosis [27] and loss of Cdc20 function leads to metaphase arrest with large-budded dumbbell morphology [28, 29]. Cdc20 is normally expressed and functions in the G2/M phase but is unstable in the G1- and S-phase of the cell cycle [30, 31]. Inactivation of thermosensitive Cdc20 mutants can achieve a G2/M-phase arrest but there are some benefits from depletion of Cdc20 activity without the associate temperature shifts as heat shock can influence a number of different parameters of yeast cell physiology [32].

1. Strains harboring *cdc20::MET3-CDC20* or *cdc20::GAL1-CDC20* can be cultured in medium allowing expression of the regulatable promoter, SD-Met for *cdc20::MET3-CDC20*, or medium containing galactose YEP-1% Raff, 1% Gal for *cdc20::GAL1-CDC20*. Culture the cells in appropriate medium until a cell density of 0.5 × 10^7 cells/mL is achieved.
2. Induce arrest of *cdc20::MET3-CDC20* by addition of methionine to a final conc of 4 mM in the medium. If using *cdc20::GAL1-CDC20* arrest the culture by collecting by the cells by centrifugation (4000 × g for 3–5 min, washing the cells 2× in prewarmed in YEP-2% Raff and then resuspended to a culture density of 0.5 × 10^7 cells/mL in YEP-2% Raff medium (*see* **Note 22**).
3. Incubate the cells in the repressive medium conditions at 30 °C for 2–3 hours (*see* **Note 23**).
4. Release the culture from the arrest by collecting the *cdc20::MET3-CDC20* strain by filtration or centrifugation onto nylon membranes washing the cells with prewarmed SD-Met medium and resuspending the cells in prewarmed SD-Met medium at a density of 1 × 10^7 cells/mL (*see* **Note 11**). Alternatively, the cells can be collected by centrifugation at 4000 × g 3–5 min, wash 2× with prewarmed SD-Met medium and resuspending in prewarmed SD-Met medium at a density of 1 × 10^7 cells /mL. Release of *cdc20::GAL1-CDC20* strains can be achieved by adding galactose to the medium to a final concentration of 1%.
5. Remove cell samples at time 0 (*see* **Note 15**).
6. Collect samples every 10–15 minutes to monitor progression through the cell cycle (*see* **Note 16**).

3.4.6 Specific Cell Cycle Arrest Induced by Inactivation of Thermosensitive cdc Mutants

An extensive collection of *cdc* mutants have been isolated in *S. cerevisiae* [15]. These mutants encode thermosensitive versions of proteins whose function is required for progression past one phase of the cell cycle. The function of the mutant protein can be rapidly inactivated by shifting cells to the non-permissive temperature leading the culture to uniformly arrest at one phase of the cell cycle. Shifting the temperature down to the permissive temperature leads reactivation of the thermosensitive protein and synchronous progression to the subsequent cell cycle phase. Widely used mutants include *cdc28*, which leads to an arrest in the G1-phase (*see* Fig. 2d), *cdc6* and *cdc7* that lead to an S-phase arrest, *cdc16, cdc23, cdc27*, and *cdc20* inducing a metaphase arrest prior to chromosome divisions, *cdc5*, *cdc14*, and *cdc15* that lead to a late anaphase/telophase arrest (*see* Fig. 2e) (*see* **Note 24**). The use of *cdc* mutants benefits from the ease of producing a uniform arrest of the culture but some limitations include a consideration that temperature shift may influence other aspects of the cells physiology [32, 33].

1. Culture the cells in YEPD or appropriate synthetic medium at the permissive temperature (usually 23–25 °C) until a density of 2–5 × 10^6 cells/mL is achieved. Culture cells in YEPD medium at 30 °C until a density of 2–5 × 10^6 cells/mL is achieved (*see* **Note 9**).
2. Shift the culture to the non-permissive temperature (usually 37 °C) (*see* **Note 25**).
3. Incubate the cell culture at the non-permissive temperature until greater that 95% of the cells display the morphology expected from the arrest (*see* **Note 26**).
4. Release the cells from arrest. This can be achieved by collecting the cells by centrifugation (4000 × g for 3–5 min), washing 2× with medium per-warmed to the permissive temperature and resuspending the cells in medium at the permissive temperature at a density of 0.5–1.0 × 10^7 cells/mL. Alternatively, the cells can be collected by filtration on membranes washed with medium prewarmed to the permissive temperature and resuspended in medium at the permissive temperature at a density of ~0.5–1 × 10^7 cells/mL (*see* **Note 11**).
5. Immediately collect cells for the time 0 sample (*see* **Note 15**).
6. Collect samples every 10–15 minutes to monitor cell cycle progression (*see* **Note 16**).

3.5 Selection Synchrony

In contrast to induced synchronization, selection protocols capture and isolate specific populations of cells, for example, G1-phase cells, from an asynchronous culture and this population can then be monitored as it proceeds through the cells division cycle.

Selection procedures such as centrifugal elutriation yield smaller numbers of cells thus limiting the amount of protein and RNA that can be isolated. These methods do benefit from being less perturbing allowing for more relevant physiological studies to be performed and from a higher degree of synchrony.

3.5.1 Centrifugal Elutriation

Cell division by budding leads to asymmetry at division in *S. cerevisiae*. Following cytokinesis, the newborn G1-phase daughter cells are smaller than the mother (Fig. 1). The larger mother cell has a larger protein synthetic capacity and will rapidly progress from G1-phase into S-phase. In contrast, the smaller daughter cells must grow in size until they reach a threshold of cell size and protein synthetic capacity is achieved that will allow them to transit G1 into S-phase [34]. Once the cells form a new bud and enter S-phase, a high proportion of growth is directed into the bud [35, 36]. This form of cell division creates a direct relationship between cell size and cell cycle position in any specific growth medium. Fractionating an asynchronous population based on cell size is one means by which cells in specific cell cycle phases can be enriched.

Centrifugal elutriation is a counter-current centrifugation technique that fractionates particles predominantly based upon size and to a lesser extent density [37, 38]. A specially modified centrifuge and rotor system are used to separate asynchronously growing cultures based on size and thus small G1-phase cells, larger S-phase cells, and the still larger G2/M phase cells can be separated and isolated based on their size (*see* Fig. 3). In this way populations of cells in specific phases of the cell cycle can be collected without the need to perturb the cells with chemical or temperature-mediated forced synchronization. One of the benefits of synchronization by centrifugal elutriation is that it can be applied to any strain, specific mutants are not required and it can be applied to haploids, or diploids and even to synchronize cells for developmental processes like meiosis and sporulation [39].

3.5.2 Selection of G1-Phase Cells by Centrifugal Elutriation

1. Culture the strain of interest in appropriate medium overnight to create a starter culture.
2. Count the cells in the culture and inoculate into 1 L of YEP-Raff, YEP-Suc, or YEP-Glyc medium in a Fernbach flask. The starting cell density should be one that will result in the cells reaching a density of 1.0–2.0 $\times$ 10^7 cells/mL after overnight growth (*see* **Notes 27** and **28**).
3. When the cells have reached a density of 1–2 $\times$ 10^7 cells/mL, collect the cells by centrifugation, at 4000 $\times$ g 5 min. Pour off the medium and save this in a save sterile bottle of flask (*see* **Note 29**).
4. Resuspend the cell pellet in 150–200 mL of the spent medium in a 250 mL conical centrifuge bottle.

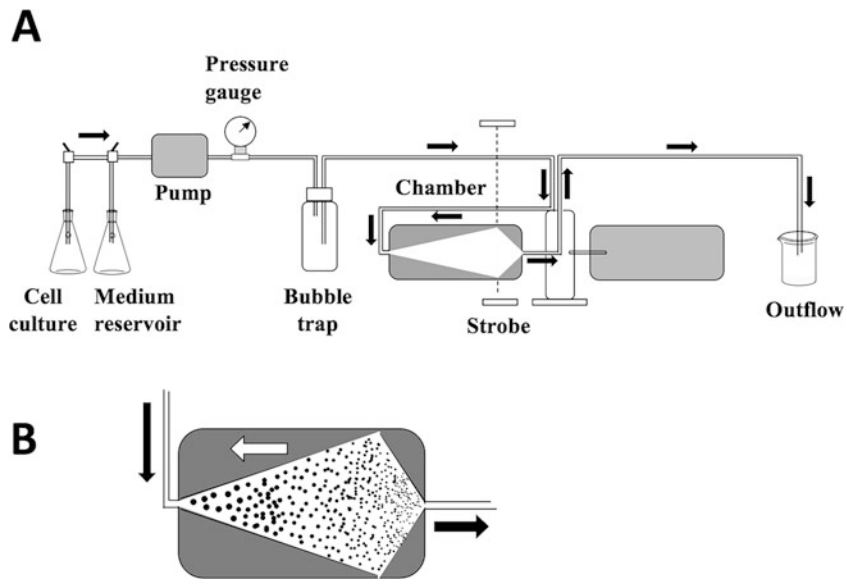

Fig. 3 (**a**) Basic set up of the centrifugal elutriation system. The black arrows indicate the direction of flow of medium from the cell culture and medium reservoir to the chamber and outflow. The cells from the reservoir are loaded into the chamber and the progress of the cells packing into the chamber can be observed through the viewport by the use of a strobe light installed in the centrifuge. Within the chamber a gradient of cells is formed and small cells can be pumped from the chamber into the outflow contained by increasing the pump speed. (**b**) Centrifugal force indicated by the white arrow is balanced by the rate of medium being pumped into the chamber shown by the black arrow, to form a gradient with the largest cells at the bottom and smallest cells at the top near the outflow. Increasing the pump speed pushes the smallest cells into the outflow for collection

5. Sonicate the cells for 3 × 15 seconds with microtip horn (*see* **Note 30**).
6. Assemble the elutriation chamber making sure that all the seals are tight.
7. Secure the separation chamber and balance into the quick release assembly.
8. Place the quick release assembly into the rotor and connect the inflow and outflow tubing.
9. Place the tethering cord into the quick release assembly.
10. Place a flask with 500 mL of 5% bleach near the pump.
11. Pump bleach into all the inflow and outflow lines and the separation chamber collecting the bleach into a waste flask.
12. Move the inflow lines into a bottle containing 1.5 L of sterile water (for the set up *see* Fig. 3).
13. Pump sterile water through the tubing and separation chamber assembly.

14. When the system has been rinsed set up a flask with the spent medium from the cell culture near the peristaltic pump.
15. Place both of the inflow tubes and the outflow tube into the spent medium containing flask.
16. Pump cold medium into the tubing through the bubble trap at a rate of 25 mL/minute and fill the chamber.
17. Continue until the tubing and chamber are filled with medium.
18. Ensure that the tubing and chamber are free of bubbles (*see* **Note 31**).
19. Precool the centrifuge to 4 °C (*see* **Note 32**).
20. Start the centrifuge running at 2400 × g.
21. Move the inflow tube that is "closed" into the centrifuge bottle with the cell suspension.
22. Open the flow to the tubing that is in the cell suspension.
23. Load cells into the elutriation chamber.
24. Place the outflow line into the centrifuge bottle containing the cell suspension.
25. Sample 20 μL of the outflow medium and place on a microscope slide. Under a microscope determine if cells are passing out of the chamber. If cells are observed decrease the pump speed until cells are no longer present in the outflow.
26. Place the outflow tube into a bottle to collect waste until greater than ½ of the cell suspension has been loaded.
27. When less than half of the cell suspension (~100 mL) is remaining place the outflow tube back into the bottle with the cells (*see* **Note 33**).
28. Continue loading until all of the cells have been loaded into the chamber and the remaining medium in the centrifuge bottle is clear.
29. Observing through the view port should display a dark front of cells in the chamber.
30. Turn off the flow from the cell suspension bottle and open the flow from the spent medium flask.
31. Place the outflow into the spent medium flask.
32. When a stable front of cells can be seen through the view port begin increasing the pump speed in 2 mL/minute increments. Sample the outflow about 1 minute after each change in the pump speed and use the microscope to look for the appearance of small unbudded cells.
33. Continue increasing pump speed until unbudded cells appear then move the outflow line into a conical 250 mL centrifuge bottle in ice.

34. Collect cells into a centrifuge bottle and recover a 10 μL sample from the outflow every 5 minutes. Place the sample into a hemocytometer counting chamber and count the cells. Alternatively, the samples can be analyzed with a Z2 Coulter Channelyzer to determine cell number and volume.
35. Collect cells until the outflow contains less than 10^6 cells/mL.
36. Change the outflow tube to a new centrifuge bottle and increase the pump speed.
37. Continue collecting fractions until the outflow displays greater than 5% budded cells at which point the separation should be stopped or the samples will become contaminated to S-phase and G2 cells.
38. Sample the cell fractions in the centrifuge bottles, count the cells and examine morphology.
39. All fractions that contain greater than 95% unbudded cells can be used for analysis of progression out of G1 and through the cell cycle but greatest synchrony will be achieved by use of a homogenous sized, unbudded population. The first bottle of cells collected will be the smallest G1-phase cell and each subsequent fraction will be larger.
40. All of the unbudded cells can be pooled but the greatest synchrony is achieved if homogeneous size fractions are collected. Concentrate the desired fractions by centrifugation and resuspend the cells in prewarmed medium at a density of 1×10^7 cell/mL.
41. Collect a cell sample at time 0 and prepare for analysis of the desired parameters of macromolecules (*see* **Note 34**).
42. Collect samples every 10–20 minutes and prepare for analysis of cell size, DNA content, morphology and any macromolecules that are of interest (*see* **Notes 16** and **34**).
43. Place the outflow tube into a bottle or flask for waste and place the inflow line into a flask of water.
44. Increase the pump speed and reduce the speed of the centrifuge to 1000 rpm to pump the remaining cells out of the chamber and into the waste.
45. When the bulk of cells have been evacuated from the separation chamber pump air into the tubing and chamber.
46. Pump in 10% bleach.
47. Pump in water to clear.
48. Pump in 70% ethanol.
49. Disassemble, clean, and sterilize the chamber, quick release assembly, and all tubing.

4 Notes

1. When selecting G1-phase cells by centrifugal elutriation 250 mL conical centrifuge bottles are advantageous since the G1-phase cells are small and in low concentration, the conical bottles concentrate the cells into a small pellet for more effective recovery following centrifugation.
2. Propidium Iodide solution is composed of 180 mM Tris base, 190 mM NaCl, 55 mM $MgCl_2$, 75 μM Propidium iodide pH 7.5. It is important to dissolve the Tris base and NaCl in water and pH to 7.5 with HCl prior to addition of $MgCl_2$ and propidium iodide, protect from light and store frozen.
3. Prepare a stock as 10 mg/mL RNase A in 10 mM sodium acetate pH 5.2, boil for 10–15 min, when cooled neutralize by addition of 0.1 volumes of 1.0 M Tris–HCl pH 8.0.
4. Currently, the only elutriation systems available are from Beckman Instruments (Fullerton, CA. USA). The JE-5.0 rotor can be used with an appropriate high-volume centrifuge. Several different elutriation chambers are available but the 40 mL chamber allows for larger volumes of cells. Other essential components of the system including peristaltic pump, pressure gauge, strobe light, and tubing can be acquired with the elutriation system.
5. The Z2 channelyzer (Beckman Coulter Life Sciences, Indianapolis, IN, USA) allows for particle counting and cell volume analysis. For *S. cerevisiae* we use this instrument with a 70 μm aperture. Other similar instruments are available and are convenient for rapidly counting cells and determining culture size homogeneity.
6. The rate of doubling and cell cycle distribution can be influenced by composition of the medium. Cells display fastest growth rates in YEPD, less favorable carbon sources delay progress through G1-phase leading to increased proportion of G1-phase cells. Cell size will be increased in YEPD relative to less favorable carbon sources.
7. Cell size will influence the OD_{600} and some mutants may be larger than wildtypes. It is helpful to count cells with a hemocytometer to determine actual cell numbers.
8. Fixed cells can be stored at 4 °C for up to one week prior to analysis.
9. Synthetic medium can also be used if cells are harboring plasmids, other carbon sources can be used. Monitor cell density by cell numbers since cell size will change during and following arrest confounding direct comparison by optical density.

10. *BAR1* strains express the Bar1 protease which degrades pheromone and so a higher concentration is required to achieve G1-phase arrest. Alternatively, delete the *BAR1* gene by homologous recombination allowing the use of lower concentrations of α-factor. Although α-factor is commercially available, for example, from Sigma-Millipore (Cat# T6901) it is relatively expensive and generating a *bar1Δ* strain can yield a significant cost saving.
11. Alternatively, cells can be collected by filtration onto nylon filter disks using a filtration apparatus. Cells can then be washed on the filter by pouring prewarmed YEPD through the filter and then resuspended in YEPD [40].
12. When arresting *bar1Δ* cells with α-factor it is not essential to wash the cells prior to addition of the pheromone. Arrest of *BAR1* cells with α-factor will be significantly improved by washing the cells with prewarmed YEPD pH 3.5 to remove secreted Bar1 protease. Bar1 is less active at low pH [41, 42].
13. Monitor the cell morphology by microscopic examination. When greater than 95% of cells are unbudded or display "shmoo" morphology the arrest is complete.
14. Holding the cells arrested for longer periods will reduce synchrony as some cells may begin to escape the arrest while others may suffer toxicity from the arrest and have difficulty proceeding into the cell cycle.
15. The time 0 sample is essential for determining the homogeneity of the culture and to set a baseline for whatever parameters are to be monitored during the course of the experiment. The parameters monitored will depend on the application but generally samples would be processed by fixing a portion the culture with 70% ethanol for DNA content analysis by flow cytometry, fixation with 3.7% formaldehyde for morphological analysis and/or tubulin staining or other immunofluorescent staining. Portions of the culture can be collected and stored at −80 °C for later analysis of RNA and or protein species.
16. The parameters monitored will depend on the application but generally samples would be processed by fixing a portion of the culture with 70% ethanol for DNA content analysis by flow cytometry, fixation with 3.7% formaldehyde for morphological analysis and/or tubulin staining or other immunofluorescent staining. Portions of the culture can be collected and stored at −80 °C for later analysis of RNA and or protein species.
17. The high concentration of HU required to achieve effective arrest makes it impractical to prepare a sterile stock solution so it is simplest to add the required amount of powder directly to the medium. Some cells are more resistant to HU and sensitivity should be tested prior to initiating the experiment.

18. Nocodazole stock solution 1.5 mg/mL in DMSO. Some cells are more resistant to nocodazole and sensitivity should be tested prior to initiating the experiment.
19. Monitor the cells for the appearance of large budded cells indicating a G2/M-phase arrest, avoid prolonged exposure to nocodazole as this will lead to cell death and poor release from the block [43].
20. The *MET3* promoter is active in the absence of methionine but rapidly inactivated upon the addition of methionine to the medium to 4 mM final concentration [44].
21. The *GAL1* promoter is induced by galactose at 1% in the medium but 1% raffinose, glycerol or other nonrepressive carbon source should be included as a carbon source. Glucose, even in low concentrations must be avoided as glucose will repress expression from the *GAL1* promoter [45, 46].
22. Inactivation of the *MET3* promoter is less complicated than transferring the cells into medium lacking galactose but cell growth in SD-met medium will be slower than cells growing in YEP-Raf + Gal.
23. Monitor the arrest by microscopic examination. When greater than 95% of cells have arrested with large buds (dumbbell morphology) the arrest is complete.
24. Most alleles of *cdc28* yield a G1-phase arrest but *cdc28-1 N* mutants arrest predominantly at the G2-phase [47].
25. It is faster and more effective to collect the cells by filtration or centrifugation, wash and resuspend the cells in medium prewarmed to the nonpermissive temperature. This achieves more rapid arrest than simply moving the culture to an incubator at the non-permissive temperature.
26. The time required to achieve a synchronously arrested culture will be at minimum the length of time required for one division cycle for those cells and may be up to 3 hours dependent on the medium used. Incubation at non-permissive temp for longer than necessary will lead to cell death and reduce the synchrony of progression upon release from the block.
27. Fernbach flasks are superior for this application owing to the large surface area allowed for the culture.
28. Any medium can be used but media containing a carbon source less favorable than glucose, typically raffinose, sucrose or glycerol allows a greater difference in size between newly budded daughter and mother cells. Additionally, media that lead to slower growth will expand the G1-phase of the cell cycle and thus enrich the population for G1-phase cells. Glucose allows

faster growth but a smaller portion of the population will be G1-phase and the newborn cells will be closer in size to the mother thus it will be more difficult to isolate a pure population of unbudded G1-phase cells [13, 48].

29. The spent growth medium will be used later in the elutriation process it should be cooled and kept sterile.
30. Sonication helps to separate cells that have clumped together and can help to separate daughter cells from mothers. Sonication should be brief and only use a microtip probe. Longer bouts of sonication can damage the small cells, reducing their viability and reducing the synchrony of progression through the cell cycle upon release.
31. Evacuating all of the air bubbles out of the tubing and separation chamber is vital to a successful fractionation. Residual air bubbles will disrupt the fluid flow and can cause changes in pressure within the separation chamber that will disrupt the cell gradient. Air bubbles can be removed by pinching off the inflow line with your fingertips and then rapidly releasing to cause a pulse of medium into the lines. Additionally, the quick release chamber can be removed from the rotor while the pump is running, and lightly tapped on its side to move bubbles out of the chamber and into the outflow line.
32. The elutriation process can be performed at room temperature but may result in reduced synchrony as the cells will continue proceeding into cycle once eluted from the chamber.
33. Other means of loading the cells are possible including just placing the inflow line into the 1 L culture. However, the method described speeds the loading process significantly.
34. Typically, cell volume and number would be determined by diluting a 100 μL sample of the cell culture into 9.9 mL of isoton II buffer and performing analysis with a Coulter Z2 Channelyzer. Samples can also be fixed in 70% ethanol for subsequent DNA content analysis by flow cytometry and a sample fixed in 3.7% formaldehyde for microscopic analysis of morphology. Other sample portions can be fixed as appropriate for immunofluorescence and/or snap frozen for subsequent analysis of protein and or RNA.

Acknowledgments

This work was supported by research grant RGPIN-2021-02898 from the Natural Sciences and Engineering Research Council of Canada.

References

1. Morgan DO (2007) The cell cycle:principles of control. New Science Press Ltd, London
2. Hartwell LH, Weinert TA (1989) Checkpoints: controls that ensure the order of cell cycle events. Science 246:629–634
3. Hartwell LH (1974) *Saccharomyces cerevisiae* cell cycle. Bacteriol Rev 38:164–198
4. Newport JW, Kirschner MW (1984) Regulation of the cell cycle during early Xenopus development. Cell 37:731–742
5. O'Farrell PH, Edgar BA, Lakich D, Lehner CF (1989) Directing cell division during development. Science 246:635–640
6. Kipreos ET, van den Heuvel S (2019) Developmental control of the cell cycle: insights from *Caenorhabditis elegans*. Genetics 211: 797–829
7. Pérez-Hidalgo L, Moreno S, Martín-Castellanos C (2008) Modified cell cycle regulation in meiosis. In: Egel R, Lankenau D-H (eds) Recombination and meiosis: crossing-over and disjunction. Springer, Berlin, Heidelberg
8. Botstein D, Fink GR (1988) Yeast: an experimental organism for modern biology. Science 240:1439–1443
9. Goffeau A, Barrell BG, Bussey H, Davis RW, Dujon B, Feldmann H et al (1996) Life with 6000 genes. Science 274(546):563–567
10. Knop M, Siegers K, Pereira G, Zachariae W, Winsor B, Nasmyth K, Schiebel E (1999) Epitope tagging of yeast genes using a PCR-based strategy: more tags and improved practical routines. Yeast 15:963–972
11. Hartwell LH, Unger MW (1977) Unequal division in *Saccharomyces cerevisiae* and its implications for the control of cell division. J Cell Biol 75:422–435
12. Amon A (1996) Mother and daughter are doing fine: asymmetric cell division in yeast. Cell 84:651–654
13. Schneider BL, Zhang J, Markwardt J, Tokiwa G, Volpe T, Honey S, Futcher B (2004) Growth rate and cell size modulate the synthesis of, and requirement for, G1-phase cyclins at start. Mol Cell Biol 24: 10802–10813
14. Lew DJ, Reed SI (1995) Cell cycle control of morphogenesis in budding yeast. Curr Opin Genet Dev 5:17–23
15. Hartwell LH, Mortimer RK, Culotti J, Culotti M (1973) Genetic control of the cell division cycle in yeast: V. Genetic analysis of *cdc* mutants. Genetics 74:267–286
16. Futcher B (1999) Cell cycle synchronization. Methods Cell Sci 21:79–86
17. Sherman F (1991) Getting started with yeast. Methods Enzymol 194:3–21
18. Tkacz JS, MacKay VL (1979) Sexual conjugation in yeast. Cell surface changes in response to the action of mating hormones. J Cell Biol 80:326–233
19. Wang PJ, Chabes A, Casagrande R, Tian XC, Thelander L, Huffaker TC (1997) Rnr4p, a novel ribonucleotide reductase small-subunit protein. Mol Cell Biol 17:6114–6121
20. Elledge SJ, Davis RW (1990) Two genes differentially regulated in the cell cycle and by DNA-damaging agents encode alternative regulatory subunits of ribonucleotide reductase. Genes Dev 4:740–751
21. Kunkel W (1980) Effects of the antimicrotubular cancerostatic drug nocodazole on the yeast *Saccharomyces cerevisiae*. Z Allg Mikrobiol 20: 315–324
22. Richardson HE, Wittenberg C, Cross F, Reed SI (1989) An essential G1 function for cyclin-like proteins in yeast. Cell 59:1127–1133
23. Dirick L, Nasmyth K (1991) Positive feedback in the activation of G1 cyclins in yeast. Nature 351:754–757
24. Stuart D, Wittenberg C (1995) *CLN3*, not positive feedback, determines the timing of *CLN2* transcription in cycling cells. Genes Dev 9:2780–2794
25. Tyers M, Tokiwa G, Futcher B (1993) Comparison of the *Saccharomyces cerevisiae* G1 cyclins: Cln3 may be an upstream activator of Cln1, Cln2 and other cyclins. EMBO J 12: 1955–1968
26. Cross FR, Blake CM (1993) The yeast Cln3 protein is an unstable activator of Cdc28. Mol Cell Biol 13:3266–3271
27. Morgan DO (1999) Regulation of the APC and the exit from mitosis. Nat Cell Biol 1: E47–E53
28. Shirayama M, Tóth A, Gálová M, Nasmyth K (1999) APCCdc20 promotes exit from mitosis by destroying the anaphase inhibitor Pds1 and cyclin Clb5. Nature 402:203–207
29. Yeong FM, Lim HH, Padmashree CG, Surana U (2000) Exit from mitosis in budding yeast: biphasic inactivation of the Cdc28-Clb2 mitotic kinase and the role of Cdc20. Mol Cell 5:501–511
30. Robbins JA, Cross FR (2010) Regulated degradation of the APC coactivator Cdc20. Cell

Div 5:23. https://doi.org/10.1186/1747-1028-5-23

31. Prinz S, Hwang ES, Visintin R, Amon A (1998) The regulation of Cdc20 proteolysis reveals a role for the APC components Cdc23 and Cdc27 during S phase and early mitosis. Curr Biol 8:750–760
32. Keuenhof KS, Larsson Berglund L, Malmgren Hill S, Schneider KL, Widlund PO, Nystrom T, Hoog JL (2022) Large organellar changes occur during mild heat shock in yeast. J Cell Sci 135. https://doi.org/10.1242/jcs.258325
33. Verghese J, Abrams J, Wang Y, Morano KA (2012) Biology of the heat shock response and protein chaperones: budding yeast (*Saccharomyces cerevisiae*) as a model system. Microbiol Mol Biol Rev 76:115–158
34. Jorgensen P, Rupes I, Sharom JR, Schneper L, Broach JR, Tyers M (2004) A dynamic transcriptional network communicates growth potential to ribosome synthesis and critical cell size. Genes Dev 18:2491–2505
35. Hartwell LH, Culotti J, Reid B (1970) Genetic control of the cell-division cycle in yeast. I detection of mutants. Proc Natl Acad Sci U S A 66:352–359
36. Howell AS, Lew DJ (2012) Morphogenesis and the cell cycle. Genetics 190:51–77
37. Lindahl PE (1948) Principle of a counter-streaming centrifuge for the separation of particles of different sizes. Nature 161:648
38. Bauer J (1999) Advances in cell separation: recent developments in counterflow centrifugal elutriation and continuous flow cell separation. J Chromatogr B Biomed Sci Appl 722:55–69
39. Stuart D, Wittenberg C (1998) *CLB5* and *CLB6* are required for premeiotic DNA replication and activation of the meiotic S/M checkpoint. Genes Dev 12:2698–2710
40. Rosebrock AP (2017) Synchronization and arrest of the budding yeast cell cycle using chemical and genetic methods. Cold Spring Harb Protoc 2017. https://doi.org/10.1101/pdb.prot088724
41. MacKay VL, Welch SK, Insley MY, Manney TR, Holly J, Saari GC, Parker ML (1988) The *Saccharomyces cerevisiae BAR1* gene encodes an exported protein with homology to pepsin. Proc Natl Acad Sci U S A 85:55–59
42. Unk I, Daraba A (2014) Synchronization of *Saccharomyces cerevisiae* cells in G1 phase of the cell cycle. Bio-protocol 4:e1273
43. Endo K, Mizuguchi M, Harata A, Itoh G, Tanaka K (2010) Nocodazole induces mitotic cell death with apoptotic-like features in *Saccharomyces cerevisiae*. FEBS Lett 584: 2387–2392
44. Cherest H, Kerjan P, Surdin-Kerjan Y (1987) The *Saccharomyces cerevisiae MET3* gene: nucleotide sequence and relationship of the 5′ non-coding region to that of *MET25*. Mol Gen Genet MGG 210:307–313
45. Lohr D, Venkov P, Zlatanova J (1995) Transcriptional regulation in the yeast GAL gene family: a complex genetic network. FASEB J 9:777–787
46. Gancedo JM (1998) Yeast carbon catabolite repression. Microbiol Mol Biol Rev 62: 334–361
47. Piggott JR, Rai R, Carter BL (1982) A bifunctional gene product involved in two phases of the yeast cell cycle. Nature 298:391–393
48. Flick K, Chapman-Shimshoni D, Stuart D, Guaderrama M, Wittenberg C (1998) Regulation of cell size by glucose is exerted via repression of the *CLN1* promoter. Mol Cell Biol 18: 2492–2501

Chapter 13

Cell Cycle Synchrony Methods for Fission Yeast, *Schizosaccharomyces pombe*

Zohreh Kianfard, Kyle Cheung, and Sarah A. Sabatinos

Abstract

The fission yeast, *Schizosaccharomyces pombe*, is a genetically tractable model organism for cell cycle and molecular genetics research. We describe methods to synchronize *S. pombe* cultures, and the benefits and limitations of each. Drug-induced synchrony is a convenient method to arrest the cell cycle. An example of the drug hydroxyurea is shown, which arrests cells in S-phase. Environmental modulation through media composition or growth conditions may also be used to synchronize cultures, most commonly with nitrogen depletion to arrest in G1-phase. Finally, examples of temperature-sensitive conditional alleles are shown which arrest the cell cycle at key transition points. Each of these methods must be assessed relative to the desired effect and the process being studied, providing the best synchrony with the fewest off-target effects.

Key words Fission yeast, *Schizosaccharomyces pombe*, cell cycle, Cdc10, Cdc22, Cdc25, Hydroxyurea block, Nitrogen arrest, Septation index

1 Introduction

Schizosaccharomyces pombe is a genetically tractable, fast-growing, and easy-to-use model organism. *S. pombe* cells divide by medial fission, suggesting the organism's common name of fission yeast. Although fission yeast experimental methods are similar to those of budding yeast (*Saccharomyces cerevisiae*), the two model organisms are distinct [1–3]. Fission yeast has a collegial international community and extensive curation tools (www.PomBase.org). Standard homologous recombination gene-targeting and expansion of newer CRISPR and recombinase methods have expanded the tools to explore *S. pombe* cell cycle regulation. In particular, fission yeast can be used to model mammalian-like DNA processes including: complex DNA replication origin structures and firing, centromere organization, and heterochromatin regulation. The molecular genetics of *S. pombe*, and its high similarity to metazoan cell

Zhixiang Wang (ed.), *Cell-Cycle Synchronization: Methods and Protocols*, Methods in Molecular Biology, vol. 2579,
https://doi.org/10.1007/978-1-0716-2736-5_13,

cycle and checkpoint processes, make fission yeast an attractive model to study cell proliferation mechanisms and their dysregulation in diseases.

The fission yeast cell cycle is approximately 2.7 hours in rich medium and at the predominant growth temperature of 32 °C; temperature and growth conditions are reviewed in articles such as [4–6]. In an actively growing fission yeast culture, approximately 70% of cells are in gap 2 (G2), and 10% in each of gap 1 (G1), synthesis (S), and mitosis (M) phases of the cell cycle. Many experiments can be performed in asynchronous cultures. However, methods that test cell growth, aging, and death frequently employ cellular synchrony to restrict effects within a cell cycle phase, or to highlight the mechanism under study. A variety of methods are commonly used to induce synchrony in fission yeast cultures. These capitalize on cell cycle inhibitory drugs, environmental conditions, and conditional alleles, and are described in this chapter.

Cell cycle arrest may be induced by adding drug to a culture. In this chapter, we describe the use of hydroxyurea (HU) to arrest cells in S-phase. HU poisons the enzyme ribonucleotide reductase, and causes dNTP depletion (e.g., [7, 8]). Replication forks slow and stall in HU, and fission yeast cells enter S-phase but arrest (e.g., [9–11]). Although nuclear division and cytokinesis are separated in *S. pombe* (discussed in Chapter 18), HU arrest in S-phase does not block cytokinesis and over time the culture will arrest with a mid-S-phase population of mononucleated cells. Consequently, HU is a useful arrest to detect resumption of DNA synthesis and the timing of S-phase exit. However, HU causes DNA replication fork instability, and activates the DNA replication checkpoint (e.g., [12]). Mutants that are DNA replication checkpoint-incompetent (e.g., *rad3*Δ, *mrc1*Δ, *cds1*Δ) lose viability (e.g., [9, 13, 14]). HU induces DNA damage even in checkpoint-competent cells, which may impact some genetic backgrounds (e.g., [15–17]). Careful choice of strains and controls will help to discern the effects of HU on DNA damage and cell cycle progression.

Numerous temperature-sensitive alleles of cell cycle genes have been characterized in *S. pombe*. These are available from many research groups and the National BioResource Program (NBRP, Japan) collection. Frequently, conditional alleles are used when the null allele does not survive in a haploid strain. This includes the cell division cycle 10 (Cdc10) gene, which regulates transcription to promote G1 to S transition in "Start". The conditional *cdc10-129* strain may be used to ablate Cdc10 and arrest cells in G1-phase (e.g., [18, 19]). Cdc22 is the enzymatic subunit of ribonucleotide reductase; heat inactivation of the *cdc22-M24* allele in a strain generates an S-phase arrest (e.g., [20]). The *cdc25-22* allele has been used extensively for G2-arrest methods (e.g., [21–23]). Temperature-sensitive strains are typically grown at a permissive temperature of 25 °C. A typical restrictive temperature to inactivate the

conditional allele protein function is 36 °C. Cold-sensitive alleles, such as the tubulin *nda3-KM311* [24], may provide alternatives for cell cycle synchrony.

We present methods to synchronize fission yeast in various cell cycle stages, and quickly assess the performance of the arrest method. The accompanying chapter "Detecting cell cycle stage and progression in fission yeast" describes methods to probe cell cycle effects within cultures that have been synchronized using these methods.

2 Materials

2.1 Fission Yeast Strains

Fission yeast strains are generally derived from the originally characterized 972/975 isolates (reviewed in [2, 3]). Strains are made by standard molecular genetics methods, as described in other methods articles. In addition to specific published strains available from fission yeast researchers, the National Bio Resource Program (NBRP) in Japan has an extensive collection of fission yeast strains; restrictions on strain use vary and are specified in the database.

2.2 Yeast Extract with Supplements Medium (YES)

A rich but undefined medium, YES can be made without supplements (yeast extract only, YE), or by adding adenine, L-histidine, L-leucine, uracil, and L-lysine to 50–225 mg/L. Yeast extract (YE) base is 5 g/L yeast extract, 30 g/L glucose in deioinized or MilliQ water. Pre-mixed YE or YES powder can be purchased in North America from MP Biologicals (Boston, MA) or Sunrise Media (California, CA). Media is made in water and autoclaved, then stored at room temperature indefinitely. Solid YES agar plates are made by adding 2% microbiology-grade agar to YES liquid, and autoclaving.

2.3 Edinborough Minimal Medium (EMM)

Synthetic and defined medium, EMM may be purchased as a stock powder from suppliers MP Biologicals or Sunrise Media. It is composed of 3 g/L potassium hydrogen phthalate, 2.2 g/L Na_2HPO_4, 5 g/L NH_4Cl, 20 g/L glucose, 20 mL/L salts (50× stock), 1 mL/L vitamins (1000× stock), and 0.1 mL/L minerals (10, 000×). EMM is made in water and autoclaved, then stored at room temperature. Supplements are added to 50–225 g/L according to the auxotrophic markers present in a given strain. EMM-nitrogen (EMM-N) is EMM without NH_4Cl added; this may be purchased as a stock powder from MP Biologicals or Sunrise Media. Alternatively, EMM-N may be made from this recipe, omitting NH_4Cl.

2.3.1 50× EMM Salts Recipe

Dissolve in water 52.2 g/L $MgCl_2 \bullet 6H_2O$, 0.735 g/L $CaCl_2 \bullet 2H_2O$, 50 g/L KCl, and 2 g/L Na_2SO_4. This solution is

autoclaved and stored at 4 °C indefinitely. This is not required if using pre-made EMM or EMM-N powder.

2.3.2 1000× EMM Vitamins Recipe

Dissolve in water 1 g/L pantothenic acid, 10 g/L nicotinic acid, 10 g/L inositol, and 10 mg/L biotin. This solution is autoclaved and stored at 4 °C indefinitely. This is not required if using pre-made EMM or EMM-N powder.

2.3.3 EMM Minerals Recipe

Dissolve in water 5 g/L boric acid, 4 g/L $MnSO_4$, 4 g/L $ZnSO_4 \bullet 7H_2O$, 2 g/L $FeCl_2 \bullet 6H_2O$, 1 g/L KI, 0.4 g/L molybdic acid, 0.4 g/L $CuSO_4 \bullet 5H_2O$, and 10 g/L citric acid. This solution is autoclaved and stored at 4 °C indefinitely. This is not required if using pre-made EMM or EMM-N powder.

2.4 Hydroxyurea (HU) Stock Solution

HU is made at 1 M in water, and then filter sterilized with a 0.2 μm filter unit. Excess HU can be aliquoted and stored at −20 °C for up to 6 months.

2.5 Orbital Shaking Water Bath

A water bath is required for quick thermal transfer and stable temperature shaking required in temperature-sensitive synchrony methods (i.e., *cdc25-M22*). Water baths should be pre-warmed to the appropriate temperature, 36 °C for a temperature block, 25 °C for release.

2.6 Cooling Pan

A pan or ice bucket filled with cooled tap water helps to speed the process of temperature decrease to permissive temperature (25 °C) when releasing cells from temperature arrest. Enough water to cover the culture depth in each flask is placed in the pan.

2.7 Thermometer

A thermometer may be used to assess culture temperature during the fast decrease of temperature from block to release. The thermometer can be cleaned, rinsed in 70% ethanol, and placed directly in the culture to monitor the liquid temperature. This is particularly important if using an air-shaking incubator to ensure that temperature increase/decrease occurs quickly.

2.8 70% Ethanol

Ethanol is diluted in purified water (i.e., MilliQ or similar) to 70% and stored in a −20 °C freezer until required.

2.9 Light Microscope

This is required for counting cell septation, in the calculation of septation indices to monitor cell cycle progression. Standard light microscopy will reveal septa and can be used. However, septa may be better visualized using differential interference contrast (DIC) or phase contrast light paths.

2.10 Vacuum Filtration System

A vacuum filtration unit such as those made by Millipore and others (i.e., Millipore XX1014702) with ground glass frit. The glass funnel (i.e., Millipore XX1014704) can be autoclaved in tinfoil to sterilize before and after use. For each sample, a sterile glass

microfiber filter (i.e., Whatman #18220555) is placed on the frit of the vacuum, and the funnel is fixed in place with an aluminum clamp.

3 Methods

The following protocols describe methods that may be used to synchronize fission yeast cultures: drug-induced synchrony; environmentally modulated synchrony; genetic synchrony using conditional alleles. Specific examples are given that can be applied to other drugs, conditions, or alleles.

3.1 Yeast Culture Growth

1. Wake yeast strains on YES-agar and grow at appropriate temperature, 30–32 °C for non-temperature sensitive strains, 25 °C for temperature-sensitive strains.
2. Inoculate 3–5 mL of YES liquid with a single colony of appropriate strain. Grow overnight at appropriate temperature with shaking at 225 rpm.
3. Inoculate an appropriate volume of EMM+supplements media from the YES culture (Subheading 3.1, **step 2**). The volume of inoculum used should give a cell density of approximately 5×10^6 cells/mL to 1×10^7 cells/mL at the start of the experiment (*see* **Notes 1–3**).
4. Grow cultures at permissive incubation temperature to an OD_{600} of approximately 0.3–0.8, corresponding to growth phase in the culture.

3.2 Culture Harvest and Septation Index Calculation

1. Remove 1 mL of culture to a microcentrifuge tube. Centrifuge 11,000 rpm (approximately 10,000 *g*) for 3 mins at room temperature.
2. Decant supernatant. Resuspend pelleted cells by pipetting, or by vortexing.
3. Remove 2 μL to place on a microscope slide. Cover with a cover glass.
4. Add 1 mL cold 70% ethanol to resuspended cells in microcentrifuge tube. Vortex and store at 4 °C.
5. At a light microscope with DIC or phase contrast, count the total number of cells and the number of cells with visible septa (refer to Fig. 1) (*see* **Note 4**).
6. Calculate the percent septated cells per time point, and plot over time.

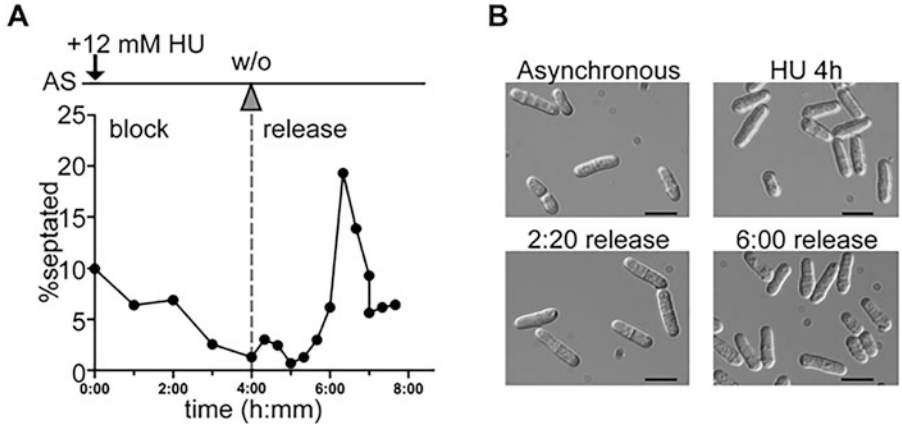

Fig. 1 (**a**) Septation index of wild-type culture (FY436) treated with 12 mM HU for 4 hours, and released into fresh EMM at 30 °C. (**b**) Sample images of the culture at time points show the impact of HU arrest on morphology and cell length during S-phase arrest and subsequent release

3.3 Drug-Induced Synchrony: Hydroxyurea (HU) Block and Release

While this protocol uses HU to induce an S-phase arrest, other compounds may also be used to block *S. pombe* cell cycle such as nocodazole, mating factor pheromone (e.g., [25]), or ATP analog with kinase mutants (e.g., [23]). This protocol may be used as a template for arrest, washing out, and monitoring release.

1. Add freshly prepared 1 M HU stock to a final concentration of 12 mM (*see* **Note 5**).
2. Immediately remove 1 mL of culture to a microcentrifuge tube and process this asynchronous (AS) time point for septation detection and ethanol fixation (Protocol 3.2).
3. Incubate cultures at permissive temperature, 225 rpm orbital shaking, for 3.5–4 hours (*see* **Note 6**). Samples may be removed during this HU block period to monitor septation and DNA synthesis (refer to Chapter 18 for detection of DNA synthesis in fixed samples by flow cytometry).
4. Remove HU by centrifugation and washes.
   (a) Wash HU-blocked cells by pouring culture into a sterile 50 mL conical tube. Centrifuge 1000 *g* for 5 mins at room temperature. Decant media.
   (b) Vortex pelleted cells and add 0.5 volume of pre-warmed media. Vortex cells in wash media, and centrifuge as in Subheading 3.3, **step 4(a)**.
   (c) Repeat Subheading 3.3, **step 4(b)** for a total of 2 washes to remove HU.
5. *Alternate wash method*: Remove HU by vacuum filtration.

(a) Assemble a sterile filtration unit with a glass microfiber filter. Apply a small amount of pre-warmed media to the filter unit to test vacuum.

(b) Pour in HU-treated culture, and allow media to flow through. Wash twice with pre-warmed media.

(c) To remove cells from filter, scrape with a sterile inoculation stick or loop.

6. Resuspend cells in 1 volume of pre-warmed growth media (YES or EMM+supplements). Return to orbital shaking incubator for continued growth at permissive temperature. Remove time points as appropriate to monitor septation and fix cells.

3.4 Environmental Control of Synchrony: Nitrogen Block and Release

1. Grow a culture in EMM + supplements to appropriate density as in Subheading 3.1. Remove an asynchronous sample for septation and fixing.
2. Harvest the remaining volume of culture in a sterile centrifuge tube.
3. Centrifuge in a clinical swinging bucket rotor, room temperature, at 1000 *g* for 5 mins. Decant media and resuspend the cell pellet.
4. Add 0.5 volume of water or EMM-nitrogen medium. Vortex cells. Centrifuge as in Subheading 3.4, **step 3**.
5. Repeat wash (Subheading 3.4, **step 4**) for a total of 2 washes in EMM-N. This removes nitrogen from the culture (*see* **Note 7**).
6. Resuspend cells in 1 volume of EMM-N medium with low supplements (7.5 to 100 mg/L) in an appropriately sized flask.
7. Incubate cells for 16–20 h at 25 °C at 225 rpm. This is the starvation step that induces a G1-arrest in *S. pombe* cultures (*see* **Notes 8** and **9**).
8. Add 1 volume of EMM + supplements to "refeed" nitrogen into the culture. Immediately remove a sample of nitrogen starved cells to assess septation and fix.
9. Shake culture at permissive temperature, 225 rpm, monitoring release from G1-phase using septation index and fixing samples as appropriate.

3.5 Conditional Allele Arrest: Temperature-Sensitive Cell Cycle Mutants

The general method here may be also applied to cold-sensitive strains, which are typically maintained at a permissive temperature of 32 °C, and blocked at a restrictive temperature of 20 °C. Water baths are essential equipment to quickly and effectively distribute heat increase/loss in these protocols; we recommend the use of orbital shaking water baths for the entire protocol.

One drawback to this method of synchrony is that cells must be treated at high temperatures to inactivate the mutant protein. Temperature shock activates stress kinase signaling, arrests the

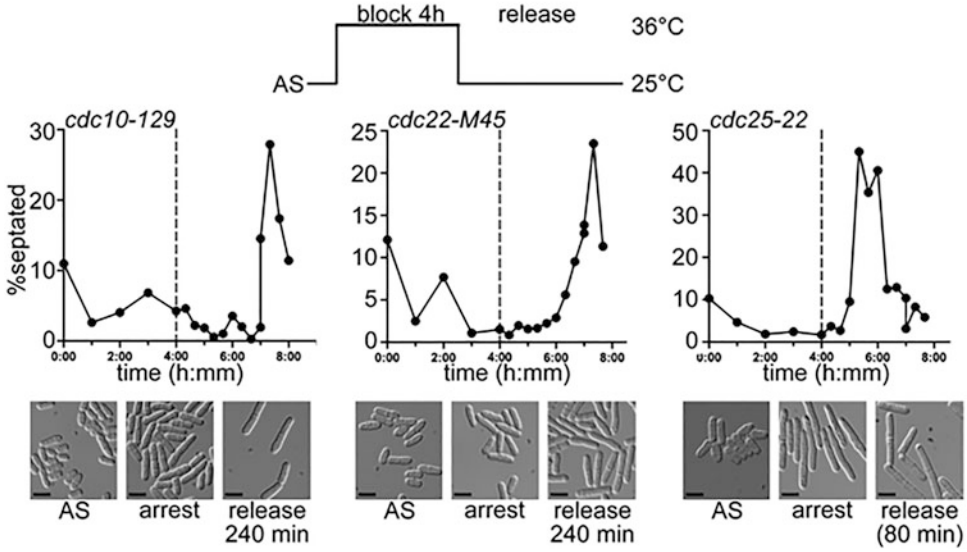

Fig. 2 Temperature block and release profile involves a shift from permissive temperature (25 °C) to restrictive temperature (36 °C). To compare alleles impacting different cell cycle arrest points, *cdc10-129, cdc22-M45,* and *cdc25-22* cultures were blocked for 4 h, and then released to 25 °C. We monitored septation at 20-min intervals to detect the next S-phase, coincident with the peak of septation. Note that both *cdc10-129 and cdc22-M45* cultures peak approximately 3.5 hours post-release (240 mins, shown), while *cdc25-22* cells show an earlier peak shown at 80 mins post-release

S. pombe cell cycle, and affects downstream targets including modifications to heterochromatin (e.g., [26, 27]). Control conditions or strains help to ensure that any unanticipated effects are caused by the process being studied and not the environmental change.

1. Grow the strain of interest at permissive temperature (25 °C) to mid-exponential phase. Remove an AS sample for septation index and to fix in ethanol (Subheading 3.2).
2. Transfer flasks to a 36 °C, pre-warmed water shaking incubator (*see* **Note 10**).
3. Shake at 36 °C for 4 hours, removing samples at least hourly to monitor septation index (*see* **Note 10**).
4. To release cells from the cell cycle block, transfer flasks to a pan of cool tap water. Monitor the decrease in culture temperature using a thermometer (*see* **Note 12**).
5. Transfer the culture(s) to the 25 °C incubator and shake at 225 rpm. Sample at 15- to 20-min intervals to monitor septation and fix samples.
6. Calculate the septation index (% septated cells, Fig. 2) of the culture to monitor the synchrony of release and the timing of cell cycle events. Since septation is coincident with S-phase,

DNA replication should be prominent at this time during release, and can be monitored directly using flow cytometry (see Chapter 18).

4 Notes

1. On many spectrophotometers, concentrations of 5×10^6 to 1×10^7 cells/mL will correspond to an optical density at 600 nm (OD600) range of 0.3–0.8. The growth curve correlating OD600 to concentration should be determined for each spectrophotometer to verify and allow use of the more convenient OD600 measurement if desired.
2. OD600 is a proxy for turbidity, and is influenced by cell volume in solution. Therefore, strains with smaller (i.e., *wee1* alleles) or longer (i.e., *cdc25-22*) morphologies will not necessarily generate consistent concentration estimations. This is particularly true if the OD600 growth curve is generated using a more uniform or wild-type morphology.
3. If the division time (t_D), total culture growth time (time), starting OD600 (OD_{start}), desired OD600 at time (OD_{end}), and culture volume ($Vol_{culture}$) are known, the following formula can be used to better estimate the inoculum volume ($Vol_{inoculum}$) to use:

$$Vol_{inoculum} = Vol_{culture} \times \ OD_{end} \times (OD_{start})^{-1} \times \left(2^{time/t_D - 1}\right)^{-1}$$

   This calculation may change if small volume pre-cultures are not saturated at the time of inoculation. Petersen and Russell [4] make excellent points about the impact of starter culture health on downstream results, indicating that care and consistency are important factors in data variation.
4. We recommend counting 3 separate fields with a minimum of 70 cells per field. Experimental replicates should be compared for peak size (i.e., degree of synchrony) and timing, although absolute numbers or timings may vary between experiments.
5. Concentrations of HU used to induce arrest vary in the literature, ranging from 8 mM to 15 mM. We have found that 12 mM is an optimal concentration of HU that promotes a good level of synchrony and apparently normal release in wild-type cells. Concentrations over 15 mM are not advised, as 20 mM HU causes irreversible effects in wild-type cells.
6. Time of HU arrest is typically 3.5 to 4 hours at 32 °C. After 4 hours, wild-type cells begin to acclimate to HU and synchrony is decreased. At 36 °C, 3.5 hours is a starting point to assess arrest. At culture temperatures of 25 °C, 4 hours in HU

is often sufficient. Arrest should be confirmed by septation and DNA content cytometry for different growth conditions using restrictive media or alternate growth temperatures.

7. Washes can be performed with EMM-N, or sterile 1× PBS or water. However, EMM-N may be a better choice to maintain cell health, as water is reported to deplete dNTP levels during washing.
8. Nitrogen arrest is frequently performed for 16 hours. A shorter time of starvation may be sufficient and can be explored. Nitrogen starvation longer than 20 hours is generally not as successful, as cells may not release once re-fed with nitrogen.
9. G1 arrest during nitrogen starvation occurs at 25 °C and generates a 1C DNA peak and a more uniform culture of small cells. Starvation medium should contain small amounts of supplements required by auxotrophic markers; otherwise, cells may not arrest or release properly.
10. If a water bath shaking incubator is not available, pans of pre-heated water can be used to shift cultures to restrictive or permissive conditions, and then follow with incubation in an air-shaking incubator at the indicated temperature. In this situation, it is important to ensure that the correct temperature has been achieved in the culture before transferring to the air shaker using a thermometer.
11. Monitoring septation at regular intervals is essential to compare cell cycle dynamics between experiments and when scaling up volumes from pilot experiments [4–6].
12. Increasing experiment volumes from small/pilot cultures to larger volumes requires particular attention to culture temperature during shifts of cell cycle block and release.

References

1. Wood V, Gwilliam R, Rajandream MA et al (2002) The genome sequence of Schizosaccharomyces pombe. Nature 415:871–880. https://doi.org/10.1038/nature724
2. Hoffman CS, Wood V, Fantes PA (2015) An ancient yeast for young geneticists: a primer on the Schizosaccharomyces pombe model system. Genetics 201:403–423. https://doi.org/10.1534/genetics.115.181503
3. Fantes PA, Hoffman CS (2016) A brief history of Schizosaccharomyces pombe research: a perspective over the past 70 years. Genetics 203: 621–629. https://doi.org/10.1534/genetics.116.189407
4. Petersen J, Russell P (2016) Growth and the environment of Schizosaccharomyces pombe. Cold Spring Harb Protoc 2016:pdb.top079764. https://doi.org/10.1101/pdb.top079764
5. Sabatinos SA, Forsburg SL (2010) Molecular genetics of Schizosaccharomyces pombe. Methods Enzymol 470:759–795. https://doi.org/10.1016/S0076-6879(10)70032-X
6. Moreno S, Klar A, Nurse P (1991) Molecular genetic analysis of fission yeast Schizosaccharomyces pombe. Methods Enzymol 194:795–823. https://doi.org/10.1016/0076-6879(91)94059-l
7. Bianchi V, Pontis E, Reichard P (1986) Changes of deoxyribonucleoside triphosphate pools induced by hydroxyurea and their relation to DNA synthesis. J Biol Chem 261: 16037–16042

8. Alvino GM, Collingwood D, Murphy JM et al (2007) Replication in hydroxyurea: it's a matter of time. Mol Cell Biol 27:6396–6406. https://doi.org/10.1128/MCB.00719-07
9. Lindsay HD, Griffiths DJ, Edwards RJ et al (1998) S-phase-specific activation of Cds1 kinase defines a subpathway of the checkpoint response in Schizosaccharomyces pombe. Genes Dev 12:382–395
10. Rhind N, Russell P (1998) The Schizosaccharomyces pombe S-phase checkpoint differentiates between different types of DNA damage. Genetics 149:1729–1737
11. Willis N, Rhind N (2009) Regulation of DNA replication by the S-phase DNA damage checkpoint. Cell Div 4:13. https://doi.org/10.1186/1747-1028-4-13
12. Boddy MN, Furnari B, Mondesert O, Russell P (1998) Replication checkpoint enforced by kinases Cds1 and Chk1. Science 280:909–912
13. Rhind N, Russell P (1998) Mitotic DNA damage and replication checkpoints in yeast. Curr Opin Cell Biol 10:749–758
14. Alcasabas AA, Osborn AJ, Bachant J et al (2001) Mrc1 transduces signals of DNA replication stress to activate Rad53. Nat Cell Biol 3:958–965. https://doi.org/10.1038/ncb1101-958
15. Dubacq C, Chevalier A, Courbeyrette R et al (2006) Role of the iron mobilization and oxidative stress regulons in the genomic response of yeast to hydroxyurea. Mol Gen Genomics 275:114–124. https://doi.org/10.1007/s00438-005-0077-5
16. Arlt MF, Wilson TE, Glover TW (2012) Replication stress and mechanisms of CNV formation. Curr Opin Genet Dev 22:204–210. https://doi.org/10.1016/j.gde.2012.01.009
17. Singh A, Xu Y-J (2016) The cell killing mechanisms of hydroxyurea. Genes (Basel) 7:E99. https://doi.org/10.3390/genes7110099
18. Matsumoto S, Yanagida M, Nurse P (1987) Histone transcription in cell cycle mutants of fission yeast. EMBO J 6:1093–1097
19. Woollard A, Nurse P (1995) G1 regulation and checkpoints operating around START in fission yeast. BioEssays 17:481–490. https://doi.org/10.1002/bies.950170604
20. Singer RA, Johnston GC (1985) Indirect suppression of the wee1 mutant phenotype in Schizosaccharomyces pombe. Exp Cell Res 158:533–543. https://doi.org/10.1016/0014-4827(85)90477-x
21. Nasmyth K, Nurse P (1981) Cell division cycle mutants altered in DNA replication and mitosis in the fission yeast Schizosaccharomyces pombe. Mol Gen Genet 182:119–124
22. Forsburg SL, Nurse P (1991) Cell cycle regulation in the yeasts Saccharomyces cerevisiae and Schizosaccharomyces pombe. Annu Rev Cell Biol 7:227–256. https://doi.org/10.1146/annurev.cb.07.110191.001303
23. Singh P, Halova L, Hagan IM (2021) Highly synchronous mitotic progression in Schizosaccharomyces pombe upon relief of transient Cdc2-asM17 inhibition. Methods Mol Biol 2329:123–142. https://doi.org/10.1007/978-1-0716-1538-6_10
24. Hiraoka Y, Toda T, Yanagida M (1984) The NDA3 gene of fission yeast encodes beta-tubulin: a cold-sensitive nda3 mutation reversibly blocks spindle formation and chromosome movement in mitosis. Cell 39:349–358. https://doi.org/10.1016/0092-8674(84)90013-8
25. Nielsen O (2016) Synchronization of S phase in Schizosaccharomyces pombe cells by transient exposure to M-factor pheromone. Cold Spring Harb Protoc 2016. https://doi.org/10.1101/pdb.prot091272
26. Allshire RC, Javerzat JP, Redhead NJ, Cranston G (1994) Position effect variegation at fission yeast centromeres. Cell 76:157–169. https://doi.org/10.1016/0092-8674(94)90180-5
27. Nguyen AN, Shiozaki K (1999) Heat shock-induced activation of stress MAP kinase is regulated by threonine- and tyrosine-specific phosphatases. Genes Dev 13:1653–1663. https://doi.org/10.1101/gad.13.13.1653

Part IV

Methods to Assess Cell Cycle Progression

Chapter 14

Analysis of Cell Cycle by Flow Cytometry

Hamid Maadi, Mohammad Hasan Soheilifar, and Zhixiang Wang

Abstract

The cell cycle of a cell is tightly controlled by several regulators. Dysregulation of cell cycle can lead to uncontrolled cell division which is one of the main characteristics of cancer cells. DNA content of a cell is changed during the cell cycle progression and can be measured by flow cytometry. In this chapter, we aim to provide a detailed protocol on how to analyze the cell cycle using flow cytometry.

Key words Cell cycle, Propidium iodide, DNA contents, Flow cytometry

1 Introduction

Cell cycle is an orchestrated process in which cell duplicates its genome and two daughter cells are created. Cell cycle progression is divided into 4 phases including gap 1 (G1), synthesis (S), gap 2 (G2), and mitosis (M). The genetic content in G1, S, G2, and late mitosis is 2n (diploid), 4n (tetraploid), 4n, and 2n respectively [1]. The events of the cell cycle are well controlled by checkpoints to ensure genome stability and proper segregation of chromosomes. Cyclin-dependent kinases (CDKs) as catalytic subunits, and cyclins as regulatory subunits are crucial cell cycle regulators.

Flow cytometry is a technique which can be used to measure DNA ploidy, cell's distribution within specific phases, and apoptotic cells using a DNA-binding fluorescent dyes. For example, the co-staining of the cells with propidium iodide (PI) and Annexin V is one of the common flow cytometric assays to quantify apoptotic cells population [2]. PI is a double-stranded DNA intercalating red-fluorescent dye which can pass through permeabilized plasma membrane. The excitation wavelength for PI fluorochrome is 488 nm and the emission wavelength is 617 nm which is proportional to DNA content.

Fluidics, optics, and electronics are three main systems of flow cytometry. Physio-chemical features of cells including cell size

Zhixiang Wang (ed.), *Cell-Cycle Synchronization: Methods and Protocols*, Methods in Molecular Biology, vol. 2579,
https://doi.org/10.1007/978-1-0716-2736-5_14,

(correlated to forward scatter signal or FSC) and complexity or granularity (correlated to side scatter signal or SSC) can be measured by flow cytometry. A single stream of cells in suspension flow pass through single or multiple lasers as optical sources. The scattered and emitted light energy can be detected by photodiodes or photomultiplier tubes. Light signals are converted to electronic signals by flow cytometry's electronic system which can be processed by the computer [3]. The most common application of flow cytometry includes but not limited to cell sorting, immunophenotyping, detection of intracellular molecules, measurement of apoptotic cells, and analysis of cell cycle [4]. In this chapter, we will explain how to analyze the cell cycle using flow cytometry.

2 Materials

2.1 Cell Culturing

1. Pipette and micropipette.
2. Pipette tips.
3. Conical 15 mL tube.
4. Vacuum pump.
5. Optical microscope.
6. Mammalian cell culture incubator (providing 37 °C and 5% CO_2).
7. Sterile 6-cm plate.
8. Centrifuge.
9. Trypsin.
10. Digital timer.
11. 1× Phosphate-Buffered Saline (PBS): dissolve the contents of one pouch of "Thermo Scientific BupH Phosphate Buffered Saline Packs" in 500 mL distilled water to obtain PBS solution with 0.1 M sodium phosphate and 0.15 M sodium chloride, pH 7.2.
12. Culturing medium: add 50 mL fetal bovine serum (FBS) and 5 mL penicillin-streptomycin mixtures (Pen-Strep) to 450 mL high glucose Dulbecco's Modified Eagle Medium (DMEM) (from Sigma- Aldrich) containing L-glutamine and sodium bicarbonate to obtain 10% FBS, 1% Pen-Strep-containing DMEM.

2.2 Staining of DNA with Propidium Iodide (PI)

1. Ice-cold 100% methanol.
2. −20 °C refrigerator.
3. Ribonuclease (RNase) buffer with 100 μg/mL concentration of RNase A: add 10 μL Triton X-100 10% and 10 μL RNase A solution from 10 mg/mL stock solution to 1 mL 1× PBS.

4. PI solution with 50 μg/mL concentration of PI: add 10 μL Triton X-100 10% and 50 μL PI solution from 1 mg/mL stock solution to 1 mL 1× PBS.

2.3 DNA Contents Analysis

1. BD Fluorescence-activated cell sorting (FACS) Canto™ II system.
2. 5 mL polystyrene round-bottom FACS tube.
3. FlowJo™ software.

3 Methods

3.1 Cell Culturing and Treatment of the Cells

1. Seed appropriate number of healthy cells in a 6-cm plate containing 3 mL culturing medium.
2. Incubate the cells in an incubator providing 37 °C and 5% CO_2 until the cells attach to the surface of the plate (24–48 h).
3. Remove the culture medium and wash the cells with 1× PBS and then add 3 mL treatment medium to the 6-cm plate (*see* **Note 1**).
4. Incubate the cells in an incubator providing 37 °C and 5% CO_2 for an appropriate time (e.g., 24 h).

3.2 Staining of DNA with PI

1. Collect the culture medium in 15 mL conical tube.
2. Add 0.8 mL trypsin to the plate and incubate the cells in an incubator for 3–5 mins (*see* **Note 2**).
3. Add 1 mL culture medium to each plate to inactivate trypsin.
4. Resuspend the cells gently by pipetting up and down and collect them in the same 15 mL conical tube containing the culture medium.
5. Wash the plate with 1× PBS and collect the remaining cells.
6. Centrifuge the cells at 1300–1500 revolutions per minute (rpm) for 5 mins.
7. Discard supernatant and add 1 mL 1× PBS to each tube and resuspend the cells gently by pipetting up and down.
8. Centrifuge the cells at 1300–1500 rpm for 5 mins.
9. Discard the supernatant and add 0.5 mL 1× PBS to each tube and resuspend the cells gently by pipetting up and down.
10. To fix the cells add 4.5 mL ice-cold 100% methanol to the cell suspension and incubate the cells at −20 °C refrigerator for 20 mins (*see* **Note 3**).
11. Centrifuge the cells at 1300–1500 rpm for 5 mins.
12. Discard the supernatant and add 1 mL Ribonuclease (RNase) buffer to each tube and resuspend the cells gently by pipetting up and down.

13. Incubate the cells on ice for 30 mins.
14. Centrifuge the cells at 1300–1500 rpm for 5 mins.
15. Discard the supernatant and add 1 mL PI solution to each tube and resuspend the cells gently by pipetting up and down.
16. Incubate the cells on ice for 5–10 mins.

3.3 DNA Contents Analysis

3.3.1 DNA Contents Analysis by BD FACS Canto™ II Machine

1. Resuspend the cells gently by pipetting up and down and transfer the cell suspension to 5 mL polystyrene round-bottom FACS tube.
2. Open BD FACSDiva software and log in into your account.
3. Open *Browser*, *Cytometer*, *Global Worksheet*, and *Acquisition Dashboard* windows by clicking on an appropriate button on the workspace toolbar (Fig. 1).
4. In the *Browser* window, click on the *New Experiment* button to create a new experiment (*see* **Note 4** and Fig. 1).
5. Double click on the New Experiment folder to open it. Then, click on the *New Specimen* button to create a new specimen and a new tube. More tubes can be added by clicking on the *New Tube* button (Fig. 1).
6. Click on the *Pointer* on the left side of new tube to activate the *Cytometer* and *Acquisition Dashboard* windows for the selected tube (*see* **Note 5** and Fig. 1).
7. In the *Cytometer* window, open the *Parameters* tab and delete all parameters except FSC, SSC, and fluorescence dye (Fig. 2).
8. Select PI from the list of fluorescence dyes.
9. Uncheck the log option for FSC, SSC, and PI parameters and check the Area (A), Height (H), and Width (W) options for all three selected parameters (Fig. 2).
10. In the *Global Worksheet* window, draw three different plots: (1) click on the *Dot Plot* button to draw a XY plot with SSC-A in the Y axis and FSC-A in the X axis (*see* **Note 6** and Fig. 3), (2) click on the *Dot Plot* button to draw a XY plot with PI-A in the Y axis and PI-W in the X axis (*see* **Note 7** and Fig. 3), (3) click on *Histogram* button to draw a XY plot with Count in the Y axis and PI-A in the X axis (*see* **Note 8** and Fig. 3).
11. Place the FACS tube in the appropriate part of BD FACS Canto™ II machine and click on the *Acquire Data* button to start analyzing the cells (Fig. 4).
12. In the *Cytometer* window, click on the *Parameters* tab and change the voltage of FSC and SSC to see the cell population in the plot (Figs. 2 and 5). Next, in the *Global Worksheet* window, click on the *Polygon Gate* button and select the cell population in FSC-A vs SSC-A plot (*see* **Note 9** and Figs. 3 and 5).

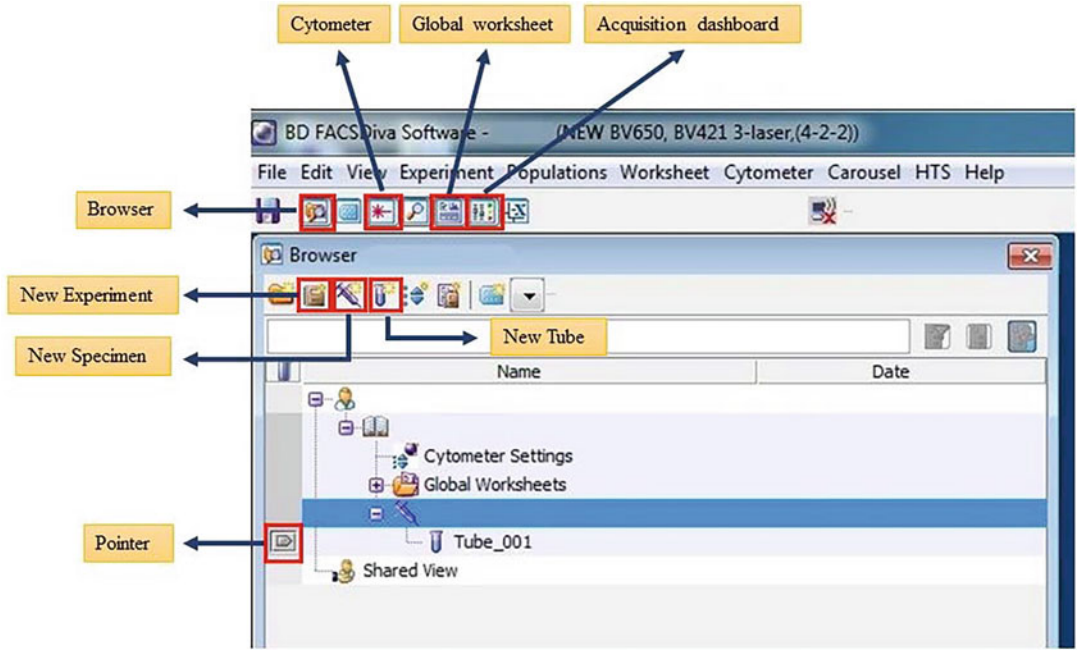

Fig. 1 Important options of BD FACSDiva software and Browser window which are needed during the cell cycle analysis

13. In the *Cytometer* window, click on the *Parameters* tab and change the voltage of PI to adjust the cell population at G1 phase after 50 and around 100 in the Y axis of PI-A vs PI-W dot plot and X axis of PI-A vs Count plot (*see* **Note 8** and Figs. 2 and 5). Next, in the *Global Worksheet* window, click on the *Polygon Gate* button and select the singlets (i.e., single cells) in PI-A vs PI-W dot plot (*see* **Note 10** and Figs. 3 and 5).
14. In *Acquisition Dashboard* window, click on the *Record Data* button to record the cell analysis data (*see* **Note 11** and Fig. 4).
15. In the *Browser* window, on the experiment option click on the right mouse button and select the *Export* option. From *Export* option export data as both *Experiments* and *FCS files* (*see* **Note 12**).

3.3.2 Analysis of Flow Cytometry Data by FlowJo™ Software

1. Open the FlowJo™ software and import the FCS file of DNA content analysis.
2. Double-click on the FCS file to open a new window showing a FSC-A vs SSC-A plot (Fig. 6).
3. Click on the *Polygon* button and select the cell population and name it as *Cells* (Fig. 6).
4. Double-click on the selected area to open a new window showing a FSC-A vs SSC-A plot of the selected cells. Change the Y axis to PI-A and X axis to PI-W. Then, click on *Transform Data Display* button and select *Linear Axis* (Fig. 7).

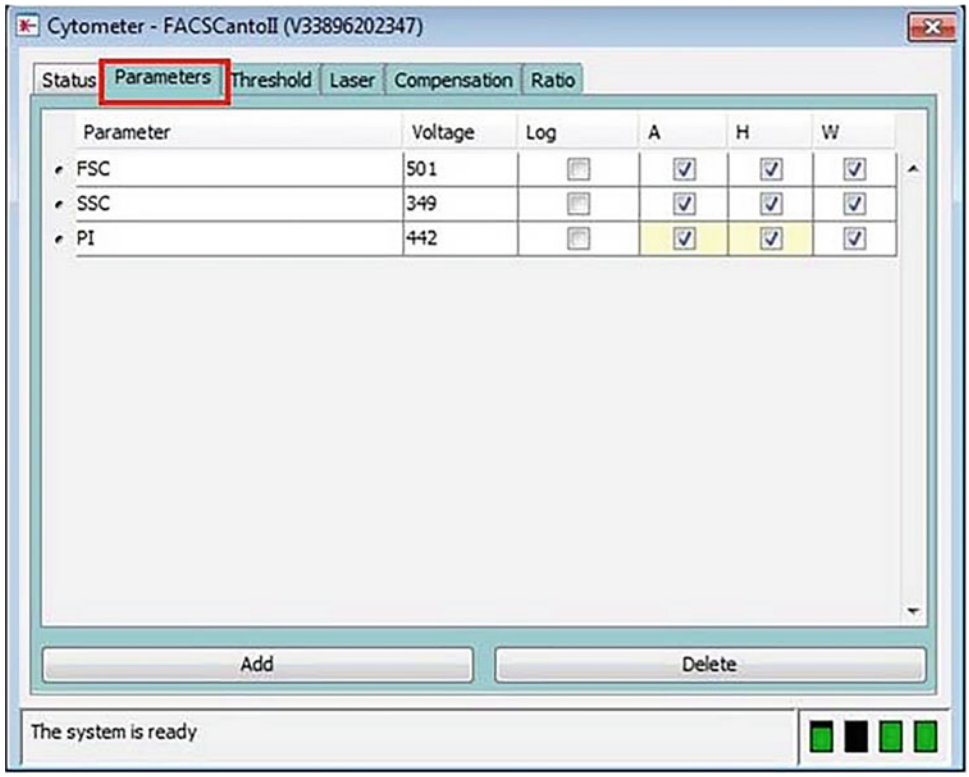

Fig. 2 A screenshot of Cytometer window and Parameters tab

5. Click on the *Polygon* button and select the singlets and name the cells as *Single Cells* (Fig. 7).
6. In the main page of the FlowJo™ software select the single cells. Then, in the FlowJo™ software toolbar, click on the *Cell Cycle* button to open a XY plot. Change the X axis to PI-A and the plot will show you the distribution of cell population in different phases of the cell cycle (Fig. 8).
7. In the same window, select the *Range* button and constrain the first peak of the plot as G1 phase and the second peak of the plot as G2 phase (*see* **Note 13** and Fig. 8).
8. In the same window, open the *Constraints* tab. Click on the *CV* option of *G1 Peak* and select = *n*. Then, click on the *CV* option of *G2 Peak* and select = *G1 CV*. Change the amount of *n:* of *G1 Peak* to obtain the lowest number for Root Mean Square Deviation (RMSD) (*see* **Note 14** and Fig. 8).
9. In the FlowJo™ software toolbar, click on the *Layout Editor* button. In the main page of the FlowJo™ software, drag the analysis results to the *Layout Editor* page and export the final report as your desired format (*see* **Note 15**).

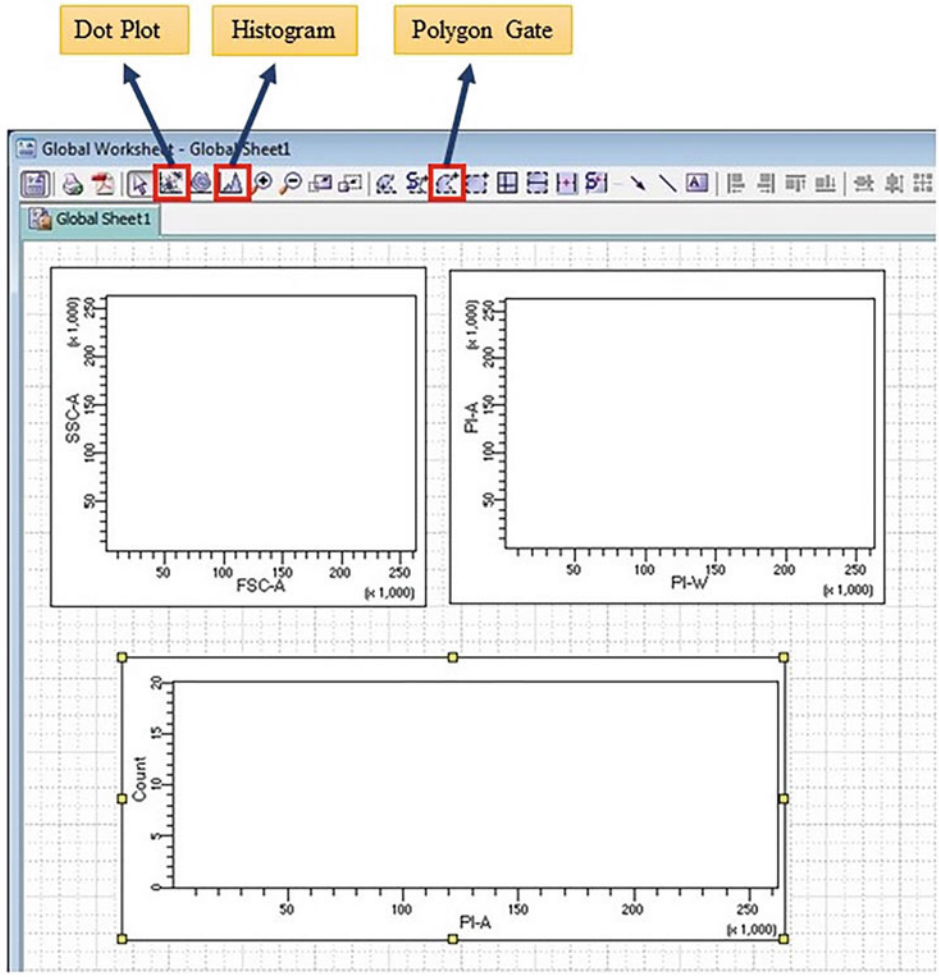

Fig. 3 A screenshot of Global Worksheet window and important options needed during the cell cycle analysis

4 Notes

1. For some experiments, the cells are needed to be starved before treatment to examine the effect of treatment on the cell cycle.
2. The incubation time depends on cell type. Optimize the incubation time before the experiment.
3. The fixed cells can be stored in −20 °C refrigerator for 1–2 months.
4. On the new experiment click on the right mouse button and select "rename" option to change the name of the experiment.
5. The color of the pointer will be changed to green after selecting the tube.

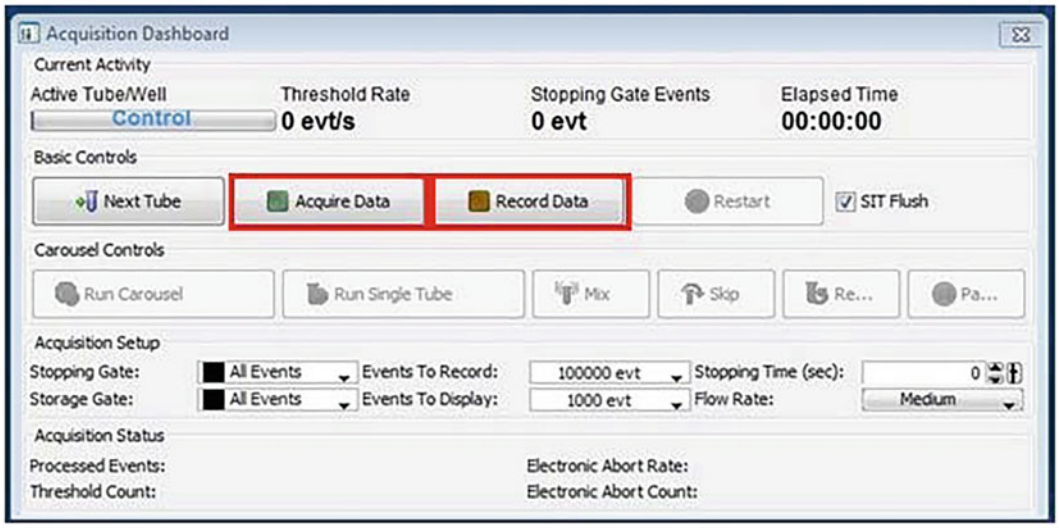

Fig. 4 A screenshot of Acquisition Dashboard and the options needed for running the samples

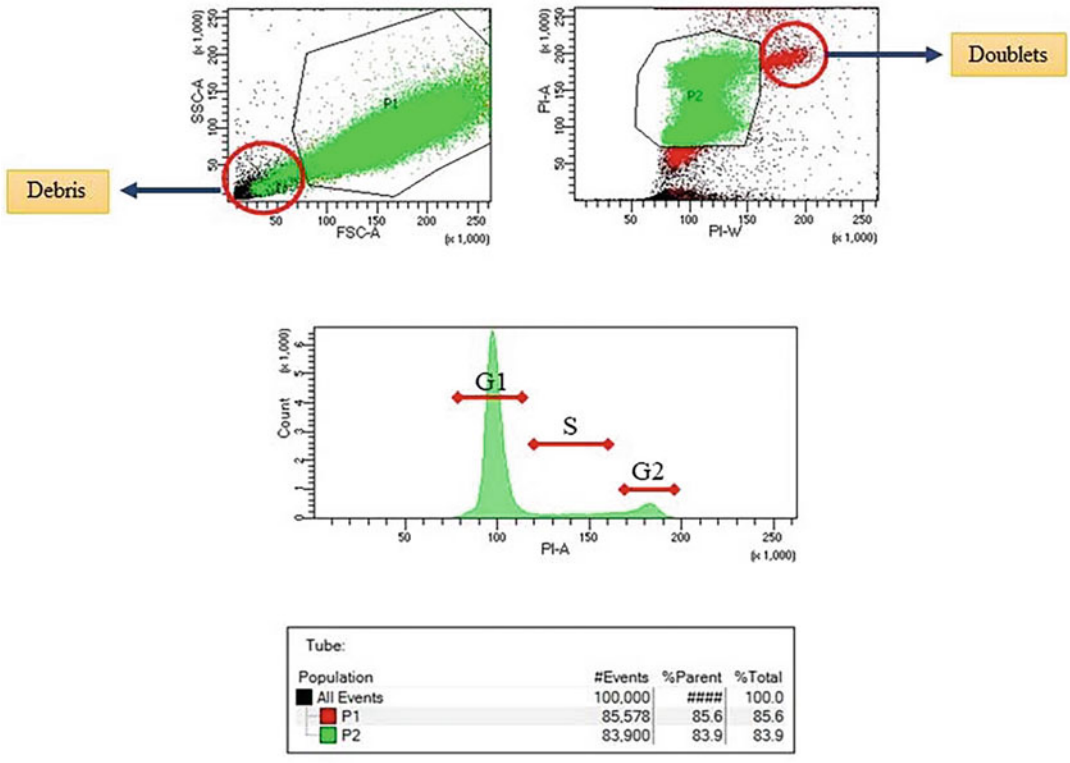

Fig. 5 An example of cell cycle analysis report. In this figure, the separation of cells from debris and singlets from doublets are shown in SSC-A vs FSC-A and PI-W vs PI-A plots, respectively. Moreover, the distribution of cell population in each phase of cell cycle is shown in PI-A vs Count plot

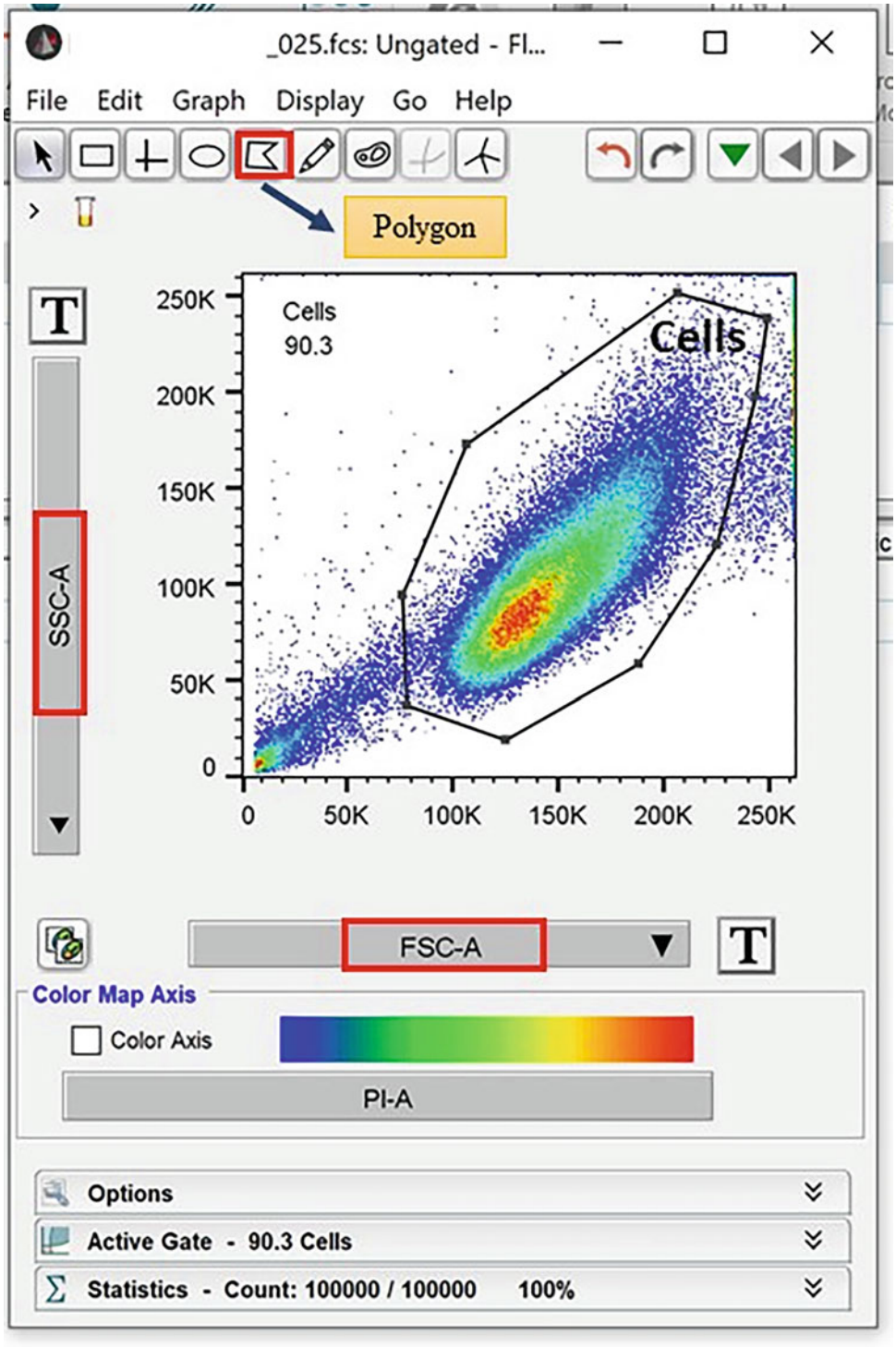

Fig. 6 A screenshot of FSC-A vs SSC-A plot from FlowJo™ software

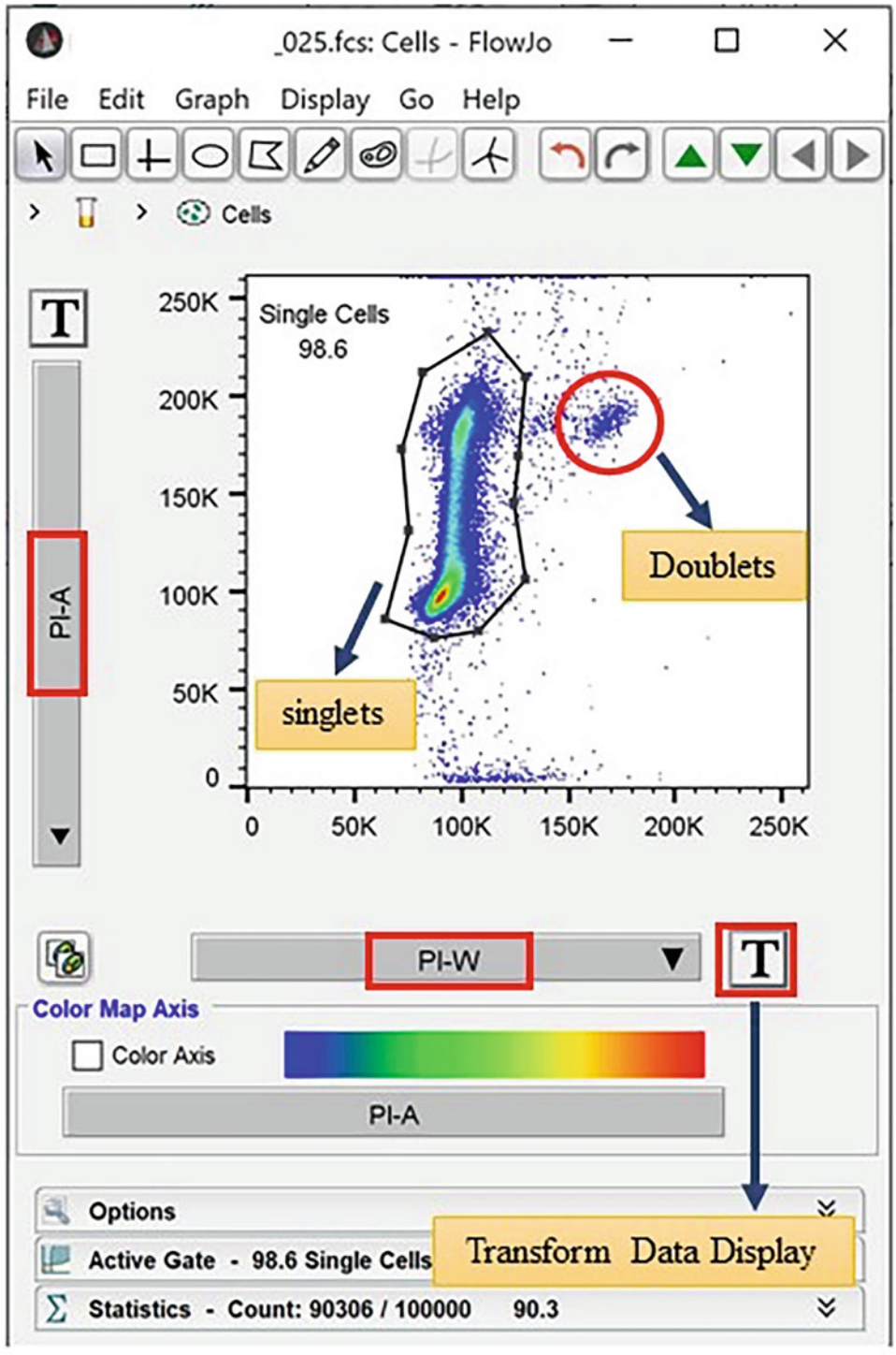

Fig. 7 A screenshot of PI-W vs PI-A plot from FlowJo™ software. The singlets and doublets are clearly separated in this plot

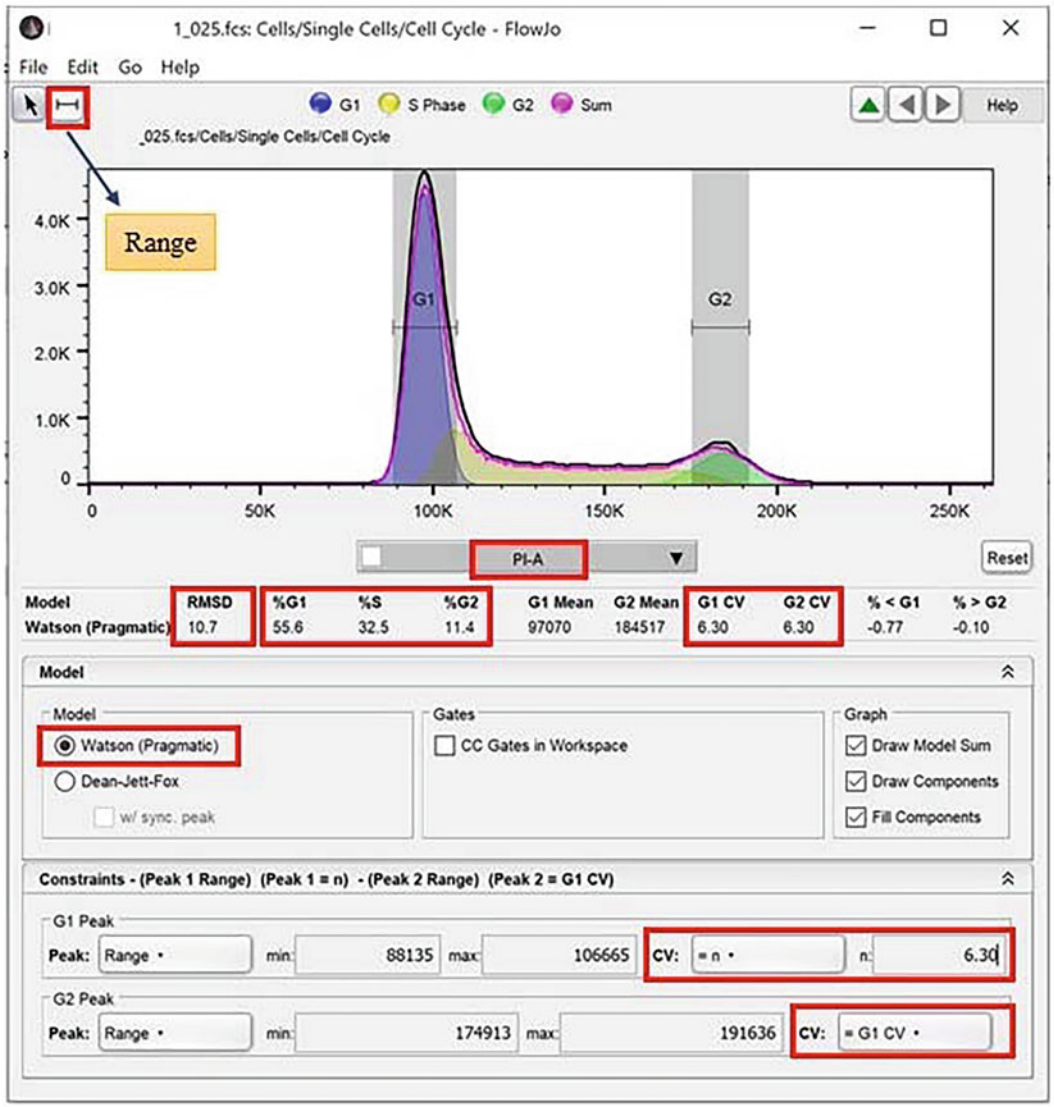

Fig. 8 A screenshot of PI-A vs count plot from FlowJo™ software. Important options and information are shown in this figure

6. The XY plot with SSC-A in Y axis and FSC-A in X axis helps us to separate the cells from debris.
7. The XY plot with PI-A in Y axis and PI-W in X axis helps us to separate single cells from doublets.
8. The XY plot with Count in Y axis and PI-A in X axis shows the cell population in each phase of cell cycle. In this plot, three phases of cell cycle can be observed: (1) First peak of the plot represents the cell population at G1 phase of the cell cycle, (2) the area between the first and second peak of the plot shows

the cell population at S phase of cell cycle, and (3) the last peak of the plot represents the cell population at the G2 phase of the cell cycle (Fig. 5).

9. Change the FSC-A voltage to locate most of the cell population in an area with FSC-A more than 50.
10. The PI fluorochrome-bound to DNA is excited by laser beam and the emitted signals are detected by detector. As cell excited by the laser beams, the detector generates a voltage pulse plot which the height of the signal is proportional to the intensity of the fluorescence signal. The width of the signal shows the time duration that detector identifies the signal. This parameter is proportional to the size of the cells. The single cells have the same width in PI-W vs PI-A and Time vs Voltage plots; however, the height (i.e., the intensity of the signal) and thereby, the area is doubled in single cells at G2 phase (4n) compared to single cells at G1 phase (2n) of the cell cycle. On the other hand, the area of doublets at G1 phase is the same as single cells at G2 phase, while the width of doublets is greater compared to single cells. This characteristic of doublets is used to separate them from singlets (Fig. 9).
11. Select at least 100,000 events for the *Events to Record* option (Fig. 4).
12. For analyzing the data with FlowJo™ software use the exported data as *FCS files*.
13. This will help the modeling algorithm to detect the right place and range of G1 and G2 phases of the cell cycle.

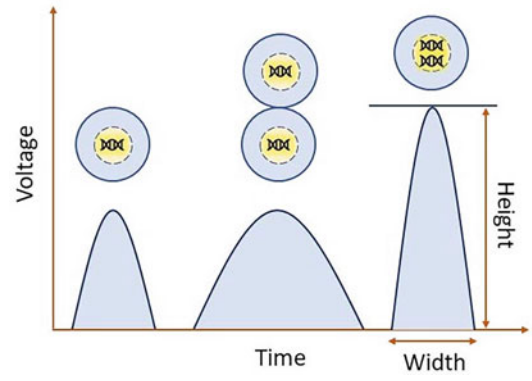

Fig. 9 A schematic figure of voltage pulse plot generated by flow cytometry. Flow cytometry generates a voltage pulse plot after detecting the emitted signals from the cell. The height of the signal is proportional to the intensity of the fluorescence and the width of the signal shows the time duration that detector detects the signal. The doublets signal is wider than singlets signals. In addition, the height of single cells signals at G2 phase is greater than the cells signal at G0/G1 phase of the cell cycle

14. The RMSD shows the accuracy of the model in recognizing the raw data. Generally, the low number of RMSD reflects the better fitness of the model to the data.
15. In the final report, the percentage of cell population in each phase of cell cycle will be shown. The sum of these percentages should be 100. If the sum is less than 100, the percentages should be scaled up proportionally.

Funding

This research has been funded by the generous support of the Stollery Children's Hospital Foundation through the Women and Children's Health Research Institute.

References

1. Trent RJ (2012) Chapter 7 – Development, aging and cancer. In: Trent RJ (ed) Molecular medicine, 4th edn. Academic Press, Boston/Waltham, pp 203–243
2. Crowley LC, Scott AP, Marfell BJ, Boughaba JA, Chojnowski G, Waterhouse NJ (2016) Measuring cell death by propidium iodide uptake and flow cytometry. Cold Spring Harb Protoc 2016(7). https://doi.org/10.1101/pdb.prot087163
3. McKinnon KM (2018) Flow cytometry: an overview. Curr Protoc Immunol 120:5.1.1–5.1.11
4. Adan A, Alizada G, Kiraz Y, Baran Y, Nalbant A (2017) Flow cytometry: basic principles and applications. Crit Rev Biotechnol 37(2): 163–176

Chapter 15

Analysis of Cell Proliferation by Three-Dimensional Culture

Xiaoyun Tang and David N. Brindley

Abstract

Three-dimensional (3D) cell culture technology is a powerful tool in cancer research and drug development. It retains several critical components of the in vivo environment, including cell-cell and cell-extracellular matrix (ECM) interactions in a 3D fashion, gradients of oxygen, nutrients and metabolic waste, and it is thus more physiologically relevant than traditional two-dimensional (2D) cell culture. Here, we describe a simple and versatile method using commercially available chamber slides and Matrigel, a surrogate ECM hydrogel, to set up a 3D culture model for breast cancer cells. In this 3D culture model, cells form aggregates or spheroids on top of a thin layer of Matrigel, which can be fixed directly onto the chamber slides for cell imaging and immunofluorescence staining. Alternatively, RNA and protein can be extracted from the cells for further investigation. This 3D cell culture model provides a useful platform for cancer research and drug development, in which the effects of novel compounds or genetic modifications can be tested.

Key words Three-dimensional cell culture, Extracellular matrix, Breast cancer cells, Matrigel, Chamber slides

1 Introduction

Traditional two-dimensional (2D) monolayer cell culture has been widely used in biological science as a valuable technology for more than seven decades [1]. However, due to the inherent constraints, culturing cells on planar and rigid surface of Petri dishes does not properly mimic the situation in vivo. Cells in 2D culture lack the three-dimensional (3D) cell-cell and cell-extracellular matrix (ECM) interactions, which are present in the in vivo environment. Concentration gradients for oxygen, nutrients, and metabolic waste exist inside the tissue, which are generated by varied proximity to blood vessels and differences in diffusion of molecules through the tissue. Cell motility, migration, and signaling are all affected by the molecular concentration gradients in vivo [2]. But these are missing in 2D culture where cells are uniformly exposed to the culture media. There are many discrepancies between results

Zhixiang Wang (ed.), *Cell-Cycle Synchronization: Methods and Protocols*, Methods in Molecular Biology, vol. 2579,
https://doi.org/10.1007/978-1-0716-2736-5_15,

obtained from 2D culture and studies in vivo [3–5]. For example, more than half of drugs selected by traditional cell culture method fail in Phase II and Phase III clinical trials due to a lack of efficacy [3], which is probably caused by the intrinsic flaws of 2D cell culture.

Since the 1980s, many techniques for 3D cell culture system have been developed. Based on the features of the media in which the cells are cultivated, these 3D culture techniques can be divided into two categories [6]: culturing cells (i) in suspension media, and (ii) with a natural or synthetic matrix (hydrogels, polylactic acid, polyglycolic acid, polyethylene glycol, etc.) (Fig. 1). Unlike the monolayer of cells in 2D culture, cells form aggregates or spheroids in 3D culture (Fig. 2). The spatial cell-cell interaction is preserved in this multicellular spheroid form. Gradients of nutrients, oxygen, and metabolic waste can be established from the periphery to the center of the spheroids [7]. The matrix used for 3D cell culture provides physical support for cells. The chemical and physical properties of the matrix can affect cell behavior. The materials of matrix can be of biological origin or they can be artificially synthesized to mimic the characteristics of ECM such as stiffness, charge, and cell compatibility [8, 9].

The importance of ECM in mammary gland morphogenesis and tumorigenesis has been well recognized [10]. Besides functioning as a biological scaffold, ECM modulates cell signaling via ECM receptors such as integrins and syndecans, which regulates the growth and differentiation of mammary epithelium [11]. Matrigel is a gelatinous protein mixture secreted by Engelbreth-Holm-Swarm mouse sarcoma cells containing various components of ECM such as laminin, collagen IV, and growth factors. Matrigel is widely used as a surrogate ECM hydrogel for 3D culture [12]. Mammary epithelial cells culture with Matrigel can establish apicobasal polarity and form organized acini [13]. Breast cancer cell lines, on the other hand, demonstrate a disorganized structure with loss of polarity, which is linked to cancer cell invasiveness [14]. Cancer cells in 3D culture also demonstrate higher radio- and chemoresistance compared to 2D culture, which is similar to the response of tumors to therapy in vivo [15].

In this protocol, we describe a 3D culture method for growing breast cancer cells on top of Matrigel. This method does not require special equipments and is easy to handle. It uses commercially available 8-well chamber slides which have small size wells. Therefore, it only needs a small amount of Matrigel to setup the 3D culture. This method can be used for investigating the effects of novel compounds or genetic modifications on breast cancer cells cultivated in 3D culture. At the end of the experiment, the cells can be fixed directly on the chamber slide for immunofluorescence staining. The chamber attached to the glass slide can be removed after staining and the cells on the slides can be mounted with cover

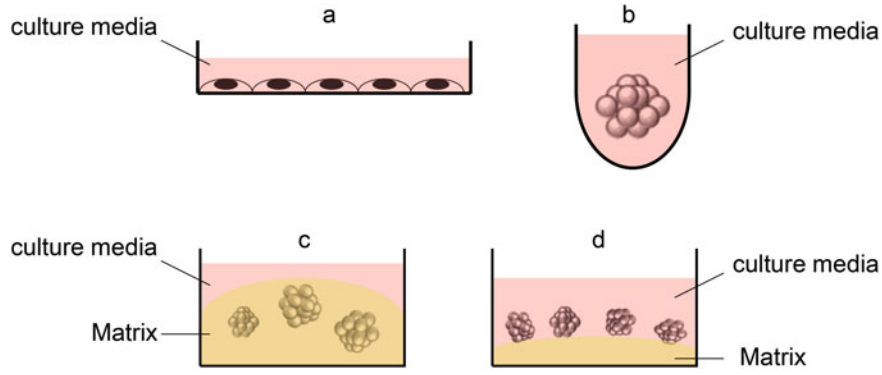

Fig. 1 Schematic diagram of 2D culture (**a**) and 3D culture (**b**–**d**). (**b**) Cells cultured in suspension. (**c**) Cells cultured in the matrix. (**d**) Cells cultured on the matrix

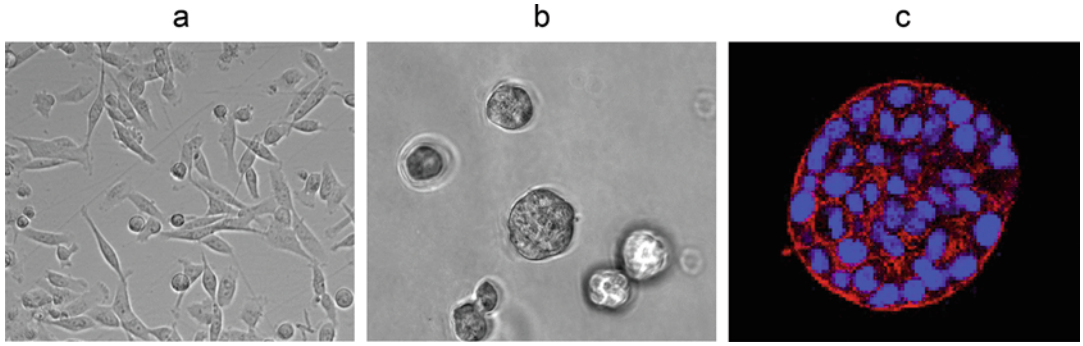

Fig. 2 Morphology of MDA-MB-231 breast cancer cells in 2D (**a**) and 3D (**b**) culture. (**c**) Confocal image of a spheroid of MDA-MB-231 cells in 3D culture. Red: actin, Blue: nuclei

slides and preserved long term at −20 °C. We also describe how to extract RNA and protein from the cells cultured by this method for further investigation.

2 Materials

1. Growth Factor Reduced (GFR) and phenol red-free Matrigel® matrix (*see* **Note 1**): Matrigel is a solubilized basement membrane preparation extracted from the Engelbreth-Holm-Swarm (EHS) mouse sarcoma, Corning Inc. Life Sciences. Matrigel is liquid between 0–10 °C and polymerizes to form a gel above 10 °C. Therefore, it must be thawed overnight on ice or in a 4 °C fridge on the day before the experiment. Pipette tips used for pipetting Matrigel must be sterile and pre-chilled in a 4 °C fridge before use. To avoid freeze and thaw, we recommend aliquoting Matrigel in small amounts in individual tubes and storing them at −80 °C.

2. Growth media: Dulbecco's Modified Eagle Media (DMEM) with 10% fetal bovine serum (FBS). Add 56 mL FBS to 500 mL low glucose DMEM in a sterile tissue culture hood. Store the growth media at 4 °C.
3. Overlay media (2×): Growth media with 4% Matrigel. For 10 wells, mix 2 mL growth media with 80 μL Matrigel in a sterile tissue culture hood (*see* **Note 2**). The 2× overlay media should be prepared freshly for each experiment and then kept on ice before use.
4. PBS: 137 mM NaCl, 2.7 mM KCl, 10 mM Na_2HPO_4, 1.8 mM KH_2PO_4 (pH 7.4). Dissolve 8 g NaCl, 0.2 g KCl, 1.42 g Na_2HPO_4, and 0.24 g KH_2PO_4 in 800 mL double-distilled water (ddH_2O). Adjust the pH to 7.4 with NaOH. Add ddH_2O to 1 L. Autoclave PBS and store it at room temperature.
5. PBS-EDTA: 137 mM NaCl, 2.7 mM KCl, 10 mM Na_2HPO_4, 1.8 mM KH_2PO_4, 5 mM EDTA adjusted to pH 7.4 with NaOH. Dissolve 8 g NaCl, 0.2 g KCl, 1.42 g Na_2HPO_4, 0.24 g KH2PO4, and 1.46 g EDTA in 800 mL double-distilled water (ddH_2O). Adjust the pH to 7.4. Add ddH_2O to 1 L. Store PBS-EDTA at 4 °C.
6. PBS-glycine buffer: 137 mM NaCl, 2.7 mM KCl, 10 mM Na_2HPO_4, 1.8 mM KH_2PO_4, 100 mM glycine (pH 7.4). Dissolve 8 g NaCl, 0.2 g KCl, 1.42 g Na_2HPO_4, 0.24 g KH_2PO_4, and 7.5 g glycine in 800 mL double-distilled water (ddH_2O). Adjust the pH to 7.4 with NaOH. Add ddH_2O to 1 L. Store PBS-glycine buffer at 4 °C.
7. 10% formalin solution: To 45 mL PBS, add 5 mL formalin and mix it well. Store 10% formalin solution at 4 °C (*see* **Note 3**).
8. Permeabilization buffer: To 49.75 mL PBS, add 0.25 mL Triton X-100 and mix it well. Store permeabilization buffer at room temperature.
9. Blocking buffer: Dissolve 0.05 g bovine serum albumin (BSA), 0.25 g NaN_3 (*see* **Note 4**), 0.1 mL Triton X-100, and 0.025 mL Tween 20 in 40 mL PBS, and add PBS to the volume of 50 mL. Store blocking buffer at 4 °C.
10. DAPI solution (1 μg/mL): Prepare 1000× DAPI stock first by dissolving 10 mg DAPI in 10 mL PBS. Prepare 1 μg/mL DAPI solution by adding 5 μL 1000× DAPI stock to 5 mL PBS. Store the 1 μg/mL DAPI solution at −20 °C and prevent light.
11. RIPA buffer: 50 mM Tris-HCl (pH 7.4), 0.1% NP40, 0.25% Na-deoxycholate, 150 mM NaCl, 1 mM EDTA, 1 mM NaF, protease inhibitor cocktail. Dissolve 790 mg Tris base, 900 mg NaCl, 0.1 mL NP40, 0.25 g Na-deoxycholate, 29 mg EDTA, and 4 mg NaF in 75 mL ddH_2O. Adjust the pH to 7.4 using

HCl. Add ddH_2O to the volume of 100 mL. Store RIPA buffer at 4 °C. The protease inhibitor cocktail is unstable in water and must be added into the buffer before use at a 1 in 100 ratio.

12. RNA STAT-60 reagent, AMSBIO.
13. Nunc™ Lab-Tek™ II Chamber Slide™ (8-well, 154,534), Thermo Scientific.
14. ProLong™ Gold Antifade Mountant, Thermo Scientific.
15. Cover slides (22 × 22 mm).

3 Methods

3.1 3D Culture of Breast Cancer Cells in 8-Well Chamber Slides

1. Thaw Matrigel at 4 °C overnight.

   Sterile pipette tips and chamber slides can also be pre-cooled at 4 °C together with the Matrigel.

   Steps 2–6 must be performed in a sterile tissue culture hood.

2. Coat the 8-well chamber slides with a thin layer of Matrigel.

   Put the chamber slides and Matrigel on ice, pipette 50 μL Matrigel on the center of a well (*see* **Note 5**). Allow the Matrigel cover the entire bottom of the well by tilting and tapping the chamber slides toward each direction of the well (*see* **Note 6**). After finishing coating all of the wells, place the chamber slides in a tissue culture incubator at 37 °C, 5% CO_2, and 95% humidity for 30–60 mins. The Matrigel will polymerize to form gel. During the waiting time, you can start to prepare cells.

3. Trypsinize cells.

   Breast cancer cells, e.g., MDA-MB-231, MCF-7 (*see* **Note 7**), or mouse 4T1 cells, etc., in 6-cm dishes should be not more than 70–80% confluency on the day of experiment. Aspirate the growth media. Wash the cells twice with PBS. Trypsinize the cells with 0.5 mL 0.05% trypsin-EDTA in a tissue culture incubator at 37 °C. Cells are resuspended in a 15-mL centrifuge tube with 10 mL growth media, and pelleted by centrifugation at 100 g for 5 mins.

4. Adjust the concentration of cells.

   Resuspend cells with 1 mL fresh growth media, pipette up and down several times to make a single-cell suspension. Count the cells with a hemocytometer. Dilute cells with growth media to the concentration of 3×10^4/mL. Mix this cell suspension with the same volume of 2× overlay media to make 1× overlay media in which the cell concentration is 1.5×10^4/mL. The 1× overlay media does not need to be kept on ice because the concentration of Matrigel is too low to polymerize. Chemicals for treatment can be added to the cells at this step.

5. Load cells on the top of Matrigel.

   Add 0.4 mL of the 1× overlay media into wells of the chamber slides pre-coated with Matrigel. Each well has 6000 cells. The cells are cultured in a tissue culture incubator at 37 °C with 5% CO_2 and 95% humidity. The formation of a spheroid in MDA-MB-231 cells takes about 7 days. Other breast cancer cell lines may have a different time range.

6. Change the overlay media.

   As the spheroids grow bigger, the overlay media need to be changed every 2–3 days. When changing the overlay media, carefully remove the old media without interfering the cell spheroids and the layer of Matrigel at the bottom (*see* **Note 8**). Add 0.4 mL freshly prepared 1× overlay media to the well.

3.2 Fix Breast Cancer Cell Spheroids in 3D Culture for Immunofluorescence Staining

1. Fix cells in 3D culture. This step must be performed in a chemical fume hood.

   Cells do not need to be rinsed prior to fixation. Carefully remove the overlay media from the wells without interfering the cell spheroids (*see* **Note 8**). Fix cells by adding 0.4 mL 10% formalin solution to wells and incubate the chamber slides at room temperature for 20 mins. Cells can also be fixed by cold 100% methanol or acetone depending on the characteristics of antigens you are interested in. Remove formalin carefully and rinse the wells once with 0.5 mL PBS. Once fixed, the slides can be stored at 4 °C with 0.5 mL PBS for up to 1 week (*see* **Note 9**).

2. Quench excess formaldehyde.

   Remove PBS in each well carefully. Add 0.5 mL PBS-glycine and incubate the chamber slides at room temperature for 10 mins. Repeat this step for three times. If the cells are fixed with methanol or acetone, this step can be skipped.

3. Permeabilize cells.

   Remove PBS-glycine in each well carefully. Add 0.4 mL permeabilization buffer and incubate the camber slides at room temperature for 10 mins. If the cells are fixed with methanol or acetone, this step can be skipped.

4. Apply blocking buffer on cells.

   Remove permeabilization buffer in each well carefully. Add 0.2 mL blocking buffer and incubate the chamber slides at room temperature for 1 h.

5. Apply primary antibody.

   Dilute primary antibodies with blocking buffer at optimized concentrations. Add 0.2 mL of the diluted antibody to wells and incubate the chamber slides at 4 °C overnight.

6. Wash cells.

   Remove the primary antibody carefully. Add 0.5 mL blocking buffer and incubate the chamber slides at room temperature for 20 mins. Repeat this step for 3 times.

7. Apply fluorescent conjugated secondary antibody.

   Dilute fluorescent conjugated secondary antibodies with blocking buffer at optimized concentrations. Add 0.2 mL of the diluted antibody to each well and incubate the chamber slides in dark at room temperature for 1 h.

8. Wash cells.

   Remove the secondary antibody carefully. Add 0.5 mL blocking buffer and incubate the chamber slides in dark at room temperature for 20 mins. Repeat this step for 3 times.

9. Nuclear staining.

   Remove blocking buffer from each well carefully. Add 0.2 mL of 1 μg/mL DAPI solution and incubate the chamber slides in dark at room temperature for 20 mins. Remove DAPI solution from each well, add 0.5 mL PBS and incubate the chamber slides in dark at room temperature for 20 mins.

10. Mount the slides.

    Remove PBS carefully. Detach the chamber with the tools provided in the package of Nunc™ Lab-Tek™ II Chamber Slide™. Remove the chamber carefully and add 1–2 drops of ProLong™ Gold Antifade Mountant to the cells of each well. Use tweezers to apply a cover slide over the cells without generating bubbles (*see* **Note 10**). Let the slides dry overnight in dark at room temperature. On the next day, seal the edge of the cover slide with nail polish (*see* **Note 11**). The sealed slides can be preserved at −20 °C for several months.

3.3 Extract Protein from Breast Cancer Cells in 3D Culture

1. Wash cells.

   Remove the overlay media carefully from the wells without interfering the cell spheroids (*see* **Note 8**). Add 0.5 mL ice-cold PBS to the wells and incubate the chamber slides at room temperature for 5 mins.

2. Dissolve Matrigel.

   Remove PBS from the wells carefully. Add 0.5 mL ice-cold PBS-EDTA to the wells. Detach the Matrigel from the bottom of the wells by gently pipetting up and down for several times. Transfer the PBS-EDTA to a 1.5-mL centrifuge tube. Wash the wells with another 0.5 mL ice-cold PBS-EDTA by pipette up and down and combine it with the previous 0.5 mL PBS-EDTA in the 1.5-mL centrifuge tube. Place the tubes on ice for 15 min and vortex the tubes every 5 mins.

3. Dissolve Matrigel.

   Inspect the tubes to check that the Matrigel has dissolved completely. If not, incubate the tubes on ice for longer time or add more ice-cold PBS-EDTA to the tubes (*see* **Note 12**).

4. Pellet and wash cells.

   Centrifuge the tubes for 5 mins at 200 g at 4 °C. The cells spheroids form loose pellets at the bottom of the tube. Aspirate most of the supernatant carefully, and wash the cell pellet with 1 mL of ice-cold PBS-EDTA. Repeat the centrifuging again, and aspirate the supernatant (*see* **Note 13**).

5. Prepare protein sample from the cell pellets.

   Add 100 μL RIPA buffer to the cell pellets. Break the cells by sonicating (*see* **Note 14**) and centrifuge the cell lysates for 10 mins at 15000 g at 4 °C. Collect the supernatants. The supernatant can be stored at −80 °C. Protein concentrations of the supernatants can be determined by BCA or Bradford method.

3.4 Extract RNA from Breast Cancer Cells in 3D Culture

Steps 1–4 must use RNase-free centrifuge tubes and pipette tips

1. Lyse cells with RNA STAT-60.

   Remove the overlay media carefully from the wells without interfering the cell spheroids (*see* **Note 8**). Add 250 μL of RNA STAT-60 to each well. Pipette up and down for several times to detach the Matrigel and cells and transfer the mixture to a 1.5-mL centrifuge tube. To get visible RNA pellets, lysates from 4 wells are combined together as one sample (1 mL in total) for RNA extraction. Incubate the tubes at room temperature for 5 mins.

2. Collect the aqueous phase containing RNA.

   Add 200 μL chloroform using a positive displacement pipette to each tube and vortex briefly. Centrifuge the tubes for 15 mins at 10,000 g at 4 °C. Transfer the upper aqueous phase to a new 1.5-mL centrifuge tube.

3. Precipitate RNA.

   Add 500 μL isopropanol to the aqueous phases. Place the tubes on ice for 30 mins. Centrifuge the tubes for 20 mins at 15000 g at 4 °C to pellet the RNA.

4. Collect RNA.

   Aspirate the supernatant carefully. Wash the RNA pellet with 1 mL 95% ethanol. Centrifuge the tubes for 10 mins at 15,000 g at 4 °C. Aspirate the supernatant carefully and repeat the centrifugation one more time. Remove excess liquid. Dry the pellet at room temperature. Dissolve the RNA pellet with 20 μL nuclease-free water. The RNA can be stored at −80 °C before use.

4 Notes

1. GFR Matrigel from Corning Inc. has lower concentrations of IGF1 (5 ng/mL vs 15.6 ng/mL), TGFβ (1.7 ng/mL vs 2.3 ng/mL), EGF (<0.5 ng/mL vs 0.7 ng/mL), PDGF (<5 pg/mL vs 12 pg/mL), and VEGF (1.0–1.5 ng/mL vs 5.0–7.5 ng/mL) compared with its standard Matrigel. GFR Matrigel is more suitable for experiments elucidating the role of growth factors, signaling-related studies, and gene expression studies. Otherwise, standard Matrigel can be used. Phenol red-free Matrigel is more suitable for experiments involving fluorescence or color detection since phenol red will interfere with the measurement. Phenol red also has estrogen-like effects should this be an issue for the experiments (*see* **Note** 7). Protein concentrations vary between different lots of Matrigel. Use the same lot for each experiment for consistency.
2. To prevent polymerization, place Matrigel on ice anytime you do not touch it during the experiment. Use pre-chilled tips to pipette Matrigel.
3. Formaldehyde is a chemical hazard. Procedures should be performed in a chemical fume hood to prevent inhalation of formaldehyde vapor. Gloves and goggles or a face shield must be worn to protect eyes and skins when handling formaldehyde solution.
4. NaN_3 is highly toxic. Wear gloves and a mask when weighing NaN_3. Avoid contact NaN_3 powder and solution with bare skin.
5. Covering the bottom of wells with Matrigel will be easier by increasing the volume of Matrigel. It does not affect the formation of spheroids, but it increases the cost. Pipette Matrigel into the wells very slowly to avoid generating bubbles on the layer of Matrigel.
6. Matrigel is viscous. You may have to tap the chamber slide to let Matrigel cover the entire bottom of the well. Do it gently and avoid splashing Matrigel on the wall of the chamber. Matrigel forms a meniscus on the bottom of the wells. To prevent polymerization of Matrigel, do not hold the slide for long. Place the slide back on ice to cool it down every 10–15 s.
7. MCF-7 cells are estrogen receptor positive. Use phenol red-free media and Matrigel for breast cancer cell lines that are estrogen receptor-positive because phenol red resembles some non-steroidal estrogens in structure and has significant estrogenic activity.
8. When changing the media, tilt the chamber slide and let the overlay media flow to one side of the wells. Aspirate the media

slowly with a 200-μL pipette. Avoid dipping the pipette tip into the media too deeply because this may damage the Matrigel on the bottom.

9. To prevent the samples from drying out, fill chamber slides with PBS and cover them with Parafilm before storing them at 4 °C.
10. Increasing the amount of ProLong™ Gold Antifade Mountant on cells will reduce the chance of generating bubbles when applying cover slides. Each cover slide covers 4 wells.
11. Only apply the nail polish at the edge of the cover slides. Avoid contaminating the areas having cells with the nail polish.
12. At least 1 mL PBS-EDTA is required for dissolving 50 μL Matrigel. If it is difficult to dissolve the Matrigel in your samples, transfer the sample into a bigger tube and add more ice-cold PBS-EDTA. Incubate the samples on ice till the Matrigel is dissolved.
13. Speed and time of the centrifugation depends on the size of the spheroids and this may need some optimization. Big spheroids are easy to pellet at the bottom of the tube. Small spheroids tend to settle at the conical area. Using a swing-out centrifuge helps to spin the cells down to the bottom of the tube.
14. Use the small probe of a sonicator to treat the cells. To prevent over-heating, sonicate the samples on ice and use short pulses with long intervals.

References

1. Yao T, Asayama Y (2017) Animal-cell culture media: history, characteristics, and current issues. Reprod Med Biol 16:99–117. https://doi.org/10.1002/rmb2.12024. RMB212024 [pii]
2. Herrmann R, Fayad W, Schwarz S, Berndtsson M, Linder S (2008) Screening for compounds that induce apoptosis of cancer cells grown as multicellular spheroids. J Biomol Screen 13:1–8. https://doi.org/10.1177/1087057107310442. 1087057107310442 [pii]
3. Arrowsmith J, Miller P (2013) Trial watch: phase II and phase III attrition rates 2011-2012. Nat Rev Drug Discov 12:569. https://doi.org/10.1038/nrd4090. nrd4090 [pii]
4. Chitcholtan K, Asselin E, Parent S, Sykes PH, Evans JJ (2013) Differences in growth properties of endometrial cancer in three dimensional (3D) culture and 2D cell monolayer. Exp Cell Res 319:75–87. https://doi.org/10.1016/j.yexcr.2012.09.012. S0014-4827(12)00404-1 [pii]
5. Hongisto V, Jernstrom S, Fey V, Mpindi JP, Kleivi Sahlberg K, Kallioniemi O, Perala M (2013) High-throughput 3D screening reveals differences in drug sensitivities between culture models of JIMT1 breast cancer cells. PLoS One 8:e77232. https://doi.org/10.1371/journal.pone.0077232. PONE-D-12-38315 [pii]
6. Langhans SA (2018) Three-dimensional in vitro cell culture models in drug discovery and drug repositioning. Front Pharmacol 9:6. https://doi.org/10.3389/fphar.2018.00006
7. Bialkowska K, Komorowski P, Bryszewska M, Milowska K (2020) Spheroids as a type of three-dimensional cell cultures-examples of methods of preparation and the most important application. Int J Mol Sci 21. https://doi.org/10.3390/ijms21176225. E6225 [pii]. ijms21176225 [pii]
8. Caliari SR, Burdick JA (2016) A practical guide to hydrogels for cell culture. Nat Methods 13:

405–414. https://doi.org/10.1038/nmeth.3839. nmeth.3839 [pii]

9. Badekila AK, Kini S, Jaiswal AK (2021) Fabrication techniques of biomimetic scaffolds in three-dimensional cell culture: a review. J Cell Physiol 236:741–762. https://doi.org/10.1002/jcp.29935
10. Ghajar CM, Bissell MJ (2008) Extracellular matrix control of mammary gland morphogenesis and tumorigenesis: insights from imaging. Histochem Cell Biol 130:1105–1118. https://doi.org/10.1007/s00418-008-0537-1
11. Spencer VA, Xu R, Bissell MJ (2007) Extracellular matrix, nuclear and chromatin structure, and gene expression in normal tissues and malignant tumors: a work in progress. Adv Cancer Res 97:275–294. https://doi.org/10.1016/S0065-230X(06)97012-2. S0065-230X(06)97012-2 [pii]
12. Kleinman HK, Martin GR (2005) Matrigel: basement membrane matrix with biological activity. Semin Cancer Biol 15:378–386. https://doi.org/10.1016/j.semcancer.2005.05.004. S1044-579X(05)00031-3 [pii]
13. Bissell MJ, Weaver VM, Lelievre SA, Wang F, Petersen OW, Schmeichel KL (1999) Tissue structure, nuclear organization, and gene expression in normal and malignant breast. Cancer Res 59:1757–1763s. discussion 1763s–1764s
14. Kenny PA, Lee GY, Myers CA, Neve RM, Semeiks JR, Spellman PT, Lorenz K, Lee EH, Barcellos-Hoff MH, Petersen OW et al (2007) The morphologies of breast cancer cell lines in three-dimensional assays correlate with their profiles of gene expression. Mol Oncol 1:84–96. https://doi.org/10.1016/j.molonc.2007.02.004. S1574-7891(07)00007-5 [pii]
15. Zschenker O, Streichert T, Hehlgans S, Cordes N (2012) Genome-wide gene expression analysis in cancer cells reveals 3D growth to affect ECM and processes associated with cell adhesion but not DNA repair. PLoS One 7:e34279. https://doi.org/10.1371/journal.pone.0034279. 10-PONE-RA-20033 [pii]

Chapter 16

BrdU Incorporation Assay to Analyze the Entry into S Phase

Jihang Yu, Zhixiang Wang, and Yi Wang

Abstract

5-Bromo-2′-deoxyuridine (bromodeoxyuridine (BrdU)), a modified nucleotide and analog of thymidine, is commonly used for detecting proliferating cells. For detection, an anti-BrdU antibody (probe) with a fluorescent dye is applied to bind the BrdU label after DNA denaturation. In this protocol, we provide the BrdU labeling method for both in vitro and in vivo studies, along with immunocytochemistry (ICC)/immunofluorescence (IF) and immunohistochemistry (IHC) staining procedures, respectively. Multicolor staining is also presented as an option to detect the co-distribution of two or multiple antigens in the same sample, making it possible to visualize the location of different molecules at the same time.

Key words 5-Bromo-2′-deoxyuridine, Thymidine analog, Bromodeoxyuridine incorporation assay, S phase, DNA synthesis

1 Introduction

Tritiated thymidine ([^{3}H] dT), a thymidine with the hydrogen α-emitting radionuclide (tritium, ^{3}H), was used to detect the cell proliferation by incorporating it into the newly synthesized DNA [1] (Fig. 1). Although [^{3}H] dT is an excellent marker of DNA synthesis, there are several drawbacks of this methodology, such as isotope usage and time-consuming (3–12 weeks) [2]. Additionally, [^{3}H] dT autoradiographs may have background noise, compared to a relatively high resolution visualized in the BrdU labeling [3]. With the advantages of rapid signal detection by immunohistochemical (IHC) method and co-labeling with multiple phenotypic markers, the BrdU method is widely performed in contemporary studies [2]. The labeling index (percentage of stained nuclei, Formula 1) can be calculated immediately after the immunocytochemical or immunohistochemical reactions [4]. Several studies of BrdU labeling have also shown it as reliable as [^{3}H] dT autoradiography method [3, 5].

Zhixiang Wang (ed.), *Cell-Cycle Synchronization: Methods and Protocols*, Methods in Molecular Biology, vol. 2579,
https://doi.org/10.1007/978-1-0716-2736-5_16,

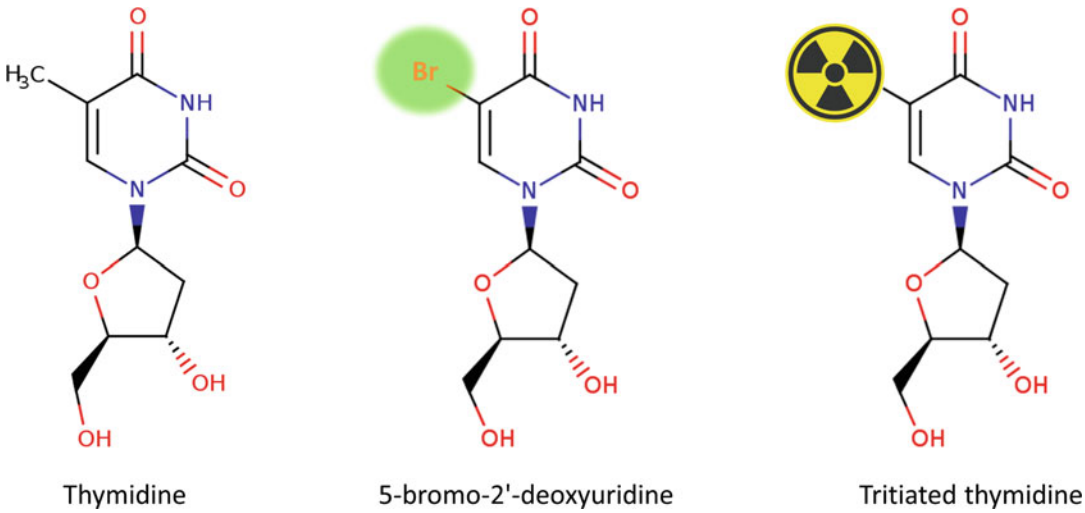

Fig. 1 The chemical structures of deoxythymidine (left), analog bromodeoxyuridine (BrdU, middle), and tritiated thymidine (right)

$$Labeling\ index\ (\%) = \frac{labeled\ cell\ number}{total\ cell\ number} \times 100\%$$

Formula 1 Calculation of labeling index. (Modified from reference [4]).

The molecular weight of BrdU is 307.10 ($C_9H_{11}BrN_2O_5$) (Fig. 1). It is soluble in water to 50 mM. Depending on specific experimental purposes, it can be injected directly into animals or incubated with cell cultures for direct tracking of cells over time, either in vivo or in vitro [6]. For example, IP (intraperitoneal) injection of BrdU into mice to isolate bone marrow may identify the proliferating hematopoietic stem cells (HSCs) directly by co-staining with HSC markers cocktail antibody and following flow cytometry [6]. As BrdU incorporates into the nucleus, this labeling alone is not suitable for morphological analyses [7]. However, combining BrdU with other markers, such as doublecortin (DCX) or polysialylated-neural cell adhesion molecule (PSA-NCAM), can recognize morphological features of immature neurons by IHC detection [7]. BrdU can also be combined with other methods to detect DNA proliferation. For instance, Ki67 monoclonal antibody, which detects all phases of proliferating cells excluding those undergoing repair [8], can be imaged by multicolor staining.

The cell cycle of the eukaryotic cells is composed of two major phases: interphase and the M (mitotic) phase. Interphase can further be divided into three steps: G (growth) 1 phase, S (synthesis)

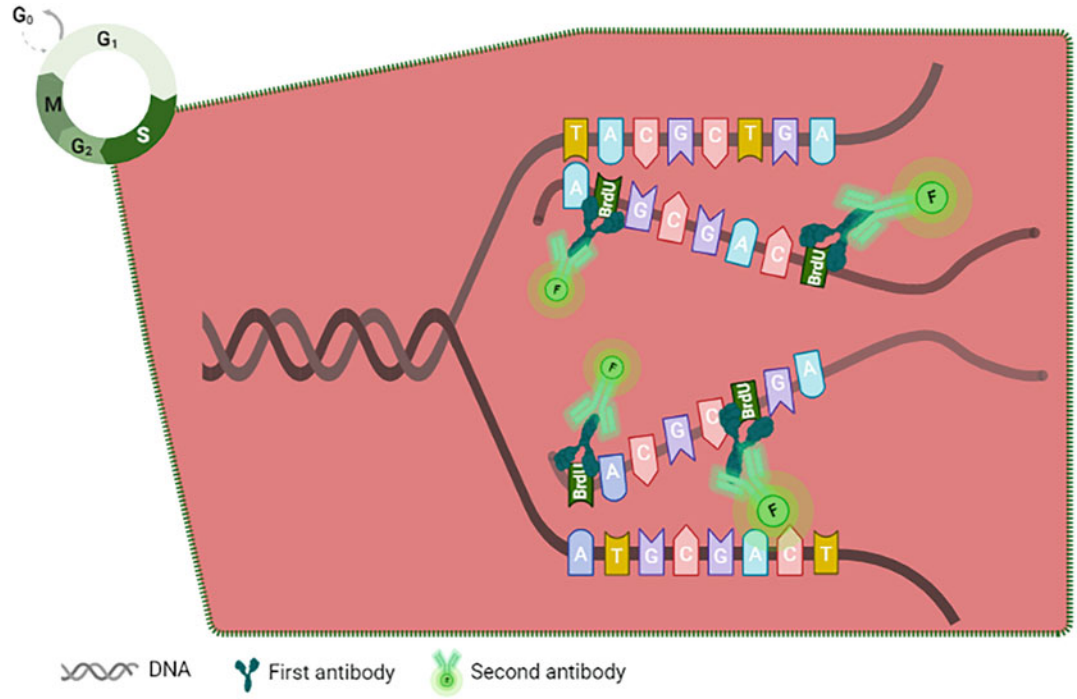

Fig. 2 The BrdU incorporation process. During the DNA S phase of the cell cycle, BrdU will replace thymidine incorporated into the newly synthesized strand. After fixation and DNA hydrolysis, the first antibody will bind BrdU, followed by the fluorescent-labeled secondary antibody to visualize and measure the signal with a microscope or flow cytometry

phase, and G (growth) 2 phase, during which the proliferative cells copy their organelles, synthesize nuclear DNA, and prepare for mitosis. DNA replication starts at the S phase, which is critical for accurate and successful cell division. During the S phase in the cell cycle, BrdU can replace thymidine in the newly synthesized DNA molecules of dividing cells, making it a unique label to identify cells entering the S phase (Fig. 2). We used this method to study the cell proliferation induced by endosomal Epidermal Growth Factor Receptor signaling [9].

2 Materials

2.1 General Lab Supplies

1. Cylinders: 100 mL, etc.
2. Pipette: 5, 10, 25 mL, etc.
3. Autoclaved glass bottle.
4. Falcon® tubes (various sizes): 5, 15 mL, etc.
5. PluriselectSupplier Diversity Partner Bundled PluriStrainer Mini 40 μm Cell Strainer and Flow Cytometry Tubes [Pluriselect, Cat# # NC1693324].

6. Eppendorf tubes.
7. 96-well round-bottom microtiter plates.
8. Hemocytometer or automated cell counter.
9. Centrifuge machine.
10. Cell scraper.
11. 0.2 μm filter.
12. Parafilm.
13. pH meter.
14. Plastic slide box.
15. Slide rack, Coplins jar [optional: deparaffinization].
16. Fat-free, poly-L-lysine coated glass slides and coverslips [Thermo Scientific™, Cat# 150067].
17. Forceps.
18. Cryostat: a machine preserves frozen tissue and section the tissue into thin slices at low temperature (−20 ~ −30 °C).
19. Cell incubator: 37 °C with 5% CO_2.
20. Fume hood.
21. Biosafety cabinet (BSC) (All BSCs must be recertified annually and after any major repairs).
22. Ice bucket.
23. Water bath [or domestic stainless steel pressure cooker, hot plate, vessel (400–500 mL) with slide rack].
24. Stereomicroscope.
25. Fluorescence microscope.

2.2 Reagents

1. poly-lysine hydrobromide.
2. BrdU.
3. BrdU Labeling/Detection Kit II* (an alternative to the BrdU powder from Abcam, which can be used for intravenous injection into the animals for in vivo labeling).
4. Cell culture medium.
5. FBS (Fetal Bovine Serum).
6. PBS (Phosphate buffered saline).
7. Double distilled water.
8. 0.25% Trypsin-EDTA (ethylenediaminetetraacetic acid).
9. 0.5 M EDTA (pH 8.0).
10. 0.4% Trypan Blue Solution.
11. Sodium azide.
12. 4% Formaldehyde in PBS.

13. Antigen Retrieval Buffer (100× Tris-EDTA Buffer, pH 9.0).
14. Antigen Retrieval Buffer (100× Citrate Buffer).
15. Tween 20.
16. tri-sodium citrate dihydrate.
17. Triton X-100.
18. Sodium Borate.
19. HCl (Hydrochloric Acid).
20. Sodium Hydroxide.
21. Xylene.
22. Methanol.
23. Ethanol.
24. TBS (Tris Buffered Saline).
25. Anti-BrdU antibody [BU1/75 (ICR1)].
26. Goat Anti-Rat IgG H&L (Alexa Fluor® 488) preadsorbed.
27. Rat IgG2a, kappa monoclonal [RTK2758].
28. Normal Goat Serum.
29. BSA (Bovine Serum Albumin).
30. Hoechst 33342 Solution.
31. DAPI (4′,6-Diamidino-2-phenylindole Hydrochloride) Staining Solution.
32. Mounting Medium.
33. 7-AAD (7-Aminoactinomycin D).

3 Methods

3.1 In Vitro Experiment

3.1.1 Slide Preparation (All of the Operations Are Performed Inside the BSC)

1. Prepare 0.1 mg/mL poly-L-lysine solution as the following table. Filter the solution with a 0.22 μm syringe filter.

Reagent	1×	__×
Poly-lysine hydrobromide	1 mg	
Sterile tissue culture grade water	10 mL	

2. Coat the coverslips with the poly-L-lysine solution at room temperature for 1 h.
3. Rinse the coverslips with sterile tissue culture grade water three times for 1 h each time.
4. Dry out the coverslips and sterilize them under UV light for at least 4 h before introducing cells and medium.

5. Transfer the poly-L-lysine coated coverslips by forceps onto the cell culture plate.
6. Store at room temperature in BSC for use.
7. Alternately, seal with Parafilm and save in 4 °C fridge for extensive storage.

3.1.2 In Vitro Adherent Cells Labeling

1. Grow cells on glass coverslips in the cell culture plate. The calculation is based on the size of a 24-well cell culture plate. The size of the vessel can be adjusted based on the experiment's purpose and imaging settings.
2. Prepare the stock BrdU solution (10 mM, 100×): dissolve 3.3 mg BrdU (ab142567) in 1 mL double distilled water.

Reagent	**1×**	**100×**	**__×**
BrdU (Abcam)	30 μg	3 mg	
ddH_2O	10 μL	1 mL	

3. Prepare the working BrdU labeling solution (10 μM): dilute 10 mM stock solution in a specific cell culture medium to make a 10 μM labeling solution.

Reagent	**1×**	**__×**
10 μM BrdU stock (1000×)	1 μL	
Cell culture medium	0.99 mL	
Total volume	1 mL	

4. Filter the 10 μM labeling solution through a 0.2 μm filter in a BSC under sterile conditions.
5. Remove the existing cell culture medium from the cells.
6. Wash cells briefly with PBS.
7. Replace PBS with 10 μM labeling solution.
8. Incubate the cells for 30 mins to 24 h at 37 °C in a 5% CO_2 incubator. The incubation time depends on cell dividing speed. One hour for rapidly proliferating cell lines and up to 24 h for primary cell lines. Pre-test the incubation time for the optimal signal-to-noise ratio is recommended.
9. Take the labeling cells from the incubator.
10. Remove the labeling solution.
11. Wash the cells twice with PBS for 5 s per wash.
12. Wash three more times with PBS for 2 mins per wash.

3.1.3 Fixation and Permeabilization (DNA Hydrolysis)

1. *Fixation*: choose one of the following two methods.
   (a) Remove PBS from the cell culture plate.
   (b) Add pre-chilled (−20 °C) 100% methanol to the cells. Incubate in the BSC or fume hood at room temperature for 5 mins. **OR** Add 4% paraformaldehyde in PBS (pH = 7.4) to the cells. Incubate at the BSC or fume hood room temperature for 10 mins.
2. Wash the cells with ice-cold PBS three times for 2 mins per wash.
3. Antigen retrieval [optional step].
   (a) Take extra caution if applying this to frozen tissue sections, especially those fixed by formaldehyde [10].
   (b) Preheat the antigen retrieval buffer (100 mM Tris, 5% [w/v] urea, pH = 9.5) to 95 °C in a water bath [11].
   (c) Mark the side of the coverslips that have cells on them.
   (d) Put the coverslips into the antigen retrieval buffer in the cover glass staining jar by a pair of forceps.
   (e) Heat the coverslips at 95 °C for 10 mins.
   (f) Transfer the coverslips from the antigen retrieval buffer to the 6-well cell culture plates, with the cells facing up.
   (g) Immerse the coverslips with PBS.
   (h) Wash the cells with PBS three times for 5 mins per wash.
4. *Permeabilization* [only for formaldehyde-fixed samples].
   (a) Remove PBS from the cell culture plate.
   (b) Add 1 mL permeabilization buffer Triton X-100 (0.1 ~ 0.25%, which can be optimized for each study) to the cells.
   (c) Incubate at room temperature for 10 ~ 20 mins.
   (d) Remove the permeabilization buffer.
   (e) Wash the cells with PBS-T three times for 5 mins per wash.

3.1.4 Staining [Standard ICC/IF Staining]

Condition: Anti-BrdU antibody rat monoclonal at 1/250 (optimization is highly recommended as the best working concentration varies for different purposes). BrdU primary antibodies from other suppliers can be used. Recently, the Anti-BrdU antibody labeled with a fluorophore (such as Alexa Fluor 647) can be directly imaged by fluorescence microscopy or high-content imaging.

1. Primary antibody incubation.
   (a) Prepare the primary antibody solution.

Reagent	1/250 first Ab dilution	_ / ___ first Ab dilution
Anti-BrdU	40 μL	
BSA	100 μL	
1× PBS-T (or TBS)	9.86 mL	
Total volume	10 mL	

(b) Prepare a humidified chamber: line tissue or paper towel soaked with water at the bottom of the chamber.

(c) Remove the blocking buffer from the samples.

(d) Drain the slides for a few seconds, but do not rinse.

(e) Wipe around the sections with tissue paper.

(f) Add the primary antibody solution to the samples.

(g) Incubate the sample slides in the humidified chamber at room temperature for 1 h or at 4 °C overnight.

2. Secondary antibody incubation.

(a) Remove the primary antibody solution from the samples.

(b) Wash with PBS three times for 5 mins per wash with gentle agitation.

(c) Prepare the secondary antibody solution (use 1/1000 as an example. The working concentration ranges from 1/200 to 1/1000. Optimization is recommended before the large batch experiment).

Reagent	1/1000 second Ab dilution	_ / ___ second Ab dilution
Goat Anti-Rat IgG H&L (Alexa Fluor® 488) preadsorbed (ab150165)	10 μL	
BSA	100 μL	
1× PBS-T (or TBS)	9.89 mL	
Total volume	10 mL	

(d) Remove PBS from the samples.

(e) Wipe around the sections with tissue paper.

(f) Add the secondary antibody solution to the samples.

(g) Incubate the sample slides in the humidified chamber at room temperature in the dark for 1 h.

(h) Remove the secondary antibody solution.

(i) Wash with PBS three times for 5 mins per wash with gentle agitation in the dark.

3. (optional step) Multicolor staining: to detect co-distribution of two or multiple antigens in the same sample.
   (a) Blocking (same as above).
   (b) Other primary antibody incubation (same steps as above with different antibodies).
   (c) Other secondary antibody incubation (same steps as above with different antibodies).
   (d) If more than two antigens are detected, continue blocking, primary and secondary antibodies incubation for the rest of the antibodies.
4. Nuclear staining.
   (a) Prepare 1.43 μM DAPI solution.

Reagent	**1×**	**__×**
10 mM DAPI (ab228549)	1.43 μL	
1× PBS	~10 mL	
Total volume	10 mL	

   (b) Remove PBS from the samples.
   (c) Wipe around the sections with tissue paper.
   (d) Add DAPI solution to the samples.
   (e) Incubate sample at room temperature for 1 h according to optimization.
   (f) Rinse the sample with PBS.
5. Mounting.
   (a) Add a drop of mounting medium.
   (b) Mount the coverslip on the slide.
   (c) Seal the coverslip with coverslip sealant to prevent drying and movement.
   (d) Image samples with fluorescent microscope according to corresponding fluorescent wavelengths and appropriate filters. For example, the green channel for BrdU (Alexa Fluor® 488. Ex: 495 nm, Em: 519 nm) and the blue channel for DAPI, respectively.
   (e) Store samples at −20 °C or +4 °C in the dark.

3.2 In Vivo Experiment

The animal protocol must be approved by the local animal care committee, and the guidelines for ethical conduct in the care and use of animals in research must be followed.

3.2.1 In Vivo Labeling

1. Intraperitoneal (IP) injection.
   (a) Dilute BrdU (ab142567) in 1× PBS to make a sterile solution of 10 mg/mL.
   (b) Filter the solution with 0.2 μM filter in BSC.
   (c) For mice, inject the BrdU solution (10 mg/mL) to a concentration of 100 mg/kg. For example, a mouse of 20 g will be IP injected with 200 μL BrdU solution (10 mg/mL).
   (d) Treated with BrdU from 30 mins to 24 h depending on the tissue types, the animals can be sacrificed according to the approved protocols. 24-h post-injection time will allow BrdU to incorporate into most tissues, while 30 mins will be good for rapidly dividing tissues such as the small intestine.
2. Oral administration.
   (a) Prepare fresh diluted BrdU (ab142567) solution (0.8 mg/mL) in drinking water and change daily. For example, a mouse of 20 g will be fed BrdU water of 225 mg/kg per day, which equals 5.625 mL of 0.8 mg/mL BrdU solution for each day.
   (b) After BrdU treatment for a certain time, the animals can be sacrificed according to the approved protocols.
3. Intravenous (IV) injection [less common method with Roche's kit].
   (a) For animal labeling, the stock BrdU labeling reagent (Roche, 2 mL per 100 g animal body weight) will be IV injected into the animal. The ideal BrdU dosage ranges from 50 to 300 mg/kg [12].
   (b) After BrdU treatment for a certain time, usually several days, the animals can be sacrificed according to the approved protocols.

3.2.2 Tissue Slices from Frozen Section Labeling

1. Cut the tissue sample to ~1 mm thick with the cryostat.
2. Cover the sample with BrdU labeling reagent (Roche).
3. Incubate the sample at 37 °C 5% CO_2 incubator. The incubation time can be optimized from 30 to 60 mins depending on the experimental purpose. For example, 30 mins for cell repair detection, and 60 mins for cell proliferation detection.
4. Locate the sample in the washing buffer (Roche).
5. Incubate the sample at 37 °C 5% CO_2 incubator for 30 mins.

3.2.3 Fixation and Permeabilization (DNA Hydrolysis)

1. Prepare 0.1 M sodium borate buffer.
   (a) Add 3.8 g sodium borate (MW = 381.4) to 100 mL ddH_2O.
   (b) Adjust the pH with a pH meter by NaOH to pH = 8.5.
2. Cut the tissue slices to ~5 μm thick by the cryostat (for frozen tissue) or microtome (for paraffin-embedded tissue) and place on poly-L-lysine glass slides.
3. [optional step: deparaffinization – only for paraffin-embedded tissue] sit the slides into a rack and wash the samples in a Coplin jar in the following order:
   (a) Xylene: 3 mins, twice.
   (b) Xylene 1:1 with 100% ethanol: 3 mins.
   (c) 100% ethanol: 3 mins, twice
   (d) 95% ethanol: 3 mins
   (e) 70% ethanol: 3 mins
   (f) 50% ethanol: 3 mins
   (g) Rinse the samples with running cold tap water.
4. Antigen retrieval [optional step]: same as above or alternative methods, for example, heat mediated antigen retrieval with citrate buffer (pH = 6) with pressure cooker [13].
   (a) Prepare sodium citrate buffer (or commercial product).
      (i) Weigh tri-sodium citrate (dihydrate) 2.94 g.
      (ii) Dissolve the tri-sodium citrate to 1 L ddH_2O.
      (iii) Mix well.
      (iv) Adjust the solution to pH = 6 with 1 N HCl.
      (v) Add 500 μL Tween 20 and mix well.
      (vi) Store at room temperature for 3 months or 4 °C for long-term storage.
   (b) Add antigen retrieval buffer into the pressure cooker.
   (c) Put the pressure cooker on the hotplate and turn on full power.
   (d) Rest the lid of the pressure cooker on top.
   (e) Transfer the slides from the tap water to the pressure cooker by forceps. [Caution: hot.]
   (f) Secure the lid of the pressure cooker properly.
   (g) Cook for 3 mins when it reaches full pressure.
   (h) Turn off the hotplate.
   (i) Put the pressure cooker in an empty sink.
   (j) Activate the pressure release valve.

(k) Ran cold water over the pressure cooker.

(l) When the pressure cooker is de-pressured, open the lid, run cold water into the cooker for 10 mins.

5. Incubate the tissue sections in 1–2 M HCl for 30–60 mins at room temperature. It is recommended to optimize the proper concentration and time for a specific experiment. A shorter incubation time can be applied by incubating cells at 37 °C.
6. [optional step] remove the HCl and neutralize it with 0.1 M sodium borate butter for 10 mins at room temperature.
7. Wash with PBS three times for 5 s per wash.

3.2.4 Blocking [Can Also Be Combined with Permeabilization Depending on Preference]

1. Prepare PBS-T (alternative: TBS-T).

Reagent	1 bottle
1× PBS (or TBS)	999 mL
Tween 20	1 mL
Total volume	1 L

2. Prepare the 10% blocking buffer.

Reagent	1×	__×
Normal goat serum (ab7481)	1 mL	
1× PBS-T (or TBS)	9 mL	
Total volume	10 mL	

3. Remove PBS and replace with the blocking buffer to the sample.
4. Incubate sample at room temperature from 30 mins to 2 h depending on the purposes.

3.2.5 Immunostaining

Tissue sample [Standard IHC staining].

Condition: Anti-BrdU antibody (ab6326) concentration 1–3 μg/mL. Perform heat mediated antigen retrieval with citrate buffer (pH = 6) before IHC staining.

Process: Similar procedure as ICC. Adjust conditions, reagents, antibodies, and counterstaining dye according to specific needs.

3.3 Flow Cytometry [Alternative Method]

3.3.1 Condition and Preparation

1. First ab: Anti-BrdU antibody (ab6326) 1/25–1/200.
2. Second ab: Goat Anti-Rat IgG H&L (Alexa Fluor® 488) pre-adsorbed (ab150165) 1/2000.

3. Isotype control: Rat IgG2a, kappa monoclonal [RTK2758] (ab18450) 2 μg for 10^6 cells. This also can be used as a negative primary antibody for ICC and IHC as necessary.
4. Prepare 1 mM EDTA solution.

Reagent	Measure
EDTA, 0.5 M	200 μL
1× PBS	~ 100 mL

5. Prepare 10% sodium azide stock solution at room temperature.

Reagent	Measure
Sodium azide	10 g
ddH_2O	100 mL

6. Prepare the resuspending solution. Store at 4 °C or in the ice bucket.

Reagent	1×	__×
FBS	1 mL	
10% sodium azide	1 mL	
1× PBS	8 mL	
Total volume	10 mL	

3.3.2 (Optional Step) Count Cell Number and Viability

1. Add 1× Trypsin-EDTA to the cells, volume according to the plate size.
2. Incubate at 37 °C 5% CO_2 incubator for a few minutes according to the character of the cells.
3. Resuspend cells in culture media.
4. Collect cells into falcon tubes (15 mL or 50 mL depending on experiments).
5. Transfer 11 μL cells into 11 μL Trypan blue solution.
6. Mix well by pipetting up and down.
7. Load 10 μL mixture to the hemocytometer or 10 μL to each side of the loading chamber of the automated cell counter.
8. Count living cell numbers manually under a stereomicroscope or automatically by the cell counter machine. Living cells are bright (no dyed), while dead cells and debris are blue.
9. The viability of the cells should be no less than 90% and ideally 95%.

3.3.3 Procedure

1. After labeling cells with BrdU (no need to culture cells on a coverslip in the cell culture plates), wash cells with 1x PBS.
2. Remove PBS from the sample.
3. Add 1 mM EDTA solution to the cell surface.
4. Gently rock the plate to remove the cells from the plate.
5. Harvest the cells into a tube.
6. Centrifuge at 300 g for 5 mins and remove the supernatant. (Optional step) Add 70% ethanol drop-wise to the cells. Fix the cells on ice for 30 mins.
7. Add 2 M HCl to the cell pellets.
8. Permeabilize cells at room temperature (22 °C) for 30 mins.
9. Neutralize the system by adding 0.1 M pH = 8.5 sodium borate buffer.
10. Centrifuge at 300 g for 5 mins and remove the supernatant.
11. Wash the sample with 1× PBS.
12. Centrifuge at 300 g for 3 mins and remove the supernatant.
13. Blocking with 10% normal goat serum in 1× PBS at room temperature for 30 mins.
14. Centrifuge at 300 g for 3 mins and remove the supernatant.
15. Add the primary antibody (ab6326) solution (calculation see above) 1 μg/1 × 10^6 cells according to the cell number.
16. Incubate at room temperature for 30 mins.
17. Centrifuge at 300 g for 3 mins and remove the supernatant.
18. Wash cells with ice-cold PBS three times by centrifuging at 300 g for 5 mins.
19. Add the secondary antibody (ab150165) solution (calculation see above).
20. Incubate at 4 °C for 30 mins in the dark.
21. Centrifuge at 300 g for 3 mins and remove the supernatant.
22. Resuspend ~1–5 × 10^6 cells/mL with *ice-cold* resuspending solution (1× PBS with 10% FBS and 1% sodium azide). An exact cell number is recommended for optimization.
23. (optional step) Add 7-ADD 5 μL (0.25 μg) per test (per 1 × 10^6 cells) for labeling dead cells.
24. Incubate at room temperature for 5 mins.
25. Filter cells with strainer flow tube (load the solution on the lid, quick spin at 300 g 1 min).
26. Collect at least 5000 events with 530/30 and 685/35 filters of a 50 mW Blue laser (488 nm) [14].

4 Notes

1. If possible, the BrdU solution should be prepared and used on the same day. The solution can be stored as aliquots at −20 °C for up to one month and equilibrate the solution to room temperature for at least 1 h before the subsequent use [15].
2. The dose and time for reagents are calculated as a reference, and the exact treatment needs to be optimized for individual experimental conditions.
3. The rationale for Triton X-100 improving the penetration of the antibody is that it can destroy cell membranes [16]. Other permeabilization buffers will be needed in the detection of membrane-associated antigens [17].
4. For tissue sections, paraffin-embedded samples need to be de-waxed before proceeding to DNA hydrolysis [18]. As most staining solutions are aqueous in the following steps, replacing wax with water will be helpful for antibody binding.
5. After deparaffinization, the samples must be kept wet until the next step to avoid causing non-specific antibody binding and further high background signals [19].
6. Microwaves may cause hot and cold spots, making uneven epitope retrieval, and rigorous boiling may induce tissue dissociation from the slide. If antigen retrieval is applied, using a water bath or pressure cooker will be better than microwaves or boiling [10].
7. Normal goat serum is an example of the blocking buffer. Usually, the serum for blocking buffer is from the same species of the secondary antibody source. However, the blocking buffer made from other sources is also available depending on the specific experimental purposes [20].
8. Typically, the primary antibody should be from the animal species different from the sample to be stained. Otherwise, the second antibody will cause high background as a result [21].
9. The reason for incubating secondary antibodies and washing in the dark is to avoid photo-bleaching of the samples [21].
10. Multicolor staining can be conducted either simultaneously (a mixture of the primary antibodies and a mixture of the secondary antibodies when incubation) or sequentially (one incubation for one antigen, then the next one) [20]. Ensure to use different sources (species) of the primary and corresponding secondary antibodies [20].

11. For counterstaining, the concentration of DAPI solution (0.5–5 μM) and incubation time (1 min to 1 h) are recommended to be optimized [20, 22].
12. Hoechst is another dye for fixed- and live-cell fluorescent staining for DNA and nuclei, primarily combined with BrdU staining [23]. It can be used to incubate samples in counter staining at a 0.1–1 μg/mL concentration for 1 min [20].
13. Positive, negative, and endogenous tissue background controls are recommended for IHC staining of tissue samples [10].
14. The force and time of the centrifugation are recommended to adjust according to cell types in preparing samples for flow cytometry [24].

5 Limitations

1. Application of BrdU labeling In vivo can adversely affect cell survival, migration, and final position in the brain [2], which may cause similar effects to corneal stem cells [25]. Ki67 is a popular alternative substitution for the detection of cell proliferation [12].
2. A 10% cross-reactivity of BrdU with 5-iodo-2'deoxy-uridine may happen in some kits such as BrdU Labeling and Detection Kit II (Roche Diagnostics) [25].
3. The denaturation conditions (heat or acid treatment) used to expose the epitope for BrdU antibodies are harsher than the "click" chemistry reaction used for 5-ethynyl-2′-deoxyuridine (EdU), another thymidine analog that can detect DNA synthesis by incorporating into the DNA of proliferating cells [26]. Also, BrdU has been shown with toxicity on the cell in a dose-dependent manner, such as mutations, breaks, and DNA instability [2].
4. Typically, in vivo BrdU labeling will be conducted by intraperitoneal injection. Although the concentration of the compound is uniform, the injection may still cause stress to animals and unstable labeling of the targeted cells [9].

Acknowledgments

This work was supported by Atomic Energy of Canada Limited's Federal Nuclear Science & Technology Program and CANDU Owners Groups (COG) Strategic Research and Development (SRD) program.

References

1. Dictionary M. *Tritiated thymidine*. [Cited 2021]. Available from: https://medical-dictionary.thefreedictionary.com/tritiated+thymidine
2. Duque A, Rakic P (2011) Different effects of bromodeoxyuridine and [3H]thymidine incorporation into DNA on cell proliferation, position, and fate. J Neurosci 31(42): 15205–15217
3. Sugihara H, Hattori T, Fukuda M (1986) Immunohistochemical detection of bromodeoxyuridine in formalin-fixed tissues. Histochemistry 85:193–195
4. Rosenstein JM, Krum JM (1994) 2 – Models of angiogenesis and the blood–brain barrier. In: Flanagan TR, Emerich DF, Winn SR (eds) Methods in neurosciences. Academic Press, San Diego, California, pp 20–32
5. Cawood AH, Savage JRK (1983) A comparison of the use of bromodeoxyuridine and [3H] thymidine in studies of the cell cycle. Cell Tissue Kinet 16:51–57
6. Matatall KA, Kadmon CS, King KY (2018) Detecting hematopoietic stem cell proliferation using BrdU incorporation. Methods Mol Biol 1686:91–103
7. Dickendesher TL, Duan Y, Giger RJ (2013) Axon regeneration. In: Cellular migration and formation of neuronal connections, pp 151–175
8. Gerdes J, Lemke H, Baisch H, Wacker HH, Schwab U, Stein H (1984) Cell cycle analysis of a cell proliferation-associated human nuclear antigen defined by the monoclonal antibody Ki-67. J Immunol 133(4):1710–1715
9. Pennock S, Wang Z (2003) Stimulation of cell proliferation by endosomal epidermal growth factor receptor as revealed through two distinct phases of signaling. Mol Cell Biol 23(16): 5803–5815
10. Abcam. Immunohistochemistry (IHC): the complete guide. [Cited 14 Oct 2021]. Available from: https://www.abcam.com/content/immunohistochemistry-the-complete-guide
11. Shi SR et al (1996) Use of pH 9.5 Tris-HCl buffer containing 5% urea for antigen retrieval immunohistochemistry. Biotech Histochem 71(4):190–196
12. Wojtowicz JM, Kee N (2006) BrdU assay for neurogenesis in rodents. Nat Protoc 1(3): 1399–1405
13. Abcam. IHC antigen retrieval protocol. [Cited 14 Oct 2021]. Available from: https://www.abcam.com/protocols/ihc-antigen-retrieval-protocol
14. Abcam. Anti-BrdU antibody [BU1/75 (ICR1)] – Proliferation Marker (ab6326). [Cited 19 Oct 2021]. Available from: https://www.abcam.com/brdu-antibody-bu175-icr1-proliferation-marker-ab6326.html
15. Abcam. BrdU (5-bromo-2'-deoxyuridine), Thymidine analog (ab142567). [Cited 18 July 2022]. Available from: https://www.abcam.com/brdu-5-bromo-2-deoxyuridine-thymidine-analog-ab142567.html?productWallTab=ShowAll
16. Karlsen OA, Berven FS, Jensen HB, Fjellbirkeland A (2011) Chapter eleven - Methanotroph Outer Membrane Preparation. Methods in Enzymology, Academic Press, 495, pp 167–176. Available from: https://doi.org/10.1016/B978-0-12-386905-0.00011-5
17. Jamur MC, Oliver C (2010) Permeabilization of cell membranes. Methods Mol Biol 588: 63–66. https://doi.org/10.1007/978-1-59745-324-0_9. PMID: 20012820
18. Abcam. BrdU staining and BrdU assay protocol. [Cited 18 July 2022] Available-from: https://www.abcam.com/protocols/brdu-staining-protocol
19. Abcam. IHC-PARAFFIN PROTOCOL (IHC-P). [Cited 18 July 2022] Available-from: https://www.abcam.com/ps/pdf/protocols/ihc_p.pdf
20. Abcam. Immunocytochemistry and immunofluorescence staining protocol. [Cited 18 Oct 2021]. Available from: https://www.abcam.com/protocols/immunocytochemistry-immunofluorescence-protocol
21. Abcam. IHC staining protocol for paraffin, frozen, and free floating sections. [Cited 18 Oct 2021]. Available from: https://www.abcam.com/protocols/immunostaining-paraffin-frozen-free-floating-protocol
22. Abcam. ab228549 – DAPI staining solution. [Cited 18 Oct 2021]. Available from: https://www.abcam.com/ps/products/228/ab228549/documents/DAPI-Staining-protocol-book-v2-ab228549%20(website).pdf
23. ThermoFisher. Hoechst 33342 solution (20 mM). [Cited 19 Oct 2021]. Available from: https://www.thermofisher.com/order/catalog/product/62249

24. Abcam. Indirect flow cytometry protocol. [Cited 19 Oct 2021]. Available from: https://www.abcam.com/protocols/indirect-flow-cytometry-protocol
25. Crane AM, Bhattacharya SK (2013) The use of bromodeoxyuridine incorporation assays to assess corneal stem cell proliferation. Methods Mol Biol 1014:65–70
26. Fatemah Chehrehasa ACBM, Dwyer P, Abrahamsen G, Mackay-Sim A (2009) EdU, a new thymidine analogue for labelling proliferating cells in the nervous system. J Neurosci Methods 177(1):122–130

Chapter 17

Assessment of Growth Plate Chondrocytes Proliferative Activity in Embryonic Endochondral Ossification via Ki-67 Immunofluorescence

Asra Almubarak and Fred B. Berry

Abstract

Cell proliferation is one of the key events that regulates organism development. In the limb, chondrocytes differentiate into a multi-layered cellular template called the growth plate. Chondrocyte proliferation is essential to provide the necessary cells that allow growth of a bone. Deregulated cell proliferation will lead to truncated bone elements. Immunofluorescence is a biological technique that uses specific antibodies to detect the subcellular localization of a proliferative marker within cellular or tissue context. In this chapter, we illustrate how to perform immunofluorescence to detect the localization of Ki-67 (a marker of actively growing/proliferating chondrocytes) in order to assess the growth fraction of the columnar chondrocytes in the growth plate in paraffin-embedded mouse tissue limb.

Key words Growth plate, Chondrocytes, Ki-67, Proliferation, Immunofluorescence, Endochondral ossification

1 Introduction

Immunofluorescence is a method used to visualize protein localization in cells or tissue. This process of protein detection is performed through employing a specific primary antibody to the targeted protein epitope. Detection can be done (a) directly via a fluorescently labeled primary antibody or (b) indirectly by utilizing a fluorophore-conjugated secondary antibody. Signals are visualized through fluorescence or confocal microscopy depending on the scope of the conducted experiment [1].

Long bone develops through a process called endochondral ossification where progenitor cells from the lateral plate mesoderm condense and form a multilayer cartilaginous template called the growth plate. The first layer of the growth plate consists of chondrocytes progenitors called the resting zone. Cells of the resting zone will then differentiate into actively proliferating columnar

Zhixiang Wang (ed.), *Cell-Cycle Synchronization: Methods and Protocols*, Methods in Molecular Biology, vol. 2579,
https://doi.org/10.1007/978-1-0716-2736-5_17,

chondrocytes. These highly proliferative chondrocytes have a critical role in controlling the longitudinal growth of limbs. Next, the columnar chondrocytes will differentiate into pre-hypertrophic chondrocytes that will exit the cell cycle, enlarge and mature to form hypertrophic chondrocytes, which will secrete a mineralized matrix to facilitate the formation of osteoblasts that will form the bone [2, 3].

Cell proliferation is a critical process during embryogenesis, tissue regeneration, and repair to generate and maintain sufficient cell numbers to establish normal size, morphology, and function of body organs. However, any disruption of such primary event due to certain pathological or genetic abnormalities can affect these biological and functional aspects. For instance, in endochondral bone development, conditional deletion of *Foxc1* and *Foxc2* genes in *Col2* positive chondrocytes in mice resulted in skeletal dysplasia with short limbs and distributive growth plate structural organization. Here, the *Col2-cre;Foxc1*$^{\Delta/\Delta}$*;Foxc2*$^{\Delta/\Delta}$ tibia growth plate shows a reduction in the columnar chondrocytes zone [4]. *Ihh* and *Fgfr3* are two major signaling molecules that regulates chondrocyte proliferation that contributes to the size and function of the long bones [5, 6]. Mutations in FGFR3 in humans cause achondroplasia which is characterized by shorter skeletal elements [7, 8].

Ki-67 is a protein, encoded by the *MKI67* gene [9], that is present only in actively growing cells and thus serves as rapid read out to determine cell proliferation. During G1, S, and G2 of the cell cycle Ki-67 localize in the nucleus, whereas in the mitosis stage the antigen tends to reposition to the surface of the chromosome. However, quiescent or resting cells do not express Ki-67 protein, which makes it an excellent marker of actively growing/proliferating cells [10, 11].

In this chapter, we will examine columnar chondrocytes growth fraction/proliferation rate in the growth plate of the mouse tibia. This assessment will be achieved through detecting the localization of the Ki-67 protein in growth plate chondrocytes of paraffin-embedded samples through indirect immunofluorescence and may be applied to other tissues (Fig. 1).

2 Materials

1. PBS (10×): 80 g NaCl, 2 g KCl, 14.4 g Na_2 HPO_4, 2.45 g K_2PO_4; volume to 1 L.
2. PBS-X Washing buffer: 1X PBS, 0.05% (250 μl) Triton X-100.
3. Citrate buffer Solution (10×): 1.47 g Tris-Sodium Citrate (dihydrate), 0.25 ml Tween-20, 450 ml dH_2, pH to 6.0 with HCl.

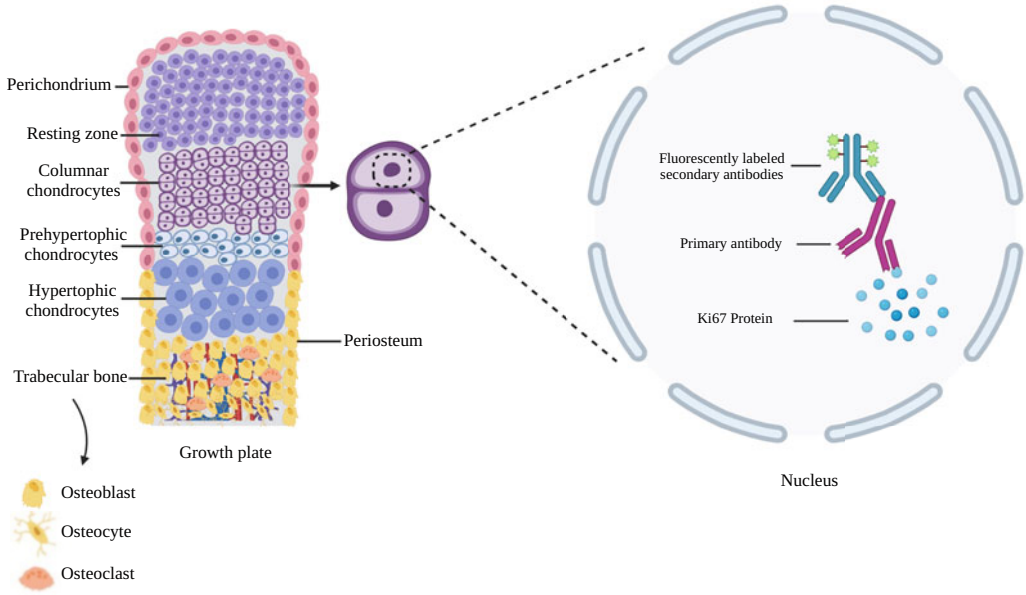

Fig. 1 Schematic diagram of the Ki-67 immunofluorescence theory. The growth plate consists of four layers of distinctively differentiated chondrocytes that will transdifferentiate to osteoblast to form the trabecular bone. Ki-67 epitopes in the columnar chondrocytes can be detected with specific anti-Ki-67 primary antibody and fluorophore-conjugated secondary antibody to enable visualization of proliferative activity. (Image was created with BioRender.com)

4. Blocking buffer: Washing buffer (1XPBS + 0.05% Triton X-100), 5% Donkey serum. The serum added to the blocking buffer must be from the same species of the secondary antibody.
5. DAPI: Dilute DAPI 1:200 in IX PBS and keep in dark.
6. ProLong Gold Antifade mountant media (Invitrogen).
7. Primary antibody: Monoclonal Rabbit anti-ki-67 (Bethyl, lot number: IHC-00375) (*see* **Note 1**).
8. Humidified chamber: Plastic container and a wet paper towel (to prevent slide dryness during incubation periods).

3 Methods

Dissect hindlimbs from mouse embryos at E14.5, E15.5, and E16.6. Then, fix the limbs with 4% paraformaldehyde, dehydrated and embedded in paraffin wax. Next, cut the paraffin blocks into Sections (5 micron) with a microtome and mount onto Superfrost plus slides (*see* **Note 2**).

3.1 Deparaffinize and Rehydrating

1. Submerge the slides in two changes of Xylene for 5 min each.
2. Immerse the slides in the slides in an alcohol gradient starting with two changes of 100% Ethanol for 5 min each, two changes of 95% Ethanol for 5 min each, 70% Ethanol for 3 min, 50% Ethanol for 3 min followed by Milli-Q water for 5 min.

3.2 Antigen Retrieval

Heating samples in citrate buffer allows accessibility of the Ki-67 epitope.

1. In a 200 ml beaker, preheat 180 ml of Milli-Q water to sub-boiling temperature (95 °C) and add 20 ml of 10× citrate buffer, and 100 μl of Tween 20 (*see* **Note 3**).
2. Submerge the slide rack in the citrate buffer and heat the slides for 20 min. Do not add the slides if the citrate buffer temperature was below 95 °C.

3.3 Permeabilization

Ki-67 is an intracellular (nuclear) antigen, therefore, permeabilization with a detergent such as Triton X-100 is a crucial step that would facilitate accessibility of the primary antibody into the cell and nucleus.

1. Incubate the slides in two changes of 1× PBSX for 5 min each.

3.4 Blocking

1. Carefully, dry the slides to not disturb the tissues, add blocking buffer that contains a serum from the same species the secondary antibody was raised (e.g., donkey serum, bovine serum albumin (BSA), or goat serum), and incubate for 1 h at RT in a humidified chamber.

3.5 Immunostaining: Primary Antibody

1. Dilute the Ki-67 primary antibody in the blocking buffer (1:200).
2. Add 100 μl of diluted Ki-67 primary antibody into each slide and cover with plastic wrap (Run one slide as a negative control with no primary antibody). Incubate overnight at 4 °C in a humidified chamber (*see* **Note 3**).

3.6 Secondary Antibody

1. The next day, wash the slides in two changes of 1× PBSX for 5 min each.
2. Dilute the secondary antibody 1:1000 in the blocking buffer, add 100 μl into each slide (including the negative control slide), and incubate for 2 h at RT in a humidified chamber in the dark to prevent photobleaching the fluorescent signal by the light.
3. Wash the slides twice with 1× PBSX for 5 min each and add DAPI for 5 min.
4. Wash slides with two changes of 1× PBS for 5 min each.

5. Mount with ProLong Gold-antifade and let slides to dry at least 4 h or overnight in dark before visualizing.
6. Store the slides at 4 °C in dark.

3.7 Multicolor Detections (Optional)

To detect co-localization of a different antigen in the same tissue section, another antibody (that can be processed through the same antigen retrieval) can be added simultaneously with the anti Ki-67 when preparing the primary antibody. This additional primary antibody must be raised in a different species than the Ki-67 antibody. For instance: mouse antibody for antigen A, and rabbit antibody for antigen B.

The corresponding secondary antibody must also be conjugated to a different wavelength to ensure having distinctive fluorescent color for each target in the slide during visualization.

3.8 Data Analysis

In order to determine chondrocytes proliferation rate, we will count the number of Ki-67-positive cells and DAPI-positive cells and calculate the ratio (*see* **Note 4**). Immunofluorescence of Ki-67 was done on wild-type embryonic mice tibia at E14.5, E15.5, and E16.5. Ki-67 proliferation ratio was calculated and plotted using SigmaPlot 13. Interestingly, the tibia growth plate chondrocytes showed a higher proliferation activity at E14.5 that will decrease at the later time point of embryonic development (Fig. 2).

4 Notes

1. Anti-Ki-67 antibodies are available as monoclonal or polyclonal, and have different animal sources such as rabbit, mouse, and chicken.
2. The Ki-67 IF protocol is also applicable to cells growing on coverslips, frozen tissue and fresh snap-frozen tissue. However, permeabilization, rehydration, and antigen retrieval steps are not required for such samples.
3. Antigen retrieval can be done on a hot plate, rice cooker or vegetable steamer or any other alternative that can bring the citrate buffer to a sub-boiling temperature (99–95) for 20 min.
4. Ki-67 signal quantification can be done manually through counting the cells or through using imaging software such as imageJ.

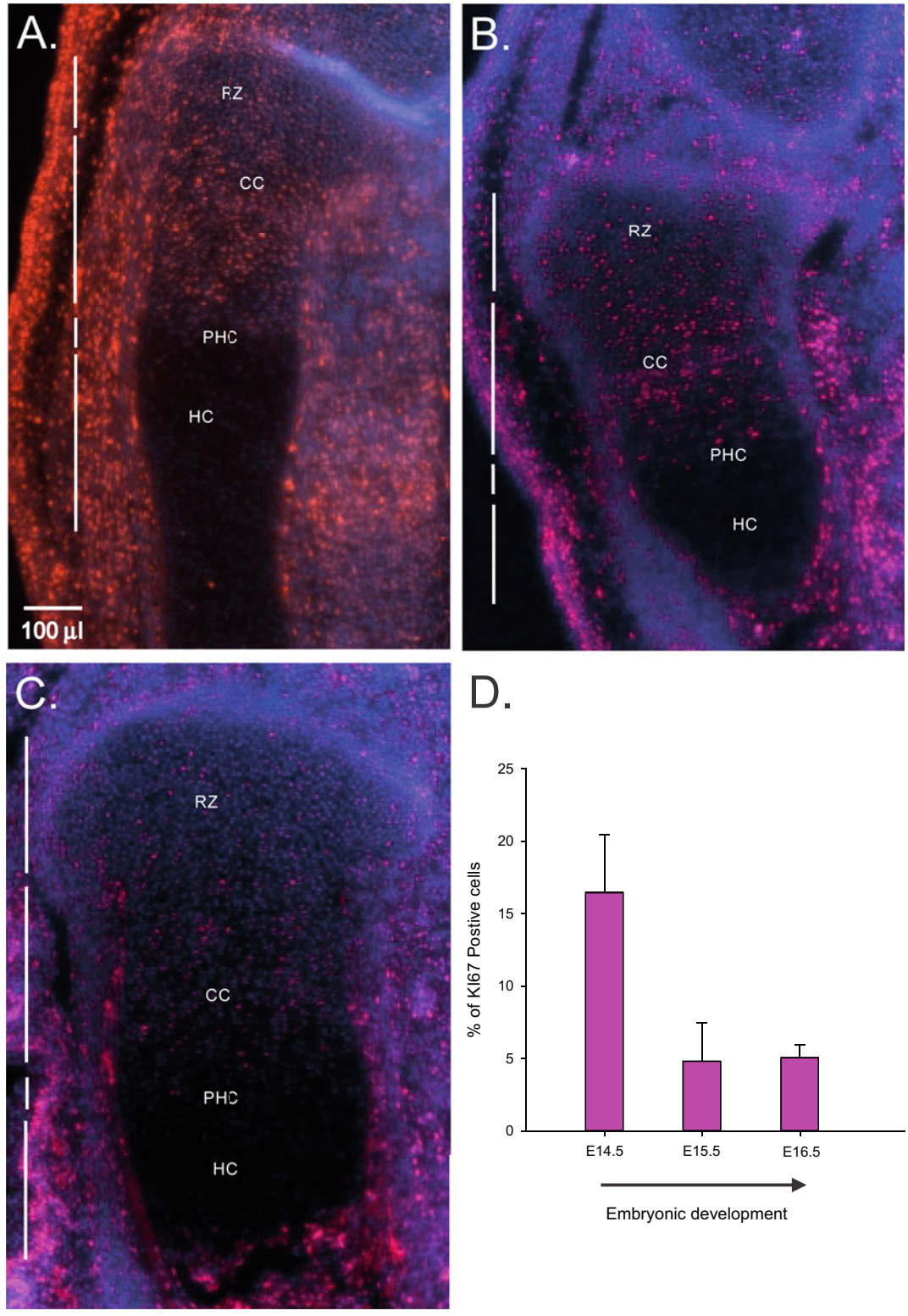

Fig. 2 The growth plate chondrocytes demonstrate higher proliferative activity at E14.5 compared to E15.5 and E16.5 during embryonic limb development. Immunofluorescence of Ki-67 was performed on mouse tibia growth plate at E14.5 (**a**), E15.5 (**b**), and E16.5 (**c**). Ki-67 positive cells were quantified and plotted (**d**). RZ resting zone, CC columnar chondrocytes, PHC prehypertrophic chondrocytes, HC hypertrophic chondrocytes

References

1. Im K, Mareninov S, Diaz MFP, Yong WH (2019) An introduction to performing immunofluorescence staining. In W. H. Yong (Ed.), Biobanking: Methods and Protocols (pp. 299–311). Springer New York
2. Sun MM-G, Beier F (2014) Chondrocyte hypertrophy in skeletal development, growth, and disease. Birth defects research. Part C. Embryo Today Rev 102:74–82. https://doi.org/10.1002/bdrc.21062
3. Yeung Tsang K, Wa Tsang S, Chan D, Cheah KSE (2014) The chondrocytic journey in endochondral bone growth and skeletal dysplasia. Birth Defects Res C Embryo Today 102: 52–73. https://doi.org/10.1002/bdrc.21060
4. Almubarak A, Lavy R, Srnic N, Hu Y, Maripuri DP, Kume T, Berry FB (2021) Loss of Foxc1 and Foxc2 function in chondroprogenitor cells disrupts endochondral ossification. J Biol Chem 101020. https://doi.org/10.1016/j.jbc.2021.101020
5. Shiang R, Thompson LM, Zhu Y-Z, Church DM, Fielder TJ, Bocian M, Winokur ST, Wasmuth JJ (1994) Mutations in the transmembrane domain of FGFR3 cause the most common genetic form of dwarfism, achondroplasia. Cell https://doi.org/10.1016/0092-8674(94)90302-6
6. Yoshida M, Hata K, Takashima R, Ono K, Nakamura E, Takahata Y, Murakami T, Iseki S, Takano-Yamamoto T, Nishimura R, Yoneda T (2015) The transcription factor Foxc1 is necessary for Ihh-Gli2-regulated endochondral ossification. Nat Commun 6: 6653. https://doi.org/10.1038/ncomms7653
7. Heuertz S, le Merrer M, Zabel B, Wright M, Legeai-Mallet L, Cormier-Daire V, Gibbs L, Bonaventure J (2006) Novel FGFR3 mutations creating cysteine residues in the extracellular domain of the receptor cause achondroplasia or severe forms of hypochondroplasia. Eur J Hum Genet 14:1240–1247. https://doi.org/10.1038/sj.ejhg.5201700
8. Lee YC, Song IW, Pai YJ, de Chen S, Chen YT (2017) Knock-in human FGFR3 achondroplasia mutation as a mouse model for human skeletal dysplasia. Sci Rep 7. https://doi.org/10.1038/SREP43220
9. Schonk DM, Kuijpers HJH, van Drunen E, van Dalen CH, Geurts Van Kessel AHM, Verheijen R, Ramaekers FCS (1989) Assignment of the gene(s) involved in the expression of the proliferation-related Ki-67 antigen to human chromosome 10. Hum Genet 83: 297–299
10. Gerdes J, Schwab U, Lemke H, Stein H (1983) Production of a mouse monoclonal antibody reactive with a human nuclear antigen associated with cell proliferation. Int J Cancer 31:13–20
11. Gerdes SJ, Lemke H, Baisch H, Wacker HH, Schwab U (1984) Cell cycle analysis of a cell proliferation-associated human nuclear antigen defined by the monoclonal antibody Ki-67. J Immunol 133:1710–1715

Chapter 18

Detecting Cell Cycle Stage and Progression in Fission Yeast, *Schizosaccharomyces pombe*

Zohreh Kianfard, Kyle Cheung, Daniel Rappaport, Sirasie P. Magalage, and Sarah A. Sabatinos

Abstract

We have previously described methods to synchronize cultures of fission yeast, *Schizosaccharomyces pombe*. In this chapter, we provide methods to detect cell cycle stage in cells and populations of *S. pombe*. These protocols used fixed samples. First, we describe sample preparation for flow cytometry of bulk DNA content. This technique allows users to monitor progression of DNA replication and detect any perturbation during the synthesis (S) phase of the cell cycle. Second, we describe methods to stain nuclei and septa of fixed yeast cells, and monitor proportions of cell cycle stages within cultures. Together, these methods provide the ability to compare cell cycle progression or delay between cultures, making use of the powerful molecular genetics tool that is *S. pombe*.

Key words Fission yeast, *Schizosaccharomyces pombe*, Cell cycle, DAPI nuclear stain, Aniline blue, septa, Flow cytometry, S-phase

1 Introduction

Schizosaccharomyces pombe shares extensive homology with metazoan models [1–3], particularly in cell cycle and checkpoint signaling pathways (e.g., [4–6]). This makes fission yeast an excellent genetic model for research of many topics, including cell signaling, metabolism, DNA replication, DNA repair, and epigenetics. In many cases, it may be useful to detect cell cycle attributes within a population, and assess the effect of a gene of interest on cell growth, division, and death. Staging samples for cell cycle distribution and phenotypes is an important tool to apply mechanistic insights from *S. pombe* to other models.

S. pombe cells are rod-shaped, and grow primarily in length during the cell cycle, ranging from approximately 8 μm to ~15 μm prior to division (e.g., [3, 4, 7]). Cell size is controlled by the cell cycle stage (e.g., [4, 5, 7, 8]). The measurement of

Zhixiang Wang (ed.), *Cell-Cycle Synchronization: Methods and Protocols*, Methods in Molecular Biology, vol. 2579,
https://doi.org/10.1007/978-1-0716-2736-5_18,

fission yeast length within a population may indicate perturbation of cell cycle progression or arrest. Fission yeast is haploid and spends most time in the G2-phase of the cell cycle, with replicated DNA (2 DNA content = 2C). However, nuclear and cell division do not happen concomitantly in actively cycling cultures of *S. pombe*. Cells enter the next cell cycle before daughter cells separate. Following G2, the 2C nucleus divides as cells enter M-phase (Fig. 1). Cells become binucleates in G1, with two separated haploid nuclei within a single cell. The G1-phase is brief and is followed by the onset of septation in the middle of the cell, a process known as medial fission. Appearance of the septum is associated with S-phase. Cytokinesis does not take place until the end of S-phase, meaning that newly separated daughter cells are already in the G2-phase following division.

Most asynchronously growing *S. pombe* cells have either one replicated (2C) nucleus, or two unreplicated (1C) nuclei. Consequently, most single *S. pombe* cells appear to have 2C DNA content, whether in G2-phase, or as binucleates in G1- or S-phases. For the purpose of DNA synthesis detection by flow cytometry, asynchronous cell populations appear as approximately 2C. DNA replication is observed as a transition from 2C toward a 4C peak in septated cells. This is observed in most asynchronous fission yeast populations, or in a G2-block and release using the *cdc25-22* temperature-sensitive strain. Methods of cell cycle synchronization that arrest cells in S-phase frequently generate a peak between 1C and 2C DNA content. This occurs because DNA synthesis is arrested while septation continues and concludes, generating two daughter cells that are stuck in S-phase. In all of these cases, synchrony and release can be monitored using flow cytometry to detect a shift of the dominant (synchronized) population during subsequent S-phase.

These cell cycle properties also allow cell staging in the G2, M, G1, and S-phases using microscopy. Septation can be assessed by light microscopy in live cultures to observe cell cycle progression (refer to Chapter 13). In fixed samples, cell cycle stage is determined by considering nuclear and septum morphologies. Fluorescence microscopy is an excellent method to assess cell cycle dynamics in fission yeast populations. Ethanol fixed cells are stained with 4′,6-diamidino-2-phenylindole (DAPI) and aniline blue to visualize DNA and septa, respectively. By visualizing DNA content and septation, cell cycle proportions can be compared to unperturbed conditions. Typical asynchronous populations of fission yeast are predominantly G2-phase (70%), with approximately 10% of the population in anaphase (M-phase), 10% binucleate without a septum (G1-phase), and 10% septated (S-phase). DNA and septum staining also allows detection of DNA mis-segregation events such as the "*cell untimely torn*" (*cut*) phenotype (reviewed in [9]), which are easily identified and quantified.

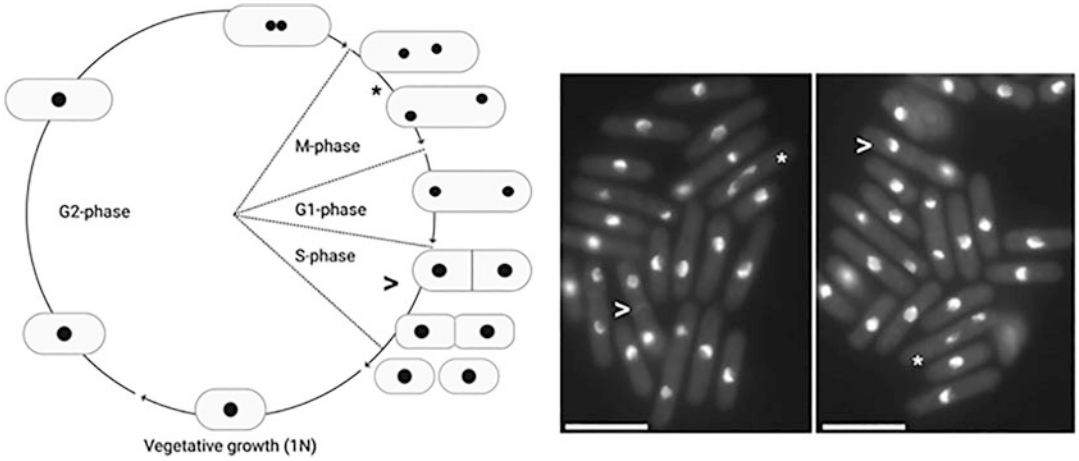

Fig. 1 DNA and septum morphologies of fission yeast cell cycle stages (left, created with BioRender.com). Sample images of a wild-type asynchronous culture are shown at right, stained with DAPI and aniline blue to detect DNA and septa, respectively. Example cells in anaphase are indicated with an asterisk (*), or an arrowhead (>) to highlight septated cells. Scale bars 10 μm

We present methods to assess cell cycle stage and effects in fission yeast. The accompanying chapter "Cell cycle stage and synchrony in fission yeast" describes various methods to synchronize yeast cultures, and then fix them in ethanol. These samples are used in this chapter to assess DNA content and cellular morphology using microscopy and flow cytometry. These methods provide powerful tools to assess progression from cell cycle block, and to detect phenotypes in mutant cultures of interest.

2 Materials and Equipment

2.1 Fixed Cell Samples

Fission yeast cultures may be stored indefinitely in 70% ethanol at 4 °C. The preceding chapter (13) describes protocols to fix large and small volumes of fission yeast. Cells may also be fixed by other methods (e.g., paraformaldehyde, glutaraldehyde), but may require permeabilization with 0.1 to 0.5% Tween-20 in water prior to using the methods in this chapter.

2.2 Flow Cytometry Staining Tubes

Flow cytometry samples are traditionally assessed in 5 mL polystyrene round-bottom tubes (e.g., Falcon brand 352052) that specifically fit the cytometer sample port. Other cytometers do not require specialty tubes, and microfuge tubes may be used for both sample preparation and acquisition.

2.3 50 mM Sodium Citrate Buffer

Sodium citrate is made up as a 0.5 M stock and autoclaved for long-term room temperature storage. Sodium citrate buffer is 50 mM, and is made from a 1:10 dilution of the 0.5 M sodium citrate stock

solution into MilliQ water as needed to make flow cytometry washes and solutions (e.g., 1× RNaseA, 1× SYTOX Green).

2.4 Ribonuclease A (RNaseA) Stock Solution

RNaseA may be purchased as a DNase-free solution from many manufacturers. Alternatively, to make RNaseA from lyophilized powder, resuspend RNaseA at 10 mg/mL in a solution of 10 mM Tris HCl, pH 7.5, 15 mM NaCl. Boil solution at 100 °C for 15 min and then cool slowly to room temperature [10]. RNaseA solution is stored at −20 °C and should be aliquoted into appropriate volumes to avoid excessive freeze/thaw cycles.

2.5 1× RNaseA Solution

Dilute RNaseA to 0.1 mg/mL in 50 mM citrate buffer.

2.6 1× SYTOX Green Solution

SYTOX Green dye is purchased from Invitrogen as a 5 mM solution in DMSO. Dilute SYTOX stock solution 1:5000 in 50 mM citrate buffer to add to flow samples in the staining step.

2.7 Sonicator

Sonicating flow samples is optional; however, sonication helps to disrupt aggregates and prevent cytometer damage. We have used both a probe microtip sonicator or water bath sonicator with good results.

2.8 Mesh Filter

Flow samples can be filtered to remove aggregates that may clog the cytometer. In-cap filter options are commonly used in metazoan flow cytometry protocols and can be used for *S. pombe* flow samples with success (i.e., Falcon 352235). Alternatively, 40–70 μm nylon mesh membrane can be purchased (i.e., Millipore NY4100010) in rolls, cut to fit a microfuge tube, and the samples pipetted on immediately before running on the cytometer.

2.9 10× Aniline Blue Stock Solution

Aniline blue is resuspended in water at 10–20 mg/mL. This is stored at 4 °C indefinitely.

2.10 Aniline Blue Working Solution

The solution is made by adding 1 mL of 10× aniline blue stock solution to 1 mL of 10× PBS and 8 mL of MilliQ water, and is stored at 4 °C.

2.11 Mounting Medium with DAPI

Mounting solution is 90% glycerol, 1% 1,4-diazabicyclo[2.2.2] octane (DABCO) (v/v/v). Mountant is aliquoted into 1 mL volumes and then is stored at −20°, protected from light. 4′,6-diamidino-2-phenylindole (DAPI) is added to 1 mg/mL and stored at −20 °C protected from light. The antifade agent DABCO preserves fluorescence of the stained cells, even after prolonged storage at 4 °C, and prevents rapid photobleaching of DAPI.

3 Methods

3.1 Flow Cytometry

Flow cytometry is an efficient method to determine bulk DNA content within cells, and to compare population-wide characteristics. We describe a robust protocol that uses SYTOX Green, a stoichiometric DNA-binding dye that is membrane impermeant and shows low cytotoxicity in living cells [11, 12] (*see* **Note 1**). SYTOX Green fluorescence is typically acquired using the FL1 detector of many commercial cytometers including the FACScan and Accuri models by Becton Dickenson. The forward scatter (FSC) detector may also be used to give population characteristics of cell size. In the case of *S. pombe* with its rod-like shape, FSC detection is useful to monitor changes in cell length between cell populations affecting cell cycle block and release. Bivariate plots of SYTOX Green and FSC, or SYTOX Green Area and Wide signals, help to distinguish cell populations within DNA that are not obvious from SYTOX Green alone [13]. Finally, consideration of DNA content (SYTOX Green) relative to cell length (using FSC as a proxy) may help to understand culture dynamics, e.g., whether a culture of cells is diploid or haploid.

1. Aliquot 1 mL of fresh 50 mM sodium citrate buffer to a microfuge tube or flow cytometry tube (*see* **Note 2**).
2. Resuspend ethanol fixed cells by vortexing, and remove approximately 250 μL (~1 to 5 × 10^6 cells) to fresh microfuge tubes (*see* **Notes 3** and **4**).
3. Vortex cells in citrate buffer and centrifuge at 11,000 rpm for 3 min. If using 5 mL polystyrene "FACS" tubes, centrifuge in a clinical swinging bucket centrifuge at 1500*g* for 3 min.
4. Decant buffer. Resuspend pelleted cells by vortexing or by agitating in a centrifuge tube rack.
5. Repeat wash step by adding 1 mL of 50 mM fresh sodium citrate buffer to each tube. Vortex and centrifuge as in Subheading 3.1, **step 3**.
6. Decant buffer and agitate cell pellet as in Subheading 3.1, **step 4**.
7. Add 500 μL of freshly prepared 1× RNaseA solution (50 mM sodium citrate + 0.1 mg/mL RNaseA) to each tube.
8. Vortex samples, and incubate at 37 °C for 2 h. Alternatively, samples can be stored at 4 °C at this step, and then incubated at 37 °C for 2 h prior to continuing on a later date.
9. Add 500 μL of 1× SYTOX Green solution (50 mM sodium citrate + 1 μM SYTOX Green) to each tube (see **Note 4**).
10. Vortex and incubate cells at 4 °C for at least 15 min, protected from light.

11. Sonicate samples to disrupt aggregates. Use a microtip sonicator set at approximately 30% power, for 5 s at low to medium power. Five bursts of 1 s may be more effective to disperse samples and break clumps. Alternatively, a water bath sonicator may be used for 5–10 s, but power settings require optimization in each setting (*see* **Note 5**).
12. *Optional*: Filter samples using 40 to 70 μm mesh filter immediately before running on the cytometer.
13. Acquire data on flow cytometer at a low flow rate for all samples and standards. On an Accuri C6 cytometer (Becton Dickenson), acquisition parameters are not altered before acquisition. SYTOX Green is detected using FL-1 Area; saving forward scatter (FSC) and side scatter (SSC) data is also useful for analysis (see **Note 6**).
14. If acquiring data using a variable detector cytometer (i.e., BD FACScan model or similar), we recommend establishing the FSC/SSC population first. Centre the largest and smallest samples in a FSC/SSC bivariate plot using voltage and gain. Next, center the FL-1 (SYTOX Green) population in linear mode, using FL-1 voltage and gain so that the brightest and dimmest populations are within the range of detection. Be aware that diploids and longer or larger cells (i.e., *cdc25-22*) will show altered characteristics compared to haploid wild-type cells.
15. Analysis can be performed on a variety of software such as FlowJo (TreeStar, BD Biosciences), FCS Express (DeNovo), or others (*see* **Note 7**). SYTOX Green histograms should be generated using a linear scale, and FL1-Area (FL1-A) signal.
16. SYTOX Green data within populations may be gated using FSC and SSC parameters; if gating is used both the gated and ungated histograms should be compared to assess the effect on SYTOX Green signals and any associated conclusions (*see* **Note 8**).
17. To judge the distribution of cell length relative to DNA content, SYTOX Green (FL1-A) versus FSC bivariate dot plots can be generated (Fig. 2).

3.2 Nucleus and Septum Staining of Cell Populations

Fission yeast cell cycle morphologies and characteristics are described in the Introduction (Subheading 1). Staining cells with a nuclear dye such as DAPI allows detection of mononucleate cells, typically in the G2-phase, and binucleates. Addition of a septum-stain such as aniline blue permits binucleate cell description as septated (S-phase) versus binucleate (G1-phase) or nuclei undergoing anaphase (M-phase). Septum stains are useful to detect defects in cytokinesis or septation establishment (e.g., [14–16]) and cell cycle re-entry (e.g., [17, 18]).

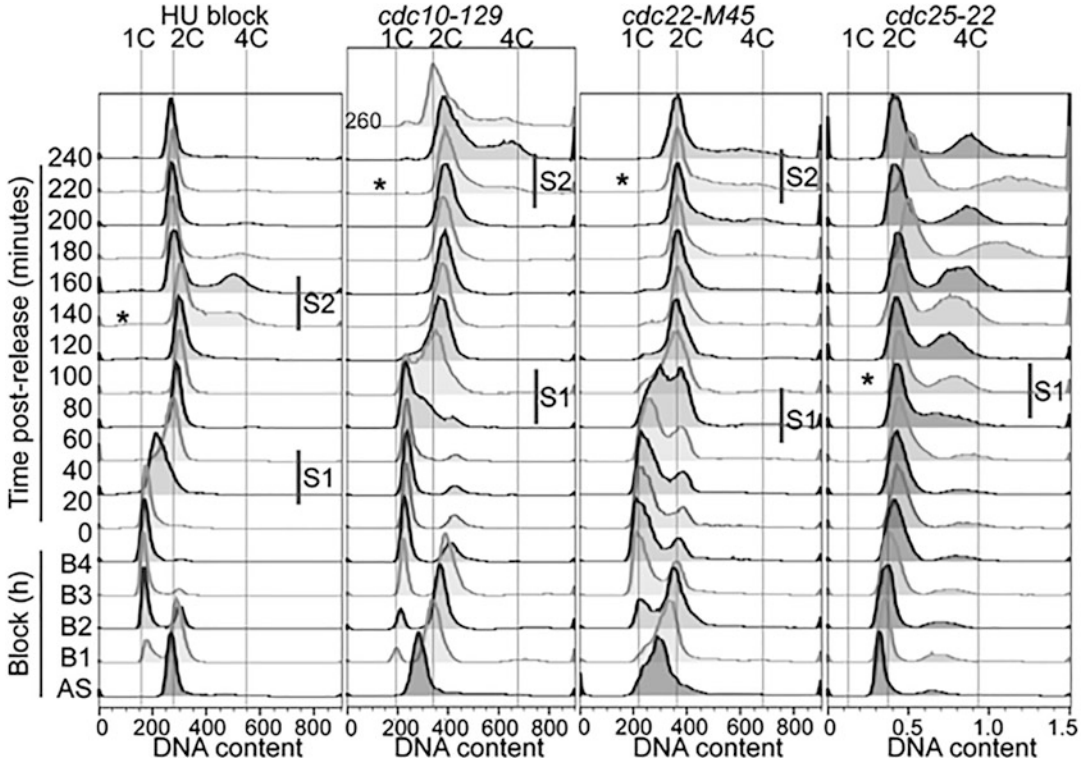

Fig. 2 Monitoring DNA content using flow cytometry following synchrony by hydroxyurea (HU) or temperature-sensitive alleles for G1/S (*cdc10-129*), S (*cdc22-M45*), or G2/M (*cdc25-22*) arrest. Samples prepared by synchrony in Chap. 13 were blocked for 4 h and released under permissive conditions, and then fixed every 20 min to monitor DNA content. Modal DNA intensities were used to show normalized peaks and compare timing of the S-phase. The S-phase is inferred by transit from 1C DNA content to 2C in cells that arrest as mononucleate G1 or S-phase populations (HU, *cdc10-129*, *cdc22-M45*). The first S-phase post-release is labeled with a line and "S1" in all samples. In cultures that arrest in G2 or in cycling populations with a predominantly 2C or binucleate population, S-phase is marked by transition from 2C to 4C. This is seen in *cdc25-22*, and second S-phases (labeled with a line and "S2") of other samples. The peak of cell septation observed by light microscopy is indicated with an asterisk (septation data is plotted in Chap. 13). An additional timepoint was acquired for *cdc10-129* at 260 min post-release and is indicated on the plot

1. Aliquot 1 mL of water into sample tubes.
2. Vortex fixed cell samples to resuspend in ethanol fixative. Remove 200–300 μL of fixed sample (1–5 × 10^6 cells total) to the appropriate tube.
3. Resuspend cells by vortexing and centrifugate 11,000 rpm for 3 min. Decant wash by pouring, and then resuspend cells by vortexing or agitating tubes against the sample tray.
4. Repeat wash steps using 1 mL water or 1× PBS, and pellet then resuspend cells as in Subheading 3.2, **step 3**.
5. Add 250 μL of Aniline blue working solution, and rotate samples for 15 to 30 min at room temperature.

6. Pellet cells as in Subheading 3.2, **step 3**. Do not disturb the pellet.
7. Remove all but ~10 μL of stain from the tube using a fine tip (p200/p20) pipette.
8. Resuspend cell pellet by pipetting up and down vigorously.
9. Apply 4 μL of stained cell suspension from Subheading 3.2, **step 8** to a glass slide. Smear cells into an area approximately 1 cm diameter using the side of the pipette tip.
10. Cover slides loosely with tinfoil, or in a darkened container. Air dry samples approximately 5 min in the dark.
11. For each sample, pipette 3–5 μL of DAPI mounting media onto a coverslip. Gently layer the coverslip, mountant-side down, onto the sample.
12. Seal the edges of the coverslip with nail varnish and dry in the dark.
13. Samples can be imaged immediately using DAPI excitation/emission parameters. We recommend also acquiring a bright-field image that can be merged with the DAPI/aniline blue image during analysis.
14. Samples on slides may be stored racked in slide storage boxes at 4 °C for several days, or −20 °C for weeks.

3.3 Assessing Cell Cycle Synchrony and Effect Using Nucleus and Septum Stain

1. Image analysis may be performed using commercial microscopy software, or open-access alternatives such as ImageJ or FIJI. In FIJI, open a file and set scale (Analyze>Set scale). This may be used to place a scale bar in each image (Analyze>Tools>Scale Bar).
2. Brightness and contrast settings should be similar across images, and should show both septa and nuclei. Absolute numbers should be tracked between images and experiments (*see* **Notes 9–11**).
3. Cells within a field can be categorized as: mononucleated (=G2-phase); anaphase (=M-phase); binucleated (=G1-phase); septated (=S-phase). An entire field of 50 to 100 cells is counted. This is repeated a minimum of 3 times for a total of 200 to 300 cells per sample. All cells in an area should be counted to avoid bias (*see* **Note 12**).
4. Cell counting can be performed in FIJI using the cell counter tool (Plugins>Analyze>Cell Counter>Cell Counter>Initialize).
5. Proportions of cells in each category are categorical data, and appropriate statistical tests are used to compare between samples. Proportions can be shown with a 95% confidence interval error bar. Excellent reviews of this topic are helpful in considering hypothesis testing and data analysis (e.g., [19]).

6. Since fission yeast grows in length during the cell cycle or when arrested in G2, cell length may be a useful measurement of treatment effect. To measure length, images opened in FIJI must have the correct scale applied, calculated from the microscope (Analyze>Set Scale). Cells may be measured from tip to tip, or from septum to tip if a septum is clearly visible, using the line drawing tool in the tool bar and the region of interest (ROI) manager. Length measurements may be exported from FIJI to a spreadsheet for analysis.

4 Notes

1. SYTOX Green has become a preferred dye for DNA staining due to its low cytotoxicity. However, care should be taken with any DNA binding dye. In this protocol, waste, consumables, and samples are disposed of in accordance with local biohazard disposal guidelines.
2. Choice of tube (microfuge tube versus polystyrene 5 mL FACS tube) is determined by the flow cytometer requirements.
3. When aliquoting fixed cells, prepare standards alongside experimental samples to process in parallel. We prepare and fix a control wild-type strain as a comparator between experiments and for DNA contents within samples. For example, the control culture serves as a baseline asynchronous population, an approximate 2C peak. We also prepare 50 mL cultures for nitrogen arrest in the G1-phase; these provide a 1C peak. We establish a vegetative diploid, and grow in a 50 mL YES culture, which provides a 4C peak. For each standard sample, we harvest the entire culture, centrifugate (1500 rpm, 5 min), resuspend the pellet, and then fix in 1 volume of cold 70% ethanol. These standards are stored at 4 °C indefinitely and are used in every experiment to suggest appropriate 1C, 2C, and 4C values.
4. All flow cytometry samples within an experiment, plus controls, should be processed at the same time. DNA staining within a batch is dependent on day-to-day variation in solutions, absolute concentration of stoichiometric DNA dye, number of cells used, and time. It is not advisable to compare between samples that are stained at different times or with different batches of buffers. Instead, trends between experiments can be compared. Absolute numbers can only be compared within samples of an experiment processed at the same time. Further, a similar number of cells should be used in each sample to ensure consistent staining and to prevent cytometer clogs; we recommend 1–5 $\times$ 10^6 total cells per sample.

5. Sonication is not an absolute requirement, but will help to disrupt aggregates and prevent clogs in the cytometer. Parameters that disrupt aggregates without disturbing samples must be determined for each sonicator; these are a guideline.
6. If desired, propidium iodide (PI) is a stoichiometric DNA-binding dye that may be used instead of SYTOX Green. PI flow is performed using the FL-2 Area detector, as the excitation/emission properties are different. 7-amino actinomycin D (7-AAD) is a sufficiently stoichiometric DNA binding dye that allows optimal detection using the FL-3 Area detector.
7. For a list of free cytometry software, refer to the Purdue University Cytometry Laboratories, http://www.cyto.purdue.edu/flowcyt/software/Catalog.htm
8. Gating in flow cytometry excludes data from analysis. This can be useful to remove non-cell debris from analysis which may obscure results. However, it is possible to remove important data events by aggressive gating (i.e., loss of a true sub-1C peak by removing all small events). We recommend testing all analyses with and without gating, and determining the impact of gated/removed cells on results. In particular, FSC/SYTOX dot plots are helpful to ensure that all cellular events are included fairly (see Fig. 2).
9. If one of DAPI or aniline blue signals appear weaker between experiments, it may signal that the stain is no longer optimal. Best imaging is obtained when septa and nuclei have similar brightness. Occasionally, DAPI in mounting media will produce dimmer signal; we typically add DAPI at 1 mg/mL to small volumes of mountant only (i.e., 1 mL) and do this more frequently.
10. Aniline blue signal is produced by binding of a dye impurity to beta-(1,3)-glucans in the *S. pombe* septum. The impurity that fluorescently marks the fission yeast septum is Sirofluor (sodium 4,4′-[carbonylbis(benzene-4,1-diyl)bis(imino)]bisbenezene sulfonate). Kippert and Lloyd (1995) reported a wide range of Aniline blue concentrations (0.25–5 mg/mL) that successfully generated septum staining, despite wide variation of Sirofluor between manufacturers and batches [20]. We find that 1 to 3 mg/mL final concentration of Aniline Blue works reliably. Greater variation occurs in staining caused by pH and/or age of the working solution. We recommend making Aniline blue working and stock solutions freshly and frequently.
11. Other stains may also be used to detect *S. pombe* septa, preferentially in non-permeabilized cells. Alternative stains include Calcofluor white or Congo red; however, these show limited

success in alcohol-fixed cells. The 70% ethanol used in these protocols is both a fixative and permeabilization agent. We predict that methanol-based fixatives would generate similar results. Calcofluor has been used in ethanol fixed cells but generates a strong signal that may interfere with DAPI detection. If using these dyes, it may be preferable to use a non-alcohol fixative.

12. We recommend that samples are blinded prior to acquisition and analysis to prevent experimenter bias and selection of "interesting" events rather than representative fields.

References

1. Wood V, Gwilliam R, Rajandream MA et al (2002) The genome sequence of Schizosaccharomyces pombe. Nature 415:871–880. https://doi.org/10.1038/nature724
2. Hayles J, Wood V, Jeffery L et al (2013) A genome-wide resource of cell cycle and cell shape genes of fission yeast. Open Biol 3: 130053. https://doi.org/10.1098/rsob.130053
3. Hoffman CS, Wood V, Fantes PA (2015) An ancient yeast for young geneticists: a primer on the *Schizosaccharomyces pombe* model system. Genetics 201:403–423. https://doi.org/10.1534/genetics.115.181503
4. Nasmyth K, Nurse P, Fraser RS (1979) The effect of cell mass on the cell cycle timing and duration of S-phase in fission yeast. J Cell Sci 39:215–233
5. Nurse P, Thuriaux P, Nasmyth K (1976) Genetic control of the cell division cycle in the fission yeast Schizosaccharomyces pombe. Mol Gen Genet 146:167–178
6. Forsburg SL, Nurse P (1991) Cell cycle regulation in the yeasts Saccharomyces cerevisiae and Schizosaccharomyces pombe. Annu Rev Cell Biol 7:227–256. https://doi.org/10.1146/annurev.cb.07.110191.001303
7. Fantes PA (1981) Isolation of cell size mutants of a fission yeast by a new selective method: characterization of mutants and implications for division control mechanisms. J Bacteriol 146:746–754. https://doi.org/10.1128/jb.146.2.746-754.1981
8. Ogden JE, Fantes PA (1986) Isolation of a novel type of mutation in the mitotic control of Schizosaccharomyces pombe whose phenotypic expression is dependent on the genetic background and nutritional environment. Curr Genet 10:509–514. https://doi.org/10.1007/BF00447384
9. Yanagida M (1998) Fission yeast cut mutations revisited: control of anaphase. Trends Cell Biol 8:144–149. https://doi.org/10.1016/s0962-8924(98)01236-7
10. (2007) RNase stock solution. Cold Spring Harb Protoc 2007:pdb.rec11030. https://doi.org/10.1101/pdb.rec11030
11. Roth BL, Poot M, Yue ST, Millard PJ (1997) Bacterial viability and antibiotic susceptibility testing with SYTOX green nucleic acid stain. Appl Environ Microbiol 63:2421–2431
12. Kolniak TA, Sullivan JM (2011) Rapid, cell-based toxicity screen of potentially therapeutic post-transcriptional gene silencing agents. Exp Eye Res 92:328–337. https://doi.org/10.1016/j.exer.2011.01.004
13. Knutsen JHJ, Rein ID, Rothe C et al (2011) Cell-cycle analysis of fission yeast cells by flow cytometry. PLoS One 6:e17175. https://doi.org/10.1371/journal.pone.0017175
14. Bohnert KA, Gould KL (2012) Cytokinesis-based constraints on polarized cell growth in fission yeast. PLoS Genet 8:e1003004. https://doi.org/10.1371/journal.pgen.1003004
15. Cortés JCG, Sato M, Muñoz J et al (2012) Fission yeast Ags1 confers the essential septum strength needed for safe gradual cell abscission. J Cell Biol 198:637–656. https://doi.org/10.1083/jcb.201202015
16. Karagiannis J, Oulton R, Young PG (2002) The Scw1 RNA-binding domain protein regulates septation and cell-wall structure in fission yeast. Genetics 162:45–58. https://doi.org/10.1093/genetics/162.1.45
17. Enoch T, Carr AM, Nurse P (1992) Fission yeast genes involved in coupling mitosis to completion of DNA replication. Genes Dev 6: 2035–2046. https://doi.org/10.1101/gad.6.11.2035

18. Bhaumik D, Wang TS (1998) Mutational effect of fission yeast polalpha on cell cycle events. Mol Biol Cell 9:2107–2123
19. Xu YJ, Kelly TJ (2009) Autoinhibition and autoactivation of the DNA replication checkpoint kinase Cds1. J Biol Chem 284: 16016–16027. https://doi.org/10.1074/jbc.M900785200
20. Kippert F, Lloyd D (1995) The aniline blue fluorochrome specifically stains the septum of both live and fixed Schizosaccharomyces pombe cells. FEMS Microbiol Lett 132: 215–219. https://doi.org/10.1111/j.1574-6968.1995.tb07836.x

INDEX

Zhixiang Wang (ed.), *Cell-Cycle Synchronization: Methods and Protocols*, Methods in Molecular Biology, vol. 2579,
https://doi.org/10.1007/978-1-0716-2736-5,

D

E

F

G

H

I

L

M

N

O

P